

REPUBLIC OF TURKEY
YILDIZ TECHNICAL UNIVERSITY
GRADUATE SCHOOL OF NATURAL AND APPLIED
SCIENCES

PRODUCTION AND MAXIMIZATION OF
POLYHYDROXYBUTYRATE FROM DIAZOTROPHIC
CYANOBACTERIA ISOLATED FROM INLAND WATERS OF
TURKEY

Tuğba DAYIOĞLU

DOCTOR OF PHILOSOPHY THESIS

Department of Chemistry

Biochemistry Program

Advisor

Prof. Dr. Barbaros NALBANTOĞLU

Co-Advisor

Assoc. Prof. Dr. Turgay ÇAKMAK

February, 2020

REPUBLIC OF TURKEY
YILDIZ TECHNICAL UNIVERSITY
GRADUATE SCHOOL OF NATURAL AND APPLIED SCIENCES

**PRODUCTION AND MAXIMIZATION OF
POLYHYDROXYBUTYRATE FROM DIAZOTROPHIC
CYANOBACTERIA ISOLATED FROM INLAND WATERS OF
TURKEY**

A thesis submitted by Tuğba DAYIOĞLU in partial fulfillment of the requirements for the degree of **DOCTOR OF PHILOSOPHY** is approved by the committee on 06.02.2020 in Department of Chemistry, Biochemistry Program.

Prof. Dr. Barbaros NALBANTOĞLU

Assoc. Prof. Dr. Turgay ÇAKMAK

Yıldız Technical University

Istanbul Medeniyet University

Advisor

Co-Advisor

Approved By the Examining Committee

Prof. Dr. Barbaros NALBANTOĞLU, Advisor

Yıldız Technical University

Prof. Dr. Ayşegül PEKSEL, Member

Yıldız Technical University

Assoc. Prof. Dr. Özgür ÇAKIR, Member

Istanbul University

Asst. Prof. Dr. Çiğdem BİLEN, Member

Yıldız Technical University

Assoc. Prof. Dr. Zafer Ömer ÖZDEMİR, Member

University of Health Sciences

I hereby declare that I have obtained the required legal permissions during data collection and exploitation procedures, that I have made the in-text citations and cited the references properly, that I haven't falsified and/or fabricated research data and results of the study and that I have abided by the principles of the scientific research and ethics during my Thesis Study under the title of Production and Maximization of Polyhydroxybutyrate from Diazotrophic Cyanobacteria Isolated from Inland Waters of Turkey supervised by my supervisor, Prof. Dr. Barbaros NALBANTOĞLU. In the case of a discovery of false statement, I am to acknowledge any legal consequence.

Tuğba DAYIOĞLU

Signature

This study was supported by the Scientific and Technological Research Council of Turkey (TUBITAK) Grant No: 2211-C and by the Republic of Turkey Ministry of Agriculture and Forestry General Directorate of Agricultural Research and Policies (TAGEM) Grant No: TAGEM/16/AR-GE/44.

*Dedicated to my family
and my beloved friend Özgenur*

ACKNOWLEDGMENTS

First of all, I wish to express my intimately thanks to my supervisor Prof. Dr. Barbaros NALBANTOĞLU, for his support and guidance throughout my Ph.D. thesis with a big smile and wise words always. Sincerely, I would like to express my gratefulness to my co-advisor Assoc. Prof. Dr. Turgay ÇAKMAK for guiding, teaching, and supporting for my studies and also for leading me interested more and more about science.

I also would like to thank TAGEM project manager, Assoc. Prof. Dr. Zeynep ELİBOL ÇAKMAK for her collaborative and guiding supports. I place on record my gratitude to Istanbul Medeniyet University for giving me the opportunity to work in their labs and for supporting this thesis with the necessary equipment, primarily to Prof. Dr. Erkan ŞAHİNKAYA for his collaborative supports on ion-exchange chromatography analysis and to Asst. Prof. Dr. Cihan AYDIN, Asst. Prof. Dr. Kübra DEMİR and Dr. Ayşe DEMİR KORKMAZ for their sincere supports. I also place on record my sense of gratitude to Asst. Prof. Dr. Mustafa YAMAN and Ömer MIZRAK for their guiding and collaborative supports on HPLC analysis.

I would like to thank my laboratory friends Dr. Satya KALIAMURTHI & Dr. Guru SELVARAJ, Aycan GEZMİŞ DEMİR, Barış BALLIK, Beyzanur NÜKYEN, Eylem Çağrıcan GÖK, Feyzullah YILMAZ, Beste ÖZGÜMÜŞ, Hind AL-JANABI, Wissem M'HIRI, and also my friends Ümmügülsüm POLAT and Pınar ÇAĞLAR for all their support, good company and for the memories that they gave to me. I also would like to thank especially my laboratory partner Dr. Mohammed Fadhıl HADDAD for supporting me all the time and for being my friend.

Ultimately I wish to express my sincere gratefulness to my father Prof. Dr. Habip DAYIOĞLU, my mother Nuran DAYIOĞLU, my sisters Büşra and Kübra DAYIOĞLU, and my brother M. Atila DAYIOĞLU for always supporting, guiding, believing in me and love me the way I am.

Tuğba DAYIOĞLU

TABLE OF CONTENTS

LIST OF SYMBOLS	ix
LIST OF ABBREVIATIONS	xi
LIST OF FIGURES	xix
LIST OF TABLES	xxiv
ABSTRACT	xxvi
ÖZET	xxvii
1 Introduction	1
1.1 Literature Review	1
1.2 Objective of the Thesis.....	11
1.3 Hypothesis	11
2 Plastics	12
2.1 History.....	12
2.2 Polymerization of Plastics	13
2.2.1 Addition Polymerization.....	14
2.2.2 Condensation Polymerization.....	15
2.2.3 Ring-Opening Polymerization (ROP).....	15
2.2.4 Other Polymerization Mechanisms	16
2.3 Molecular Structure.....	16
2.3.1 Organization of Molecular Structure	17
2.3.2 Thermoplastic and Thermosetting.....	18
2.3.3 Additives of Plastics	20
2.4 Recycling Process.....	20
2.4.1 Degradation of Plastics.....	21

3	Biodegradable Plastics and Bioplastics	23
3.1	Biodegradable Plastics	23
3.1.1	Starch-based Biodegradable Plastics.....	23
3.1.2	Polycaprolactone (PCL).....	23
3.1.3	Polyethylene Succinate (PES)	24
3.1.4	Polyvinyl Alcohol (PVA)	24
3.1.5	Biodegradation by Plastic Eating Organisms	25
3.2	Bioplastics	26
3.2.1	Bioplastics from Renewable Resources.....	27
3.2.2	Bio-based Bioplastics: Polyhydroxyalkanoates (PHAs)	28
4	Cyanobacteria	35
4.1	Cyanobacteria and Taxonomy.....	35
4.1.1	Class: Cyanophyceae	35
5	Material and Methods	47
5.1	Materials.....	47
5.1.1	Chemicals.....	47
5.1.2	Devices.....	51
5.1.3	Media.....	54
5.2	Experimental Methods.....	58
5.2.1	Sampling of Cyanobacteria	58
5.2.2	Selection of Cyanobacteria	61
5.2.3	Preparation of Inoculum	67
5.2.4	Screening PHB Levels of Cyanobacteria	67
5.2.5	Studies on Selected Species.....	72
6	Results and Discussion	83
6.1	Sampling Parameters of Water	83
6.2	Isolation and Identification of Cyanobacteria.....	84
6.2.1	Purification and Selection of Nitrogen-Fixing Cyanobacteria	84
6.2.2	Genetic Identification of Nitrogen-Fixing Cyanobacteria	90
6.3	Effect of Inoculum	100

6.4	Screening and Selecting the Best PHB Producer Cyanobacteria Species	100
6.4.1	Quantitative Analyzes of PHB	102
6.4.2	Other Measurements	109
6.5	Studies on Selected Species	119
6.5.1	Medium Trial	119
6.5.2	HPLC Analysis	119
6.5.3	Detailed Experiments on Selected Species.....	124
6.5.4	Maximization of Extraction Techniques	131
6.5.5	Environmental Stress Applications	132
6.5.6	Identification of PHB by FTIR Analysis.....	142
6.6	Conclusions	145
References		147
Publications from the Thesis		156

LIST OF SYMBOLS

bp	Basepair
β	Beta
°C	Centigrade degree
C	Concentration
dw	Dry weight
R	Functional groups
Tg	Glass transition temperature
g	Gram
g	Gravity force (for centrifuge)
kb	Kilobasepair
L	Liter
MPa	Megapascal
mVA	Megavolt ampere
Tm	Melting point
m	Meter
Mt	Metric tons
μ	Micro
μE	Microeinsteins
μl	Microliter
μm	Micrometer
μmol	Micromole
mg	Milligram
ml	Milliliter

mM	Millimolar
M	Molar
ng	Nanogram
nm	Nanometer
N	Normal
ω	Omega
rpm	Revolutions per minute
V	Volume

LIST OF ABBREVIATIONS

DCDDH	1,2-dihydroxy-3,5-cyclohexadiene-1,4-dicarboxylate dehydrogenase
Nile red	9-diethylamino-5H-benzo[a]phenoxazine-5-one
A	Absorbance
AcOH	Acetic acid
AcC	Acetyl cellulose
ABS	Acrylonitrile-butadiene-styrene
ADP	Adenosine diphosphate
ATP	Adenosine triphosphate
APC	Allophycocyanin (Phcobiliprotein)
$\text{Al}_2(\text{SO}_4)_3\text{K}_2\text{SO}_4\cdot 2\text{H}_2\text{O}$	Aluminum potassium sulfate dihydrate
NH	Amine
NH_2	Amino
NH_3	Ammonia
NH_4Cl	Ammonium chloride
$(\text{NH}_4)_6\text{Mo}_7\text{O}_{24}\cdot 4\text{H}_2\text{O}$	Ammonium molybdate tetrahydrate
$\text{NiSO}_4(\text{NH}_4)_2\text{SO}_4\cdot 6\text{H}_2\text{O}$	Ammonium nickel sulphate hexahydrate
ASEAN	Association of Southeast Asian Nations
δ_{as}	Asymmetric deformation (bend)
V_{as}	Asymmetric stretch
BLASTn	Basic Local Alignment Search Tool-Nucleotide
HMG	β -Hydroxy β -methylglutaryl
BPA	Bisphenol A

BG11	Blue-green medium
H ₃ BO ₃	Boric acid
BSA	Bovine serum albumin
Cd(NO ₃) ₂ ·4H ₂ O	Cadmium nitrate tetrahydrate
CaCl ₂ ·2H ₂ O	Calcium chloride dihydrate
Ca(NO ₃) ₂ ·4H ₂ O	Calcium nitrate tetrahydrate
C; C ₄	Carbon
CO ₂	Carbon dioxide
COOH	Carboxyl
(C)	Chloroform
(CD)	Chloroform: dichloromethane (1: 1)
Chl	Chlorophyll
Cr(NO ₃) ₃ ·7H ₂ O	Chromium (III) nitrate heptahydrate
CoCl ₂ ·6H ₂ O	Cobalt (II) chloride hexahydrate
Co(NO ₃) ₂ ·6H ₂ O	Cobalt (II) nitrate hexahydrate
CoA	Coenzyme A
MARPOL	Convention for Prevention of Marine Pollution
CuSO ₄ ·5H ₂ O	Copper (II) sulfate pentahydrate
d	Day
DNA	Deoxyribonucleic acid
D	Dextro
DSC	Differential scanning calorimetry
H ₂ O	Dihydrogen monoxide (Water)
DMSO	Dimethyl sulfoxide
dH ₂ O	Distilled water

ddH ₂ O	Double-distilled water
ET	Electron transfer
Eq	Equation
EtOH	Ethanol
Na ₂ -EDTA	Ethylenediaminetetra acetic acid disodium salt dihydrate
EDTA	Ethylenediaminetetraacetic acid
ECHA	European Chemicals Agency
EFSA	European Food Safety Authority
EU	European Union
FAME	Fattyacylmethylester
Fe	Ferrum (Iron)
FTIR	Fourier transform infrared spectroscopy
FW	Freshwater
GC	Gas Chromatography
HFR	halogenated flame retardant
CTAB	Hexadecyltrimethylammonium bromide
HDPE	High-density polyethylene
HPLC	High-performance liquid chromatography
h	Hour
HCl	Hydrochloric acid
H ₂	Hydrogen
HB	Hydroxybutyrate
OH	Hydroxyl
FeSO ₄ ·7H ₂ O	Iron (II) sulfate heptahydrate
FeCl ₃	Iron (III) chloride

IMU	Istanbul Medeniyet University
L	Levorotary
LDPE	Low-density polyethylene
MgSO ₄ ·7H ₂ O	Magnesium sulfate heptahydrate
MnCl ₂ ·4H ₂ O	Manganese (II) chloride tetrahydrate
MnSO ₄ ·4H ₂ O	Manganese (II) sulfate Tetrahydrate
(M)	Methanol
MeOH	Methanol
(MAWD)	Methanol: acetone: water: dimethylformamide (40: 40: 18: 2)
CH ₃	Methyl
CH ₂	Methylene
MP	Microplastic
min	Minute
Mo	Molybdate
MHET	Mono-(2-hydroxyethyl)terephthalic acid
NCBI	National Center for Biotechnology Information
NAD	Nicotinamide adenine dinucleotide
NADP	Nicotinamide adenine dinucleotide phosphate
N; N ₂	Nitrogen
BG11-NP	Nitrogen and phosphorous-deprived blue-green medium
BG11-N	Nitrogen-deprived blue-green medium
Z8-N	Nitrogen-deprived Z8 medium
OD	Optical density
O ₂	Oxygen

PO ₄	Phosphate
P; P ₂	Phosphorus
PAE	Phthalate
PC	Phycocyanin (Phcobiliprotein)
PE	Phycoerythrin (Phcobiliprotein)
P3HP	Poly (3-hydroxypropionate)
PHV; P3HV	Poly (3-hydroxyvalerate)
P4HB	Poly (4-hydroxybutyrate)
P5HV	Poly (5-hydroxyvalerate)
Nylon 11	Poly ω -undecanamide
PBDE	Polybrominated diphenyl ethers
PBS	Polybutylene succinate
Nylon 6	Polycaprolactam
PCL	Polycaprolactone
PC	Polycarbonate
PEEK	Polyetheretherketone
PE	Polyethylene
PES	Polyethylene succinate
PET	Polyethylene terephthalate
PHA	Polyhydroxyalkanoate
PHB; P3HB	Polyhydroxybutyrate; poly (3-hydroxybutyrate); poly (3- β -hydroxybutyrate); poly[(<i>R</i>)-3-hydroxybutyric acid]
PLA	Polylactic acid
PCR	Polymerase chain reaction
PMMA	Polymethyl methacrylate

PPS	Polyphenylene sulfide
PP	Polypropylene
PS	Polystyrene
PTFE	Polytetrafluoroethylene
PVA	Polyvinyl alcohol
PVC	Polyvinyl chloride
KBr	Potassium bromide
KH_2PO_4	Potassium dihydrogen phosphate
KI	Potassium iodide
K_2HPO_4	Potassium phosphate dibasic anhydrous
K_2SO_4	Potassium sulfate
PCA	Protocatechuic acid
Pca34	Protocatechuic acid 3,4-dioxygenase
PQQ	Pyrroloquinoline quinone
RC	Reaction center
R	Rectus (Right)
NADH	Reduced nicotinamide adenine dinucleotide
NADPH	Reduced nicotinamide adenine dinucleotide phosphate
Ref.	Reference
RNA	Ribonucleic acid
rRNA	Ribosomal ribonucleic acid
ROP	Ring-opening polymerization
s	Second
S-layer	Serrated external layer
Na_2CO_3	Sodium carbonate

NaCl	Sodium chlorite
SDS	Sodium dodecyl sulfate
$\text{Na}_2\text{SiO}_3 \cdot 9\text{H}_2\text{O}$	Sodium metasilicate nonahydrate
$\text{Na}_2\text{MoO}_4 \cdot 2\text{H}_2\text{O}$	Sodium molybdate dihydrate
NaNO_3	Sodium nitrate
$\text{Na}_2\text{WO}_4 \cdot 2\text{H}_2\text{O}$	Sodium tungstate dihydrate
H_2SO_4	Sulfuric acid
δ_s	Symmetric deformation (bend)
v_s	Symmetric stretch
TPA	Terephthalic acid
TPADO	Terephthalic acid 1,2-dioxygenase
TPATP	Terephthalic acid transporter
THF	Tetrahydrofuran
EMBL	The European Molecular Biology Laboratory
TAGEM	The Republic of Turkey Ministry of Agriculture and Forestry General Directorate of Agricultural Research and Policies
SH	Thiol
TDS	Total dissolved solids
TAG	Triacylglycerol
Tris-HCl	Tris(hydroxymethyl)aminomethane hydrochloride; trizma hydrochloride
TBE	Tris-borate-EDTA
PAGEV	Turkish Plastic Industrialists Research and Development Foundation
ULT	Ultra-low temperature

UV	Ultraviolet
UV-Vis	Ultraviolet-visible
UNEA	United Nations Environment Assembly
$\text{VOSO}_4 \cdot 6\text{H}_2\text{O}$	Vanadium (IV) oxide sulfate hexahydrate
Vit.	Vitamin
ZnCl_2	Zinc chloride
$\text{ZnSO}_4 \cdot 7\text{H}_2\text{O}$	Zinc sulfate heptahydrate

LIST OF FIGURES

Figure 1.1	Map of microplastic (MP) locations of Arctic snow	1
Figure 1.2	Litter and microplastic distribution on the World water systems	2
Figure 1.3	Global marine litter composition and its effects on organisms	3
Figure 1.4	Ecosystem impacts of marine plastic on biota	4
Figure 1.5	Plastic debris from the stomachs of Serrasalmid fishes from the Amazon River	4
Figure 1.6	Summary of the trophic network for the intake of plastic by three guilds of serrasalmid fishes in the Amazon River	5
Figure 1.7	Members of the International Waste Platform	6
Figure 1.8	Plastic consumption of Turkey in (a) isochronal terms and (b) increasing by years	7
Figure 1.9	Protection mechanism for nitrogenase against O ₂ in A. vinelandii	8
Figure 2.1	Summary illustrating historical stages in the development, production, and use of plastics	13
Figure 2.2	Some plastic polymers	14
Figure 2.3	Polystyrene's addition polymerization mechanism from styrene monomer	15
Figure 2.4	Polyamide's condensation mechanism from diacid and diamine	15
Figure 2.5	Hydrolytic ring-opening polymerization of caprolactam to produce nylon 6	16
Figure 2.6	Schematic representation of linear, branched, and crosslinked polymers	16
Figure 2.7	Structural representation of semicrystalline and amorphous polymers	17
Figure 2.8	Schematic diagram of the semicrystalline morphology, showing amorphous regions and crystallites	17

Figure 2.9	DSC thermogram of melting endotherm for a semicrystalline polymer and a glass transition for an amorphous material	18
Figure 3.1	Molecular structure of polycaprolactone	23
Figure 3.2	Molecular structure of polyethylene succinate	24
Figure 3.3	PVA utilization by symbiotic bacteria	24
Figure 3.4	PVA degradation pathway by various enzyme systems	25
Figure 3.5	PET metabolism by <i>Ideonella sakaiensis</i>	26
Figure 3.6	Chemical structure of (a) PLLA and (b) PDLA	27
Figure 3.7	Chemical structure of (a) succinate acid, (b) 1,4-butanediol, and (c) polybutylene succinate (PBS)	28
Figure 3.8	Structure of polyhydroxyalkanoates	29
Figure 3.9	3- β -hydroxybutyrate pathway in ketogenesis	29
Figure 3.10	Biosynthetic pathway of PHB	30
Figure 3.11	Model for the system of PHB synthesis control	31
Figure 3.12	Examples of PHA matrices fabricated for medical use	32
Figure 4.1	Taxonomy of Cyanobacteria	35
Figure 4.2	Cyanobacterial noncyclic electron flow of the photosynthetic apparatus	37
Figure 4.3	Comparative anatomy of the photosynthetic apparatus in Cyanobacteria	37
Figure 4.4	Anatomy of Cyanobacterial cell wall	38
Figure 4.5	Cyanobacterial gas vacuoles and lipid droplets	38
Figure 4.6	Germination of Cyanobacterium from akinete	39
Figure 4.7	Akinete, heterocyst, and vegetative cells	39
Figure 4.8	Formation of heterocysts, nitrogen fixation, and cellular accumulation	40
Figure 4.9	Taxonomy of the studied Cyanobacteria	41
Figure 4.10	Microscope and diagram image of <i>Nostoc</i> sp.	42
Figure 4.11	Microscope image of <i>Anabaena</i> sp.	42
Figure 4.12	Microscope image of <i>Cylindrospermopsis</i> sp.	43
Figure 4.13	Microscope image of <i>Anabaenopsis</i> sp.	43
Figure 4.14	Microscope image of <i>Nodularia</i> sp.	44

Figure 4.15	Microscope image of <i>Calothrix</i> sp.	44
Figure 4.16	Microscope image of <i>Microchaete</i> sp.	45
Figure 4.17	Microscope image of <i>Chlorogloeopsis</i> sp.	45
Figure 4.18	Microscope image of <i>Mastigocladus</i> sp.	46
Figure 4.19	Microscope image of <i>Nodosilinea</i> sp.	46
Figure 5.1	Sampling locations of Cyanobacteria species from IMU Culture Library	59
Figure 5.2	Sampling locations of Cyanobacteria species from paddy fields	60
Figure 5.3	Sampling from paddy fields.....	60
Figure 5.4	Ion-exchange chromatography	61
Figure 5.5	Purification process of nitrogen-fixing Cyanobacteria.....	62
Figure 5.6	Thermo-shaker and nanodrop respectively	64
Figure 5.7	Gel electrophoresis and gel electrophoresis scanner	65
Figure 5.8	Thermocycler (PCR)	67
Figure 5.9	Light microscope imaging system	68
Figure 5.10	Scheme of the steps of developed Sudan black B quantification technique.....	69
Figure 5.11	FTIR	70
Figure 5.12	PHB responsible FTIR peaks	70
Figure 5.13	Microplate spectrophotometer.....	71
Figure 5.14	Lyophilizer and homogenizer, respectively	74
Figure 5.15	Chlorophyll a, b and carotenoids absorbance spectra	75
Figure 5.16	Fluorescence microscope imaging system.....	77
Figure 5.17	Soxhlet extraction and evaporation with rotary.....	79
Figure 5.18	Gas chromatography	82
Figure 6.1	Selection of isolates on BG11 and BG11-N media in the same two-sided Petri dish.....	87
Figure 6.2	Growing rate on BG11-N, Z8-N, and Z8 media respectively	87
Figure 6.3	Selection of best primers on gel electrophoresis image.....	92
Figure 6.4	Gel electrophoresis image of Cyanobacteria species	93
Figure 6.5	Sudan black B method PHB calibration curve.....	102

Figure 6.6	PHB content of Cyanobacteria species by Sudan black B method.....	103
Figure 6.7	PHB responsible FTIR peak at 1720 cm ⁻¹	105
Figure 6.8	PHB responsible FTIR peak at 1735 cm ⁻¹	106
Figure 6.9	PHB concentration ratio of 1720 cm ⁻¹ /1652 cm ⁻¹	107
Figure 6.10	PHB concentration ratio of 1735 cm ⁻¹ /1652 cm ⁻¹	108
Figure 6.11	TAG concentration ratio of Cyanobacteria species	110
Figure 6.12	Oligosaccharide and polysaccharide concentration ratios of Cyanobacteria species.....	111
Figure 6.13	Total chlorophyll-a concentration in Cyanobacteria species.....	113
Figure 6.14	Total carotenoid concentration in Cyanobacteria species.....	114
Figure 6.15	Phycoerythrin concentration changes in Cyanobacteria species.....	116
Figure 6.16	Phycocyanine concentration changes in Cyanobacteria species.....	117
Figure 6.17	Allophycocyanine concentration changes in Cyanobacteria species.....	118
Figure 6.18	Lutein concentrations in selected Cyanobacteria.....	120
Figure 6.19	Zeaxanthin concentrations in selected Cyanobacteria	121
Figure 6.20	Canthaxanthin concentrations in selected Cyanobacteria	121
Figure 6.21	Chlorophyll-a concentrations in selected Cyanobacteria	122
Figure 6.22	Alpha-carotene concentrations in selected Cyanobacteria.....	123
Figure 6.23	Beta-carotene concentrations in selected Cyanobacteria.....	123
Figure 6.24	B ₂ vitamin concentrations in selected Cyanobacteria	124
Figure 6.25	PHB calibration curve of sulphuric acid digestion in the quartz tube.....	125
Figure 6.26	PHB percentage in dry weight (dw) by sulphuric acid digestion method.....	125
Figure 6.27	PHB concentration by Sudan black B dye method	126
Figure 6.28	Cyanobacterial growth rates	127
Figure 6.29	Chlorophyll-a amounts in selected species.....	128
Figure 6.30	Carotenoid amounts in selected species.....	128

Figure 6.31	Saccharide calibration curve	129
Figure 6.32	Total saccharide amounts in selected species.....	129
Figure 6.33	Protein calibration curve.....	130
Figure 6.34	Protein amounts in selected species	130
Figure 6.35	Nile red images.....	131
Figure 6.36	PHB percentage in dry weight (dw) of selected species after different extraction manipulations	132
Figure 6.37	Calibration curve of PHB in the microplate.....	134
Figure 6.38	PHB amounts of <i>Calothrix</i> sp. IMU10 in the quartz tubes	134
Figure 6.39	PHB amounts of <i>Calothrix</i> sp. IMU10 in in the microplate.....	135
Figure 6.40	PHB amounts of <i>Nostoc</i> sp. IMU11 in the quartz tubes.....	136
Figure 6.41	PHB amounts of <i>Nostoc</i> sp. IMU11 in the microplate	136
Figure 6.42	PHB amounts of <i>Anabaena</i> sp. IMU18 in the quartz tubes.....	137
Figure 6.43	PHB amounts of <i>Anabaena</i> sp. IMU18 in the microplate.....	137
Figure 6.44	PHB amounts of selected Cyanobacteria against environmental manipulation	138
Figure 6.45	Chlorophyll-a amounts of selected species in different stress conditions	139
Figure 6.46	Carotenoid amounts of selected species in different stress conditions.....	140
Figure 6.47	FAME analysis of <i>Calothrix</i> sp. IMU10	141
Figure 6.48	FAME analysis of <i>Nostoc</i> sp. IMU11.....	141
Figure 6.49	FAME analysis of <i>Anabaena</i> sp. IMU18.....	142
Figure 6.50	FTIR spectra of <i>Calothrix</i> sp. IMU10.....	144
Figure 6.51	FTIR spectra of <i>Nostoc</i> sp. IMU11.....	144
Figure 6.52	FTIR spectra of <i>Anabaena</i> sp. IMU18.....	144

LIST OF TABLES

Table 1.1	PHB producing organisms	9
Table 2.1	Properties and applications of commercially important plastics...	18
Table 2.2	Polymer degradation routes.....	22
Table 3.1	Polymer degradation routes.....	30
Table 5.1	Chemicals, solutions, and kits.....	47
Table 5.2	Experimental devices.....	51
Table 5.3	BG11 medium recipe	54
Table 5.4	Z8 medium recipe.....	55
Table 5.5	Allen medium recipe.....	56
Table 5.6	FW medium recipe	57
Table 5.7	Micronutrient solution recipe	58
Table 5.8	Vitamin mix recipe	58
Table 5.9	CTAB extraction buffer recipe.....	63
Table 5.10	5xTBE buffer recipe	65
Table 5.11	Primer pairs.....	66
Table 5.12	PCR program	66
Table 5.13	Preparation of calibration series of D-glucose in distilled water...	76
Table 5.14	Preparation of calibration series of BSA in distilled water	77
Table 5.15	Extraction parameters	79
Table 5.16	Environmental stress factors of experimental groups.....	80
Table 5.17	FAME extraction buffer recipe	81
Table 6.1	Dynamic properties of water samples	83
Table 6.2	Salinity, ammonium and nitrate level of water samples	84
Table 6.3	Classification of selected isolates based on microscope images....	84
Table 6.4	BG11 (+), BG11-N (-N), and BG11-NP (-N-P) medium trial	88
Table 6.5	Nanodrop measurements.....	91
Table 6.6	Primer order	92
Table 6.7	Genomic and morphologic information of identified Cyanobacteria.....	94
Table 6.8	Images of Cyanobacteria in BG11-N and BG11-NP medium	100

Table 6.9	Allen, BG11, FW, and Z8 medium trial.....	119
Table 6.10	Culture flasks during inoculation by various media	133
Table 6.11	Band assignments of FTIR	143

Production and Maximization of Polyhydroxybutyrate from Diazotrophic Cyanobacteria Isolated from Inland Waters of Turkey

Tuğba DAYIOĞLU

Department of Chemistry

Doctor of Philosophy Thesis

Advisor: Prof. Dr. Barbaros NALBANTOĞLU

Co-advisor: Assoc. Prof. Dr. Turgay ÇAKMAK

Plastic has an essential importance in our lives. However, the disposal of these non-biodegradable plastics poses a threat to our environment. In addition to their chemical and physical properties, biocompatible and biodegradable polyhydroxyalkanoates (PHA) have the potential to be alternative to petroleum-based plastics. Polyhydroxybutyrate (PHB), which is the most common derivative of PHA, is generated as an alternative petrochemical plastics due to their biodegradable qualifications. In this thesis, twelve Cyanobacteria species from the paddy fields of Edirne were isolated, and with twelve Cyanobacteria species from the IMU culture library, which were also collected from Turkey's inland waters have been identified on morphologic and genomic base. Studied diazotrophic Cyanobacteria have been investigated for their PHB contents, which is biodegradable, renewable, biologically suitable, non-toxic, and environmentally friendly bioplastics. The best culture medium selection has been performed, and

Calothrix sp. IMU10, *Nostoc* sp. IMU11, and *Anabaena* sp. IMU18 have been selected as the best diazotrophic PHB producer Cyanobacteria. Also, PHB analysis methods and the maximization of extraction technics have been investigated. Furthermore, valuable Cyanobacterial by-products such as fatty acid methyl ester and tri acyl glycerol, saccharide, chlorophyll-a, carotenoid, riboflavin, protein, and phycobiliprotein have been measured.

Keywords: PHB, Cyanobacteria, genomic identification, nitrogen deprivation

Türkiye'nin İç Sularından İzole Edilen Diazotrofik Siyanobakterilerden Polihidroksibutirat Üretimi ve Maksimizasyonu

Tuğba DAYIOĞLU

Kimya Bölümü

Doktora Tezi

Danışman: Prof. Dr. Barbaros NALBANTOĞLU

Eş-Danışman: Doç. Dr. Turgay ÇAKMAK

Plastik hayatımızda oldukça büyük bir öneme sahiptir. Bununla birlikte, biyolojik olarak bozunmayan bu plastiklerin kirliliği çevremize tehdit oluşturmaktadır. Kimyasal ve fiziksel özelliklerine ek olarak, biyolojik olarak uyumlu ve biyolojik olarak parçalanabilir polihidroksialkanoatlar (PHA), petrol bazlı plastiklere alternatif olma potansiyeline sahiptir. PHA'nın en yaygın türevi olan polihidroksibutirat (PHB), biyolojik olarak parçalanabilir nitelikleri nedeniyle petrokimyasal plastiklere bir alternatif olarak üretilmiştir. Bu tezde, Edirne'nin çeltik tarlalarından on iki siyanobakteri türü saflaştırılmış ve yine Türkiye iç sularından toplanan IMU kültür kütüphanesinden on iki siyanobakteri türü ile morfolojik ve genomik düzeyde tanımlanmıştır. Çalışılan diazotrofik Siyanobakteriler biyoçözünür, yenilenebilir, biyolojik olarak uygun, toksik olmayan ve çevre dostu biyoplastikler olan PHB içerikleri yönünden

arařtırılmıřlardır. En iyi besi-yeri belirlenmiř ve *Calothrix* sp. IMU10, *Nostoc* sp. IMU11 ve *Anabaena* sp. IMU18 en iyi diazotropik PHB üretici Siyanobakteri olarak seçilmiřtir. Ayrıca, PHB analiz metotları ve ekstraksiyon tekniklerinin maksimizasyonu arařtırılmıřtır. Bunların yanında, yağ asidi metil ester ve tri açıl gliserol, sakkarit, klorofil-a, karotenoid, riboflavin, protein ve fikobiliprotein gibi deęerli Siyanobakteriyel yan ürünler ölçölmüřtür.

Anahtar Kelimeler: PHB, Siyanobakteri, genomik tanımlama, azot yoksunluğu

1

Introduction

1.1 Literature Review

Plastics are petroleum-based chemicals that have used worldwide since the 1950s [1]. The word of plastic originated from “plastikos,” which means “able to be molded into different shapes” due to plastic polymers can be mold, extruded, cast, spun or applied as a coating, have variable usage in industry, agriculture, and especially in packaging [2].

Approximately 10 percent of the waste we produce is plastic, and increasing usage of plastics and their durability create significant waste problem [1]. Only plastic production has been computed to be 8300 million metric tons (Mt), and by 2050 approximately 12000 Mt of plastic waste is foreseen to be in environment, and every year, between 1.15-2.41 million metric tons of plastic enter the ocean via global riverine systems which makes rivers primarily responsible for the marine plastic pollution [3]. Though removing some marine plastic is possible, it is time-intensive, expensive, and inefficient, but for the microplastics (MP)(0.1 μm –5 mm), it is more complicated, formidable, and expensive and now well evidenced that this plastic negatively impacts marine life [4].

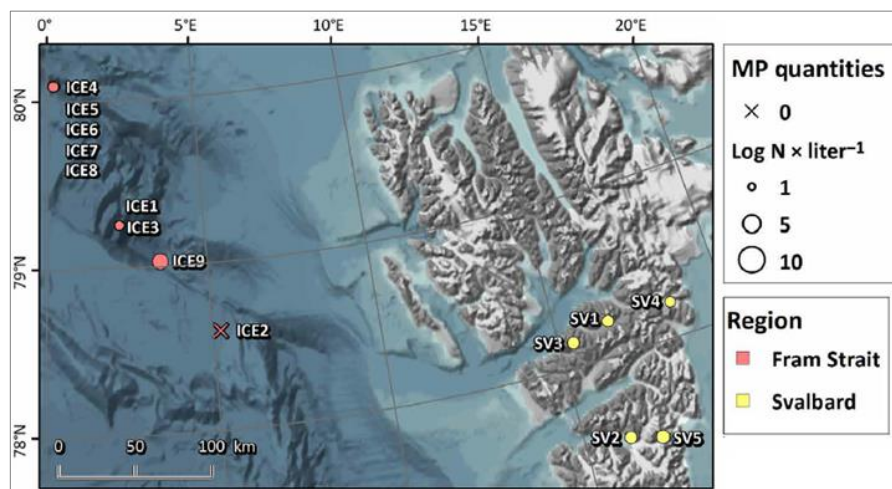


Figure 1.1 Map of microplastic (MP) locations of Arctic snow

Plastics have been reported in environments close to urban centers, terrestrial areas, and freshwater ecosystems, and new studies showed that plastic has also been found in Polar Regions, including Arctic beaches, water column, sea ice, sea surface, and the seafloor (Fig. 1.1) [5].

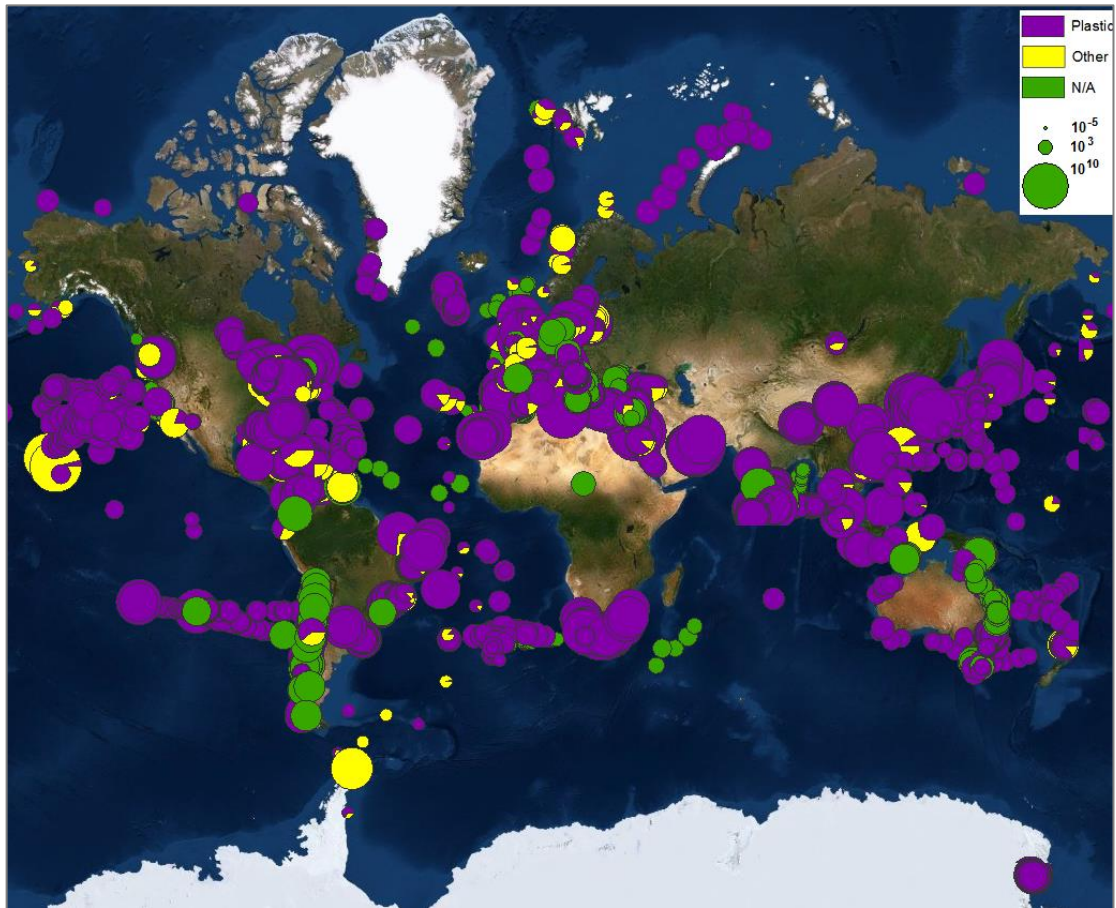


Figure 1.2 Litter and microplastic distribution on the World water systems

Marine plastics pollution is a widespread problem affecting many countries, and globally the most polluting countries are China, Indonesia, the Philippines, Vietnam, and Sri Lanka [6]. The composition of litter in the world's oceans is mostly plastics, and plastic litter has become a severe threat to the marine environment, aquatic life, and humankind (Fig 1.2, 1.3) [7].

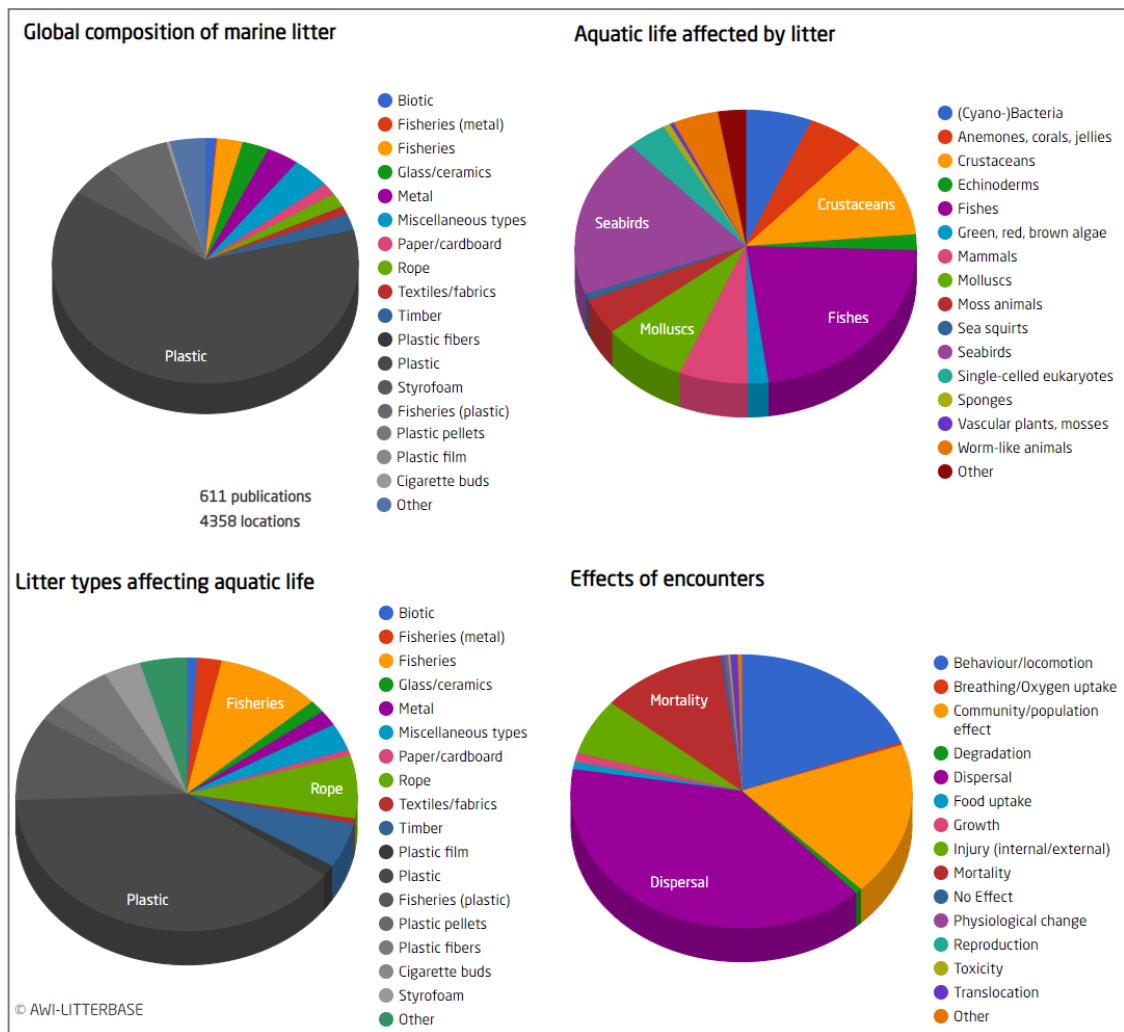


Figure 1.3 Global marine litter composition and its effects on organisms

Recent studies have demonstrated nanosized polystyrene plastics which are also used in products such as waterborne paints, toothpaste, and biomedical products, to be hazardous, for instance, by reducing the filter-feeding activity of mussels (*Mytilus edulis*), causing mortality of copepods upon ingestion (*Tigriopus japonicus*) [3], and interfering with algal photosynthesis [8]. Figure 1.4 demonstrates the ecosystem impacts of marine plastic on biota, which are negative, except for algae and bacteria [4].

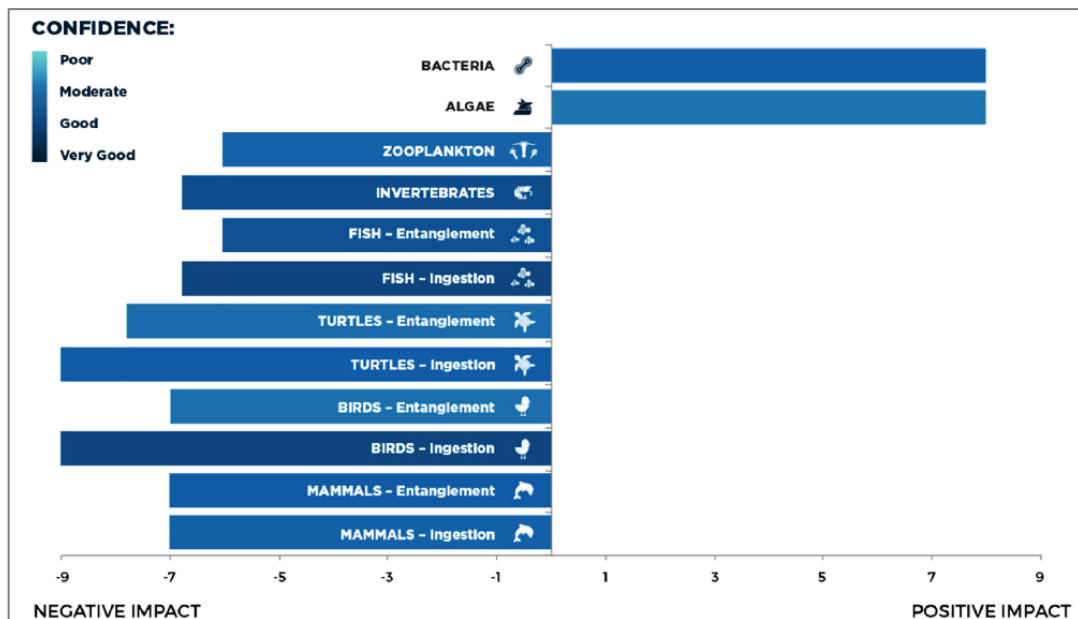


Figure 1.4 Ecosystem impacts of marine plastic on biota

A study on stomach contents of Amazon River fishes of family Serrasalminidae (Fig 1.5) showed that plastic presence and their major trophic pathways and potential routes for plastic intake (Fig 1.6), and pointed up plastic debris can be a danger to animals and humans who consume fish [9].

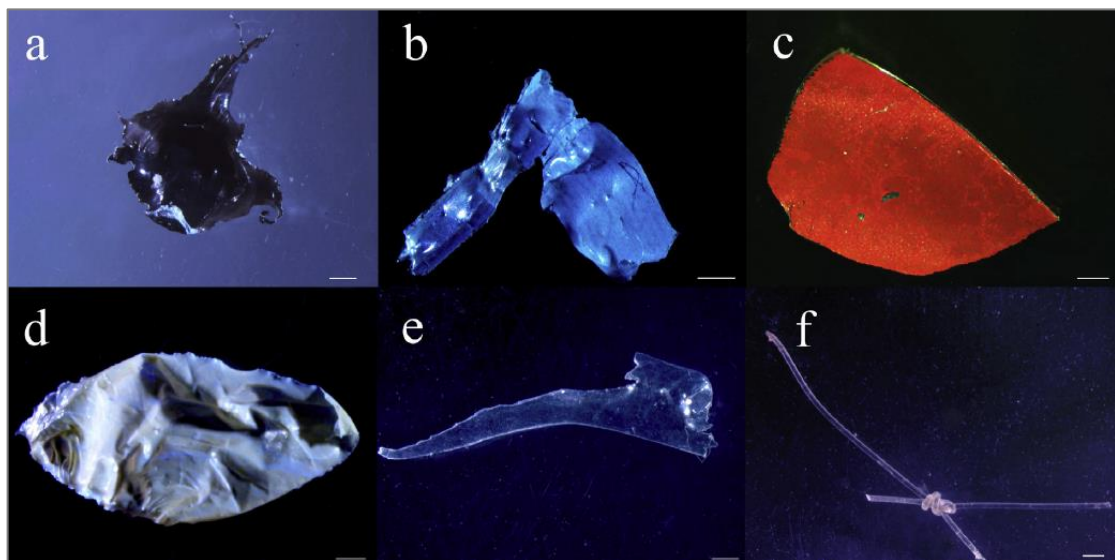


Figure 1.5 Plastic debris from the stomachs of Serrasalminid fishes from the Amazon River

(Fragments (a-e) and filaments (f), and of the colors black (a), blue (b), red (c), white (d), and transparent (e, f)) *Scale bar $\frac{1}{4}$ 1 mm

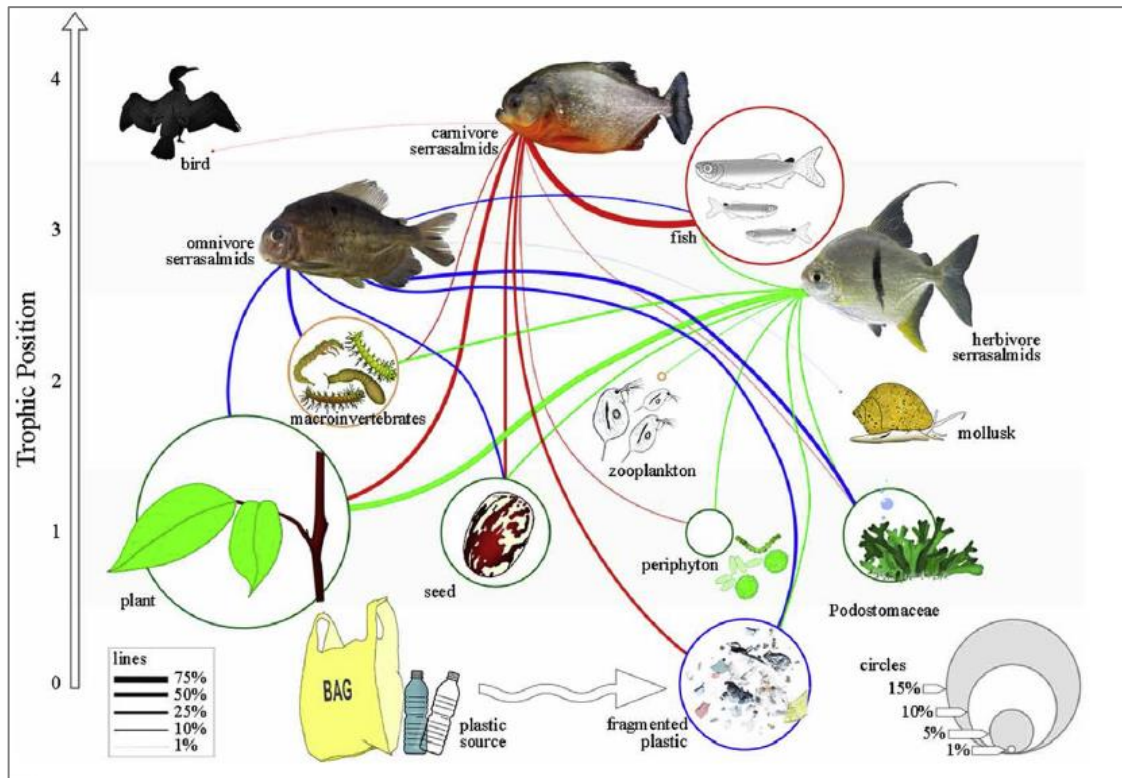


Figure 1.6 Summary of the trophic network for the intake of plastic by three guilds of serrasalmid fishes in the Amazon River

A model that is using published data on plastic ingestion by seabirds has been adjusted and predicted that by 2050, plastic will be found in the digestive parts of 99% of all seabird species, which 95% of the individual species [10].

The World is now more sensitive about the plastic, especially on health and environment, including harmful effects on wildlife and the qualities of cities and forests [2]. The G7 Leaders' statement in 2018 placed a spotlight on ocean plastics pollution [6]. The Association of Southeast Asian Nations Conference 2017 (ASEAN) on "Reducing Marine Debris in the ASEAN Region" highlighted regional cooperation to reduce plastics pollution at its originating sources [6]. Since its first session (UNEA-1) in 2014, the United Nations Environment Assembly (UNEA) attached importance of marine plastic pollution and microplastics [6], and they made some activities such as cleaning seas, sharing concepts, knowledge, programs, and opportunities by their Voluntary Commitment [11]. Also, the Sixth International Marine Debris Conference agreed to collaborate with the International Waste Platform's members (Fig. 1.7) [11].

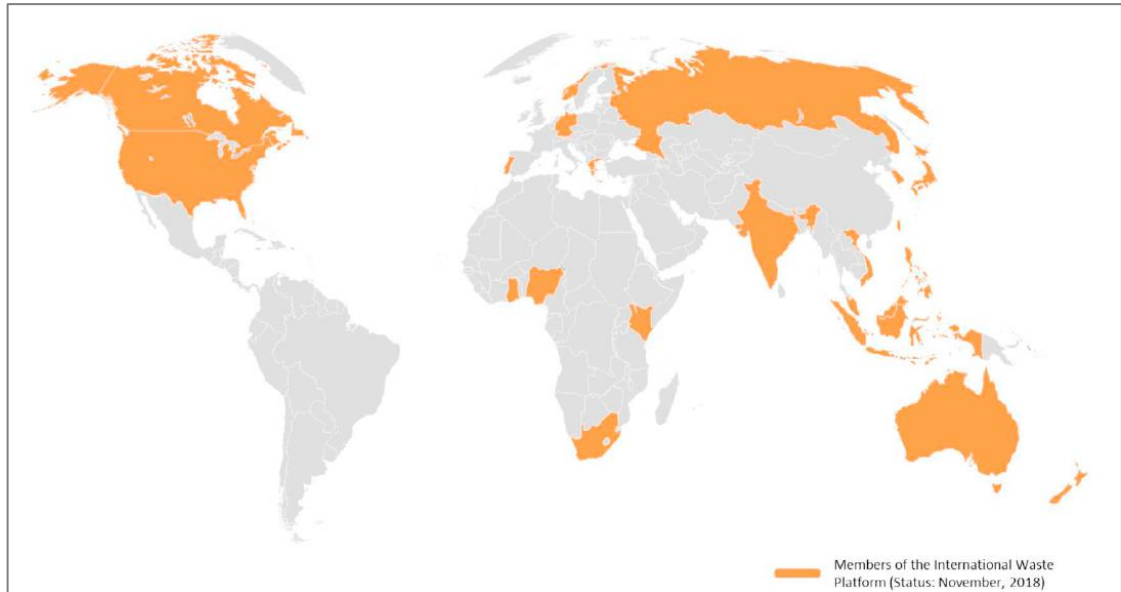


Figure 1.7 Members of the International Waste Platform

Seeking to reduce production, use, and disposal of plastic bags, the world's largest economies encourage charging for plastic bags, restrictive use, recycling, and even a complete banish has been implemented [12]. With this aim the in 2016 distribution of plastic bags were banned in California (USA), Denmark and Austria achieved 80-100% plastic recovery from wastes, in Ireland, the plastic bag tax was launched in 2002 [12], and at 01.01.2019, Turkey Republic Environment and Urban Ministry declared Environment Law (No: 2872) of “Principles and Procedures for Pricing of Plastic Bags” which may cause a decrease in PAGEV’s 2019 March report (Fig. 1.8) [13]. Moreover, the interchanging of conventional plastic polymers with biodegradable plastics has been used as an alternative for reducing the environmental accumulation of plastic debris [12].

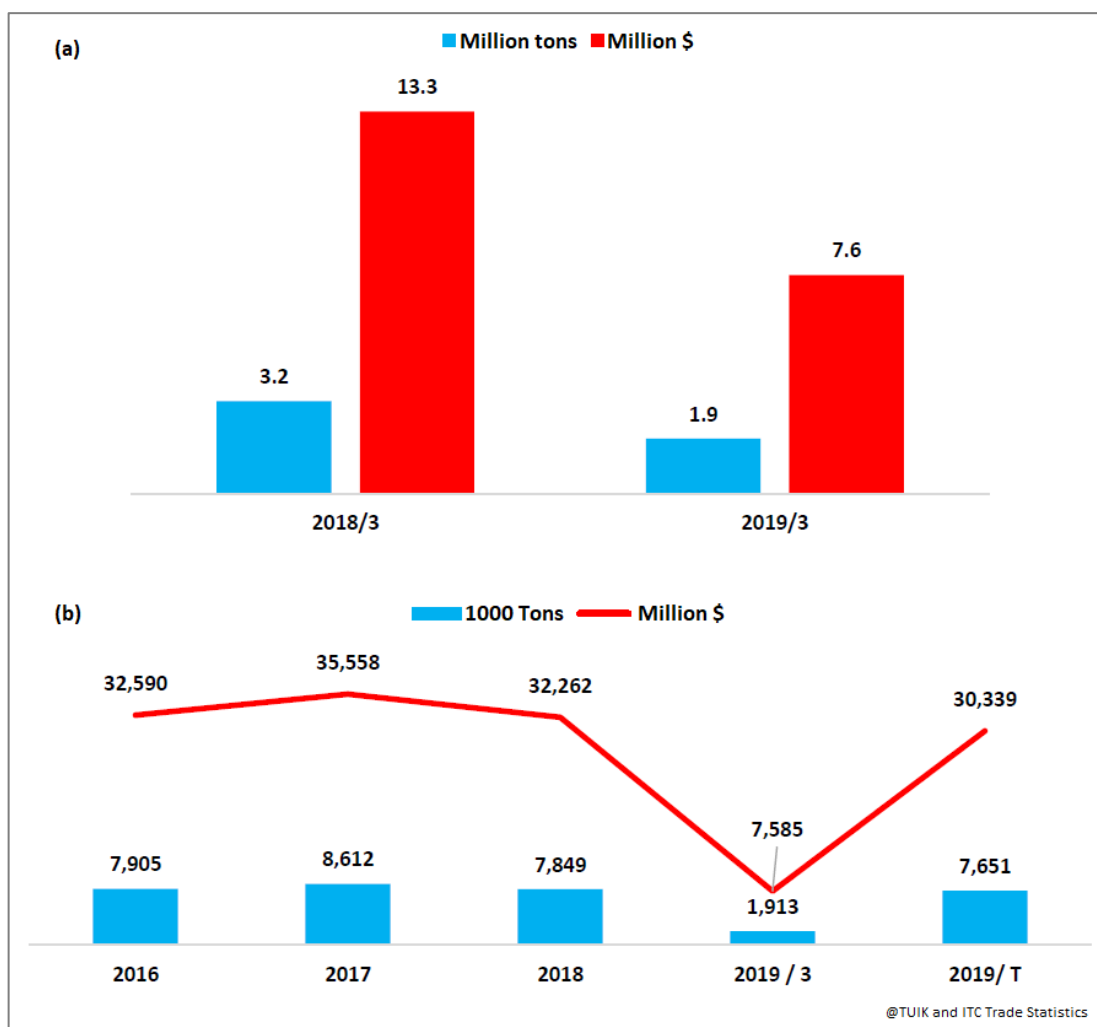


Figure 1.8 Plastic consumption of Turkey in (a) isochronal terms and (b) increasing by years

Having considered the benefits of plastics with comparison of the problems, the properties of PHB as a natural based compound, including thermoplastic processability, biocompatibility, piezoelectricity, optical purity, resistance to water, high biodegradability, make it a valuable alternative to petroleum-based plastics and would be a good alternative for new waste management strategies [14].

PHB is generally produced by nitrogen-fixing organisms when nutrients are limited, such as nitrogen and phosphorus [15]. PHB accumulation via nitrogenase in nitrogen-fixing microorganisms occurs for the protection of nitrogenase from O_2 damage which summarized in Figure 1.9 [16]:

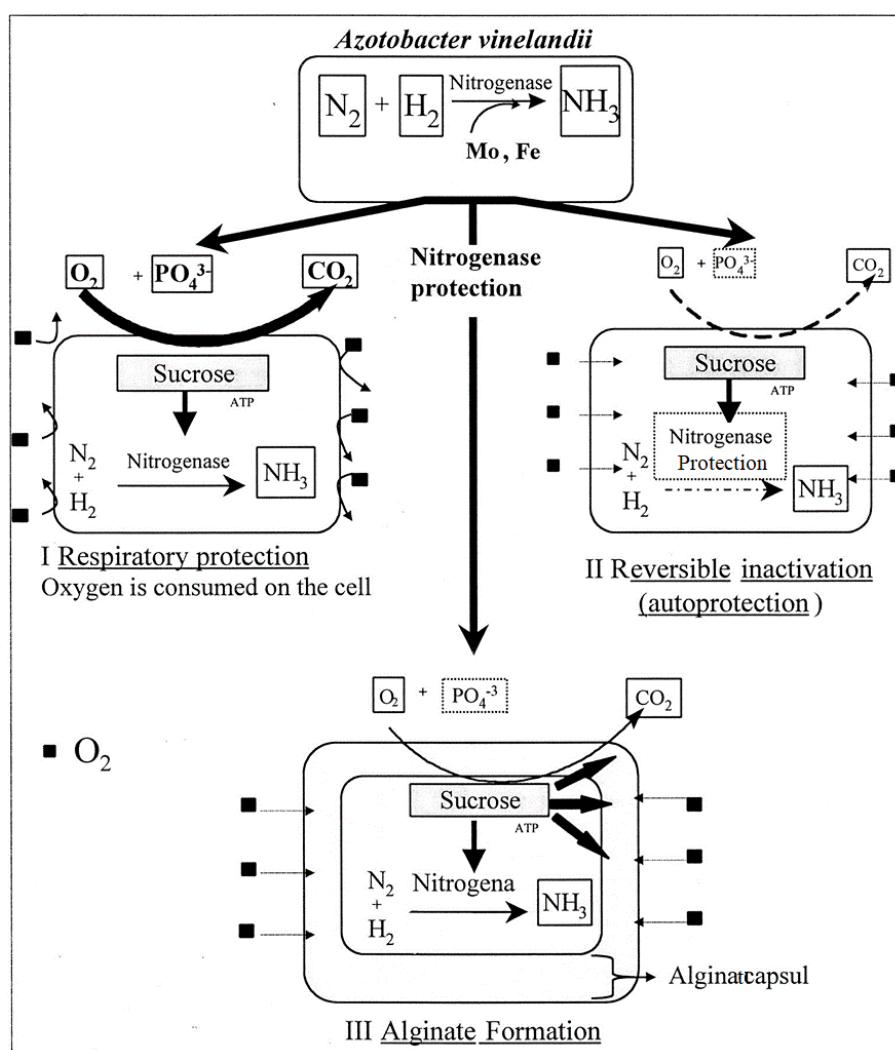


Figure 1.9 Protection mechanism for nitrogenase against O_2 in *A. vinelandii*

The activation of Sll0783 gene cluster is reported as PHB producing responsible protein in nitrogen starvation for being able to fix nitrogen for all of the heterotrophic bacteria, which includes Proteobacteria, Actinobacteria, and Cyanobacteria [17]. Also, adapting to nitrogen deficiency is controlled by the PII-signaling protein and transcription factor NtcA in [17]. It is notified that nitrogen depletion accumulates expression of sigE and overexpression enhances acetyl-CoA and organic acids (citrate) levels, and the addition of acetate as a carbon source accumulates PHB in Cyanobacteria [18].

PHB producing organisms are listed in the following Table 1.1:

Table 1.1 PHB producing organisms

	<i>Species</i>	<i>Method</i>	<i>PHB Amount in dw</i>	<i>Ref.</i>
<i>Plants</i>	<i>A. thaliana</i> (in the cytoplasm)	transformation	27%	[19]
	<i>A. thaliana</i> (in the plastid)	transformation	40%	[19]
	<i>A. thaliana</i> (in the peroxisome)	transformation	0.6%	[19]
	Corn (in the plastid)	transformation	6%	[19]
<i>Bacteria</i>	<i>Alcaligenes eutrophus</i>	+ gluconate	46-85%	[20]
	<i>Alcaligenes eutrophus</i>	+ propionate	26-36%	[20]
	<i>Alcaligenes eutrophus</i>	+ octanoate	38-45%	[20]
	<i>Bacillus megaterium</i> QMB1551	transformation + glucose	20%	[21]
	<i>Klebsiella aerogenes</i>	transformation + molasses	65%	[22]
	<i>Methylobacterium rhodesianum</i> MB1267	+ fructose, methanol	30%	[23]
	<i>Methylobacterium extorquens</i> ATCC 55366	+ methanol	40-46%	[24]
	<i>Pseudomonas oleovorans</i>	+ gluconate	1.1-5%	[20]
	<i>Pseudomonas oleovorans</i>	+ octanoate	50-60%	[20]
	<i>Pseudomonas putida</i> GPp104	+ octanoate	12-22%	[20]
	<i>Sphaerotilus natans</i>	mutation + glucose	40%	[25]
<i>Cyanobacteria</i>	<i>Anabaena cylindrical</i> 10 C	acetate + propionate	2%	[26]
	<i>Aulosira fertilissima</i>	phosphate-limitation + acetate, citrate, KH_2PO_4	77%	[14]
	<i>Chloroglea fritschii</i>	+ acetate	10%	[27]
	<i>Nostoc muscorum</i>	phosphate-limitation + 1% glucose, 1% acetate	16.4%	[14]

	<i>Nostoc muscorum</i>	dark+2%acetate	35%	[28]
	<i>Nostoc muscorum</i>	phosphate-limitation dark+ glucose,acetate	46%	[29]
	<i>Nostoc muscorum</i>	+11% acetate, 0.08% propionate, pH 8.1	31.4%	[30]
	<i>Nostoc muscorum</i>	phosphate-limitation +aeration,CO ₂	21.5%	[31]
	<i>Nostoc muscorum</i> NCCU-442	phosphate-limitation 7.5 pH, 30°C, 10:14 h light:dark periods +0.4% glucose, 1 g/L NaCl	26.37%	[32]
	<i>Oscillatoria limosa</i>	+acetate	6%	[33]
	<i>Spirulina maxima</i>	+acetate	3.1%	[34]
	<i>Spirulina platensis</i>	phosphate-limitation	3.5%	[14]
	<i>Spirulina platensis</i>	+acetate	2.9%	[35]
	<i>Spirulina subsalsa</i>	nitrogen-limitation + 5% NaCl	7.45%	[14]
	<i>Synechococcus elongates</i>	nitrogen-limitation + 1% sucrose	17.15%	[14]
	<i>Synechococcus</i> sp. MA19	nitrogen-limitation	27%	[36]
	<i>Synechococcus</i> sp. MA19	phosphate-limitation	55%	[37]
	<i>Synechocystis</i> sp. PCC6714	nitrogen,phosphate- limitation	16.4%	[38]
	<i>Synechocystis</i> sp. PCC6803	phosphate-limitation + fructose, acetate	38%	[14]
	<i>Synechocystis</i> sp. PCC6803	phosphate-limitation + glucose,acetate	29%	[39]

Photoautotrophic PHB accumulation by Cyanobacteria is considerably less expensive when compared to bacteria due to these organisms require water, minerals, CO₂, and light with no needed to carbon source [40]. But usage of plants

is a kind of a waste of agricultural crops which were required for the food industry, contrary to Cyanobacteria where can grow even at the deserts in bioreactors.

1.2 Objective of the Thesis

Plastics are essential for our life, but their pollution also has significant importance. Bioplastics lead an essential solution for the plastic problem. Starting from this point of view, we have planned to produce renewable, biologically suitable, biodegradable, non-toxic, and environmentally friendly bioplastics by isolation of Cyanobacteria species from Turkey's inland waters. With this aim Cyanobacteria species isolated from paddy rice fields and enriched with Cyanobacterial species from IMU Culture Library. Studies based on selecting the best bioplastic raw material (PHB) producing species and also the best extraction and analysis methods. In addition, species were investigated for their valuable by-products such as tri acyl glycerol (biodiesel raw material), carbohydrate, carotenoid, phycobiliprotein, protein, and vitamin.

1.3 Hypothesis

Exploring and applications of Cyanobacteria species for production PHB may lead a practical solution for plastic problems, and also usage of Cyanobacteria would be a good alternative to expenses for no needed to carbon sources and agricultural fields. Furthermore, identified species can be used for biodiesel (tri acyl glycerol), pharmacology, and agriculture industry.

2.1 History

The first plastic usage has been reported in prehistoric Mesoamerica, where Mayans used it to get rubber ball, human figurines, rubber bands to form axes, and liquid rubber for medicines and painting by obtaining the latex from *Castilla elastica* tree [41].

In 1839, vulcanized rubber, and polystyrene (PS) discovered [42]. Developments on polymers such as polyvinyl chloride (PVC) continued through the 19th century (Fig. 2.1) [42]. But the first truly synthetic polymer named Bakelite was developed in 1907 [1]. Whinfield and Dickson discovered the PET in 1941, and in the 1950s, they produced the first polyester film, and in the following 1970s they generated the first polyester bottle resin [42].

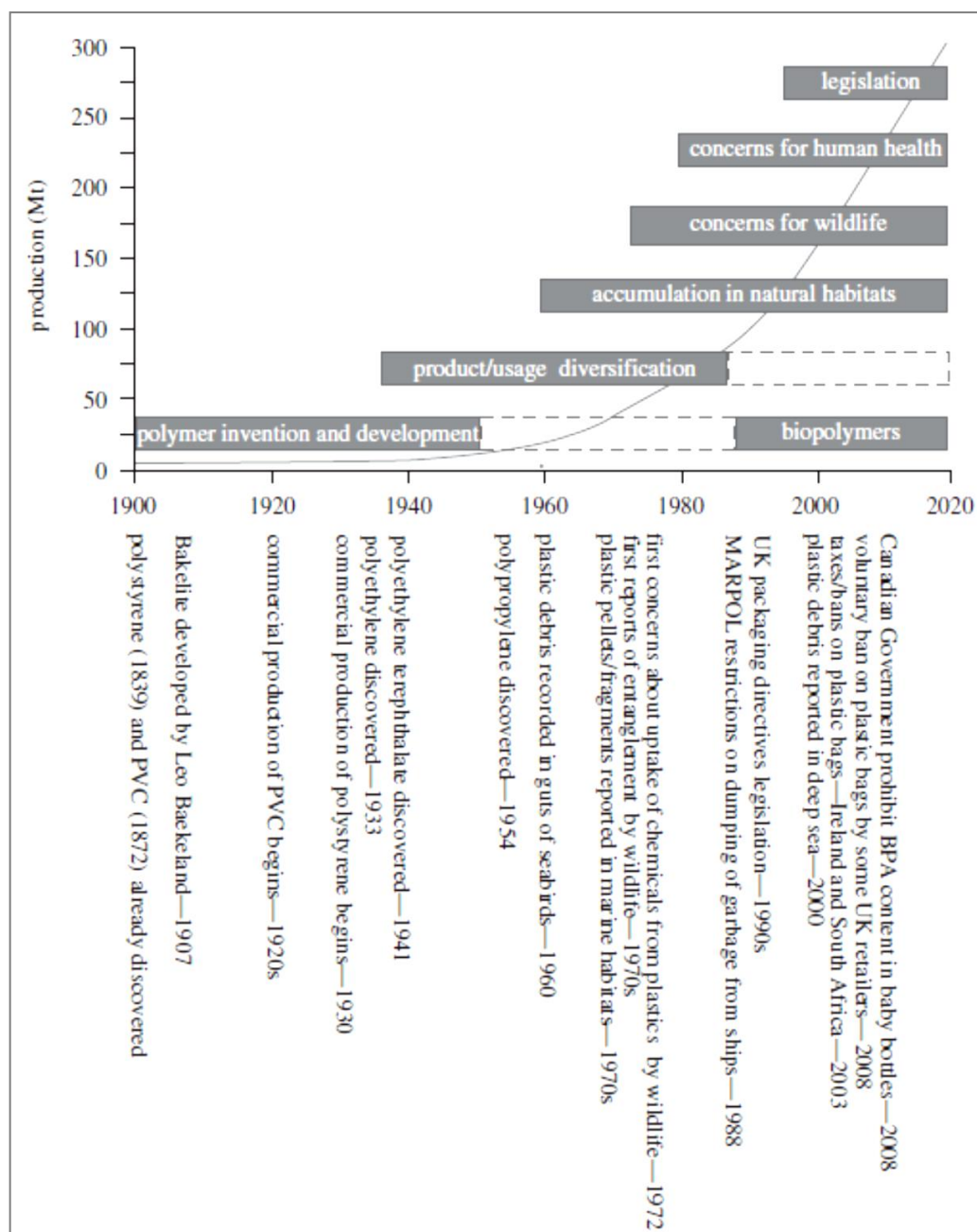


Figure 2.1 Summary illustrating historical stages in the development, production, and use of plastics *Mt: millions, BPA, bisphenol A; PVC, polyvinyl chloride

2.2 Polymerization of Plastics

The polymerization process is made up of polymer synthesis by chemically bonded smaller molecules, which are called repeating units [8]. Various polymerization reactions are classified based on reaction mechanisms such as addition, ring-opening, condensation, and other mechanisms. Plastic polymers are having different molecular structures (Fig. 2.2) by using different starting materials and polymerization processes and techniques [43].

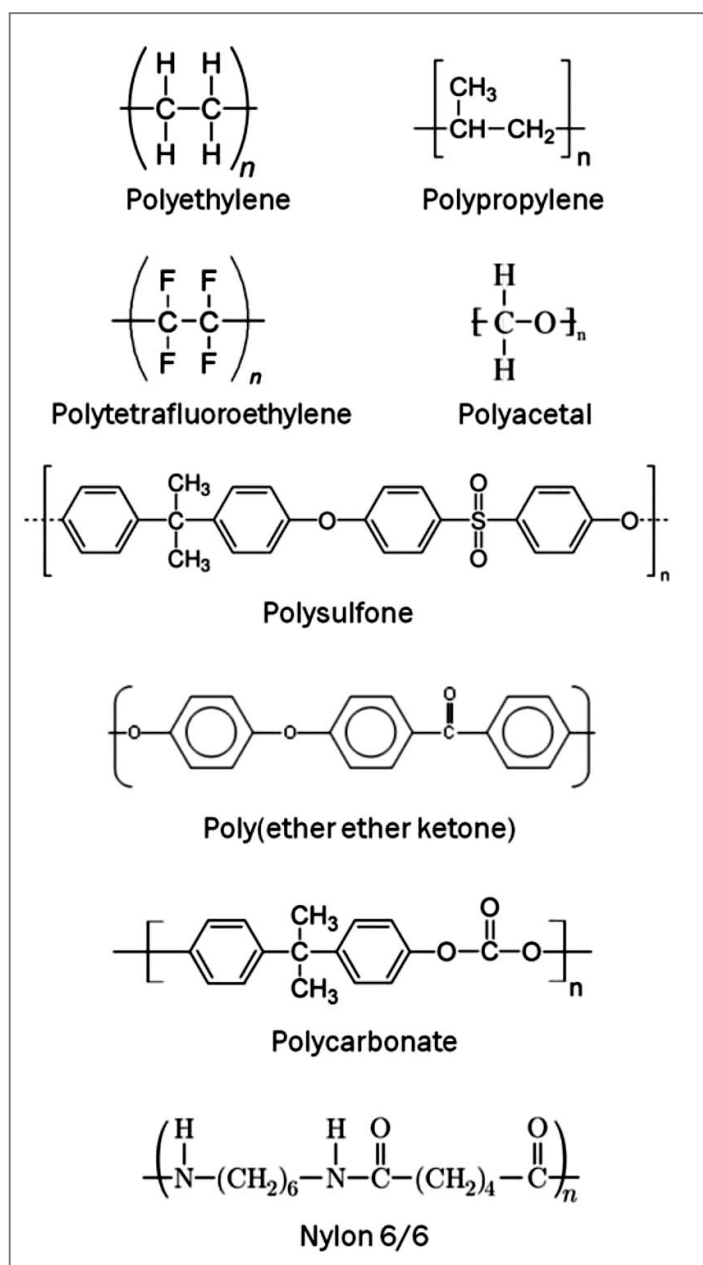


Figure 2.2 Some plastic polymers

2.2.1 Addition Polymerization

Addition (chain) polymerization is the formation through an exothermic reaction of polymers from carbon-carbon double-bonded monomers (Fig. 2.3), which makes them are generally chemically inert [43]. Conventional plastics produced through addition polymerizations such as polyethylene, polystyrene, polyvinyl chloride, and polypropylene.

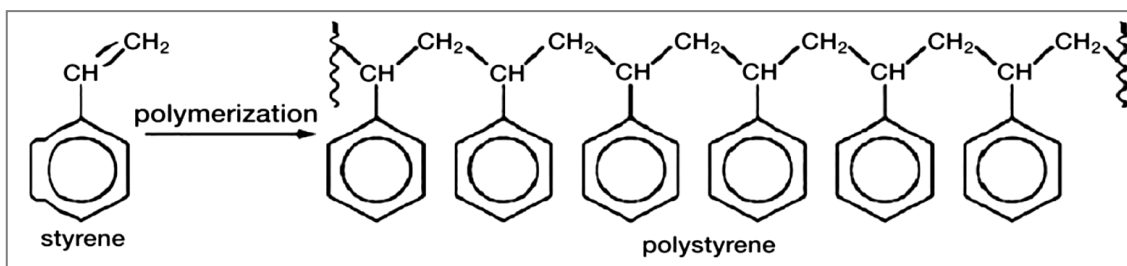


Figure 2.3 Polystyrene's addition polymerization mechanism from styrene monomer

2.2.2 Condensation Polymerization

Condensation (step-growth) polymerization is an endothermic reaction, and polymers are formed by a stepwise response of molecules with different functional groups and produce water, or other small molecules such as methanol, which makes them susceptible to hydrolytic molecular degradation at high temperatures (Fig. 2.4) [43]. Common examples include thermoplastic polyesters, polyamides, and polycarbonate in which form high-molecular-weight chains.

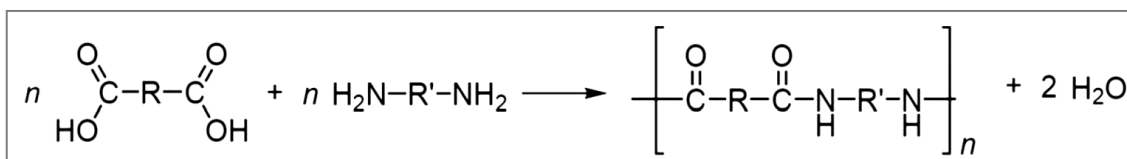


Figure 2.4 Polyamide's condensation mechanism from a diacid and a diamine

2.2.3 Ring-Opening Polymerization (ROP)

Ring-opening polymerization utilizes cyclic monomers (Fig. 2.5) and yields high molecular weight in a shorter time, which makes it a superior method for a specific application such as adhesives, coatings, composites, elastomers, and fibers [8]. Common examples are polypropylene oxide, polyoxymethylene, polycaprolactone, polytetramethylene oxide, and polydimethylsiloxane.

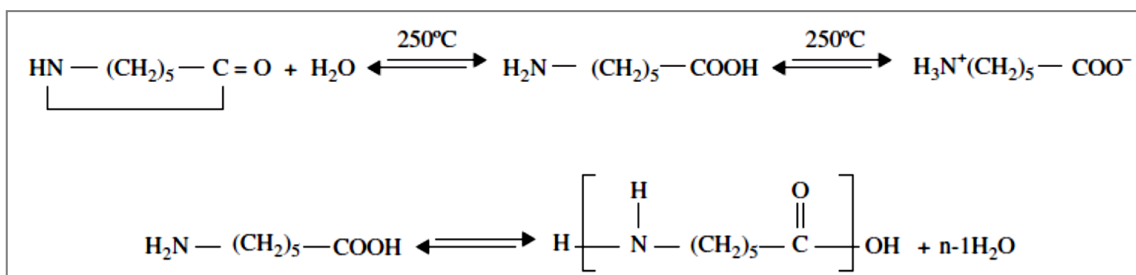


Figure 2.5 Hydrolytic ring-opening polymerization of caprolactam to produce nylon 6

2.2.4 Other Polymerization Mechanisms

Plasma and chain transfer polymerization are some of the other polymerization mechanisms. In chain transfer, the growing chain's active center is transferred to another molecule, and in plasma polymerization, the polymer, which is highly branched and cross-linked to surfaces, is produced by using the partially ionized gas (plasma) [8].

2.3 Molecular Structure

The chain structures of polymers could be as linear (polyethylene, PVC, polystyrene, and polyamides), branched (low-density polyethylene (LDPE)), and cross-linked polymer (epoxies, rubber) as can be seen in Figure 2.6 [8].

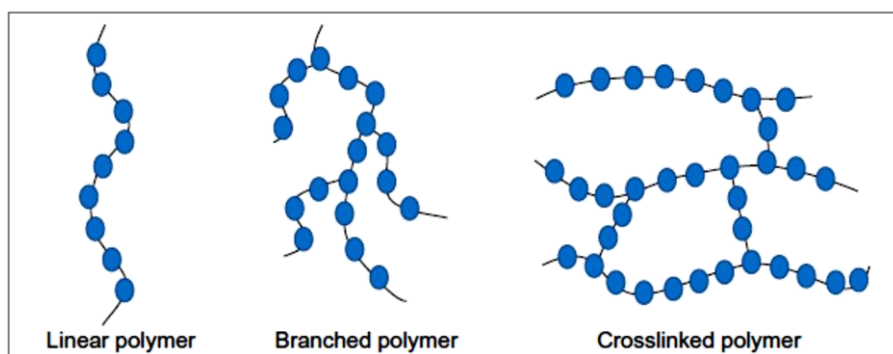


Figure 2.6 Schematic representation of linear, branched, and crosslinked polymers

The individual chains are not bonded covalently, alternatively on intermolecular forces, such as Van der Waals forces, hydrogen bonding, and dipole-dipole interactions, to keep the strings from disentangling [43].

2.3.1 Organization of Molecular Structure

The plastics can be a semicrystalline or amorphous form (Fig. 2.7).

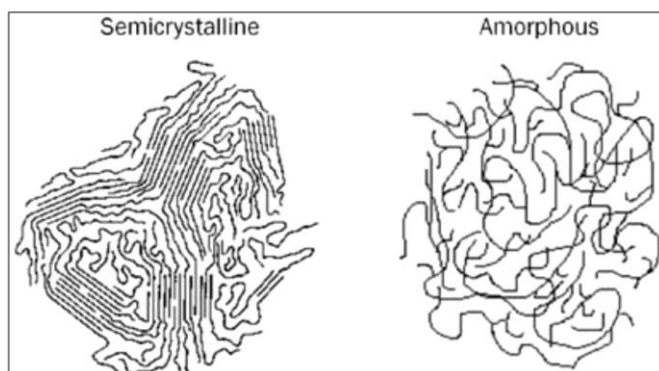


Figure 2.7 Structural representation of semicrystalline and amorphous polymers

Amorphous molecules are arranged randomly, whereas crystalline molecules are arranged in close order, and between these molecules, semicrystalline materials have crystalline regions (crystallites), in an amorphous matrix (Fig. 2.8) [44].

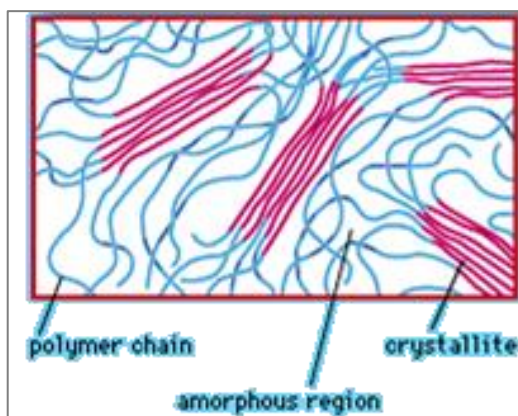


Figure 2.8 Schematic diagram of the semicrystalline morphology, showing amorphous regions and crystallites [44]

Semicrystalline polymers, including polyacetal, polyethylene, and nylon, are opaque or translucent and has distinct melting point, higher tensile strength and modulus, better organo-chemical resistance, higher density and mold shrinkage, better creep and fatigue resistance while, amorphous polymers such as polycarbonate, polystyrene, and polyphenylsulfone, are transparent and has lower organo-chemical resistance and density, softened over a wider range of temperature, higher flexibility and better toughness [43].

Semicrystalline polymers undergo a distinct melting transition and have a melting point (T_m) instead of amorphous polymers. Because when a sufficient temperature is reached in semicrystalline polymers, the crystallinity results in melting, but when amorphous polymers are heated above their glass transition temperature (T_g), they do not truly melt but only soften (Fig. 2.9) [43].

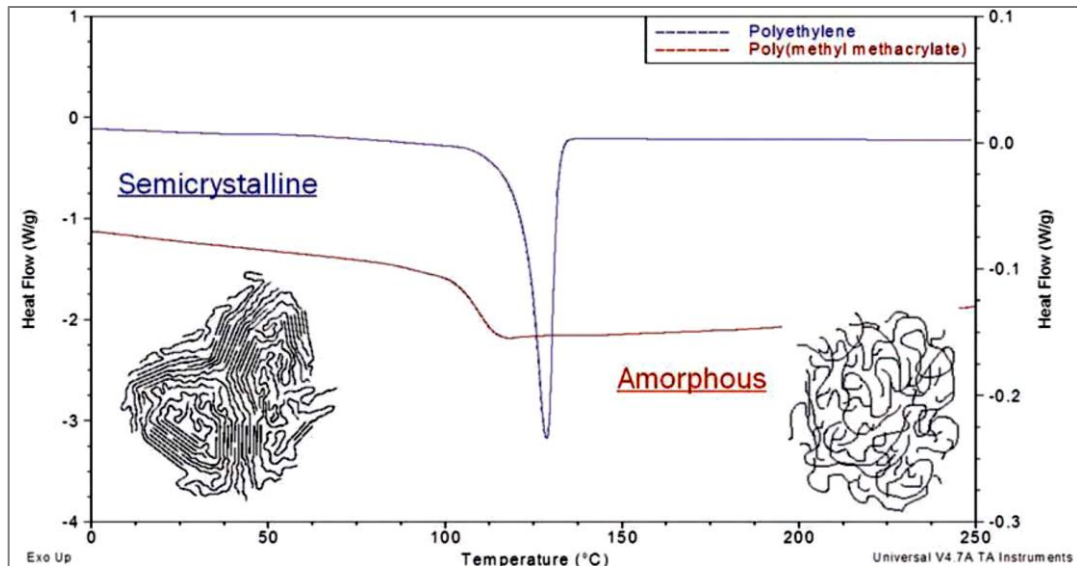


Figure 2.9 DSC thermogram of melting endotherm for a semicrystalline polymer and a glass transition for an amorphous material

2.3.2 Thermoplastic and Thermosetting

Plastics can also be classified into thermoplastics and thermosets by their thermodynamic and molecular structures (Table 2.1) [44].

Thermoplastics may have low or extremely high molecular weight and can be molded repeatedly due to their structure may be amorphous or semicrystalline, while thermosets are amorphous cannot be reheated or remolded [44].

Table 2.1 Properties and applications of commercially important plastics

Polymer Family and Type	Typical Products and Applications
Thermoplastics	
Carbon-chain	
High-density polyethylene (HDPE)	milk bottles, cable, and wire insulation, toys

Low-density polyethylene (LDPE)	packaging film, agricultural mulch, grocery bags
Polypropylene (PP)	bottles, toys, food containers
Polystyrene (PS)	foamed food containers, eating utensils
Acrylonitrile butadiene styrene (ABS)	appliance housings, pipe fittings, helmets
Polyvinyl chloride (PVC) (unplasticized)	pipe, window frames, conduit, home siding
Polymethyl methacrylate (PMMA)	impact-resistant windows, canopies, skylights
Polytetrafluoroethylene (PTFE)	nonstick cookware, self-lubricated bearings
Heterochain	
Polyethylene terephthalate (PET)	recording tape, transparent bottles
Polycarbonate (PC)	compact discs, sporting goods, safety glasses
Polyacetal	bearings, showerheads, gears, zippers
Polyetheretherketone (PEEK)	machine, aerospace, and automotive parts
Polyphenylene sulfide (PPS)	machine parts, electrical equipment, appliances
Cellulose diacetate	photographic film
Polycaprolactam (nylon 6)	bearings, gears, pulleys
Thermosets	
Heterochain	
Polyester (unsaturated)	automobile panels, boat hulls
Epoxies	laminated circuit boards, aircraft parts, flooring
Phenol formaldehyde	electrical connectors, appliance handles
Urea, and melamine formaldehyde	Dinnerware, countertops

Polyurethane	rigid and flexible foams for upholstery, insulation
--------------	---

*Rearranged from Encyclopædia Britannica

2.3.3 Additives of Plastics

Plastics are generally combined with additives such as plasticizers, colorants, reinforcements, and stabilizers to maximize performance [42]. Plasticizers are used to change the odor, biodegradability, flammability, and cost of the product and especially the Tg of the plastic [44]. Various inorganic oxides are used as colorants to give colors to the plastics, while reinforcements (silica, talc, carbon black, mica, etc.) are used to enhance the mechanical properties of plastic and stabilizers are added to get rid of the effects of aging of plastic [44]. In these groups, the most concerning types of additives are phthalates (PAEs), bisphenol A (BPA), and polybrominated diphenyl ethers (PBDE) due to their extensive interaction on the human body, especially on babies and children by food and drink packages and toys [1].

On the European Union (EU) framework report 2018 it has mentioned that the both European Food Safety Authority (EFSA) European Chemicals Agency (ECHA) and agree that there is evidence that BPA has endocrine-disrupting properties, but also EFSA stated that BPA has no health risk for consumers of any age group [45].

Studies showed that children and infants are the most sensitive and the females also more sensitive than the males to PAEs which tend to migrate into foods by the time and the temperature and promote the risk of mutagenesis, teratogenesis, and carcinogenic effect since they are not bound to the plastic matrix chemically [46]. Moreover, the supporting study has declared that diethylhexyl phthalate has been detected in natural mineral water packages and food samples [46].

2.4 Recycling Process

The conventional method for disposing of solid waste is embedding in the soil of landfills, but with the awarning of the worldwide effect of plastic pollution, recycling processes importance improving day by day. Most of the recycling efforts on the collection have focused on separated containers and deposit systems, after

sorting process followed by chopping and grinding, then dried the washed chips molds or extruded directly into fibers [44].

Generally, thermoplastics can be recycled more effectively than thermosets [44]. The other limitations of recycling of plastics are differences in molecular weight, contamination by non-plastics and additives or by different polymers in the making up process which makes the mixed material will not be suitable for the following operations [44].

Commonly recycled plastics such as PVC, PP, ABS, and PS have the potential for transformation into children's toys and food containers (generally PS); also, their different levels of halogenated flame retardant (HFR) residues may occur health risks especially for children [47].

2.4.1 Degradation of Plastics

Photo, thermal or biological degradation of plastics (Table 2.2) have been characterized in changes of material properties (optical, mechanical or electrical characteristics, in crazing, erosion, cracking, discoloration, phase delamination or separation) by chemical transformation, the formation of functional groups, and bond scission [6].

Table 2.2 Polymer degradation routes

<i>Factors (requirement/ activity)</i>	Photo- degradation	Thermo- oxidative degradation	Biodegradation
<i>Active agent</i>	UV-light or high-energy radiation	Heat and oxygen	Microbial agents
<i>Requirement of heat</i>	Not required	Higher than the ambient temperature required	Not required
<i>Rate of degradation</i>	Initiation is slow. But propagation is fast	Fast	Moderate
<i>Other consideration</i>	Environment-friendly if high-energy radiation is not used	Environmentally not acceptable	Environment-friendly
<i>Overall acceptance</i>	Acceptable but costly	Not acceptable	Cheap and very much acceptable

Producing environmentally friendly bioplastics from the start would have overcome collecting, health, and limited substrate problems, both without spending money on the recycling process.

Biodegradable Plastics and Bioplastics

3.1 Biodegradable Plastics

Biodegradable plastics are degradable plastics produced by petroleum-based polymerization and not able to show all the properties of plastic [40].

3.1.1 Starch-based Biodegradable Plastics

Starch-linked plastics are made up of starch and plastic polymer (starch-polyethylene), and while their starch can degrade by soil microorganisms, the polymer fragments remain due to their non-biodegradable structure [40]. Herewith starch-based plastics are not truly acceptable for being biodegradable.

3.1.2 Polycaprolactone (PCL)

Polycaprolactone is a biodegradable, partially-crystalline synthetic polyester (Fig. 3.1) with a low melting point at 60°C, and is degraded by the action of many microorganisms such as *Penicillium sp.* strain 26-1, *Aspergillus sp.* strain ST-01 [48].

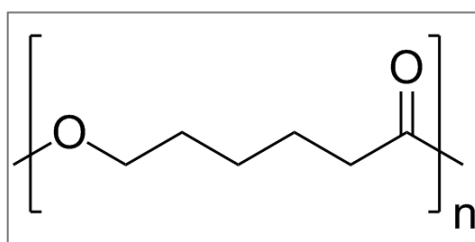


Figure 3.1 Molecular structure of polycaprolactone

PCL can be degraded by lipase and esterase enzymes, and the degradation rate is dependent on the degree of crystallinity and molecular weight [48]. The chemical structure of a PCL and two cutin monomers are similar, which may lead to cutinase activity act as a PCL depolymerase [49].

3.1.3 Polyethylene Succinate (PES)

Polyethylene succinate (Fig. 3.2) is an aliphatic synthetic polyester that is synthesized from dicarboxylic acids and glycols with high melting points, can be biodegraded by *Amycolatopsis sp.* HT-6 [48].

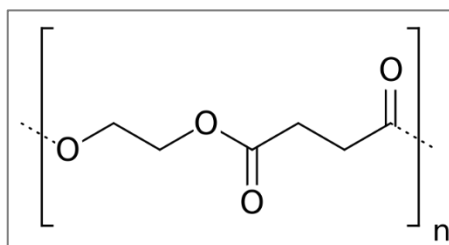


Figure 3.2 Molecular structure of polyethylene succinate

3.1.4 Polyvinyl Alcohol (PVA)

Polyvinyl alcohol (PVA) (Fig. 3.4) is a water-soluble thermoplastic vinyl polymer which can be mineralized by microorganisms of genus *Pseudomonas* [49]. In a symbiotic relationship, *Pseudomonas putida* VM15A releases the growth factor pyrroloquinoline quinone (PQQ), which enables the growth of *Pseudomonas sp.* VM15C on PVA (Fig. 3.3) [49].

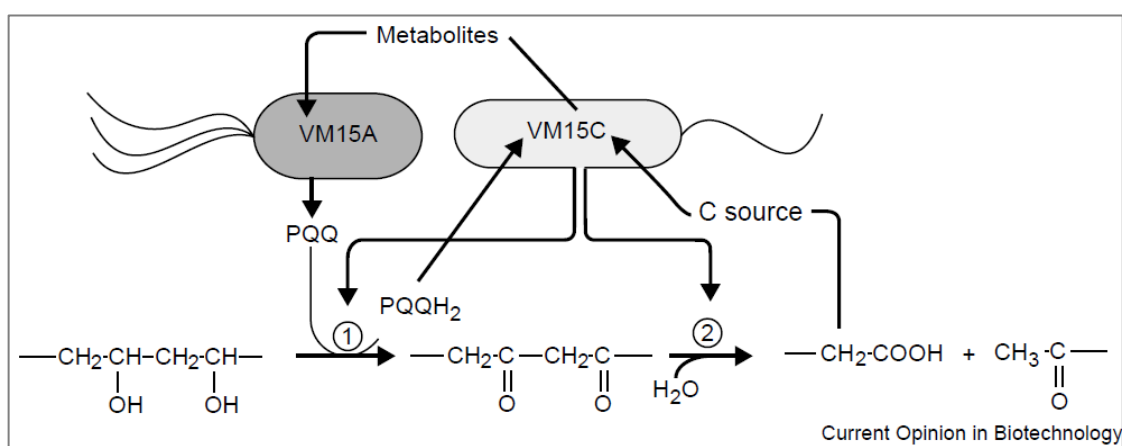


Figure 3.3 PVA utilization by symbiotic bacteria

*1:PQQ-dependent PVA dehydrogenase; 2:oxidized PVA hydrolase

PVA degradation starts with dehydrogenase or oxidase reaction, then it's followed by hydrolase or aldolase reaction as can be investigated in Figure 3.4 [49]:

dehydrogenase (DCDDH), and PCA 3,4-dioxygenase (Pca34) to form protocatechuic acid (PCA) [52].

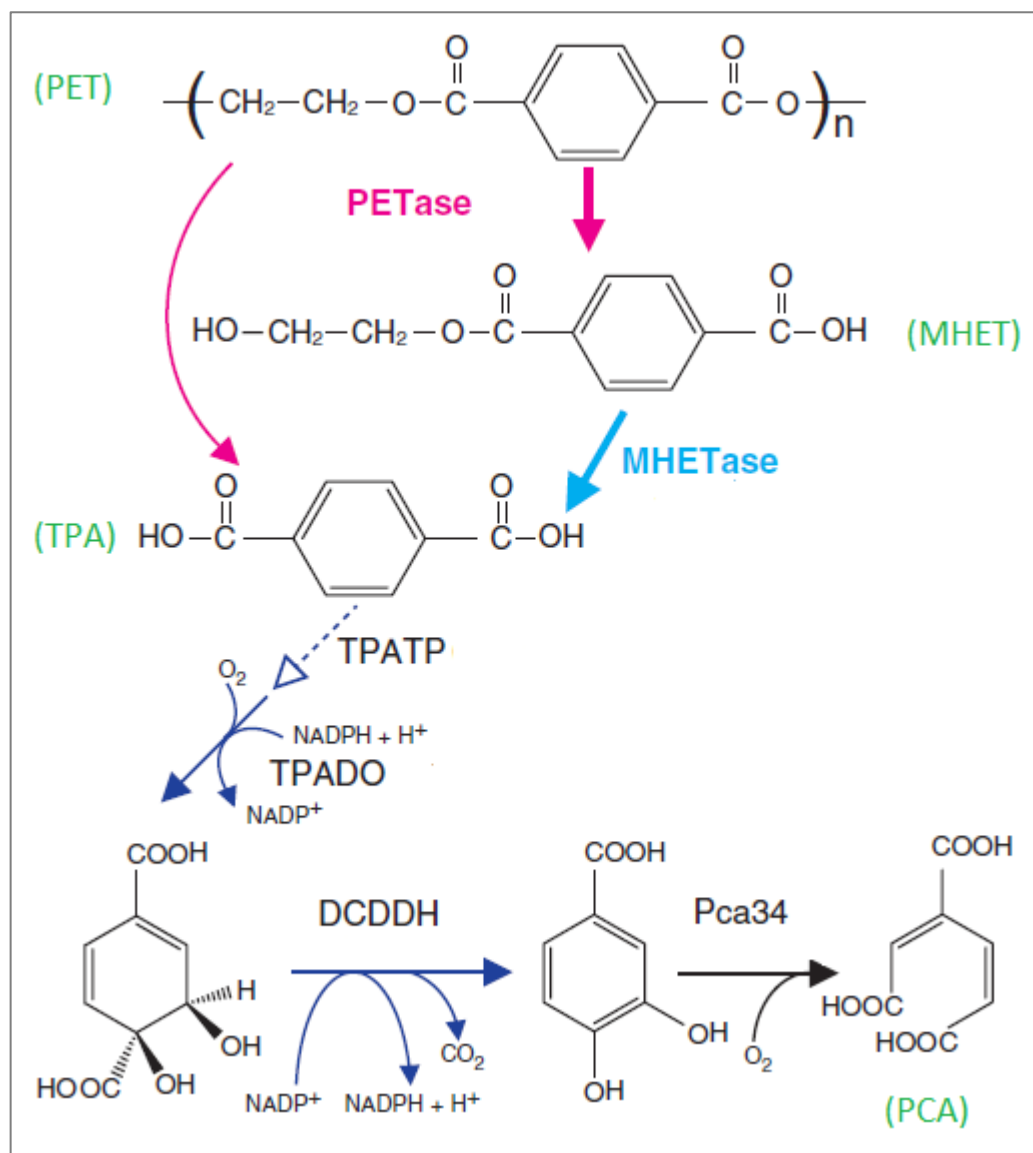


Figure 3.5 PET metabolism by *Ideonella sakaiensis*

Degradation of plastics is a better alternative to overcome the recycling process of plastics even if not recent studies showed that some biodegradable plastics had not been properly analyzed to clarify their degradation rates in the real marine environment [12].

3.2 Bioplastics

Bioplastics are synthesized from renewable resources or biomass, and they have the ability to recycle into useful metabolites by microorganisms and enzymes [40].

3.2.1 Bioplastics from Renewable Resources

Bioplastics that are produced from renewable resources are utilized chemically, and they are not entirely biodegradable [48]. This point of view, this group may not be seen as real bioplastic and can be addressed as “semi-bioplastics” due to not synthesized by living organisms and also being an evolutionary step between biodegradable plastics and bio-based plastics.

3.2.1.1 Nylon, Polyethylene (PE), and Acetyl Cellulose (AcC)

Nylon-6 can be degraded to soluble oligomers by the enzyme systems, and polyethylene (PE) is degraded under nitrogen or carbon limited conditions by lignin-degrading fungi [49]. Even though Nylon 11 and PE can be synthesized from renewable resources, they are not totally biodegradable, while acetyl cellulose (AcC) can be biodegradable or non-biodegradable, depending on the acetylation degree [48].

3.2.1.2 Polylactic Acid (PLA)

PLA is a thermoplastic that can be synthesized by ring-opening polymerization of lactide or by condensation polymerization of lactic acid [48]. PLA exists in the three stereoisomer forms: PLLA and PDLA, and between both, a stereo complex can be formed. (Fig. 3.6) [53].

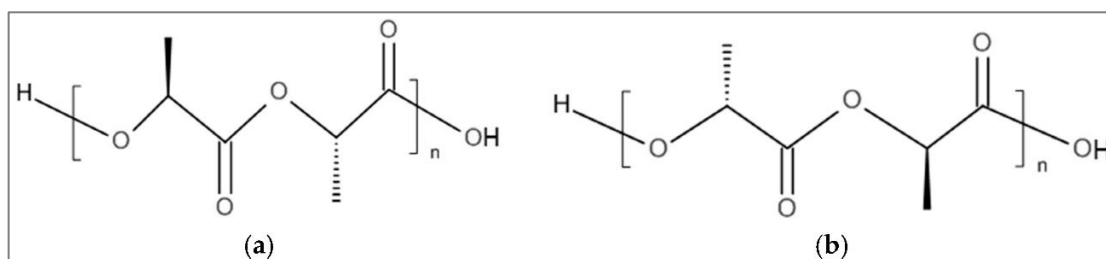


Figure 3.6 Chemical structure of (a) PLLA and (b) PDLA

Degradation of PLA in the environment takes a long time due to only a few PLA degrading microorganisms that have been isolated and identified, such as genus *Amycolatopsis* and *Saccharotrix* and also PLA-degrading microorganisms are not widely distributed [48]. Besides, the enzymes cannot reach inside, while

enzymatic degradation proceeds only on the polymers' surface, which made PLA need for the industrial composting process [53].

PLA's high modulus of elasticity, high transparency, high strength, and easy processing make it a suitable polymer for processing, on the other hand, its slow crystallization rate, low heat distortion temperature, and high brittleness can make it not affordable [53].

3.2.1.3 Polybutylene Succinate

Polybutylene succinate (PBS) can be synthesized from dicarboxylic acids and glycols as PES [48] but also can be synthesized from renewable resources, which are bio-based succinic acid and 1,4-butanediol [53] (Fig. 3.7).

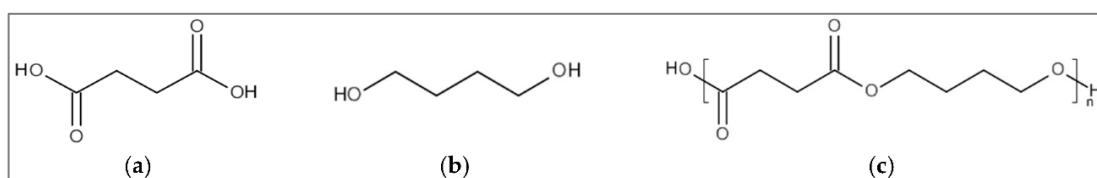


Figure 3.7 Chemical structure of (a) succinate acid, (b) 1,4-butanediol, and (c) polybutylene succinate (PBS)

PBS can be biodegraded by *Amycolatopsis sp.* HT-6 [48]. PBS also has desirable properties such as high flexibility and thermal stability in spite of its stiffness and melt viscosity [53].

3.2.2 Bio-based Bioplastics: Polyhydroxyalkanoates (PHAs)

Bio-based bioplastics, which are the family of polyhydroxyalkanoates (PHAs), are entirely utilized by organisms and 100% biodegradable polymers without forming any toxic byproducts [48].

3.2.2.1 Molecular Structure of PHAs

PHAs constitute a family of polyesters with carbon length ranging from C₃ to C₁₄ of different hydroxyl alkanoic acids (HAs), which based on a functional group (R) and consisting number of -CH₂ in the molecular structure, PHAs can be varied as defined in the following Figure 3.8 [40].

	$\left[\text{O} - \underset{\text{R}}{\text{CH}} - (\text{CH}_2)_x - \overset{\text{O}}{\parallel}{\text{C}} \right]_n$		
X=1	R= Hydrogen	Poly (3-hydroxypropionate)	P3HP
	R= Methyl	Poly (3-hydroxybutyrate)	PHB (P3HB)
	R= Ethyl	Poly (3-hydroxyvalerate)	PHV (P3HV)
X=2	R= Hydrogen	Poly (4-hydroxybutyrate)	P4HB
X=3	R= Hydrogen	Poly (5-hydroxyvalerate)	P5HV

Figure 3.8 Structure of polyhydroxyalkanoates

Among the 150 types of PHA monomers, poly (3- β -hydroxybutyrate) (PHB), which is also known as ketone body in mammal fat metabolism (Fig. 3.9), is the best-known characterized (Table 3.1) PHA [40].

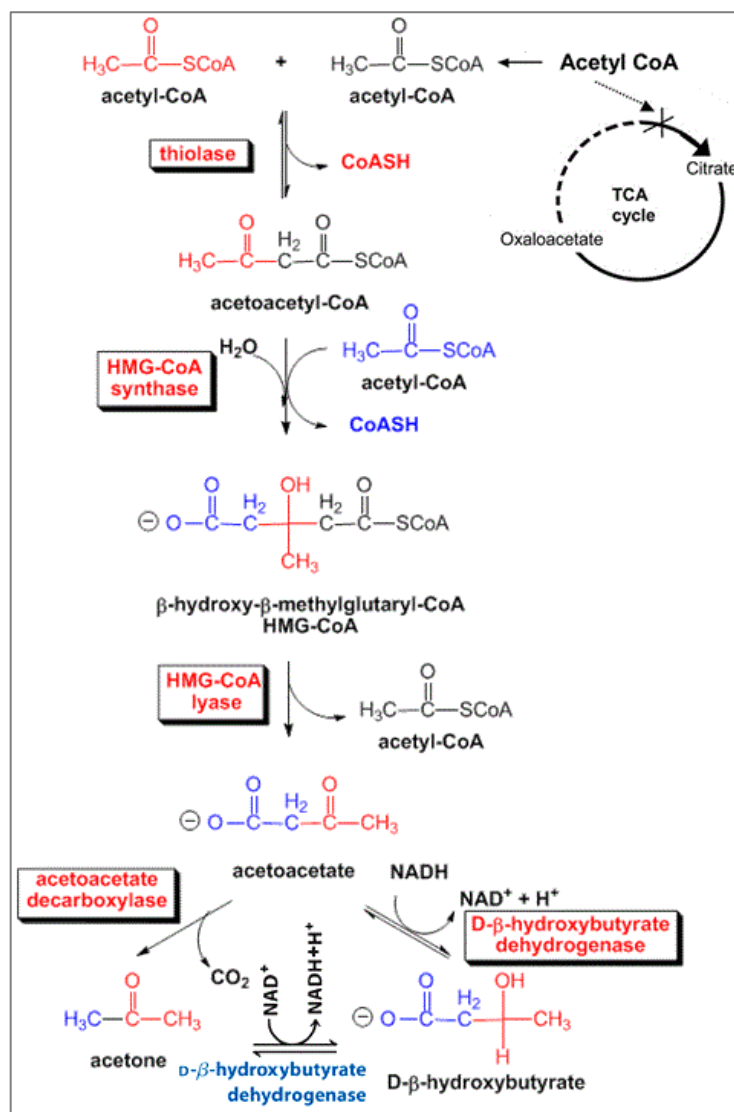


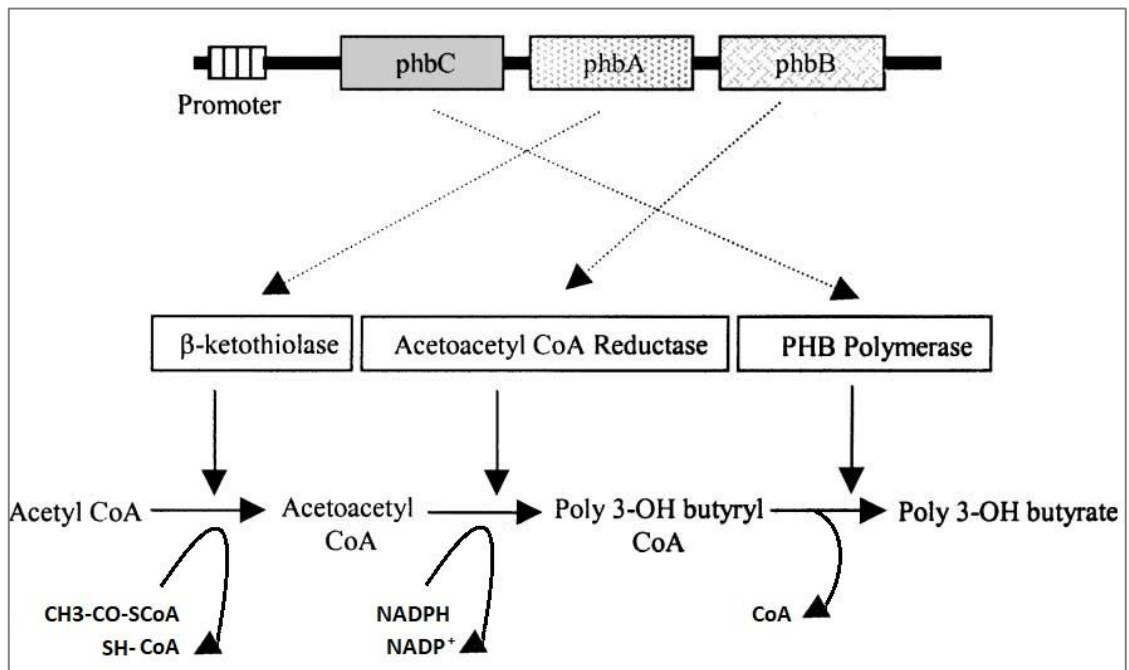
Figure 3.9 3- β -hydroxybutyrate pathway in ketogenesis [54]

Table 3.1 Polymer degradation routes

	Tm (°C)	Tg (°C)	Tensile strength (MPa)	Tensile modulus (MPa)	Absorption rate
P(4HB)	60	-51	50	70	8-52weeks
P(3HB)	180	1	36	2500	2 years

3.2.2.2 Synthesis Mechanism

PHB is synthesized in microorganisms by the action of β -ketoacyl-CoA thiolase (*phbA*), acetoacetyl-CoA reductase (*phbB*), and PHB polymerase (*phbC*) in three-steps, as shown in Figure 3.10 [20].

**Figure 3.10** Biosynthetic pathway of PHB

The imbalance of the C/N ratio and NADPH/ATP ratio have an effect on PHB accumulation in both chemolithotrophic bacteria and Cyanobacteria [55]. In *Synechococcus* sp. strain MA19, it was understood for the first time that under nitrogen-limited cultivation, which causes an imbalance in the C/N ratio, results in the production of PHB due to posttranslational control of acetyl phosphate on PHB synthase regulation (Fig. 3.11) [55]. In this model (Fig. 3.11), under the limitation of nitrogen, phosphotransacetylase promotes acetyl phosphate for indicating acetyl-CoA flux, which activates PHB synthase for PHB synthesis [55].

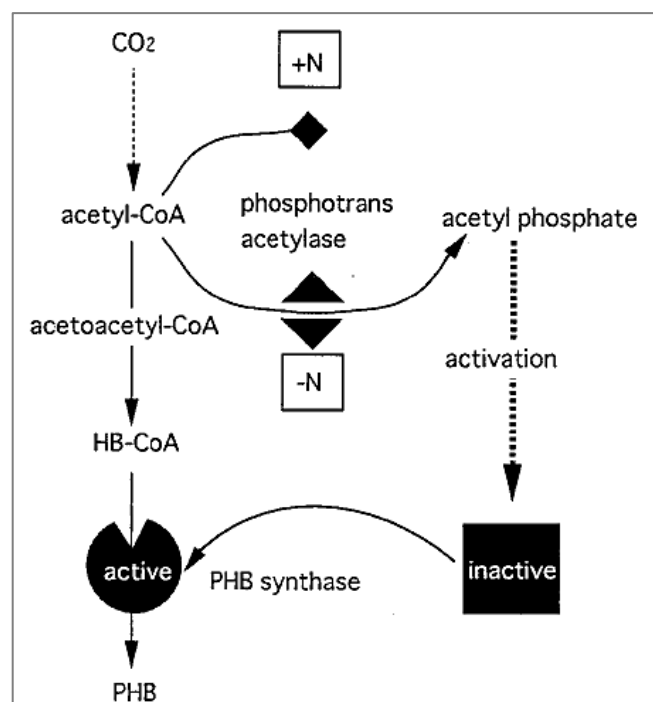


Figure 3.11 Model for the system of PHB synthesis control

3.2.2.3 Degradation

The PHA depolymerases are serine hydrolase enzymes which are responsible for the degradation of PHAs in microorganism [49]. The percentage of PHB-degrading microorganisms appraised to be 0.5-9.6% in the environment such as in soil (*Pseudomonas lemoigne*, *Aspergillus fumigatus*, *Acidovorax faecalis*, *Variovorax paradoxus*, and *Comamonas* sp.), anaerobic and activated sludge (*Pseudomonas* sp., *Illyobacter delafieldi*, *Alcaligenes faecalis*), lake water and seawater (*Pseudomonas stutzeri*, *Comamonas testosterone*) [48].

3.2.2.4 Advantages and Usages

PHAs have a high degree of polymerization, are highly crystalline, optically active, stereochemical regularity in repeating units, piezoelectric, and insoluble in water, which makes them competitive with polypropylene [20]. Also, PHAs composition can change their physical properties, with the presence of aromatic monomers, leading to new applications in biotechnological fields, medical, and pharmaceutical [56]. Items produced from PHAs such as meshes and fibers for sutures show promise for medical use, pellets and microspheres for drug delivery,

films for usage in post-surgery recovery and agricultural applications [15], are shown in the following Figure 3.12:



Figure 3.12 Examples of PHA matrices fabricated for medical use

PHAs are widely used for the fabrication of disposable items, such as razors, utensils, feminine hygiene products, diapers, cosmetic containers, shampoo bottles and cups [20], bottles, fibers, and several products of commercial and packaging interest, especially for their biodegradability and hydrophobicity specialties [40].

In the agriculture sector, PHAs are used to enhance nitrogen fixation in plants with the producing microorganisms and can be used as urea fertilizer coat to be used in rice fields or for herbicides and insecticides [57], yet Cyanobacteria are known to strengthen nitrogen ratio in rice fields as a biofertilizer [58], which can also produce PHB. One of the other specialized applications of P3HB and P3HV in agriculture is the controlled release of pesticides [57].

PHAs are potentially applicable to medical research such as surgical sutures, vein valves, and targeted drug delivery [18]. The biocompatibility property of PHB makes them be applied in the medical field, especially for their non-toxicity via 3-hydroxybutyric acid, which produced after the degradation of PHB, which is normal human blood constituent [56]. Besides, PHB or P(HB-co-HV) did not affect platelet responses when in contact with blood [15]. In response to the needs of

tissue engineering, PHAs can be used as tissue scaffold and absorbable polymer, in medical applications [40].

The other most notable feature of PHB except for being biocompatible in medical applications is their slow biodegradation rate [59], which means PHA implants and other medical devices on animals do not need the removing surgery [15] and also release and long term dosage control of bioactive compounds such as medicines, drugs, hormones, herbicides, and insecticides can be operated by biodegradable PHAs carriers [20].

Owing to the piezoelectric properties in surgical sutures, bone plates, and blood vessel replacements, PHAs are used as osteosynthetic materials for the stimulation of bone growth [20].

Also, PHAs are useful as being stereoregular, that can operate the chemical synthesis of optically active and enantiomerically pure compounds, as chiral precursors [20].

3.2.2.5 PHB-producing Microorganisms

PHB most commonly found in prokaryotes, including Cyanobacteria [21]. Polyhydroxybutyrate (PHB) first discovered in *Bacillus megaterium* in 1927. *Cupriavidus necator* (the synonyms are *Ralstonia eutropha*, *Hydrogenomonas eutropha*, *Alcaligenes eutrophus*, and *Wautersia eutropha*) which is the paradigm of microbial PHA biosynthesis [15] is the most frequently used and the most studied bacterium in industrial applications due to its ability to produce PHB from different carbon sources [56].

PHB producer microorganisms can be divided into two groups. First group microorganisms which are bacteria and Cyanobacteria can accumulate PHB especially in nutrient-limited stress conditions such as nitrogen and phosphorus [56], the second group producers are acquired by mutation (change in the nucleotide sequence of a short region of a genome) such as *Azotobacter vinelandii* or recombination (results in a restructuring of part of a genome) such as *Escherichia coli* [60].

Apart from bacteria and Cyanobacteria, transgenic plants have been started to produce PHB. First, PHB production in plants was reported in *Arabidopsis thaliana* (model plant) by a transformation from *Agrobacterium tumefaciens* then followed by *Cupriavidus necator* and then studies were carried on transgenic plant *Brassica napus* (canola) [40].

Photoautotrophic PHAs accumulation by Cyanobacteria and transgenic is considerably less expensive when compared to bacteria due to these organisms require water, minerals, CO₂, and light with no needed to carbon source [40]. But usage of plants is a kind of a waste of agricultural crops which were required for the food industry, contrary to Cyanobacteria where can grow even at the deserts in bioreactors.

4.1 Cyanobacteria and Taxonomy

Cyanobacteria are photosynthetic prokaryotes that are widespread in wetlands, rivers, lakes, springs, ponds, and streams, and they have a noteworthy role in the oxygen, nitrogen, and carbon kinetics of environments [61]. Also, rice fields are noted as a source for nitrogen-fixing Cyanobacteria [58]. The exact timing of the first Cyanobacteria like microbe appearance on the World was although not yet sure thought more than two billion years ago and played a significant role in the accumulation of oxygen for the early atmosphere [61].

Taxonomy of the Cyanobacteria is detailed in Figure 4.1 from empire to order base as follows:

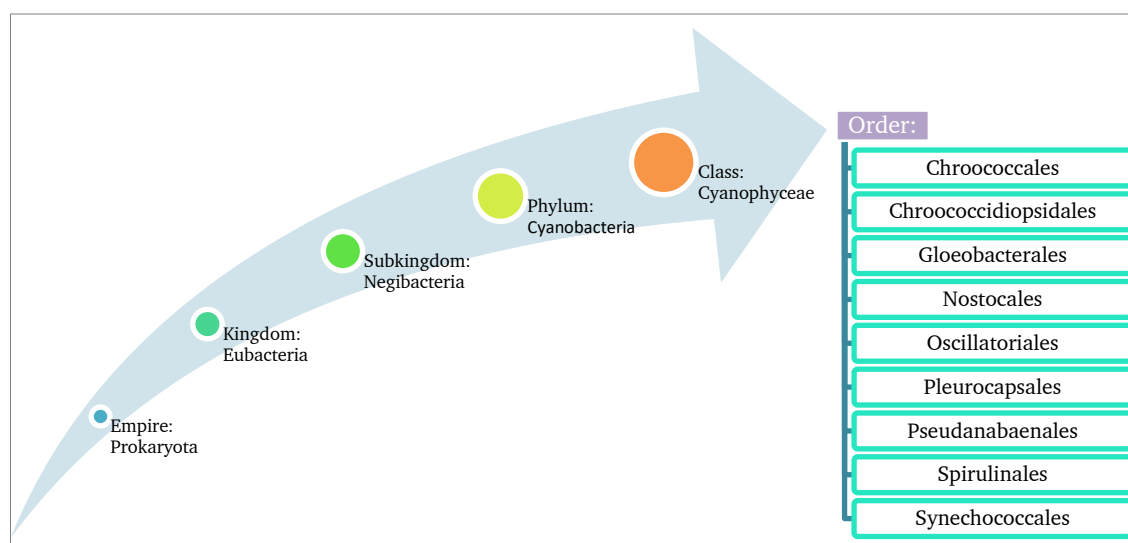


Figure 4.1 Taxonomy of Cyanobacteria

4.1.1 Class: Cyanophyceae

Cyano word is derived from the Greek language, which means blue and often referred to as blue-green algae, Cyanobacteria, or blue-green bacteria due to their prokaryotic form with no membrane-bounded organelles and their usually blue-

green (sometimes grey, blackish brownish, or purple but never bright green) color [62]. The blue-green color occurs from photosynthetic pigments such as phycocyanin (blue) and chlorophyll-a (green) (have no chlorophyll b) [62].

The photosynthetic apparatus contains two different reaction centers (RC I and II) (Fig. 4.2) [63]. Excitation of reaction centers can produce cyclic electron flow, which coupled to ATP synthesis, and the specific role of reaction center II is the photolysis of water [63]. Reaction centers I and II are interconnected through the electron transport chain, and when the centers are simultaneously excited, the electron transport produces ATP by oxidation of water with the reaction of NADP [63]. Reaction centers I and II and the electron transport system are placed into membranes, which are mostly thylakoid for Cyanobacteria species except for Gloeobacters within the cell membrane (Fig. 4.3) [63].

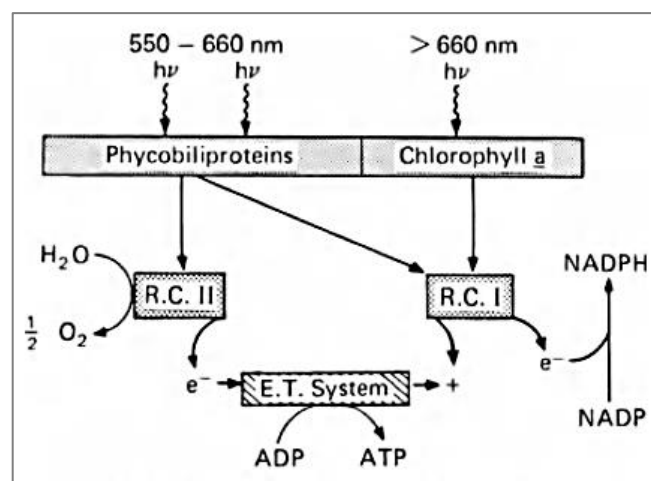


Figure 4.2 Cyanobacterial noncyclic electron flow of the photosynthetic apparatus

*R.C; reaction center, ET; electron transfer

Cyanobacteria	Pigment Antenna	Reaction Center & Electron Transfer System	Schematic Diagram
Gloeobacter	Subcortical layer	Cell membrane	
All others	Phycobilisome	Thylakoid membrane	

Figure 4.3 Comparative anatomy of the photosynthetic apparatus in Cyanobacteria

The Cyanobacterial cell is surrounded by trichome (formation of a row of cells), filament (sheath surrounds the trichome), cell wall (a serrated external layer and a layer of hair-like fibers composed from glycoprotein called oscillin), peptidoglycan layer (N-acetylmuramic acid, N-acetylglucosamine, and several different amino acids), cell membrane, periplasmic space (filled with peptidoglycan fibrils generally) and junctional pores to cross walls of neighbor cells (Fig. 4.4) [64].

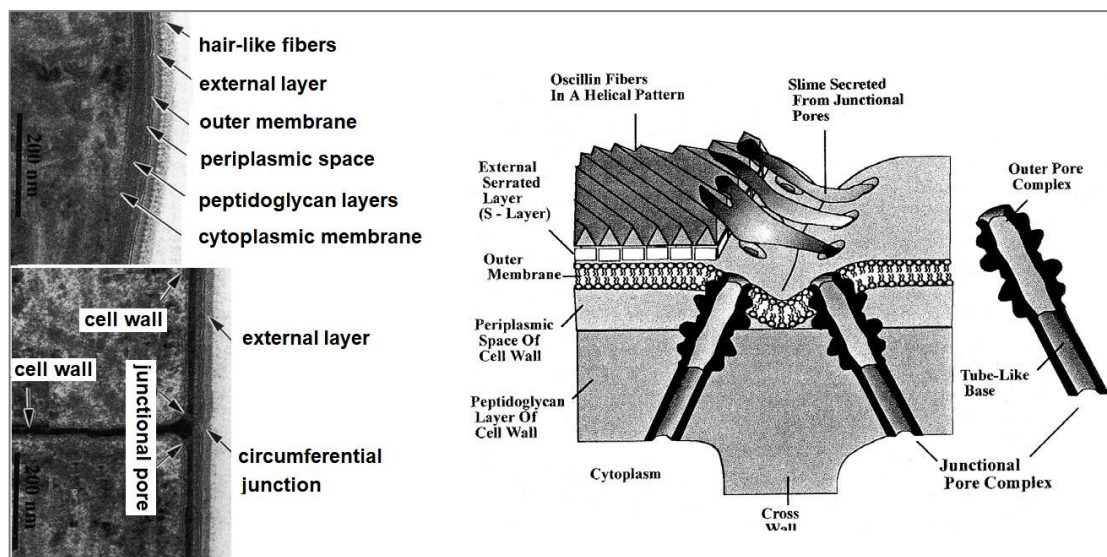


Figure 4.4 Anatomy of Cyanobacterial cell wall

Cyanobacterial cells can be single cells, colonial or filamentous with a characteristic thick cell wall that can be surrounded by mucous [62] and especially gas vacuole features that allow them to buoyancy in water (Fig. 4.5) [64].

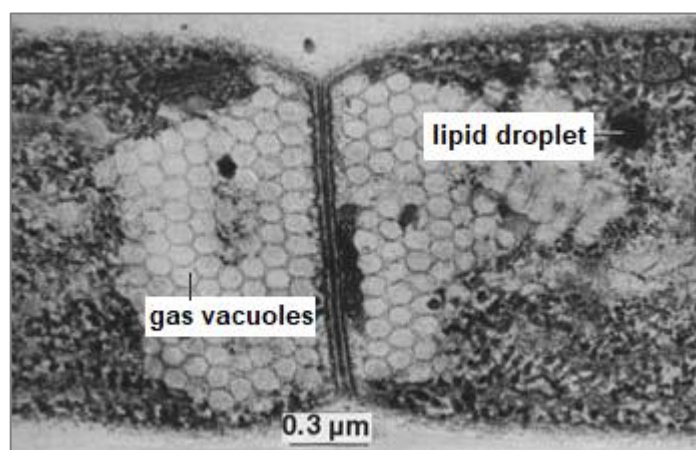


Figure 4.5 Cyanobacterial gas vacuoles (honeycombs) and lipid droplets (black dots)

Akinetes are generally larger sized vegetative cells with high concentrations of glycogen and cyanophycin (Fig. 4.6) and can be compared to endospores (Gram-positive bacteria) without being resistant to environmental extremes [64]. Also, Cyanobacteria species are noted as biodiesel source for their high lipid and TAG (tri acyl glycerol) contents [56], [65], [66].

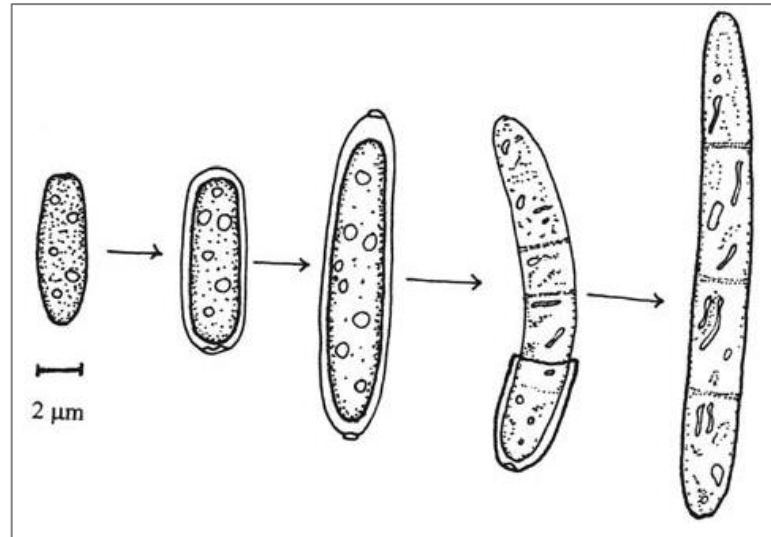


Figure 4.6 Germination of Cyanobacterium from akinete

Akinetes have full of storage products, whereas heterocysts appear empty and larger than vegetative cells in the light microscope (Fig. 4.7) [64].

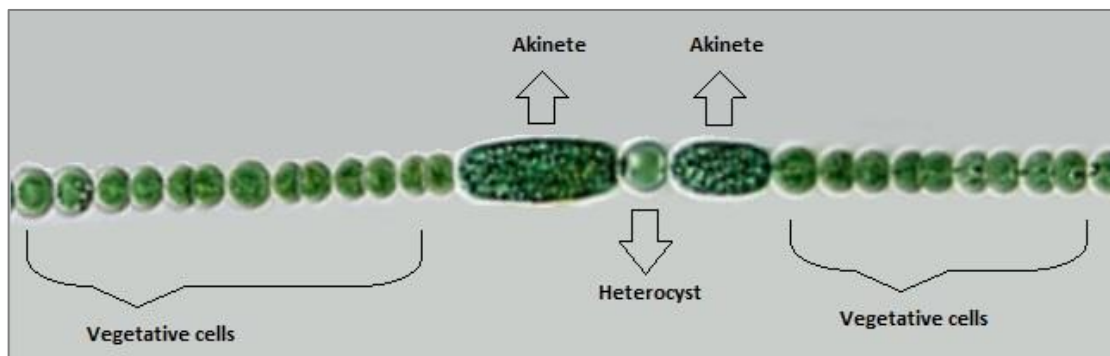


Figure 4.7 Akinete, heterocyst, and vegetative cells

Heterocysts are photosynthetically inactive, almost anoxic, which is ideal for O_2 sensitive nitrogenase enzyme, and serves nitrogen fixation under aerobic conditions [64]. Heterocysts formation and the diffusion of cellular components were summarized following Figure 4.8 [64]:

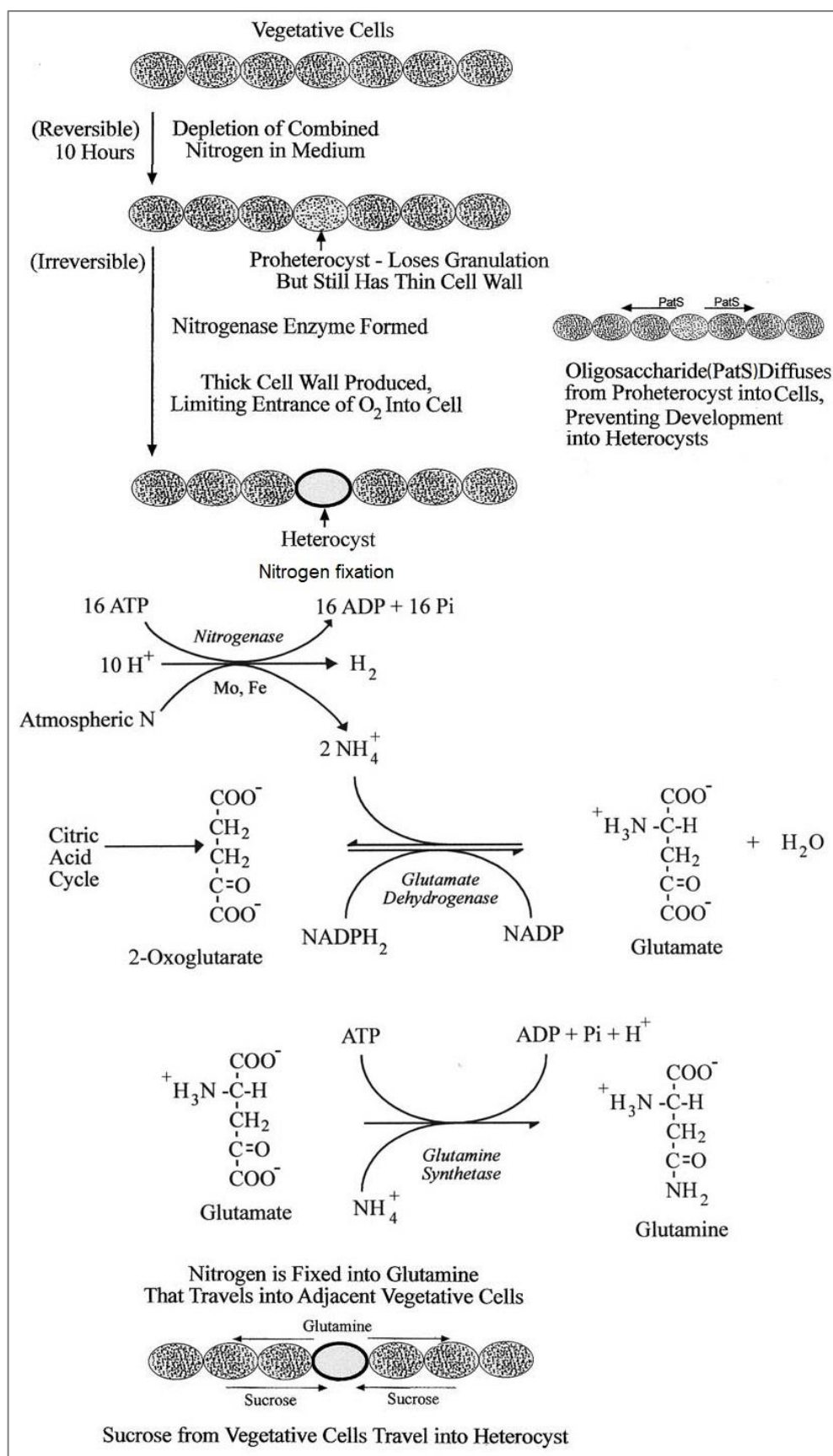


Figure 4.8 Formation of heterocysts, nitrogen fixation, and cellular accumulation

4.1.1.1 Taxonomy of Studied Cyanobacteria

Taxonomy of the studied Cyanobacteria are listed in following Figure 4.9:

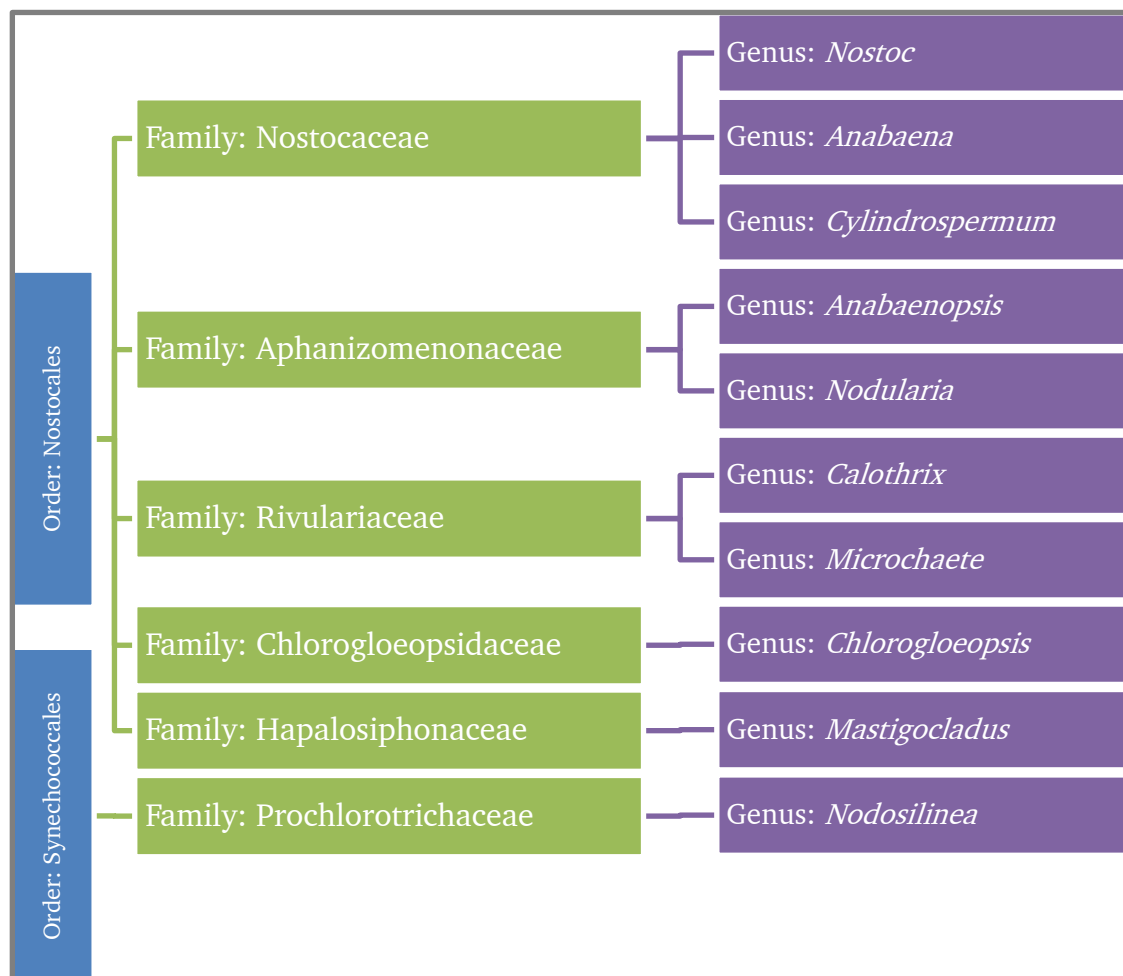


Figure 4.9 Taxonomy of the studied Cyanobacteria

4.1.1.1.1 *Nostoc*

Nostoc (Figure 4.10) has an individual vegetation cycle, and they can grow in freshwater and also in soil [67]. Long filamentous cells sometimes coiled due to mucilage sheath. Heterocytes generally placed terminal and repeats after vegetative cell groups likewise akinetes.

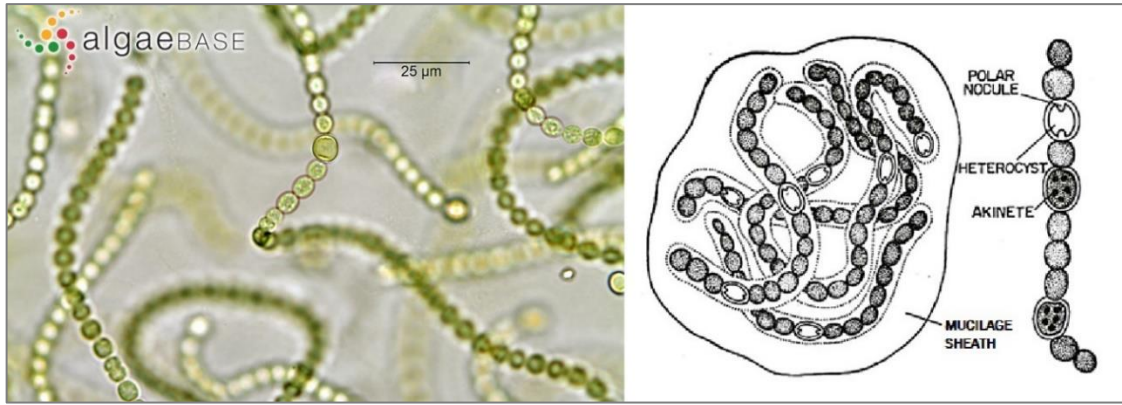


Figure 4.10 Microscope and diagram image of *Nostoc* sp.

4.1.1.1.2 *Anabaena*

Anabaena is formed straight, curved, or coiled unbranched filaments (trichomes) within 7-12 μm diameter [62]. Colorless cylindrical, spherical, or barrel-shaped cells are generally without mucilage sheaths, and trichomes are uniserial and metameric (3-9 heterocytes develop intercalary in certain distances one from another) [67] (Fig.4.11) [68].

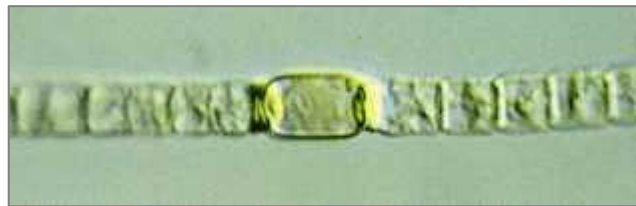


Figure 4.11 Microscope image of *Anabaena* sp.

4.1.1.1.3 *Cylindrospermopsis*

Cylindrospermopsis has a planktonic form that can be obtained from water such as diatoms, and during bloom, formation makes differ from other Cyanobacteria with has no surface scum [62]. Apart from *Anabaena*, cells are small (2-4 μm width, and 2-9 μm height), yellowish or pale blue-green, and the end cells often conical or sharply pointed [62]. The mucilaginous sheath is absent, and heterocysts (2-4 μm width, and 3-10 μm height) are elongated and always terminal [62]. Akinetes (3-5 μm width, and 7-16 μm height) are ellipsoidal and rounded at the ends and distant from apical heterocysts [62] (Fig.4.12) [68].



Figure 4.12 Microscope image of *Cylandrospermopsis* sp.

4.1.1.1.4 *Anabaenopsis*

Planktonic *Anabaenopsis* species prefer alkaline and saline or highly mineral waters such as paddy fields species [67]. Colorless cells generally tangled spiral metameric trichomes, Heterocytes, and akinetes spherical or oval and intercalary (Fig.4.13) [67].

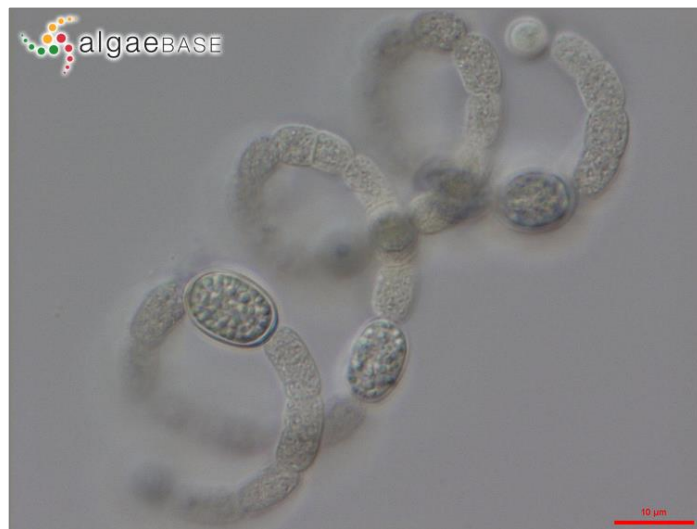


Figure 4.13 Microscope image of *Anabaenopsis* sp.

4.1.1.1.5 *Nodularia*

Nodularia cells are narrow barrel-shaped, isopolar, unbranched, curved, and covered with cell sheath, which is opened at both ends [67]. Metameric heterocytes and akinetes are irregular, and except for benthic species, only planktonic species have gas vesicles (Fig.4.14) [67].



Figure 4.14 Microscope image of *Nodularia* sp.

4.1.1.1.6 *Calothrix*

Calothrix cells have a worm-like form due to their heteropolar filamentous trichomes [67]. Filament starts with one hemispherical heterocyte and follows by big akinetes and gradually shrinking vegetative cells (Fig.4.15) [68].



Figure 4.15 Microscope image of *Calothrix* sp.

4.1.1.1.7 *Microchaete*

Microchaete cells are broad, barrel-shaped, isodiametric, and the apical cell is always rounded by sheath firm [67]. Heterocytes basal, hemispherical, spherical, and akinetes develop near the bases [67] (Fig.4.16).



Figure 4.16 Microscope image of *Microchaete* sp.

4.1.1.1.8 *Chlorogloeopsis*

Chlorogloeopsis cells are pale blue-green, rounded, and thallus forms are irregular-rounded trichomes with 3-20 cells, usually without particular mucilage sheath [67]. Irregular heterocytes are terminal and intercalary without akinetes [67] (Fig.4.17).



Figure 4.17 Microscope image of *Chlorogloeopsis* sp.

4.1.1.1.9 *Mastigocladus*

Mastigocladus cells are olive-green, irregularly coiled, composed of tangled filaments. Heterocytes are intercalary, and akinetes are very rare, which placed on the old cells [67] (Fig.4.18).

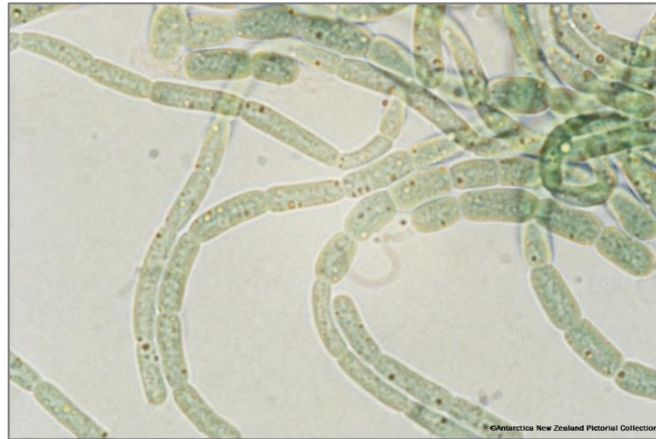


Figure 4.18 Microscope image of *Mastigocladus* sp.

4.1.1.1.10 *Nodosilinea*

Nodosilinea shows long, solitary, uniseriate trichomes within a thin sheath that forms spirals, with similar vegetative and apical cell shapes [69] (Fig.4.19).

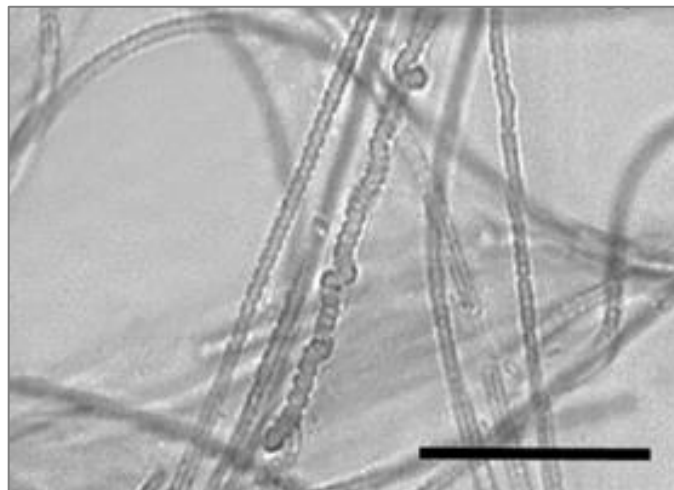


Figure 4.19 Microscope image of *Nodosilinea* sp.

5

Material and Methods

5.1 Materials

5.1.1 Chemicals

Chemicals and kits used in this thesis were listed in Table 5.1:

Table 5.1 Chemicals, solutions, and kits

CAS Number	Company	Product Code	Name
64-19-7	Sigma	27225-R	Acetic acid
67-64-1	Merck	1.000.202	Acetone
9002-18-0	Sigma	A1296	Agar
9012-36-6	Sigma	A9539	Agarose
7784-24-9	Sigma	1.01047	Aluminium potassium sulfate dodecahydrate
631-61-8	Acros Organics	218365000	Ammonium acetate
12125-02-9	Sigma	A943	Ammonium chloride
1185-57-5	Alfa Aesar	A11199	Ammonium iron (III) citrate
12054-85-2	Alfa Aesar	11831	Ammonium molybdate (para) tetrahydrate
6484-52-2	Merck	101187	Ammonium nitrate
7785-20-8	Sigma	574988	Ammonium nickel (II) sulfate hexahydrate
7783-20-2	Merck	101217	Ammonium sulfate
7727-54-0	Sigma	A3678	Ammonium persulphate

1245-13-2	Sigma	B9643-1L	Bicinchoninic acid solution
58-85-5	Sigma	B4501	Biotin
10043-35-3	VWR	33601-261	Boric acid
10035-04-8	Biofroxx	1186KG001	Calcium chloride dihydrate
13477-34-4	VWR	22388292	Calcium nitrate tetrahydrate
10022-68-1	Sigma	642045	Cadmium nitrate tetrahydrate
67-66-3	VWR	22.711.324	Chloroform
7789-02-8	Sigma	379972	Chromium (III) nitrate nonahydrate
77-92-9	Alfa Aesar	36664	Citric acid anhydrous
68-19-9	Alfa Aesar	A14894	Cobalamin (Vitamin B ₁₂)
7791-13-1	VWR	CC0349	Cobalt (II) chloride hexahydrate
7758-99-8	Labochem international	LC-4502.3	Copper (II) sulphate pentahydrate
7758-98-7	Sigma	C2284	Copper sulfate solution
75-09-2	IsoLab	914.013.2501	Dichloromethane
60-29-7	Honeywell	10315081	Diethyl ether
60-00-4	Alfa	A10713	Ethylenediaminetetra-acetic acid (EDTA)
6381-92-6	Sigma	E5134	Ethylenediaminetetra-acetic acid disodium salt dihydrate (Na ₂ -EDTA)
1239-45-9	Sigma	e7637	Ethidium bromide
	Supelco	CRM47885	FAME mix (37 component)
50-99-7	Appllichem	A0883	Glucose anhydrous (D+)
110-54-3	Merck	1.043.712	n-Hexane
7365-45-9	Alfa Aesar	A14777	HEPES

506-12-7	Alfa Aesar	L05928	Heptadecanoic acid
7647-01-0	Sigma	7102	Hydrochloric acid
	Bioline	BIO-33053	HyperLadder™ 1kb
	Cargille	16490	Immersion oil Type A
7705-08-0	Alfa Aesar	12357	Iron (III) chloride
3522-50-7	Aldrich	F6129	Iron (III) citrate
7782-63-0	Sigma	12354	Iron (II) sulfate heptahydrate
10034-99-8	Merck	1,0588601	Magnesium sulphate heptahydrate
13446-34-9	Alfa Aesar	36526	Manganese (II) chloride tetrahydrate
10034-96-5	Alfa Aesar	A17615	Manganese (II) sulfate monohydrate
67-56-1	Merck	20.864.320	Methanol
68-12-2	Sigma	227056	<i>N,N</i> -Dimethylformamide
67-68-5	AppliChem GmbH	A3006	Dimethyl sulfoxide (DMSO)
	Bioline	BIO-21105	MyTaq™ DNA Polymerase
	Bioline	BIO-37111	MyTaq™ Reaction Buffer
7385-67-3	Sigma	N3013	Nil Red
108-95-2	Sigma	P1037	Phenol
9001-77-8	Sigma	P3752	Phosphatase, acid from potato
29435-48-1	Sigma	363502	Poly[(R)-3-hydroxybutyric acid] (PHB)
7758-02-3	Sigma	243418	Potassium bromide
0838401 709	Merck	1,05101	di-Potassium hydrogen phosphate anhydrous
7778-77-0	Appllichem	A3095,1000	Potassium dihydrogen phosphate cell culture grade

7447-40-7	Merck	1,04936	Potassium chloride
7681-11-0	VWR	26850,23	Potassium iodide
7778-80-5	Sigma	31270	Potassium sulfate
67-63-0	VWR	437423R	2-Propanol
9048-46-8	Sigma	P0914-5AMP	Protein standard
39450-01-6	Sigma	P2308	Proteinase K from Tritirachium album
144-55-8	Sigma	31437	Sodium bicarbonate
101855321	Sigma	13418	Sodium chloride
100187927 4	Sigma	L3771	Sodium dodecyl sulfate (SDS)
1310-73-2	VWR	28248298	Sodium hydroxide
144-55-8	VWR	27775,293	Sodium hydrogen carbonate
7631-95-0	Abcr	AB106776	Sodium molybdate anhydrous
7631-99-4	VWR	27950298	Sodium nitrate
10213-79-3	Sigma	71746	Sodium metasilicat pentahidrat
10213-10-2	Sigma	72069	Sodium tungstate dihydrate
7664-93-9	Sigma	40254	Sulfuric acid semiconductor grade PURANAL™ (Honeywell 17831), 95-97%
4197-25-5	Sigma	199664	Sudan Black B
77-86-1	Sigma	T1503	Trizma base (Tris-Base)
1185-53-1	Sigma	T5941	Trizma hydrochloride (Tris-HCl)
9002-93-1	Sigma	X100	Triton™ X-100
7732-18-5	Sigma	W4502	Water (RNAase Free)
123334-20- 3	Sigma	233706	Vanadium (IV) oxide sulfate hydrate
7646-85-7	Abcr	AB117501	Zinc chloride anhydrous

7446-20-0	Alfa Aesar	33399	Zinc sulfate heptahydrate
-----------	------------	-------	---------------------------

5.1.2 Devices

Devices used in this thesis were listed in Table 5.2:

Table 5.2 Experimental devices

Name	Company	Series/Code
Agitator rotator	WiseMix	RT-10
Analytical balance	Shimadzu	ATX224
Autoclave	Nuve	OT 90L
Automatic pipettes	Eppendorf	2.5 μ l/20 μ l/200 μ l/1000 μ l/5000 μ l
Biological chamber	Fitotron	SGC 120
Biosafety cabinet	Labconco	Logic + /Class II, Type A2
Block thermostat/ Nitrogen evaporator	Teknosem	TAB-24
Centrifuge	Beckman Coulter	Allegra X-15R Benchtop
Centrifuge	Eppendorf	5418R
Drying oven	Binder	ED 53
Electrophoresis	Thermo Scientific	Cast (7309) B1A Mini Gel Electrophoresis systems
Electrophoresis power source	VWR	300 V
Fluorescence microscope	Zeiss	Axiovert A1 with Colibri 7/ AxioCam 503 color
Fluorescence microscope	Nikon	H600L
Freeze dryer (Lyophilizer)	Christ	Alpha 1-2 LDplus

Freezer (-10°C/ -22°C)	Inoksan	EMP.70.95.02-40
Freezer (-2°C/ +8°C)	Inoksan	EMP.140.80.03
FTIR	Perkin Elmer	Spectrum Two
GC (Gas chromatograph)	Thermo Scientific	Trace 1310
GC column	Agilent	DB-23 (60 m, 0.25 mm, 0.25 µm)/ 122-2362
Gel electrophoresis scanner	The Azure	c200
Homogenizer	MP Biomedicals	FastPrep-24™ 5G
HPLC analytic column	Agilent	Eclipse XCD-C18, 5 µm, 4.6x150 mm
HPLC analytic column	Agilent	Zorbax C8 (5 µm, 4.6x250 mm, PN 880952-706)
HPLC (high-performance liquid chromatography)	Shimadzu	Prominence LC-20A
HPLC (high-performance liquid chromatography)	Shimadzu	Nexera-i lc-2040c 3d
Ice maker	Scotsman	AF 80
Incubator	Thermo Scientific	IGS60
Incubator/ Shaker	Mikrotest	LMS MCI-55
Incubator/ Shaker	Sartorius stedim Biotech	Certomat BS-T
Ion-exchange chromatography	DIONEX	AS-DV, ICS-5000 ⁺ DC/SP
Ion-exchange chromatography analytical column	Thermo Scientific	Dionex IonPac™ AS9-HC RF1C™ 4X250 mm
Ion-exchange chromatography guard column	Thermo Scientific	Dionex IonPac™ AG9-HC RF1C™ 4X50 mm

Light microscope	Nikon	Eclipse Ni U with DS-Ri2
Light microscope	Nikon	Eclipse 100 LED
Magnetic stirrer hotplate	VWR IKA	VMS-C7 S1
Magnetic stirrer hotplate	VWR	VMS-A
Magnetic stirrer hotplate	IKA	RTC
Magnetic stirrer hotplate	Heidolph	MR Hei-Tec
Microplate spectrophotometer	Thermo Scientific	MULTISKAN GO
Microwave	Arçelik	MD 574 S
Multi-parameter reader	YSI	ProPlus
Nanodrop / Fluorometer	DeNovix	DS-11+
pH- meter	Mettler Toledo	FiveEasy
Rotary evaporator	Heidolph	Hei-VAP Gold 3
Shaker	VWR	Advanced Orbital Shaker Model 5000
Thermocycler / PCR	Bio-Rad	T100 PCR Thermal Cycler, TS-100
Thermo-shaker	Grant-bio	PHMT with PSC24N
Thermo-shaker for microplates	Grant-bio	PHMP
Ultra-low temperature freezer (ULT)	Haier Biomedical	DW-86L628
UV-Vis spectrophotometers	Shimadzu	UV-2600
Vortex	BioSan	Multi-Vortex V-32
Water baht	Mikrotest	LMS MSB 6
Water purification system	Merck Millipore	Direct-Q 5 UV

5.1.3 Media

5.1.3.1 BG11, BG11-N, and BG11-NP Medium Recipes

BG11 (Blue-Green Medium) is a commonly used medium for Blue-green alga, which are also named as Cyanobacteria [70]. BG11 was prepared by addition 10.0 ml from stock solutions 1 to 8, and 1.0 ml from stock solution 9 into approximately 900 ml of double-distilled water (ddH₂O) in the order specified while stirring continuously (Table 5.3). Total volume made up to 1 liter with ddH₂O. The pH arranged to 7.1 and autoclaved. After the medium has been cooled, stored at +4°C temperature. For Petri dishes, 14.0 g agar added per liter of the medium [71].

BG11-N [72] was prepared same as BG11 medium except for addition of NaNO₃ (Stock solution 1), and for BG11-NP medium, NaNO₃ (Stock solution 1) and K₂HPO₄ (Stock solution 2) did not add to BG11 medium, but also K₂SO₄ (174.259 g/mol) added instead of K₂HPO₄ (174.2 g/mol).

Table 5.3 BG11 medium recipe

<i>Stocks</i>	<i>Component</i>	<i>per liter</i>	<i>Final Concentration</i>
1	NaNO ₃	150 g	17.6 mM
2	K ₂ HPO ₄	4 g	0.23 mM
3	MgSO ₄ ·7H ₂ O	7.5 g	0.3 mM
4	CaCl ₂ ·2H ₂ O	3.6 g	0.24 mM
5	Citric acid·H ₂ O	0.6 g	0.031 mM
6	Ferric ammonium citrate	0.6 g	0.021 mM
7	Na ₂ EDTA·2H ₂ O	0.1 g	0.0027 mM
8	Na ₂ CO ₃	1.6 g	0.19 mM
9	Trace metal solution:	1 ml	
	H ₃ BO ₃	2.86 g/L	46 mM
	MnCl ₂ ·4H ₂ O	1.81 g/L	9 mM

	ZnSO ₄ ·7H ₂ O	0.22 g/L	0.77 mM
	Na ₂ MoO ₄ ·2H ₂ O	0.39 g/L	1.6 mM
	CuSO ₄ ·5H ₂ O	0.079 g/L	0.3 mM
	Co(NO ₃) ₂ ·6H ₂ O	49.4 mg/L	0.17 mM

5.1.3.2 Z8 and Z8-N Medium Recipes

Z8 medium has been tried to compare the growth of Cyanobacterium [73] for Cyanobacterial growth, which described in Table 5.4 [74]. After autoclave, medium stored at +4°C temperature. For Petri dishes, 14.0 g agar added per liter of the medium. Z8-N medium prepared the same as the Z8 medium except for the addition of NaNO₃.

Table 5.4 Z8 medium recipe

<i>Component</i>		<i>Amount/L ddH₂O</i>
MgSO ₄ ·7H ₂ O		0.25 g
NaNO ₃		0.467 g
Ca(NO ₃) ₂ ·4H ₂ O		59 mg
NH ₄ Cl		31 mg
Na ₂ CO ₃		0.02 g
FeCl ₃	28 g /L in 0.1 N HCl	0.1 ml
Na ₂ EDTA	39 g/L in 0.1 N NaOH	0.095 ml
Gaffron micronutrients in 1L ddH ₂ O:		1 ml
H ₃ BO ₃	3.1 g	
MnSO ₄ ·4H ₂ O	2.23 g	
ZnSO ₄ ·7H ₂ O	0.22 g	

$(\text{NH}_4)_6\text{Mo}_7\text{O}_{24}\cdot 4\text{H}_2\text{O}$	0.088 g	
$\text{Co}(\text{NO}_3)_2\cdot 6\text{H}_2\text{O}$	0.146 g	
$\text{VOSO}_4\cdot 6\text{H}_2\text{O}$	0.054 g	
$\text{Al}_2(\text{SO}_4)_3\text{K}_2\text{SO}_4\cdot 2\text{H}_2\text{O}$	0.474 g	
$\text{NiSO}_4(\text{NH}_4)_2\text{SO}_4\cdot 6\text{H}_2\text{O}$	0.198 g	
$\text{Cd}(\text{NO}_3)_2\cdot 4\text{H}_2\text{O}$	0.154 g	
$\text{Cr}(\text{NO}_3)_3\cdot 7\text{H}_2\text{O}$	0.037 g	
$\text{Na}_2\text{WO}_4\cdot 2\text{H}_2\text{O}$	0.033 g	
KBr	0.119 g	
KI	0.083 g	

5.1.3.3 Allen Medium Recipe

The Allen medium was prepared as described in Table 5.5, and the pH was adjusted at 7.8 [75]. After autoclave, medium stored at +4°C temperature. For Petri dishes, 14.0 g agar added per liter of the medium.

Table 5.5 Allen medium recipe

<i>Component</i>		<i>Amount/L ddH₂O</i>
HEPES buffer		2.3 g
NaNO ₃		1.5 g
K ₂ HPO ₄ ·7H ₂ O	6 g/L ddH ₂ O	5 ml
MgSO ₄ ·7H ₂ O	6 g/L ddH ₂ O	5 ml
Na ₂ CO ₃	4 g/L ddH ₂ O	5 ml
CaCl ₂ ·2H ₂ O	2.5 g/L ddH ₂ O	10 ml
Na ₂ SiO ₃ ·9H ₂ O	4.64 g/L ddH ₂ O	10 ml
Citric acid·H ₂ O	4.8 g/L ddH ₂ O	1 ml
P-IV metal solution 1L ddH ₂ O:		1 ml

Na ₂ EDTA·2H ₂ O	0.75 g	
FeCl ₃ ·6H ₂ O	0.097 g	
MnCl ₂ ·4H ₂ O	0.041 g	
ZnCl ₂	0.005 g	
CoCl ₂ ·6H ₂ O	0.002 g	
Na ₂ MoO ₄ ·2H ₂ O	0.004 g	

5.1.3.4 FW (Freshwater) Medium Recipe

First soil-extract* prepared for the FW medium. 50 g soil was boiled in 500 ml ddH₂O for 30 min, then centrifuged at 5500 rpm for 15 min, filtered (0.45 µm PTFE), and double autoclaved. The following FW medium was prepared, as described in Table 5.6 [76]. After autoclave vitamin mix added to medium with sterile syringe and filter (0.45 µm PTFE), then pH was adjusted at 6.5 with HCl and stored at +4°C temperature. For Petri dishes, 14.0 g agar added per liter of the medium.

Table 5.6 FW medium recipe

<i>Stocks</i>	<i>Component</i>	<i>Stock recipe</i>	<i>Amount/L ddH₂O</i>
1	Ca(NO ₃) ₂ ·4H ₂ O	0.2 g/100 ml	20 ml
2	K ₂ HPO ₄	0.1 g/100 ml	10 ml
3	MgSO ₄ ·7H ₂ O	0.1 g/100 ml	25 ml
4	Na ₂ CO ₃	0.1 g/100 ml	20 ml
5	Na ₂ SiO ₃ ·5H ₂ O	0.1 g/100 ml	50 ml
6	Ferric-citrate	0.1 g/100 ml	10 ml
7	Citrit acid	0.1 g/100 ml	10 ml
8	Soil-extract	* Described above	30 ml
9	Micronutrient solution	**Table 5.7	5 ml
10	Vitamin mix	*** Table 5.8	1 ml

Table 5.7 Micronutrient solution recipe

<i>Solution</i>	<i>Component</i>	<i>Stock recipe</i>	<i>Amount</i>
Solution I	ddH ₂ O		881 ml
	ZnSO ₄ ·7H ₂ O	0.1 g/100 ml	1 ml
	MnSO ₄ ·H ₂ O	0.0758 g/100 ml	2 ml
	H ₃ BO ₃	0.2 g/100 ml	5 ml
	Co(NO ₃) ₂ ·6H ₂ O	0.02 g/100 ml	5 ml
	Na ₂ MoO ₄ ·2H ₂ O	0.02 g/100 ml	5 ml
	CuSO ₄ ·5H ₂ O	0.0005 g/100 ml	1 ml
	EDTA (Triplex III)		0.4 g
Solution II	ddH ₂ O		100 ml
	FeSO ₄ ·7H ₂ O		0.7 g
	EDTA (Triplex III)		0.4 g

** Solution I and II autoclaved separately then combined after cooling

Table 5.8 Vitamin mix recipe

<i>Component</i>	<i>Amount/100 ml ddH₂O</i>
Vit. B ₁ (Thiamine HCl)	100 mg
Vit. H (Biotin)	0.025 mg
Vit. B ₁₂ (Cyanocobalamin)	0.015 mg

***added aseptically to autoclaved and cooled medium

5.2 Experimental Methods

5.2.1 Sampling of Cyanobacteria

Selected Cyanobacteria that were collected from paddy fields, where Cyanobacterial biodiversity is high and some other diazotrophic Cyanobacteria

species, which were already isolated from different thermal water resources and volcanic lakes of Turkey had been employed.

5.2.1.1 Cyanobacteria from Thermal Waters and Hot Springs

Cyanobacterial species of Istanbul Medeniyet University's (IMU) culture library has been planned to investigate for their PHB production. The Cyanobacterial species of IMU library were already collected from thermal and hot spring waters and lakes (mostly volcanic) by supporting of "The Republic of Turkey Ministry of Agriculture and Forestry General Directorate of Agricultural Research and Policies" project numbered as TAGEM/12/AR-GE/13 as labeled following figure 5.1:



Figure 5.1 Sampling locations of Cyanobacteria species from IMU Culture Library

5.2.1.2 Cyanobacteria from Paddy Fields

The first part of the thesis study was to isolate Cyanobacteria from paddy fields that were known to host a broad range of Cyanobacterial species which can produce PHB [58]. Isolation has been made in three terms as of May, June, and especially in July when the rice plant is grown, from paddy fields of Balabancık, Ipsala, Yeni Karpuzlu, Enez, and Büyük Mandıra (Fig. 5.2).

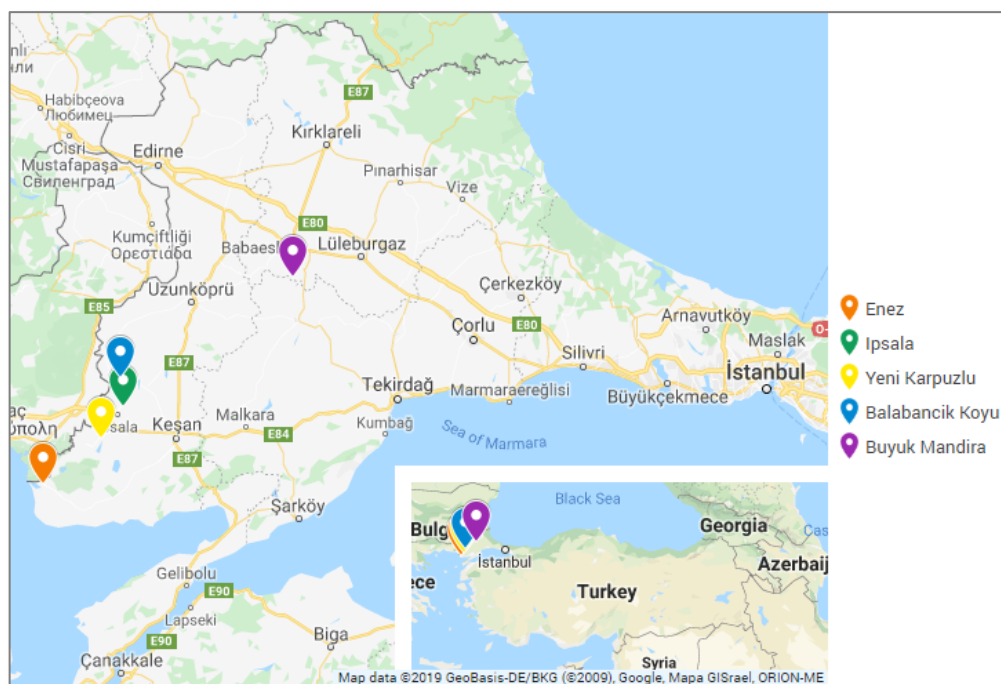


Figure 5.2 Sampling locations of Cyanobacteria species from paddy fields

Samples were collected from water (Planktonic samples), soil (Epipellic), stone (Epilithic), and plant (Epiphytic). We made direct sampling from soil (Epipellic), stone (Epilithic), plant (Epiphytic), and the plankton net was employed for planktonic samples (Fig. 5.3).



Figure 5.3 Sampling from paddy fields

Water's pH, conductivity, temperature, and total dissolved solids (TDS) have been measured by multi-parameter reader and salinity, ammonium, and nitrate level of

water samples measured by ion-exchange chromatography with Dionex IonPac AS9-HC RF1C column (4x250 mm) (mobile phase: 9mM NaCO₃, flow rate:1) [77] (Fig. 5.4).



Figure 5.4 Ion-exchange chromatography

5.2.2 Selection of Cyanobacteria

5.2.2.1 Purification

Samples were inoculated in liquid BG11 and spread on solid BG11 medium prepared with or without nitrogen. Incubating samples in nitrogen plus and minus media lets select nitrogen-fixing Cyanobacteria from a Cyanobacterial/micro-algal bulk. Techniques such as antibiotic treatment have also been used for the species for obtaining the axenic cultures, then identified by microscopically via serial dilution which was summarized as follows: 10 ml from the sample was transferred into flasks with 190 ml BG11-N medium then incubated by shaking with continuous light. 2 ml sample taken from the flasks and transferred to the next 50 ml flasks. The process was repeated for every 15 days, and the microscopic investigation was performed after 15 days to identify the Cyanobacteria and determine the purity. The purification process of nitrogen-fixing Cyanobacteria which were collected from paddy fields in summary, followed by sampling, incubated in BG11/ BG11-N liquid media, separation by serial dilution method, again incubated in different liquid/solid media such as BG11-N, Z8 and Z8-N, examination by microscope imaging, and collecting in liquid nitrogen for cryopreservation, as shown in Figure 5.5:

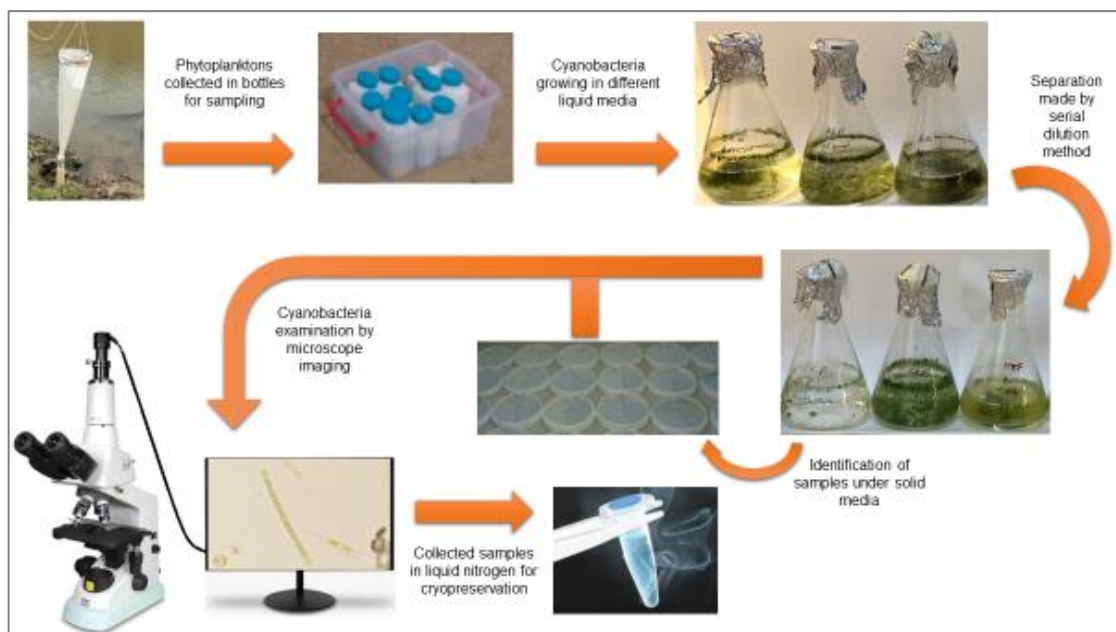


Figure 5.5 Purification process of nitrogen-fixing Cyanobacteria

Likewise, formerly purified samples that exist in Istanbul Medeniyet University culture collection were also spread on BG-11 and BG11-N agar for the selection of diazotrophic Cyanobacteria. Also, the Z8 medium and its nitrogen deprived version of Z8-N tried to compare the Cyanobacteria growth. The identified pure Cyanobacteria were transferred in solid and liquid media as stocks. Microscopic imaging has been made continuously to check the purity of samples.

5.2.2.2 Identification

5.2.2.2.1 DNA Extraction

Genomic DNA was extracted from Cyanobacterial species following the phenol-chloroform method [77–79]:

Washed (dH₂O) and centrifuged (10,000g 2 min) 100 mg (minimum) Cyanobacterial biomass washed with 4% Triton 100x and centrifuged again (10,000g 2 min). 400 µl extraction buffer (Table 5.9) pre-warmed to 60°C and added on the pellet, then vortexed for 1 min at maximum speed. 40 µl SDS (10%) and 10 µl proteinase K (20 mg/ml) added to the mix in the Eppendorf tube and vortexed for the 5 min and then incubated at 60°C for 1 h by thermo-shaker (300 rpm) (Fig. 5.6). After incubation, the Eppendorf tube upended for three times and

400 μ l phenol: chloroform (1:1) (caution: phenol is high carcinogenic, work under cabin) added, and rotated (20 rpm speed) by inversion for 2 min. The upper-aqueous phase (including DNA) transferred into a new Eppendorf tube after settled down for 1 min at 4°C of centrifugation at 14,000 g for 10 min at 4°C. 300 μ l isopropanol added to the tube and mixed by agitator rotator for 3 min at 20 rpm speed, and incubated for at least for 1h or uttermost overnight till the DNA became visible. After that, the solution centrifuged at 14,000 g for 15 min at 4°C, and the supernatant discarded with caution. The DNA pellet washed with 750 μ l cold ethanol (70%) and rotated by inversion at 20 rpm for 2 min and then again centrifuged at 14,000 g for 2 min at room temperature to the formation of the pellet. The supernatant was thrown out, and the pellet left to dry in the sterile cabinet for 10 minutes while the tube was open. Then 300 μ l sterile T₁₀E₁ (10mM Tris-HCl EDTA pH 8.0; 1mM Na₂EDTA pH 8.0) was added (or RNAase Free Water), and nanodrop (Fig. 5.6) was read at a wavelength between 260-280 nm to measure the concentration of the DNA. Concentration (C) was adjusted around 50 ng/ μ l for 300 μ l volume, according to the dilution equation ($C_1V_1 = C_2V_2$), to get good bands for gel electrophoresis. After the quantification, 50 μ l taken in as aliquotes and stored at -80°C for further analysis.

Table 5.9 CTAB extraction buffer recipe

<i>Component</i>	<i>Amount</i>
CTAB (Hexadecyltrimethylammonium bromide)	1 g
5 M NaCl	10 ml
1 M Tris-HCl (pH 8)	5 ml
0.5 M EDTA (pH 8)	2 ml
ddH ₂ O	33 ml



Figure 5.6 Thermo-shaker and nanodrop respectively

5.2.2.2.2 Gel Electrophoresis

The first gel electrophoresis was used to determination of the band' molecular weight, which gave good specify of DNA quality for the polymerase chain reaction (PCR), and then gel electrophoresis used again to see the amplification proficiency of DNA after PCR. 1% solution of agarose has been prepared by dissolving 0.45 g of agarose in 450 ml of 0.5x TBE buffer, which diluted (1/10) from 5X TBE buffer solution (Table 5.10), and placed in a microwave for 5 min, then left for cooling, after that 5 μ l of 10 mg/ml ethidium bromide (caution: high carcinogenic, work under cabin) added into agarose mix before it gets solid, mixed well and poured slowly in the electrophoresis tank for polymerization of the agarose solution. The electrophoresis comb with 14 teeth was used to mold wells during gel formation. After 30 min electrophoresis comb was removed, and the electrophoresis tank was filled upon the gel with a 0.5x TBE buffer solution. First, 3 μ l of 1kb ladder added than 3 μ l of per sample (DNA: before PCR, 16S rRNA: after PCR) were loaded to the separated wells mixed with 2 μ l 6x loading buffer, and the gel was run at 85 mVA 90 volts for 1:15 min (Fig. 5.7). Afterward, the gel was picturized by gel electrophoresis scanner (Fig. 5.7) for the identification of the isolated DNA band' quality. Since both the dull, blurry, thick, dark, or smearing bands were recognized as bad resolutions for gel electrophoresis, these samples were diluted and tried again or started from the DNA extraction, whereas visible and not smeared bands were accepted as good results.

Table 5.10 5xTBE buffer recipe

<i>Component</i>	<i>Amount</i>
Tris base	27 g
Boric acid	14 g
0.5 M EDTA (pH 8.0)	10 ml
ddH ₂ O	490 ml

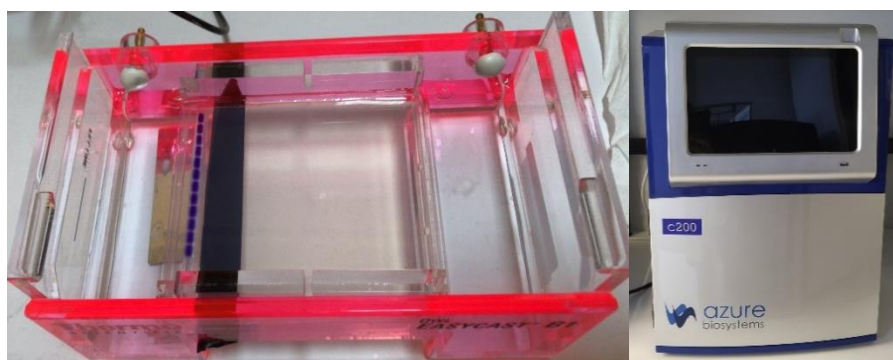


Figure 5.7 Gel electrophoresis and gel electrophoresis scanner

5.2.2.2.3 Amplification of the 16S rRNA Gene via Polymerase Chain Reaction

PCR performs DNA amplification from genomic DNA containing a partial 16S ribosomal RNA region [81]. Ten primers (Table 5.11), which determined by the literature studies, have been designed by Sentromer DNA Technology limited company (©2009-2020 <https://www.sentromer.com/>) and were attempted to select the best primers for the amplification of the Cyanobacterial DNA. After PCR amplification, first gel electrophoresis of the primers, then 16S rRNA sent to sequence analysis to Sentromer DNA Technology limited company (©2009-2020 <https://www.sentromer.com/>) and results investigated on Chromas v2.6.4 (a tool for viewing and editing chromatograms from Sanger sequences) and the NCBI databases with BLASTn search (<https://blast.ncbi.nlm.nih.gov/Blast.cgi>). Selected primers have been used for all Cyanobacterial DNA samples for the amplification of 16S rRNA.

Table 5.11 Primer pairs

<i>Primer name</i>	<i>Type*</i>	<i>5' Primer sequences 3'</i>	<i>Ref.</i>
pA	F	AGA GTTTGATCC TGG CTC AG	[82]
B23S	R	CTT CGC CTC TGTGTGCCT AGGT	[82]
CYA108F	F	ACG GGT GAG TAA CRC GTR A	[83]
CYA16S SCYR	R	CTT CAY GYA GGC GAG TTG CAGC	[83]
16S545R	R	ATT CCG GAT AAC GCT TGC	[82]
CYA359F	F	GGG GAA TCT TCC GCA ATG GG	[84]
CYA781R	R	GAC TAC AGG GGT ATC TAA TCC	[84]
27F	F	AGA GTT TGA TCM TGG CTC	[65]
27FR	F-R	TTG GGC GTA AAG CGT AG	[85]
809R	R	GCT TCG GCA CGG CTC GGG TCG ATA	[86]

*F: Forward, R: Reverse

Primers diluted (10 μ l in 190 μ l of ddH₂O) for a polymerase chain reaction. First 5 μ l extracted DNA, 5 μ l master mix, 1 μ l from diluted forward primer, 1 μ l from diluted reverse primer, and 12 μ l ddH₂O added in a sterile PCR tube, then 1 μ l DNA polymerase added and placed in a thermocycler (Fig. 5.8) according to program detailed in Table 5.12. After amplification, 16S rRNA sent to Sentromer DNA Technology limited company (©2009-2020 <https://www.sentromer.com/>) for Sanger sequence analysis. Results investigated on Chromas v2.6.4 (a tool for viewing and editing chromatograms from Sanger sequences) and the NCBI databases with BLASTn search (<https://blast.ncbi.nlm.nih.gov/Blast.cgi>) and species entered the database of NCBI.

Table 5.12 PCR program

	<i>Step 1</i>	<i>Step 2</i>	<i>Step 3</i>	<i>Step 4</i>	<i>Step 5</i>	<i>Step 6</i>	<i>Step 7</i>
<i>Temperature</i>	94. 0°C	94. 0°C	50. 0°C	72. 0°C	Go to step 2	72. 0°C	12. 0°C
<i>Time</i>	0:5:0	10:01:0	0:1:30	0:2:0	30 cycle	0:7:0	∞



Figure 5.8 Thermocycler (PCR)

5.2.3 Preparation of Inoculum

The Cyanobacteria species have been sustained in BG11-N medium by refreshing every 15-20 days, since isolation in May 2017. Exponentially growing Cyanobacteria cells were harvested by centrifugation at 2000 g for 3 min, washed with ddH₂O, and used as inoculum (5%) for experiments.

5.2.4 Screening PHB Levels of Cyanobacteria

5.2.4.1 Experimental Design

Cyanobacterial species were cultivated under the continuous light intensity of 100 $\mu\text{E}/(\text{m}^2/\text{s})$ at 25°C by orbital shaking at 120 rpm speed. Both 50 ml BG11-N medium (as the control) and BG11-NP medium (the experimental group for observation the effect of phosphorous) in 100 ml flasks to enhance PHB production. Triplicate samples were collected on the 5th and the 10th days of incubation. Cells monitored by light microscope imaging with Nikon Eclipse Ni light microscope (Fig. 5.9) with Nikon Y-TV 55 optic camera by using NIS-Elements BR 4.40.00 64-bit program.

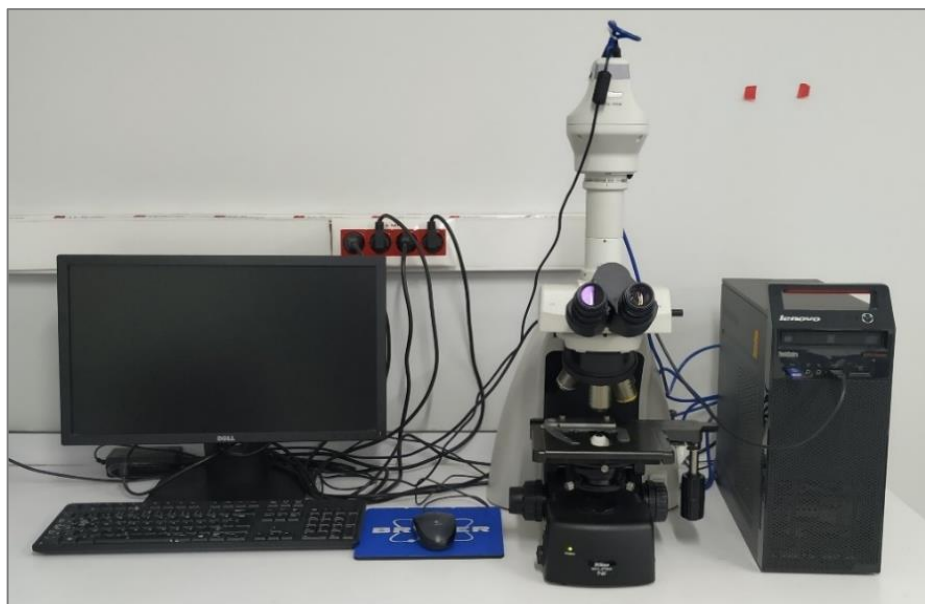


Figure 5.9 Light microscope imaging system

5.2.4.2 Analysis

5.2.4.2.1 Sudan Black Dye Method

The schematic steps of the Sudan black technique for investigating PHB content are explained in Figure 5.10 [87]. 1 ml sample was collected, centrifuged at 7500 g, and washed with ddH₂O [87]. Sudan black B solution (16 mg/ml ethanol) prepared in 70% ethanol [88] and 400 µl added into Cyanobacteria samples, then incubated by shaking for 20 min at 35°C [87]. The stained samples were centrifuged at 7500 g and washed three times with ddH₂O to get rid of not fixed dye. In the last step, 1 ml ddH₂O was added to the stained cell pellet homogenized, then its UV spectrum was read at 670 nm and also virtualized on immersion oil by x100 microscope objective [87].

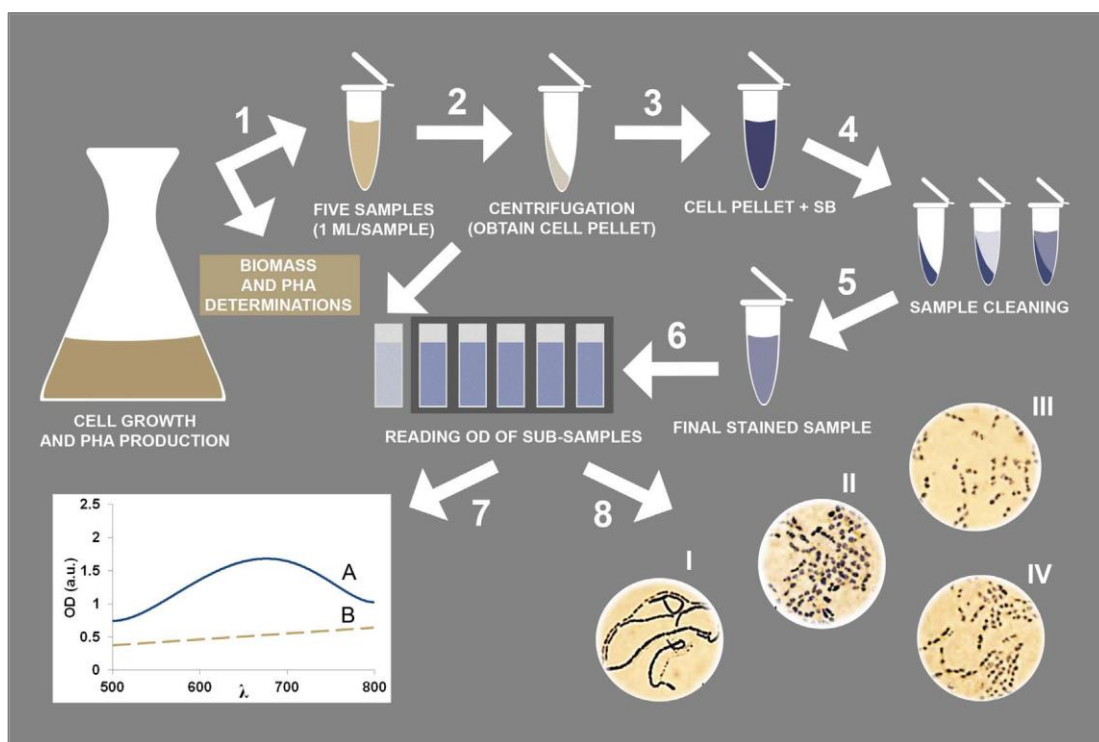


Figure 5.10 Scheme of the steps of developed Sudan black B quantification technique

5.2.4.2.2 FTIR (Fourier Transform Infrared Spectroscopy) Analysis

The collected 2 ml cells were centrifuged for 5 min at 2000 g and frozen in -80°C for 24h, then dried by lyophilizer at 40°C for 12h. After drying with the lyophilizer, powdered-like cells were analyzed between $4000\text{--}400\text{ cm}^{-1}$ wavenumber range absorbance spectrums with 64 scanings of the FTIR Spectrometer (Fig. 5.11) [89].

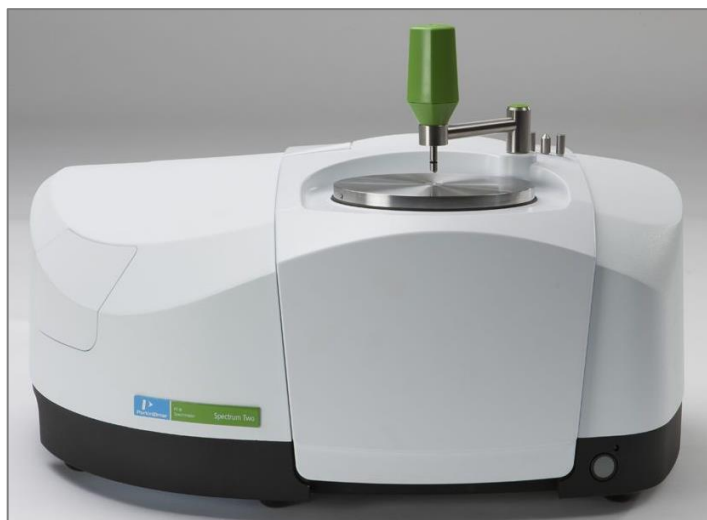


Figure 5.11 FTIR

PHB gives (C=O) transmission bands at 1720 cm^{-1} [90] and 1735 cm^{-1} [91] absorbance, which depends on the degree of crystallinity (Fig 5.12). 1720 cm^{-1} and 1735 cm^{-1} bands were used to identify the PHB feedstock separately.

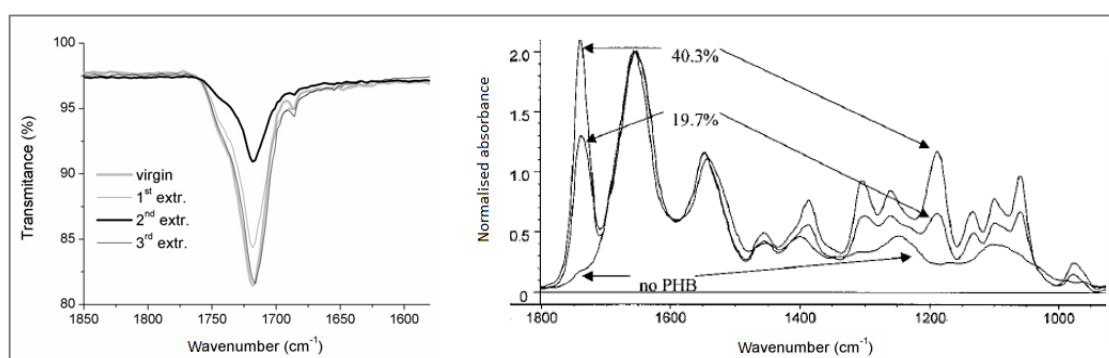


Figure 5.12 PHB responsible FTIR peaks

Also, 2 ml samples were collected on the 7th day of the incubation to measure the triacylglycerol (TAG), oligosaccharide, and polysaccharide amounts. FTIR peak values attributed to ester group (C=O) vibration of TAG (1744 cm^{-1}), membrane-bound oligosaccharide (C–OH) bond (1145 cm^{-1}), and stretching of the (C–O) (C–OH) groups of polysaccharide (1045 cm^{-1}) [89].

The amide I band (1652 cm^{-1}) was taken as a reference for FTIR spectra normalization and ratio determination [92].

5.2.4.2.3 Total Chlorophyll-a & Carotenoid Analysis Method

Cyanobacterial samples (100 mg) were vortexed with 500 µl water and centrifuged at 2000 rpm for 3 min. 500 µl of 90% acetone was added into the cells, then vortexed and mixed by agitator rotator for 15 min, and centrifuged at 15000 rpm for 5 min. 150 µl from the supernatant were placed into 96 well F sterile microplates and the absorbances were measured by microplate spectrophotometer (Fig. 5.13) at 470, 630, 647, 664, and 750 nm against a 90% acetone blank. The concentration of total chlorophyll-a and carotenoid were calculated according to the following equations [93]:

$$\text{Chlorophyll-a } [\mu\text{g/ml}] = (11.85(A_{664}-A_{750}) - 1.54(A_{647}-A_{750}) - 0.08(A_{630}-A_{750})) \quad (5.1)$$

$$\text{Chlorophyll-b } [\mu\text{g/ml}] = (-5.43(A_{664}-A_{750}) + 21.03(A_{647}-A_{750}) - 2.66(A_{630}-A_{750})) \quad (5.2)$$

$$\text{Total carotenoid } [\mu\text{g/ml}] = (1000(A_{470}) - (1.86[\text{Chl-a}]) - (74.08[\text{Chl-b}]))/206 \quad (5.3)$$



Figure 5.13 Microplate spectrophotometer

5.2.4.2.4 Determination of Phycobiliproteins

Samples (10 ml) were centrifuged at 3000 rpm for 5 minutes and washed with buffer (1M Tris-HCl, pH 8.1), and 5x volume of the buffer were added into the cell pellet to extract pigments and for the destruction of the cell wall of the strains were obtained by continuous freezing at -20°C and thawing at +4°C, then sonication (10 min/ 30 sec per cycles). After centrifugation at 12,000 rpm for 10 min, separation of cell fragments was done, and supernatants were measured spectrophotometrically in 96 well microplate at A₅₆₂ nm for phycoerythrin (PE), A₆₁₅ nm for phycocyanin (PC), and A₆₅₂ nm for allophycocyanin (APC) by

microplate spectrophotometer. The concentration of phycobiliprotein pigments was calculated by using the following formulas [94]:

$$PE \text{ [mg/ml]} = [(A_{562}) - 2.41(PC) - 0.849(APC)]/9.62 \quad (5.4)$$

$$PC \text{ [mg/ml]} = [(A_{615}) - 0.474(A_{652})]/5.34 \quad (5.5)$$

$$APC \text{ [mg/ml]} = [(A_{652}) - 0.208(A_{615})]/5.09 \quad (5.6)$$

5.2.5 Studies on Selected Species

5.2.5.1 Medium Trial for Growth of Cyanobacteria

BG11, Z8, Allen, and FW solid media were tried to find the best Cyanobacterial growth on selected species.

5.2.5.2 Experimental Design

Selected Cyanobacterial species were cultivated under the continuous light intensity of $100 \mu\text{E}/(\text{m}^2/\text{s})$ at 25°C by orbital shaking at 120 rpm speed. Both 100 ml BG11-N medium (as the control) and BG11-NP medium (the experimental group) in 250 ml flasks were used as triplicates for each species and samples collected on the 5th and the 10th days.

5.2.5.2.1 HPLC Analysis

5.2.5.2.1.1 Carotenoid Analysis

The extraction buffer (2 ml, 50% MeOH-50% THF) added on 0.1 g wet sample and vortexed, then filtered by PTFE filters ($0.45 \mu\text{m}$) [95]. Zorbax C8 reverse phase HPLC column ($5 \mu\text{m}$, $4.6 \times 250 \text{ mm}$) was used with the 0.8 min flow rate by the 95% MeOH: 5% THF of the mobile phase. Following equation used for calculation of carotenoids [96]:

$$x = \frac{1 \times (\text{HPLC area}) \times (\text{dilution ratio})}{(\text{standard area}) \times (\text{amount of sample})} \times 100 \quad (5.7)$$

* (amount of sample= 0.1 g) (dilution ratio= 2ml) (standard area= 320,000 (lutein); 280,000 (β -carotene))

5.2.5.2.1.2B₂ (Riboflavin) Vitamin Analysis

Wet cyanobacterial samples (0.1 g) were autoclaved at 121°C for 30 minutes with a 4 ml buffer (0.1 N HCl). The pH was arranged ~4.5 with 2.5 N sodium acetate. After three hours of enzymatic incubation at 37°C with 0.1 ml phosphatase acid enzyme, the tubes were adjusted to 10 ml with 1N HCl, then filtered with filters (Chromafil 45/25 mm) and vialled [96] [97]. Samples have been measured on HPLC by Eclipse XCD-C18 column (5 μ m, 4.6x 150 mm) with the water: methanol (75:25) mobile phase [96].

5.2.5.3 Experimental Design with Negative Control

Selected three Cyanobacterial species were cultivated under the continuous light intensity of 100 μ E/(m²/s) at 25°C by orbital shaking at 120 rpm speed. Both 50 ml BG11 medium (as the negative control), BG11-N medium (as the control), and BG11-NP medium (the experimental group) in 100 ml flasks were used as triplicates for each species and samples collected on the 5th and the 10th days.

5.2.5.3.1 PHB Measurements

Sudan black B dye and sulphuric acid digestion method were investigated both to determine PHB production of Cyanobacterial species.

5.2.5.3.1.1 Sudan Black B Dye Method

Cyanobacterial sample (1 ml) was collected, centrifuged (7500 g), and washed with dH₂O, then Sudan black B solution 400 μ l added into samples and incubated by shaking for 20 min at 35°C [87]. The stained samples were centrifuged (7500g), washed three times with dH₂O, then again suspended with 1 ml dH₂O [87]. The UV spectrum was read at 670 nm.

5.2.5.3.1.2 Sulphuric Acid Digestion Method

Cyanobacterial medium (10 ml) was centrifuged at 6000 rpm for 30 min, and the pellet was dried in a lyophilizer (Fig. 5.14) at 40°C for 12h. The dry weights of the pellets were measured, then suspended in 2 ml ddH₂O and homogenized (Fig.

5.14). 2 ml of 2N HCl was added into the suspension and heated in a water bath at 95°C for 2 hours, then centrifuged for 20 min at 6000 rpm [98].



Figure 5.14 Lyophilizer and homogenizer, respectively

Chloroform (5 ml) was added into the tubes (lids closed) and left overnight on an incubator at 28°C with shaking at 150 rpm, then centrifuged for 20 min at 6000 rpm [99]. 0.1 ml from chloroform phase replaced in the clean glass tubes and dried at 40 °C for 15 min. 5 ml concentrated sulfuric acid (H_2SO_4) (caution: work with a plastic coat, gloves, goggles, etc.) was added into the tubes and 10 mg of PHB standard (Sigma 363502) for calibration curve. Vials closed and heated in a water bath at 100°C for 20 min for the conversion of PHB polymers to crotonic acid. The PHB amount was measured by measuring crotonic acid at A_{235} nm in a UV spectrophotometer against the blank of sulphuric acid [98]. PHB production and the percentage were calculated by the cells dry weight (dw) and PHB amount which was determined by the calibration curve. The calibration curve was constituted from PHB's serial diluted concentrations which were 15.25 $\mu\text{g/ml}$, 7.8125 $\mu\text{g/ml}$, 3.90625 $\mu\text{g/ml}$, and 0 $\mu\text{g/ml}$.

5.2.5.3.2 Growth Measurements

Cyanobacterial growth was recorded by optical density (OD) of 1 ml culture suspension at 680 nm ($\text{OD } A_{680}$) [100], which is responsible for chlorophyll-a (Fig. 5.15). The most abundant pigment is chlorophyll a [101], which means its content is parallel with the cell division.

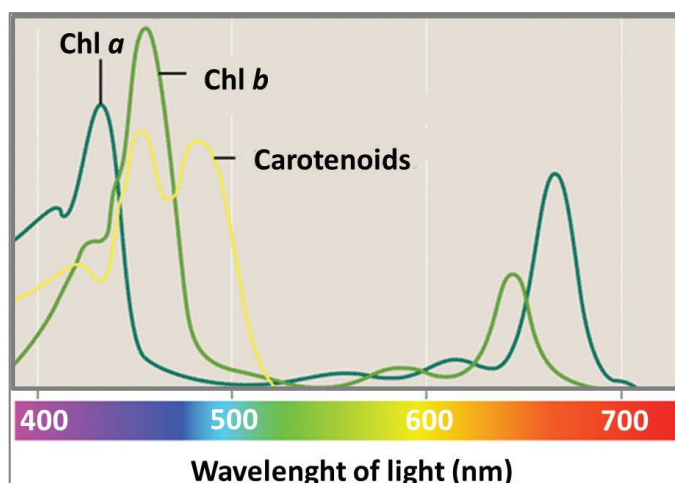


Figure 5.15 Chlorophyll a, b and carotenoids absorbance spectra [101]

5.2.5.3.3 Chlorophyll-a & Carotenoid Measurements

Cyanobacterial cells (2 ml) were harvested on the 0, 3, 5, 7, and 10th days of incubation. The protocol [102] followed by centrifugation (15,000 g for 7 min) and the supernatant was removed. 1 ml pre-cooled methanol (+4°C) added to the cells and mixed with homogenization, then covered with aluminum foil and incubated at +4°C for 20 min, and bluish color has been observed. Samples were centrifuged at 15,000 g for 7 min, and absorbance of the supernatant was measured by microplate spectrophotometer at 470 nm, 665 nm, and 720 nm, the chlorophyll-a (Chl-a) and carotenoid calculated by following equations [102]:

$$\text{Chl-a } (\mu\text{g/ml}) = 12.9447 (A_{665} - A_{720}) \quad (5.8)$$

$$\text{Carotenoids } [\mu\text{g/ml}] = [1,000 (A_{470} - A_{720}) - 2.86(\text{Chl-a } (\mu\text{g/ml}))] / 221 \quad (5.9)$$

5.2.5.3.4 Saccharide Measurements

Cyanobacterial cells (1 ml) were harvested on the 0, 3, 5, 7, and 10th days of incubation and centrifuged at 15000 g for 5 min, and supernatants were removed. 1 ml pre-cooled methanol (+4°C) added to the samples and mixed by homogenization, then tubes were covered with aluminum foil and incubated at +4°C for 20 min, and bluish or purple color has been observed. Samples were centrifuged at 15000 g for 5 min, then supernatants were discarded, and 500 μl dH_2O and 500 μl 5% phenol (caution: high carcinogenic, work in fume hood) were

added into the pellets and D-glucose (Applichem A0883) calibration solutions which were described in Table 5.13. After 15 min incubation at room temperature, 60 μ l of each sample, and 150 μ l of 96% sulfuric acid were transferred to 96-well microplate and incubated again for 5 min at room temperature [103]. Samples saccharide content was measured by a microplate spectrophotometer at 490 nm and calculated from the calibration curve.

Table 5.13 Preparation of calibration series of D-glucose in distilled water

<i>Tube number</i>	<i>Glucose solution [μl] (500 μg ml⁻¹)</i>	<i>dH₂O [μl]</i>	<i>Glucose concentration [μg ml⁻¹]</i>
1	25	475	25
2	50	450	50
3	75	425	75
4	100	400	100
5	300	200	300
6	500	0	500

5.2.5.3.5 Protein Measurements

Lysis buffer (50 mM Tris–HCl pH 8.0, 2% SDS, 10 mM EDTA) was prepared, and 500 μ l buffer added into frozen cell pellets (50-100mg) in (at -80°C and hurriedly thawed at 37°C). Homogenized cells (10 cycles with mixing for 30 sec) were incubated at laboratory temperature for 15 min at agitator rotator, then centrifuged at 5000g for 20 min at 4°C. 200 μ l of pre-heated (60°C) working reagent (4% copper sulfate solution: bicinchoninic acid solution, 1:50) (caution: safe from light) was added to the supernatant and incubated at 60°C for 30 minutes. Then measured by microplate spectrophotometer at 562 nm absorbance spectrum at room temperature for protein determination [89]. The protein standard (Bovin Serum Albumin (BSA)) (Sigma P0914-5AMP) was prepared according to Table 5.14 to obtain a protein calibration curve.

Table 5.14 Preparation of calibration series of BSA in distilled water

<i>Tube number</i>	<i>BSA (0.5 mg/ml)</i>	<i>Water</i>
1	0 μ l	10 μ l
2	1.5 μ l	8.5 μ l
3	3 μ l	7 μ l
4	5 μ l	5 μ l
5	7.5 μ l	2.5 μ l
6	10 μ l	0 μ l

5.2.5.3.6 Fluorescence Imaging via Nile Red Dye

Cyanobacterial samples (1 ml) were harvested, and the UV absorbance was measured at 720 nm. After that, the final concentrations were arranged to 0.2 OD by BG11 media for the Nile red (9-diethylamino-5Hbenzo[a]phenoxazine-5-one) encolouring of the living cells. After dilution, 250 μ l Nile red solution (1 μ g/ in DMSO) was added into 9.8 ml cell suspension and mixed by agitator rotator for 10 min in the dark. Then, a fluorescence microscope (Zeiss Axiovert A1 with Colibri 7, Axiocam 503 color) (Fig. 5.16) used to observe the Cyanobacterial lipid content at 530 nm excitation and 570 nm emission wavelengths [104].

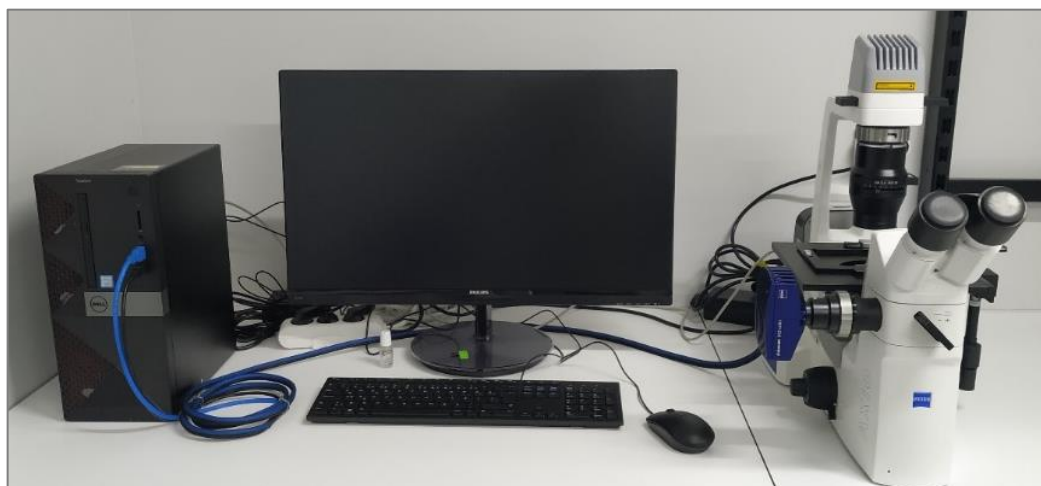


Figure 5.16 Fluorescence microscope imaging system

5.2.5.4 Maximization of Extraction Techniques

5.2.5.4.1 Sodium Hypochlorite Extraction

Cyanobacterial samples (10 ml) were centrifuged (2000 g, 5 min) and freeze-dried. Then Cyanobacterial biomass was mixed with 4% sodium hypochlorite at agitator rotator for 20 min. Then centrifuged (2000 g, 5 min) to separate the dead cells and rinsed twice with dH₂O, and followed by centrifugation (2000 g, 5 min) and cleaning with acetone for drying [105].

5.2.5.4.2 Soxhlet Extraction

Soxhlet extraction (Fig. 5.17) based on Yellore and Desai's method [106]. Cyanobacterial biomass was suspended in methanol for pre-extraction and kept overnight at 4°C for the removal of pigments. Then centrifuged for 5 min at 8,000 rpm and supernatants were discarded. The obtained pellet was dried at 60°C, then extracted in 150 ml hot chloroform by soxhlet apparatus for 30 h. Extraction followed by evaporation, precipitation (with 2x cold diethyl ether), and then filtered with Whatman glass microfiber filters (GF/C 125 mm). After centrifugation (10,000 g for 20 min), the pellet was washed with 10 ml diethyl ether and 10 ml acetone and evaporated (Fig. 5.18) [32]. Then transferred in a glass tube by dissolving in chloroform. The samples were placed in an incubator at 40°C for drying. Then 5 ml chloroform added to cells for investigation of PHB contents, which were measured by the sulphuric acid digestion method [98] as described above.



Figure 5.17 Soxhlet extraction and evaporation with rotary

Selected Cyanobacteria species were investigated in different extraction parameters which were described in following Table 5.15:

Table 5.15 Extraction parameters

<i>Pre-extraction</i>	<i>Soxhlet extraction</i>
Methanol (M)	Chloroform (C)
Methanol: acetone: water: dimethylformamide [40: 40: 18: 2] (MAWD)	Chloroform (C)
Methanol (M)	Chloroform: dichloromethane [1: 1] (CD)

5.2.5.5 Environmental Stress Applications

Selected three Cyanobacterial species were cultivated in the 100 ml BG11-N media in 250 ml flasks under the continuous light intensity of $100 \mu\text{E}/(\text{m}^2/\text{s})$ at 25°C by orbital shaking at 120 rpm speed. Sampling made on the day of the 5th and 10th days of incubation. Following environmental stress factors were chosen as experimental groups were described in following Table 5.16, based on the literature, to improve PHB production. Group-N used as the control group, which was incubated in the BG11-N medium (pH 7.1). The experimental groups were incubated at dark conditions with %0.4 acetic acid (AcOH) addition in BG11-N medium (pH 7.1) at 25°C temperature which was represented the main group-A, while pH was adjusted to 8.5 for the group-B and samples of the group-C were grown at the cold temperature ($+10^\circ\text{C}$).

Table 5.16 Environmental stress factors of experimental groups

<i>In BG11-N</i>	<i>Group -N</i>	<i>Group -A</i>	<i>Group -B</i>	<i>Group -C</i>	<i>Ref.</i>
%0.4 AcOH addition	-	+	+	+	[28], [31], [107]
Dark incubation	-	+	+	+	[100], [107], [28]
Basic pH (8.5)	-	-	+	-	[28]
Cold ($+10^\circ\text{C}$)	-	-	-	+	[66]

Results have been estimated by the sulphuric acid digestion method [98]. Also, the Greiner UV Star F Bottom 96 well microplate used for the comparison of quartz tubes, which had been used already for the sulphuric acid digestion method. The microplate has been measured at UV 235nm by the Microplate spectrophotometer (Multiskan GO).

5.2.5.5.1 Chlorophyll-a & Carotenoid Measurements

The protocol [102] was carried out as described above, especially for the determination of chlorophyll-a content of the Cyanobacterial cells to the investigation of the growth.

5.2.5.5.2 GC Measurements of FAME Products

The edited [108] [109] fatty acid methyl ester (FAME) extraction, transesterification, and Gas chromatography (GC) analysis of Cyanobacteria was started with harvesting 10 ml Cyanobacterial samples which placed in screw-capped tubes. Samples were centrifuged at 3000 g for 5 min, and then supernatants were discarded. 305 μ l extraction buffer (Table 5.17) added into the cells and incubated for 2 h at 80°C in Thermo-Shaker with 750 rpm. After samples were cooled to room temperature, 300 μ l 0.9% NaCl and 300 μ l hexane were added onto them and vortexed for 20 min. Samples were centrifuged (3000 g, 3 min, 20°C) and 150 μ l upper phases of hexane were transferred in snap vials. Helium gas was used as a carrier with a 1ml/min flow rate in DB-23 (Agilent, 60 m/0.25 mm/0.25 μ m) column of TRACE 1310 Gas Chromatograph (Fig. 5.19). The oven temperature was programmed at 120°C with 5 min hold, then 5°C increased up to 230°C with 275 FID temperature [108]. Supelco 37 component FAME mix (CRM47885) used as a FAME standard.

Table 5.17 FAME extraction buffer recipe

Extraction solution		+ Internal standard (5 μ l)	
Methanol	98 ml	Heptadecanoid acid	10 mg
H ₂ SO ₄	2 ml	Hexane	1 ml



Figure 5.18 Gas chromatography

5.2.5.6 Identification of PHB

The identification of PHB, which extracted by soxhlet extraction, was made by FTIR.

5.2.5.6.1 FTIR Analysis

PHB extracts were analyzed between 4000-400 cm^{-1} wavenumber range absorbance spectrums of the PerkinElmer Spectrum Two FTIR Spectrometer [89].

6.1 Sampling Parameters of Water

We investigated the dynamic water parameters like pH, conductivity, and total dissolved solids (TDS) temperature (Table 6.1). Paddy fields' conductivity levels were not so high, and the water temperature changed between 24.5-26.5°C on May, 29-37°C in June, 32.4-37.2°C in July. The measured temperature degrees were suitable for Cyanobacterial growth. The pH values of all samples were close to neutral pH, which were also favorable for Cyanobacterial growth.

Table 6.1 Dynamic properties of water samples

<i>Location</i>	<i>pH</i>			<i>Conductivity m/s</i>			<i>TDS mg/ L</i>			<i>Temperature °C</i>		
	<i>May</i>	<i>June</i>	<i>July</i>	<i>May</i>	<i>June</i>	<i>July</i>	<i>May</i>	<i>June</i>	<i>July</i>	<i>May</i>	<i>June</i>	<i>July</i>
<i>Enez</i>	7.3	8.2	7.8	1450	1700	1400	820	850	910	26.5	29.5	32.4
<i>Ipsala</i>	7.1	7.5	7.1	2020	1950	2065	1025	970	890	25.3	33.1	34.2
<i>Yeni Karpuzlu</i>	6.9	7.8	7.5	2350	2600	2400	980	1300	1520	24.5	36.7	34.5
<i>Balabancik Koyu</i>	7.1	8.1	7.9	1420	1240	1310	810	610	820	26.2	36.6	37.2
<i>Buyuk Mandira</i>	7.4	8.3	7.2	1070	1180	1480	630	580	505	24.5	29.4	33.5

The parameters of salinity and nitrogen forms, which are ammonium and nitrate, are essential for Cyanobacterial diversity. The low salinity levels promote Cyanobacterial growth and via Cyanobacterial growth, nitrogen forms as ammonium in paddy fields. Investigated salinity, ammonium, and nitrate parameters of paddy fields (Table 6.2) showed that ammonium levels were the dominate nitrogen forms for all sampling terms and the salinity levels were

suitable for Cyanobacterial growth on paddy fields with under the degree of 600 ppm, except for Buyuk Mandıra location with not significant importance.

Table 6.2 Salinity, ammonium and nitrate level of water samples

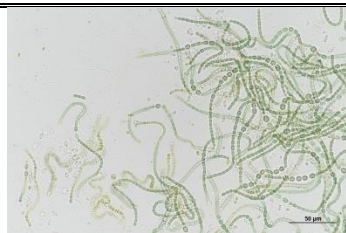
<i>Location</i>	<i>Salinity (ppm)</i>			<i>Ammonium (mg/L)</i>			<i>Nitrate (mg/L)</i>		
	<i>May</i>	<i>June</i>	<i>July</i>	<i>May</i>	<i>June</i>	<i>July</i>	<i>May</i>	<i>June</i>	<i>July</i>
<i>Enez</i>	360	420	580	4.8	11.8	18.5	0.65	0.8	0.85
<i>Ipsala</i>	410	620	480	6.2	22.4	28.7	4.2	4.5	2.3
<i>Yeni Karpuzlu</i>	280	470	510	3.2	11.2	10.3	1.2	0.7	1.4
<i>Balabancık Koyu</i>	510	470	560	7.1	26.3	21.4	0.8	3.2	1.1
<i>Buyuk Mandıra</i>	680	810	690	5.3	26.5	27.2	0.25	1.3	2.6





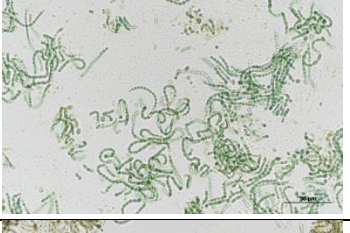
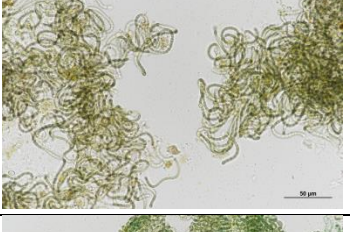

6.2 Isolation and Identification of Cyanobacteria


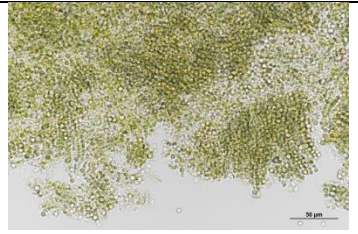

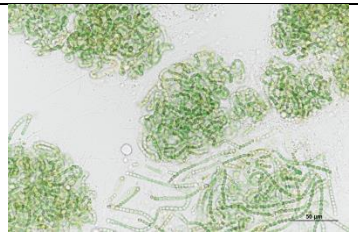
6.2.1 Purification and Selection of Nitrogen-Fixing Cyanobacteria

The nitrogen-fixing Cyanobacteria which were collected from paddy fields, selected and identified in family level by microscope imaging after the purification process, which based on morphological characteristics by classification key [110], as shown in Table 6.3:

Table 6.3 Classification of selected isolates based on microscope images (x40)

Nostocaceae	Ipsala	29-30 July	

Nostocaceae	Balabancik Koyu	07-09 June	
Nostocaceae	Enez	29-30 July	
Rivulariaceae	Ipsala	29-30 July	
Rivulariaceae	Enez	19-21 June	
Nostocaceae	Yeni Karpuzlu	19-21 June	
Nostocaceae	Balabancik Koyu	19-21 June	
Nostocaceae	Balabancik Koyu	29-30 July	

Nostocaceae	Ipsala	07-09 June	
Nostocaceae	Enez	19-21 June	
Rivulariaceae	Yeni Karpuzlu	21 May	
Rivulariaceae	Yeni Karpuzlu	21 May	

The selection of nitrogen-fixing Cyanobacteria from Istanbul Medeniyet University culture collection has been carried out on plates of the BG11/BG11-N medium (Fig. 6.1). BG11 (+), BG11-N (-N), and BG11-NP (-N-P) media tried to enhance PHB production (Table 6.4). Also, Z8 and Z8-N medium have been compared for the growth of all Cyanobacterium, too (Fig. 6.2). After all observations, we investigate that is the best medium for both Cyanobacterial growth and selection is BG11-N.

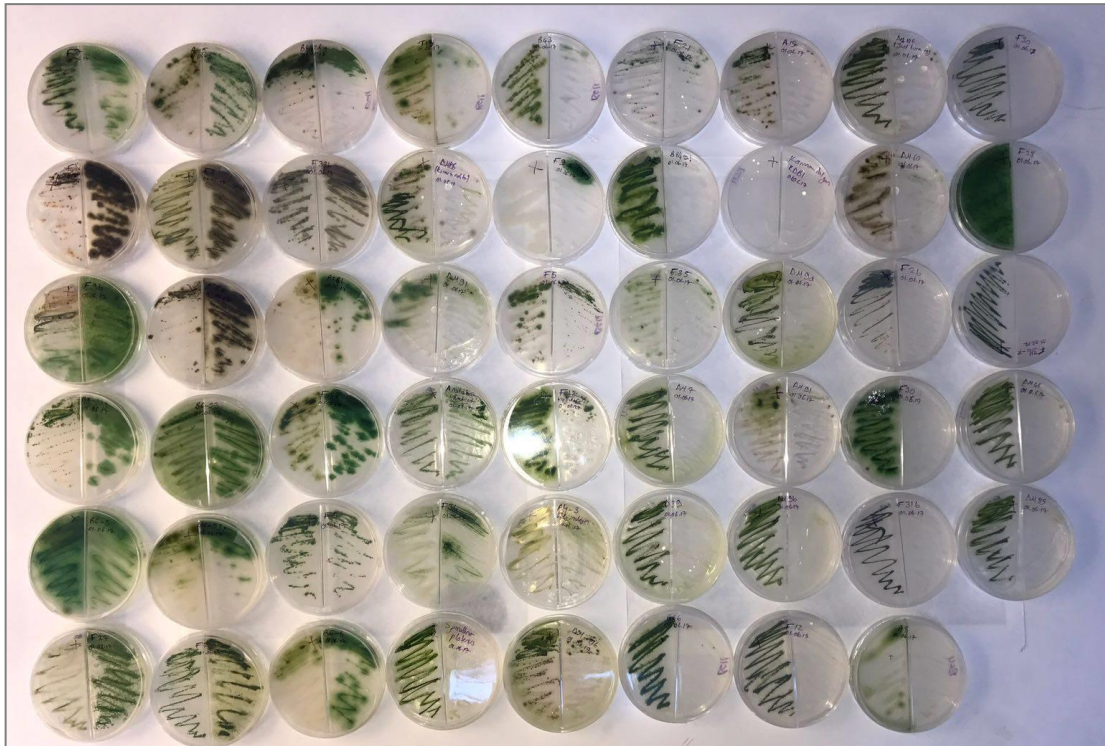


Figure 6.1 Selection of isolates on BG11 (Left side) and BG11-N (Right side) media in the same two-sided Petri dish

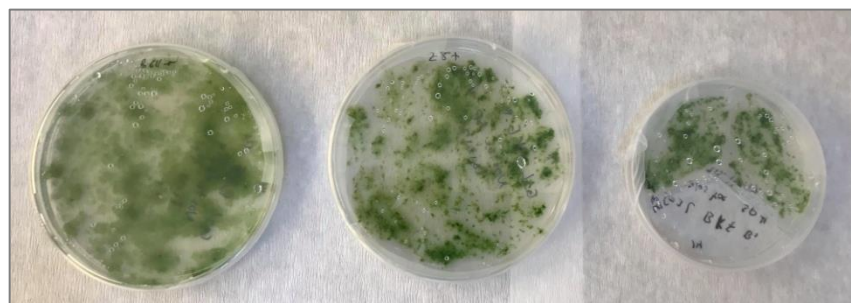





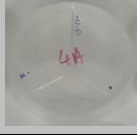

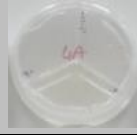

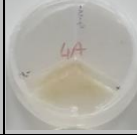
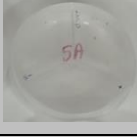




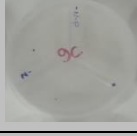




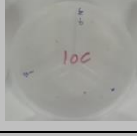




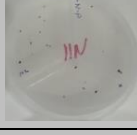





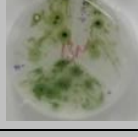



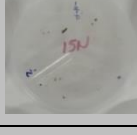

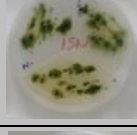

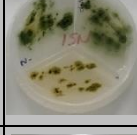
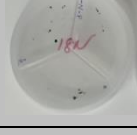

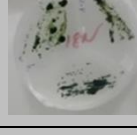

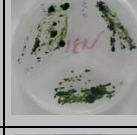





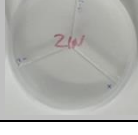
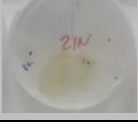



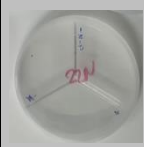

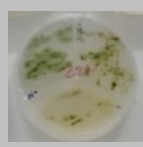



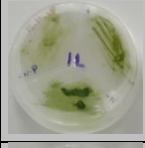
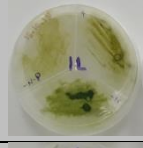
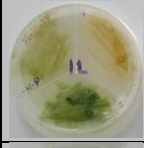
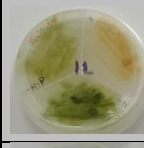

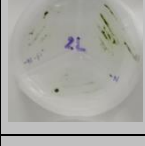

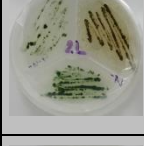
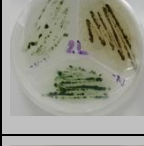

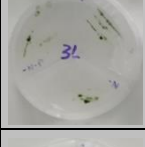

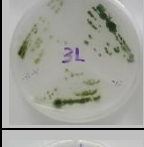
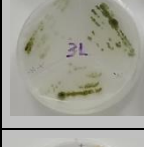
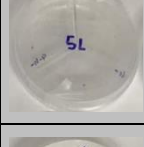
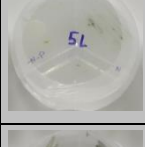
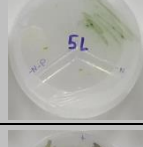
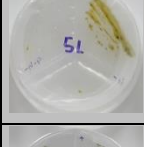
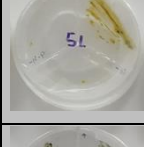
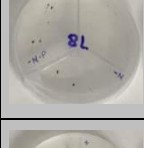
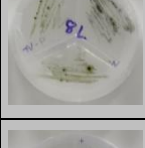

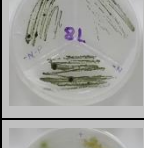
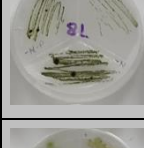
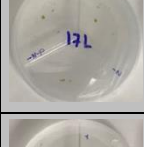
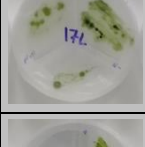
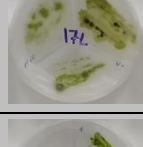
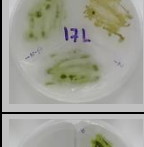
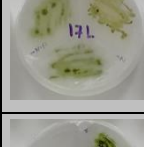
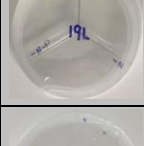
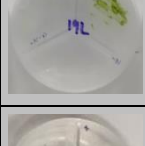


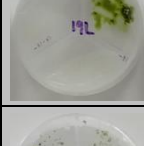

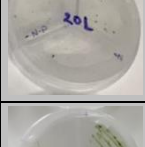
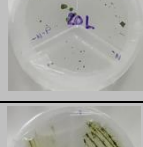
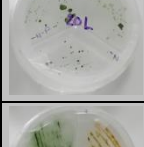


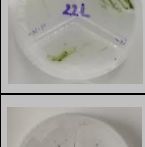
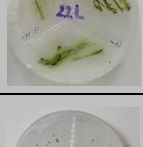
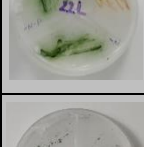



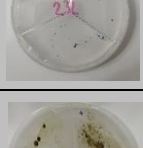







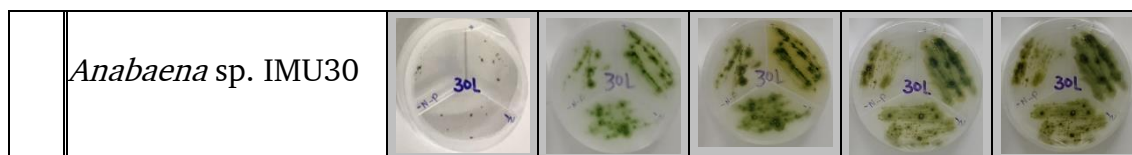


Figure 6.2 Growing rate on BG11-N, Z8-N, and Z8 media respectively

Table 6.4 BG11 (+), BG11-N (-N), and BG11-NP (-N-P) medium trial

<i>Species from Edirne paddy fields</i>	<i>Species Name*</i>	<i>0th</i>	<i>5th</i>	<i>10th</i>	<i>15th</i>	<i>20th</i>
	<i>Nostoc</i> sp. IMU02					
	<i>Cylindrospermum</i> sp. IMU04					
	<i>Cylindrospermum</i> sp. IMU05					
	<i>Calothrix</i> sp. IMU09					
	<i>Calothrix</i> sp. IMU10					
	<i>Nostoc</i> sp. IMU11					
	<i>Nostoc</i> sp. IMU13					
	<i>Nostoc</i> sp. IMU15					
	<i>Anabaena</i> sp. IMU18					
	<i>Nostoc</i> sp. IMU019					
	<i>Calothrix</i> sp. IMU21					

IMU culture library species	<i>Calothrix</i> sp. IMU22					
	<i>Nostoc</i> sp. IMU1					
	<i>Mastigocladus</i> sp. IMU2					
	<i>Chlorogloeopsis</i> sp. IMU3					
	<i>Nodosilinea</i> sp. IMU5					
	<i>Anabaena variabilis</i> sp. IMU8					
	<i>Nodularia</i> sp. IMU17					
	<i>Nostoc</i> sp. IMU19					
	<i>Nostoc</i> sp. IMU20					
	<i>Microchaete</i> sp. IMU22					
	<i>Anabaenopsis</i> sp. IMU23					
	<i>Trichormus</i> sp. IMU26					



*Named after identification

6.2.2 Genetic Identification of Nitrogen-Fixing Cyanobacteria

Genomic DNA is extracted from Cyanobacterial species by the phenol-chloroform method and the concentration of the DNA measured by nanodrop (Table 6.5).

Before PCR performing DNA amplification from genomic DNA containing a partial 16S ribosomal RNA region for Cyanobacterial species, all primers (Table 6.6) tried to find the best PCR products. With this aim, two species were chosen one from *Nostoc*, one from *Calothrix* species, and six primer groups were selected as pA-B23S (P1+2), pA-B23S-16S545R (P1+2+5), CYA108F- CYA16S SCYR(P3+4), CYA359F- CYA781R (P6+7), 27F- 27FR (P8+9), and 27F- 809R (P8+10) (Fig. 6.3). After PCR, two primer couples had shown the best bands for both species, which were CYA359F-CYA781R (P6+7) and 27F-809R (P8+10) primer couples. Also, CYA108F- CYA16S SCYR (P3+4) primer couples were worked for both species, but with the low band quality for especially *Calothrix* species besides these primes gave bands more than one for *Nostoc* species. CYA359F-CYA781R gave 200 bp (base pair) and 27F-809R gave 400 bp after PCR. 27F (Forward 27 : (AGAGTTTGATCMTGGCTC) and 809R (Reverse 809 : (GCTTCGGCACGGCTCGGGTCGATA)) primer couples were selected for the ability of amplification more base pairs which can help to investigate the genome of Cyanobacteria species more detailed.

Table 6.5 Nanodrop measurements

	<i>Species Name*</i>	<i>ng/μl</i>	<i>260/280</i>
<i>Species from Edirne paddy fields</i>	<i>Nostoc</i> sp. IMU02	79.05	2.08
	<i>Cylindrospermum</i> sp. IMU04	32.73	1.68
	<i>Cylindrospermum</i> sp. IMU05	10.38	1.39
	<i>Calothrix</i> sp. IMU09	83.04	1.64
	<i>Calothrix</i> sp. IMU10	04.77	1.73
	<i>Nostoc</i> sp. IMU11	42.54	1.85
	<i>Nostoc</i> sp. IMU13	99.62	2.01
	<i>Nostoc</i> sp. IMU15	98.75	1.40
	<i>Anabaena</i> sp. IMU18	80.64	2.05
	<i>Nostoc</i> sp. IMU019	72.12	2.07
	<i>Calothrix</i> sp. IMU21	20.26	1.93
	<i>Calothrix</i> sp. IMU22	66.83	2.03
<i>IMU culture library species</i>	<i>Nostoc</i> sp. IMU1	10.01	1.59
	<i>Mastigocladus</i> sp. IMU2	37.03	2.46
	<i>Chlorogloeopsis</i> sp. IMU3	47.48	1.67
	<i>Nodosilinea</i> sp. IMU5	46.09	2.19
	<i>Anabaena variabilis</i> sp. IMU8	67.74	1.95
	<i>Nodularia</i> sp. IMU17	28.60	1.79
	<i>Nostoc</i> sp. IMU19	15.93	1.93
	<i>Nostoc</i> sp. IMU20	52.66	1.94
	<i>Microchaete</i> sp. IMU22	32.73	1.97
	<i>Anabaenopsis</i> sp. IMU23	30.92	1.68
	<i>Trichormus</i> sp. IMU26	32.08	2.26
	<i>Anabaena</i> sp. IMU30	48.61	1.60

*Named after identification

Table 6.6 Primer order

Number	1	2	3	4	5	6	7	8	9	10
Primer	pA	B23S	CYA108F	CYA16S SCYR	16S545R	CYA359F	CYA781R	27F	27FR	809R

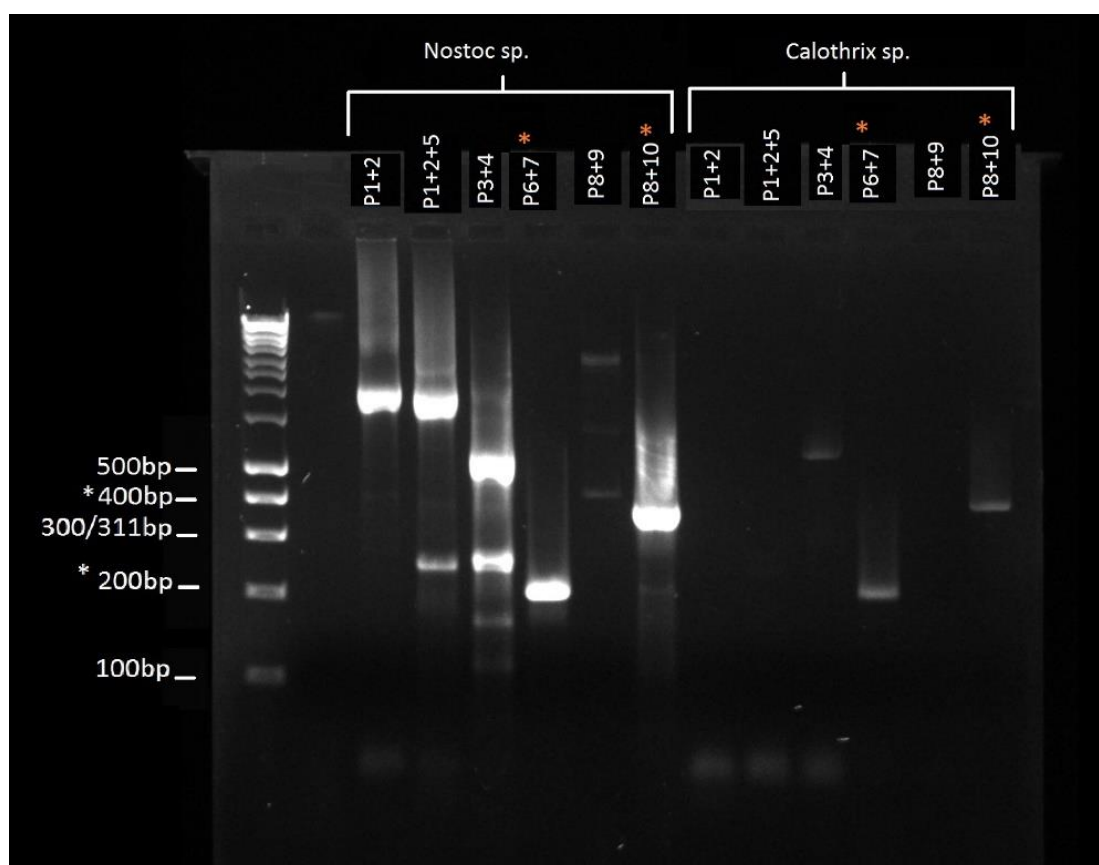


Figure 6.3 Selection of best primers on gel electrophoresis image

The extracted genomic DNA of Cyanobacteria species by the phenol-chloroform method was used for PCR amplification by using the 27F and 809R primers, then gel electrophoresis was employed (Fig 6.4).

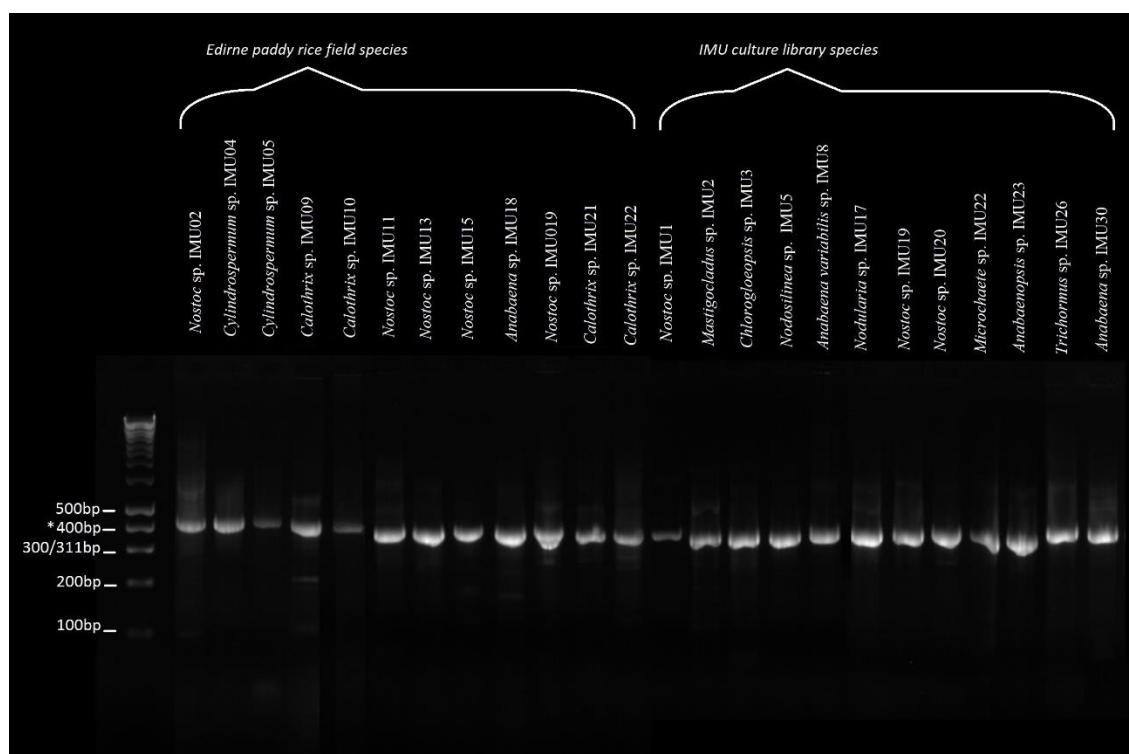

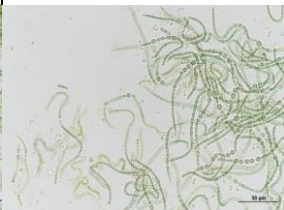



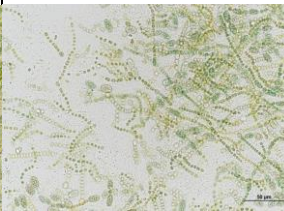

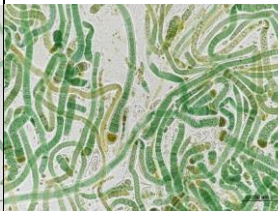


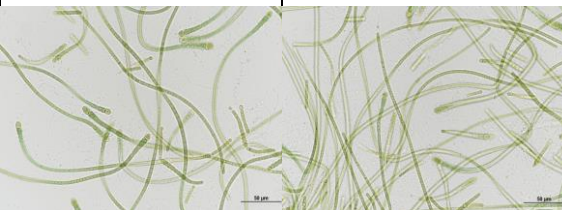
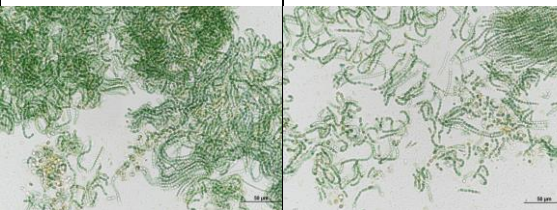
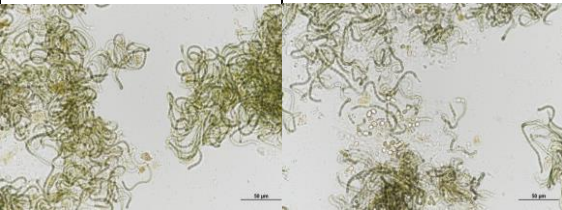
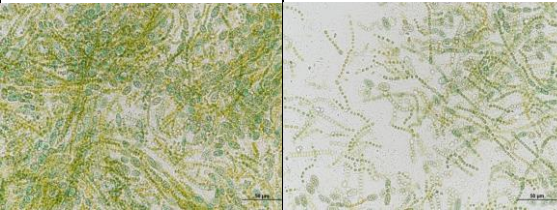
Figure 6.4 Gel electrophoresis image of Cyanobacteria species




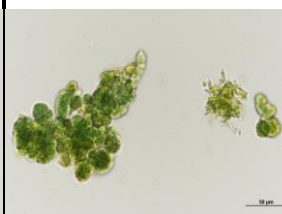
*Named after identification

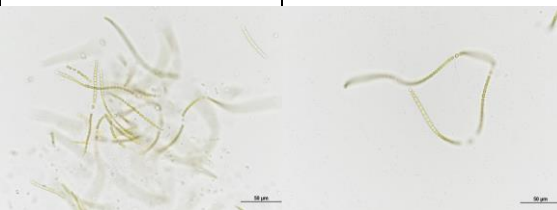
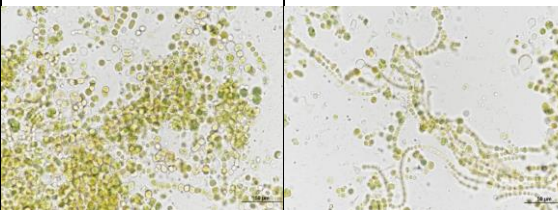
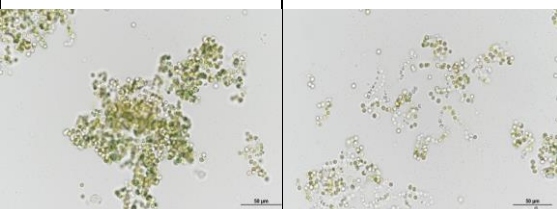

After amplification, 16S rRNAs of Cyanobacteria and 27F-809R primers were sent to Sentromer DNA technology limited company (©2009-2020 <https://www.sentromer.com/>) for Sanger sequence analysis. Results investigated on Chromas v2.6.4 and the nucleotide sequences were analyzed on the NCBI database. As a final point, BLASTn search (<https://blast.ncbi.nlm.nih.gov/Blast.cgi>) results were used for the identification. Genomic and morphologic information results of diazotrophic Cyanobacteria were summarized in the following Table 6.7:

Table 6.7 Genomic and morphologic information of identified Cyanobacteria

											
Name/Family:			<i>Nostoc</i> sp. IMU02 / Nostocaceae			Name/Family:			<i>Cylandrospermum</i> sp. IMU04 / Nostocaceae		
Location:			Ipsala Paddy Field / 40.9557680 N 26.4117180 E			Location:			Balabancik Koyu Paddy Field / 41.0402400 N 26.4005100 E		
Harvester:			Muhammad Haddad, Tuğba Dayioğlu, Turgay Çakmak, Zeynep Elibol Çakmak			Harvester:			Muhammad Haddad, Tuğba Dayioğlu, Turgay Çakmak, Zeynep Elibol Çakmak		
Harvesting date:			29-30 July 2017			Harvesting date:			07-09 June 2017		
Sequence info:			GAATCTWKCCTTCAGGTCGGGATAACTACTGGAACG GTGGCTWATACCGGATGTGCCGAAAGGTGAAAGGYT WGCCTGCCTGAAGATGARCTCGCGTCTGATTAGCTAGT TGGTGTGTAAGAGCGCACCAAGCGGACGATCAGTAR CTGGTCTGARAGGATGATCAGCCACACTGGGACTGAR ACACGGCCAGACTCTACGGGAGGCAGCAGTGGGG AATTTTCGCAATGGGCGAAAGCCTGACGGARCAATA CCGCGTGAGGGARGAAGGCTCTTGGGTTGTAAACCTC TTTTCTCAAGGAATAASTTC			Sequence info:			KCTGGCTTCMGGTCGGGACACAGTTGGAAACGACT GCTAATACCGGATATGCCGAGAGGTGAAAGATTAAAT GCCTGGAGATGARCTCGCGTCTGATTAGCTAGTTGGT GGGGTAAGARCCTACCAAGGSGACGATCAGTAGCTGG TCTGARAGGATGATCAGCCMCAGCTGGGACTGARACAC GGCCCARACTCTACGGGAGGCAGCAGTGGGGAAATTT TCCSCAATGGGCGAAAGCCTGACGGARCMATACSCG TGAGGGAGGAAGGCTCTTGGGTCGTAACCTCTTTTC TCAGGAAAAAATGACGGTACCTGAGGAATAAGC ATCSGCTAATCCGTG		
NCBI Accession			MN649241			NCBI Accession			MN653635		
Project info			TAGEM/16/AR-GE/44			Project info			TAGEM/16/AR-GE/44		
EMBL / Gen Bank No			Name of the strain			Homology			EMBL / Gen Bank No		
Name of the strain			<i>Nostoc spongiaeforme</i> FACHB-130			Homology			Name of the strain		
JX872517.1			96%			Homology			<i>Cylandrospermum</i> sp. ACSSI 043		
KY283043.1			91%								
											
Name/Family:			<i>Cylandrospermum</i> sp. IMU05 / Nostocaceae			Name/Family:			<i>Calothrix</i> sp. IMU09 / Rivulariaceae		
Location:			Enez Paddy Field / 40.722994 N 26.093973 E			Location:			Ipsala Paddy Field / 40.9557680 N 26.4117180 E		
Harvester:			Muhammad Haddad, Tuğba Dayioğlu, Turgay Çakmak, Zeynep Elibol Çakmak			Harvester:			Mohammad Haddad, Tuğba Dayioğlu, Turgay Çakmak, Zeynep Elibol Çakmak		
Harvesting date:			29-30 July 2017			Harvesting date:			29-30 July 2017		
Sequence info:			GAGTAACGCGTGARAATTTGGCTTCAGGTCGGGGACA ACCACTGGAAACGGKGGCTAATACCGGATATGCCGAR AGGTGAAAGGSTTGTGCTGAARATAARCTCGCGTC TGATTAGCTAGTTGGTGGGTAAGARCCCTACCAAGGC GACSATCAGTAGCTGGTCTGARAGGATGATCAGCCMC ACTGGGACTGARACACGGCCCARACTCTACGGGAGG SAGCAGTGGGGAATTTTCCSAAATGGGCGAAAGCCTG ACGGARCAATACCGCGTGAGGGARGAAGGSTCTTGGG TCGTAAACCTCTTTTCTCAGGGAAAAAAGGATGACG GTACCTGARGAAGAAGCATCGGCTAATCCGTGCCAG CAGCCGCGGTAAATACGGAGGATGCAAGCGTTATCCGG AATGATTGGGCGTAAAGGTCGCGAGGTGGTACTGTA AGTCTGCTGTTAAARAGCAAGGCTCMACCTTGTAAAA GCGGKGAAACTACARAA			Sequence info:			TAGCTAGTTGGTGKGGTAAGARCGCACCMAGGCGAC GATCAGTAGCTGGTCTGARAGGATGATCAGCCMCAGT GGGACTGAGACACGGSCCAGACTCTACGGGAGGCAG CAGTGGGGAATTTTCCGCAATGGGCGAAAGCCTGACG GARCAATACCGCGTGARGGAGGAARGCTCTTGGGTTG TAAACCTCTTTTCTCMR		
NCBI Accession			MN653634			NCBI Accession			MN653639		
Project info			TAGEM/16/AR-GE/44			Project info			TAGEM/16/AR-GE/44		
EMBL / Gen Bank No			Name of the strain			Homology			EMBL / Gen Bank No		
Name of the strain			<i>Cylandrospermum</i> sp. NIES-4074			Homology			Name of the strain		
AP018269.1			92%			Homology			<i>Calothrix</i> sp. 9-SKD-2014		
LC011972.1			95%								

					
Name/Family: <i>Calothrix</i> sp. IMU10 / Rivulariaceae			Name/Family: <i>Nostoc</i> sp. IMU11 / Nostocaceae		
Location: Enez Paddy Field / 40.722994 N 26.093973 E			Location: Yeni Karpuzlu Paddy Field / 40.8599640 N 26.3224540 E		
Harvester: Mohammad Haddad, Tuğba Dayioğlu, Turgay Çakmak, Zeynep Elibol Çakmak			Harvester: Mohammad Haddad, Tuğba Dayioğlu, Turgay Çakmak, Zeynep Elibol Çakmak		
Harvesting date: 19-21 June 2017			Harvesting date: 19-21 June 2017		
Sequence info: AKSSGAKGCTTACCATGCAAGTCGAACGGTCTCTTCGG AGATAGTGGCGGACGGGTGAGTAACGCGTGAGAATCT AGCTCTAGGTCTGGGACAACCATTTGAAACGGTGGST AATACTGGATGTGCCGAGAGGTGAAAGGCTTGTGCC TAGAGATGAGCTTCCGTTCAGATTAGCTAGTAGGTGTG GTAARGGCGCACCTAGGCGACGATCTGTAGCTGGTCT GARAGGACGATCAGCCACACTGGAACGARACACGGT CCAGACTCCTACGGGAGGACGAGTGGGGAAATTTCC GCAATGGGCGAAAGCCTGACGGARCAATACCGCGTGA GGGAGGAAGGCTCTTGGGTTGTAAACCTCTTTTCTCA AGGAAGATAATGACGGTACTTGAGGAATAAGCATCGG CTAACTCCGTGCCAGCAGCCGGTAATACGGAGGAT GCAAGCGTTATCCGGAATGATTGGGCGTAAAGCGTCC GCAGGTGGTTTAAAGATCTGTGTAAAGAGTGAGG CTTAACCTCATAAGGGCAATGGAACCTGCTGAACCTAG AGTACGTTCCGGGCAAGGGGAATCCAGTGATGCGG TGAAATGCGTAGAGATTGGGAAGAACCGGTGGCGA AAGCGCTTGCTAGGCCGTAACCTGACACTGAGGACG AAAGCTAGGGGAGCGAATGGGATTAGATACCCAGTA GTCCTAGCCGTAACGATGGATACTAGGCGTTGTCTG TATCGACCCGAGCCGKKGCCSAARAMCAA			Sequence info: ACTGGAACGGKGGCTAATACCRGATGTGCCRAGAGG TGAAAGGCTTKCTGCCTGAAGATGARCTCGGCTCTGA TTAGTAGTGTGGTGTGGTAAGAGCSCACCARGGCSAC KATCARTAKCTGGTCTGARARGATGATCASCNCWCCT GGGACTGARACACSGCCASACTCTACGGGAGGCMG CWGTGGGGAATTTCCSCARTGGGCRAAASCTGACR GARCAATACCGCGT		
NCBI Accession MK929008			NCBI Accession MK929013		
Project info TAGEM/16/AR-GE/44			Project info TAGEM/16/AR-GE/44		
EMBL / Gen Bank No	Name of the strain	Homology	EMBL / Gen Bank No	Name of the strain	Homology
HE974991.1	<i>Calothrix parietina</i> CCAP	96%	KX913930.1	<i>Nostoc carneum</i> MBDU 015	89%
					
Name/Family: <i>Nostoc</i> sp. IMU13 / Nostocaceae			Name/Family: <i>Nostoc</i> sp. IMU15 / Nostocaceae		
Location: Balabancık Koyu Paddy Field / 41.0402400 N 26.4005100 E			Location: Balabancık Koyu Paddy Field / 41.0402400 N 26.4005100 E		
Harvester: Mohammad Haddad, Tuğba Dayioğlu, Turgay Çakmak, Zeynep Elibol Çakmak			Harvester: Mohammad Haddad, Tuğba Dayioğlu, Turgay Çakmak, Zeynep Elibol Çakmak		
Harvesting date: 19-21 Jun 2017			Harvesting date: 29-30 July 2017		
Sequence info: GGGTGAGTAACGCGTGAGAATCTAGCTCTAGGTCCGG GACAACCACTGGAAACGGTGGCTAATACCGGATGTGC CSAGAGGTAAAGGCTTGTGCTARAGATGARCTCS CGTCTGATTAGCTAGTARGTGTGGTAAGARGCGACCT AGGCGACGATCAGTAGCTGCTGARAGGATGATCAG CCACACTGGGACTGARACACGGCCAGACTCCTACGG GAGGCAGCAGTGGGGAATTTCCGCAATGGGCGAAAG CCTGACGGARCAATACCGCGTGAGGGAGGAAGGCTCT TGGGTTGTAAACCTCTTTTCTCAGGGAATAAAAAATG AARGTACCTGAGGAATAAGCATCGGCTAACTCCGTGC CMGCAGCCSCGGTAATACGGARGATGCAAGCGTTATC CSGAATGATTGGGCGTAAAGGGTCCSAGGTGGCCCT GTA			Sequence info: TWACGCGTGAGAATCTARCTCTAGGTCCGGGACMAC CACTGGAACCGGTGGCTAATACCGGATGTGCCGAAAG GTGAAAGATTATTGCCTAGARATGARCTCGGCTCYG ATTARCTWGTGGGTGGTAAGARGCGACCAAGGCG ACGATCAGTASCTGGTCTGARARGATGAWCRGCCACA CTGGGACTGARACACGGCCARACTCCTACGGGAGGY MGCAGTGGGGAATTTCCGSAATGGGSGAAAGCCTGA CSGASCAATACCGCGTGAGGGARGAAGGSTCTTGGGK TGTAACCTCTTTTCTCAGGGAATAAAAAATGAAGGT ACCTGAGGAATAAGCATCGGCTAACTCCGTGSCAGCA GCCGCGGTAATACSGAGGATGCMAGCGTTATCCGGA TGATTGGGCTAAAGCGTCCGAGGTGGCACTGTAAG TCTGCTGTTAAAGARCAAGGCTCAACCTTGTAAAGGC AGTGGAACACTACMGARCTAGAGTACGTTCCGGGCG ARGGAATTCCTGGTGTAGCGGTGAAATGCGTAGAGAT CAGGAAGAACCCGGTGGCGAAAGCGCTCTGCTAGGC CGTAAC		
NCBI Accession MK928973			NCBI Accession MN653636		
Project info TAGEM/16/AR-GE/44			Project info TAGEM/16/AR-GE/44		
EMBL / Gen Bank No	Name of the strain	Homology	EMBL / Gen Bank No	Name of the strain	Homology
AB087403.2	<i>Nostoc</i> sp. KU001	97%	KX442796.1	<i>Nostoc</i> sp. IPPAS B-1212	94%

					
Name/Family:	Anabaena sp. IMU18 / Nostocaceae		Name/Family:	Nostoc sp. IMU019 / Nostocaceae	
Location:	Ipsala Paddy Field / 40.9557680 N 26.4117180 E		Location:	Enez Paddy Field / 40.722994 N 26.093973 E	
Harvester:	Mohammad Haddad, Tuğba Dayioğlu, Turgay Çakmak, Zeynep Elibol Çakmak		Harvester:	Mohammad Haddad, Tuğba Dayioğlu, Turgay Çakmak, Zeynep Elibol Çakmak	
Harvesting date:	07-09 June 2017		Harvesting date:	19-21 June 2017	
Sequence info:	AGTAACGCGTGAGAATCTAGCTTCAGGTCGGGGACAA CCACTGGAAGCGGTGGCTAATACCGGATGTGCCGAAA GGTGAAARATTTATTGCCTGAAGATGARCTCGCGTCT GATTAGCTAGTTGGTGTGGTAAGARCGCACCMAGGSG ACGATCAGTAGCTGGTCTGARAGGATGATCAGCCACA CTGGGACTGARACACGSGCCARACTCCTACSGGAGGS AGCAGTGGGGAATTTCCGCAATGGCGGAAAGCCTGA CGGARCAATACCGCGTGAGGGAGGAAGGSTCTTGGGT TGTAACCTCTTTTCTCAGGGAATAAAAAATGAARGT ACCTGARGAATAAGCATCGGCTAACTCCSTGCCMGCA GCCGCGGTAATACGGARGATGCAAGCGTTATCCGGAA TGATTGGGCGTAAAGCGTCCGAGGTGGCACTGTAAG TCTGCTGTTAAAGARCAAGGCTCAACCTTGTAAGGC AGTGGAACACTACAGARCTAGAGTACGTTCCGGGCGA GGGAATTCCTGTGTARCGGTGAAATGCGTAAARATC ARGAAGAACACCGGTGGCGAAAGCGCTCTGCTAGGCC GTAAGTGA		Sequence info:	CTACTGGGGTATCTAATCCCATTCGCTCCCTARCTTT CGTCCCTCAGCGTCAGTTACGGCCYAGTAGCACGCTT TCSCCACCGGTGTTCTTCTGATCTCTACGCAITTCAC CGTACACCAAGAAATTCCTGCTACCCCGAAACGCACTC TAGCTCTGTAGTTTCCACTGSTCTTATGAGGTTAAGCC TCACTCTTTAAACAGCAGAMTTACAGGGCCACCTGSGG ACCCTTTACGCGCAATCATTCGGGAWAACGCTTGSAT CCTCCGTATTACCGCGGCTGCTGGSACGGAGTTAGCC GAWGCTATTTCCTCAGGTACCTTCAITTTTTTATTCCC TGARAAAARAGGTTTACAACCCAARARCCTTCCYCCY CACGCGGTATTGCTCCGTGAGGTTTCCSCCATTTGSGG AAAATTCGCCACTGSTGCCTCCGTAGGARTCTGGGC CGKGTCTCAGTCCACG	
NCBI Accession	MK929012		NCBI Accession	MN866121	
Project info	TAGEM/16/AR-GE/44		Project info	TAGEM/16/AR-GE/44	
EMBL / Gen Bank No	Name of the strain	Homology	EMBL / Gen Bank No	Name of the strain	Homology
AP018216.1	Anabaena variabilis NIES-23	96%	AM711525.1	Nostoc sp. PCC 8976	95%
					
Name/Family:	Calothrix sp. IMU21 / Rivulariaceae		Name/Family:	Calothrix sp. IMU22 / Rivulariaceae	
Location:	Yeni Karpuzlu Paddy Field / 40.8599640 N 26.3224540 E		Location:	Yeni Karpuzlu Paddy Field / 40.8599640 N 26.3224540 E	
Harvester:	Mohammad Haddad, Tuğba Dayioğlu, Turgay Çakmak, Zeynep Elibol Çakmak		Harvester:	Mohammad Haddad, Tuğba Dayioğlu, Turgay Çakmak, Zeynep Elibol Çakmak	
Harvesting date:	21 May 2017		Harvesting date:	21 May 2017	
Sequence info:	TTGGAAACGGYGGCTAATACYGGATGTGCCAGAGGTT RAAAGGYTTGCTGCCTGAAGATKAGCTCSGCTCTGATT ARCTAGTWGGWGTGGTAASAGCGCACCTAGGCGACG ATCWGTASCTGGTCTGARAGGATGAYCAGSCACACTG GGAAGTACAGACCGGYCCAGACTCTACGGGAGGCAGC AGTGGGGAATTTCCGCAATGGGCGAAAGCCTGACGG ARCAATACCSGCTGAGGGAGGAAGGSTYTTGGGTTGT AAACCYCTTTTCTCASGGAATAAKTTCTGAAGGTACCT GARGAATCMGCATCGGCTAAGTCCGTGCCAGCAGCCG CGGTAATACSGAGGATGCMAGCGTTATCCGGAATGAT TGGGCGTAAAGCGTCCGAGGTGGYWWKAAAGTCT GCTGTTAAAGAGTGAGGCTTAACCTCATAAARGCAGT GGAAACTACATGARCTAGAGTGCGGTGCGGGYAGARG GAATTCYVGTGTAGCGGTGAAATGCGTAGAKATYRG GAAGAACACCRGTGGCGAAAGCGCTYTRCTRGGYCKS MACTGACACTGAGGAGCAAAAGCTAGGGGAGCGAAT GGGATTAGATACCCC		Sequence info:	TAACGCGTGAGAATCTGTMTTCAGGTGCGGGACAA CACTTGAAGATGACTGCTAATACCGGATGTGCCSAAAGG TGAAAGATTTATTGCTCGAATTTGAGCTCGCGTCMGA TTAGCTAGTWGGTGGGTGAAGARACTACTAGGCATC GATCTGTAGCTGGTCTGARAGGACGATCAGCCACACT GGRACCTGARACACGCTCCAGACTCCTACGGGAGGSAG CAGTGGGGAATTTCCGCAATGGGCGAAAGCCTGACG GARCAATACCGCGTGAGGGACGAAGGCYTTGGGTYG TAAACCTCTTTTCTCAAGGAAGAWTTWSACRGRKCTT GAGGAAWAAGCATCGGCTAAMTCTGTGCCMGACGCC SCGGTAATACAGAGGATGCRMGCGTTWTCCSGAATG ATTGGGCGTAAARCGTCCSCASGTGTTTWWAARTC TGCTGTTWAAGCGTGTGGCTCAACCMCMTACAGGSG GTGAAACTATRAGACTAGAGTATGTTAKGGGTAGA GGGAATTCYCMGTGTAGCGGTGAAATGCGTAGAGATT GGGAARAAMACCGGTGGCGAAAGCGCTCTGCTA	
NCBI Accession	MN865212		NCBI Accession	MN865214	
Project info	TAGEM/16/AR-GE/44		Project info	TAGEM/16/AR-GE/44	
EMBL / Gen Bank No	Name of the strain	Homology	EMBL / Gen Bank No	Name of the strain	Homology
KM019924.1	Calothrix membranacea SAG1410-1	90%	FJ661021.1	Calothrix sp. PCC 7103 isolate DBSU 2	91%

					
Name/Family:	<i>Nostoc</i> sp. IMU1 / Nostocaceae		Name/Family:	<i>Mastigocladus</i> sp. IMU2 / Hapalosiphonaceae	
Location:	Aygir Lake-Suphan / 38.838416 N 42.822410 E		Location:	Meliksah Hot spring / 40.164102 N 32.944384 E	
Harvester:	Turgay Çakmak, Zeynep Elibol Çakmak		Harvester:	Turgay Çakmak, Zeynep Elibol Çakmak	
Harvesting date:	May 2014		Harvesting date:	June 2017	
Sequence info:	AGTGGCGGACGGGTGARTAACGCGTGAGAATCTARCTCAGGTGCGGGATAACTACTGGAAACGGTGGCTAATACCGGATGTGCCGAAAGGTAAAGGCTTGTGCCTGAAATGARTCGCGCTCTGATTAGCTAGTTGGTGTGGTAAAGCGCACCAAGGCGTCSATCAGTAGCTGGTCTGARAAGATGATCAGCCACACTGGGACTGARACACGGCCCARACTCCTACGGGAGGCAGCAGTGGGGAATTTCCGCAATGGGCGAAAGCCTGACGGARCAATACCGCGTGAGGGAGGAAGGCTCTTGGGTGTAAACCTCTTTTCTCAAGGAATAAAAAATGAAGGKACTTGAGGAATAAGCATCGCTAACTCGGTGCCAGCAGCCGGTAATACGGAGGATGCAAGCGTTATCCGGAATGATTGGCGTAAAGCGTCCGCAGGKGCATGTAAGTCTGCTGTAAAGAGCAAAGCTTAACCTTTGAAAAGCAGTGGAACCTACATAGCTAGAGTACGTTTCGGGGCARARGGAATTCTGGTGTAGCGGTGAATGCGTARAGATCAGGAAGAACACCGGTGGCGAARGCGCTCTGCTAGGCCGTAACCTGACACTGAGGGACGAAAGCTAGGGGA		Sequence info:	TAACGCGTGAGAATCTAACTTCMGGTTCGGGACAACMTTGGGAAACCGATGCTAATACCGGAWGTGCGTGAAGTGAAAGGCTTGTGCCTGAAATGARCTCGCGTCTGATTARCTAGTTGGTAGTGAAGGGACTACCAAGGCGACATCATARCTGGTCTGARAGGATGATCAGCCMCMCTGGAACCTGARACACSGTCCAGACTCTACGGGAGGCAGCAGTGGGGAATTTCCSAAATGGGCGAAAGCCTGACGGARCAATACCGCGTAGGGARGAAGGCTCTTGGGTGTAAACCTCTTTTCTCA	
NCBI Accession	MK929009		NCBI Accession	MN865220	
Project info	TAGEM/12/AR-GE/13 - TAGEM/16/AR-GE/44		Project info	TAGEM/12/AR-GE/13 - TAGEM/16/AR-GE/44	
EMBL / Gen Bank No	Name of the strain	Homology	EMBL / Gen Bank No	Name of the strain	Homology
CP003548.1	<i>Nostoc</i> sp. PCC 7107	98%	KM376998.1	<i>Mastigocladus laminosus</i> PUPCCC 515.6	94%
					
Name/Family:	<i>Chlorogloeopsis</i> sp. IMU3 / Chlorogloeopsidaceae		Name/Family:	<i>Nodosilinea</i> sp. IMU5 / Prochlorotrichaceae	
Location:	Dutlu Hot spring 40.153854 N 31.904695 E		Location:	Malikoy Hot spring 39.763197 N 32.390247 E	
Harvester:	Turgay Çakmak, Zeynep Elibol Çakmak		Harvester:	Turgay Çakmak, Zeynep Elibol Çakmak	
Harvesting date:	Jun 2017		Harvesting date:	June 2017	
Sequence info:	TAACGSGTGAGAATCTARCTTCAGGTCSGGGACMACCCTGGAAACGGTGGCTAATACCGGATGTGCCGAAAGGTGAAAGATTTATTGCGCTGAAGATGARCTCGCGTCTGATTAGCTAGGTGTGGTAAGAGCGCACCTAGGCGACGATCAGTAGCTGGTCTGARAGGATGATCAGCCACACTGGGACTGARACACGGCCAGACTCTACGGGAGGCAGCAGTGGGGAATTTCCGCAATGGGCGAAAGCCTGACGGARCAATACCGCGTGAGGGAGGAAGGSTCTTGGGTGTAAACCTCTTTTCTCAGGGAATAAAAAATGAAGGTACCTGAGGAATAAGCATCGGCTAACTCCGTGCCAGCAGCGCGGTAATACGGARGATGCAAGCGTTATCCGGAATGATTGGCGTAAAGGGTCCGAGGTGGCAATGTAAGCTGTCTGTTAAAGAATGAGGCTCAACCTCATACAGCAGTGGAACCTACATAGCTAGAGTGCCTTCGGGGTAGARGAATTYCTGGTGTAGCGGTGAAATGCGTAGATATCAGGAAGAACCCGGTGGCGAAAGCGCTCTACTAGGCCGCAACTGACACTGAGGGACGAAAGCTAGGGGA		Sequence info:	CTACAGGGGTATCTAATCCCTTCGCTCCCTAGCTTTTCGTCCTCAGCGTCAGTTGTGGCCAGTAGAGCGCCTTCGCCACTGGTGTCTTCCCGATATCTAGCATTTCACCGCTACACCGGGAATTCCTCTACCCCTACACACTCAAGTTCCCGATTTCCATTGSCGATCCACAGTTGARCTGTGACCTTTGACAACAGACTTAARAAACCGCCTGSGGACGCTTTAGCCCCAATAATTCGGAWAACGCTTGSCCTCTCCGTCTTACCGCGGCTGTGGCAGCGAGTTAGCCGAGGCTTATTCCTCTGGKACCGCTCAGTTCTTCTCCAGARAAAAAGGTTTACAACCCCTAAGGSCCTCTCCCTCAACCGCGCTTGTCCGTGAGGTTGSGCCCAATTGSGGAATTCCTCCACTGCTGCTCCGTARGARTCTGGGCCGTGTCTCARTCCAGTGTGGSTGAWCATCTCTTARAACAGCTACTGATCGTCGCTTGTGAGCCCTTACCTCACCAACTARCTAATCAGAMGCGAGTTTCATCTCAGGSCATAAATGTTTCACTCTCGGCACATTGGGTATTARCCACCGTTTCCMGTTGGKTGKCCCC	
NCBI Accession	MN865249		NCBI Accession	MN865219	
Project info	TAGEM/12/AR-GE/13 - TAGEM/16/AR-GE/44		Project info	TAGEM/12/AR-GE/13 - TAGEM/16/AR-GE/44	
EMBL / Gen Bank No	Name of the strain	Homology	EMBL / Gen Bank No	Name of the strain	Homology
JN166685.1	<i>Chlorogloeopsis</i> sp. GSP606-1	97%	KF246481.1	<i>Nodosilinea</i> sp. CENA512	95%

					
Name/Family:	<i>Anabaena variabilis</i> sp. IMU8 / Nostocaceae		Name/Family:	<i>Nodularia</i> sp. IMU17 / Aphanizomenonaceae	
Location:	Hidirlar Hot spring / 39.839879 N 27.160581 E		Location:	Hidirlar Hot spring / 39.839879 N 27.160581 E	
Harvester:	Turgay Çakmak, Zeynep Elibol Çakmak		Harvester:	Turgay Çakmak, Zeynep Elibol Çakmak	
Harvesting date:	Jun 2017		Harvesting date:	Jun 2017	
Sequence info:	GGGTGARTAACGCGTGAGAATCTACATTYAGGTCGGG GACAACCACTGGAAACGGTGGCTAATACCGGATGTGC CGAGAGGTAAAGGTTGCCGCTGARAATGAGCTCG CGTCTGATTAGCTAGTTGGGGTGTAAAGARACCA AGGCGACGATCAGTAGCTGCTGARAGGATGATCAG CCACACTGGGACTGARACACGCCAGACTCCTACGG GAGGCAGCAGTGGGGAATTTCCGCAATGGCGAAAG CCTGACGGARCAATACCGCGTGAGGGAGGAAGGCTCT TGGGTTGTAAACCTCTTTTCTCAGGGAAGAAAAAAT GACGGTACCTGAGGAATAAGCATCGGCTAAGTCCGTG CCAGCAGCCGCGTAAATACGGARGATGCAAGCGTTAT CCGGAATGATTGGGCGTAAAGGTCGCGAGGTGGCAC TGTAAGTCTGCTGCAARARCAAGGSTCAACCTTGTA AAGGCAGTGGAACTACAGAGCTAGAGTACGTTCCGG GCAGAAGGAATTCCTGGTGTAGCGGTGAATGCGTAG AGATCAGGAAGAACACCGGTGGCGAAAGCGTTCTGCT AGGCCTGTACTGACACTGAGGACGAAAGCTAGGGGA GCGAATGGGATTAGATACCC		Sequence info:	GGGTGAGTAACGCGTGAGAATCTGGCTTCAGGTCGGG GACAACCACTGGAAACGGTGGCTAATACCGGATATGC CGAGAGGTGAAAGATTAATTGGCTGAAGATGAGCTCG CGTCTGATTAGCTAGTTGGGAGTGAAGARACTACCA AGGSGACGATCAGTAGCTGGTCTGARAGGATGATCAG CCACACTGGGACTGARACACGCCAGACTCCTACGG GAGGCAGCAGTGGGGAATTTCCGCAATGGCGAAAG CCTGACGGARCAATACCGCGTGAGGGAGGAAGGCTCT TGGGTTGTAAACCTCTTTTCTCAGGGAAGAAAAAAT GACGGTACTTGAGGAATAAGCATCGGCTAAGTCCGTG CCAGCAGCCGCGTAAATACGGAGGATGCAAGCGTTAT CCGGAATGATTGGGCGTAAAGGTCGCGAGGTGGCTG TGAAAGTCTGCTGTTAAAGATGAGGCTCAACCTCAT CAGARCACTGGAACTACAGAGCTAGAGTGCCTCGG GGTAGAGGGAATTCCTGGTGTAGCGGTGAATGCGTA GATATCAGGAAGAACACCGGTGGCGAAGGCGCTCTAC TAGGCCCACTGACACTGAGGGACGAAAGCTAGGG GAGCGAATGGGATTAGATACCCAGTAGTCTAGCCG TAAACGATGGATACTA	
NCBI Accession	MK928972		NCBI Accession	MN595301	
Project info	TAGEM/12/AR-GE/13 - TAGEM/16/AR-GE/44		Project info	TAGEM/12/AR-GE/13 - TAGEM/16/AR-GE/44	
EMBL / Gen Bank No	Name of the strain	Homology	EMBL / Gen Bank No	Name of the strain	Homology
AY274616.1	<i>Anabaena variabilis</i> CIBNOR 23	97%	DQ185231.1	<i>Nodularia harveyana</i> 'Huebel 1983/300'	96%
					
Name/Family:	<i>Nostoc</i> sp. IMU19 / Nostocaceae		Name/Family:	<i>Nostoc</i> sp. IMU20 / Nostocaceae	
Location:	Kizilcahamam Hot spring / 40.469602 N 32.638608 E		Location:	Kizilcahamam Hot spring / 40.469602 N 32.638608 E	
Harvester:	Turgay Çakmak, Zeynep Elibol Çakmak		Harvester:	Turgay Çakmak, Zeynep Elibol Çakmak	
Harvesting date:	Jun 2017		Harvesting date:	Jun 2017	
Sequence info:	AGTAACGCGTGAGAATCTAGCTTCAGGTCGGGGACAA CCACTGGAAACGGTGGCTAATACCGGATGTGCCAAA GGTGAAAGATTATTGCCTGAAGATGARCTCSCGTCT GATTAGCTAGTAGTGTGGTAAGARCGCACCTAGGCG ACGATCAGTAGCTGCTGARAGGATGATCAGCCACA CTGGGACTGARACACGGCCARACTCCTACGGGAGGC AGCAGTGGGGAATTTCCSCAATGGCGAAAGCCTGA CGGARCAATACCGCGTGAGGGAGGAAGGCTCTTGGGT TGTAACCTCTTTTCTCAGGGAATAAAAAATGAAGGT ACCTGARGAATAAGCATCGGCTAAGTCCGTGSCAGCA GCCGCGGTAAACGGARGATGCAAGCGTTATCCGGAA TGATTGGGCGTAAAGGTCGCGAGGTGGCAATGTAAG TCTGCTGTTAAAGAATGAGGCTCAACCTCATACCGAGC AGTGGAACACTACATAGCTWGAGTGCGTTCCGGGTAG AGGGAATTCCTGGTGTAGCGGTGAAATGCGGTAGATAT CAGGAAGAACACCGGTGGCGAAAGCGCTCTACTAGGC CGCACTGACACTGAGGGACGAAAGCTAGGGGAGCG AATGGGATT		Sequence info:	ACTTAGGTACTAGTGGCGGACGGGTGAGTAACGCGT GAGAATCTGGCTTCAGGTCGGGACAACTGGAAA CGGTGGCTAATACCGGATGTGCCCAAGGTAAAGGC TTGCCGCTGAAGATGARCTCGCGTCTGATTAGCTAG TAGGKGGGTAAAGCCTACCTAGGCCAGCATCAGTA GCTGCTGARAGGATGATCAGCCAGCACTGGGACTGA RACACGCCCARACTCCTACGGGAGGCAGTGGGG AATTTCCGCAATGGCGAAAGCCTGACGGARCAATA CCGCGTGAGGGAGGAAGGCTCTTGGGTTGTAAACCTC TTTTCTCAGGGAAGACACAATGACGCTACCTGAGGA ATAAGCATCGGCTAAGTCCGTGCCGAGCGCGGTA ATACGGAGGATGCAAGCGTTATCCGGAATGTTGGGC GTAAGCGTCCGAGGTGGCTATGTAAGTCTGCTGTT AAAGAGTGAGGCTCAACCTCATAAGARCACTGGAAC TACATGGGTAGAGTGCGTTCCGGGTAGAGGGAATCC TGGTGTAGCGGTGAAATGCGTATATCARGAAGAAC ACCGGTGGCGAAAGCCTCTGCTAGGCCGCACTGAC ACTGAGGACGAAAGCTAGGGAGCGCAATGGGA	
NCBI Accession	MN865246		NCBI Accession	MN865215	
Project info	TAGEM/12/AR-GE/13 - TAGEM/16/AR-GE/44		Project info	TAGEM/12/AR-GE/13 - TAGEM/16/AR-GE/44	
EMBL / Gen Bank No	Name of the strain	Homology	EMBL / Gen Bank No	Name of the strain	Homology
AP018180.1	<i>Nostoc carneum</i> NIES-2107	97%	JQ070066.1	<i>Nostoc punctiforme</i> UAM 393	99%

					
Name/Family:	<i>Microchaete</i> sp. IMU22 / Rivulariaceae		Name/Family:	<i>Anabaenopsis</i> sp. IMU23 / Aphanizomenonaceae	
Location:	Beypazari Hot spring / 40.065153 N 32.048973 E		Location:	Dutlu Hot spring / 40.153854 N 31.904695 E	
Harvester:	Turgay Çakmak, Zeynep Elibol Çakmak		Harvester:	Turgay Çakmak, Zeynep Elibol Çakmak	
Harvesting date:	Jun 2017		Harvesting date:	Jun 2017	
Sequence info:	AGTGGCGGACGGGTGAGTAACGCGTGAGAATCTAGCT CTTGGTCGGGGACAACAGTTGAAACGACTGCTAATA CCGGATGTGCCGGAAGGTGAAAGATTATTGCCAAGA RATGAGCTCGCTCTGATTAGCTAGTAGGTGGTAA GAGCGCACCTAGGCGACGATCAGTAGCTGGTCTGARA GGATGATCAGCCACACTGGGACTGARACACGGCCAG ACTCCTACGGGAGGCAGCAGTGGGGAAATTTCCGCAA TGGGCGAAAGCCTGACGGARCAATACCGCGTGAGGG AGGAAGGSTCTTGGGTCTGTAACCTCTTTTCTCAGGG AAGAATCAAGTGACGGTACCTGAGGAATAAGCATCGG CTAAGTCGCTGCCAGCMGCCGCGGTAATACGGAGGAT GCAAGCGTTATCCGGAATGATTGGGCGTAAAGCGTTC GCAGGTGGCTGTGAAGTCTGCTGTTAAAGAAATGAGG CTCAACCTCMTCAAAGCAGTGGAACCTACACGGCTAG AGTGSCTTGGGGCAGARGGAATTCCTGGKGTARCGG TGAAATGCGTAGAGATCARGAAGAACACCGGTGGCGA AAGCGCTCTGCTAGGCCGCAACTGACACTGARGGAMA AAAGCTAGGGGA		Sequence info:	CGGGGACMACCAGCGGAAACGGTGGCTAATACCGGA TATGCCGAAAAGGTGAAAGGCTARCTGCCTGAAGATGA RCTCSCGTCTGATTARCTARTTGGTAGAGTAAGARCT ACCMAGSGAGCAGTACGTAGCTGTGARAGGATGA TCAGCCACACTGGGACTGARACACGGCCAGACTCCT ACGGGAGGCAGCAGTGGGGAATTTCCSCMATGGGC GAAASCCTGACGGAGCAATACCCSGTGAGGGAGGAAG GSTCTTGGGTGTAAACCTCTTTCTCMAGGAAGAAA AAAATGACGGTACTTGAGGAATAAGCATCSGCTAAT CCGTGSCAGCAGCCGCGKAATACGGAGGATGCAAGC GTTATCCGGAATGATTGGGCGTAAAGCGTCCGCGAGT GGCTGTGTAAGTCTGCTGTTAAAGAAATGAGGCTCAAC CTCATCAAAGCRGTGGAACTACACSGSTAGAGTGCG TTCGGGGTARAGGGAATTCCTGGTGTACCGGTGAAAT GCGTAGATATCAGGAAGAACACCGGTGGCGAAAGCGC TCTGCTAGGCCG	
NCBI Accession	MN866117		NCBI Accession	MN595301	
Project info	TAGEM/12/AR-GE/13 - TAGEM/16/AR-GE/44		Project info	TAGEM/12/AR-GE/13 - TAGEM/16/AR-GE/44	
EMBL / Gen Bank No	Name of the strain	Homology	EMBL / Gen Bank No	Name of the strain	Homology
KX458494.1	<i>Microchaetaceae</i> CENA550	97%	AM773302.1	<i>Anabaenopsis</i> cf. AB2002/25	94%
					
Name/Family:	<i>Trichormus</i> sp. IMU26 / Nostocaceae		Name/Family:	<i>Anabaena</i> sp. IMU30 / Nostocaceae	
Location:	Malikoy Uyuz Thermal spring / 39.763197 N 32.390247 E		Location:	Kizilcahamam Thermal spring / 40.469602 N 32.638608 E	
Harvester:	Turgay Çakmak, Zeynep Elibol Çakmak		Harvester:	Turgay Çakmak, Zeynep Elibol Çakmak	
Harvesting date:	Jun 2017		Harvesting date:	Jun 2017	
Sequence info:	GGATTAGTGGCGGACGGGTGAGTAACGCSTGAGAAT CTGGCTTCAGGTCTGGGACAACCACTGGRRRCGGKGG CTAATACCGGATGTCCSAGAGGTGAAAGGCTTGCTG CCTGAAGATGARCTTGGCTCTGATTAGCTAGTTGGTG GGGTAAGAGCCTACCAAGGCGACGATCARTARCTGGT CTGARAGGATGATCAGCCMACTGGGACTGARACAC		Sequence info:	GACGGGTGAGTAACGCGTGAGATCTACATTYAGGTC GGGGACAACCACTGGAACGGTGGCTAATACCGGATG TGCCGAGAGGTAAAAGGCTTGCCGCTGARAATGAGC TCGCGTCTGATTAGCTAGTTGGGGGTGAAGARACCA CAAAGGCGACGATCAGTAGCTGTCTGARAGGATGAT CAGCCACACTGGGACTGARACACGGCCARACTCCTA CGGGAGGCAGCAGTGGGGAATTTCCGCAATGGGCG AAAGCCTGACCGGARCAATACCGCGTGAGGGAGGAAG GSTCTTGGGTGTAAACCTCTTTCTCAGGGAAGAAAA AAATGACGGTACCTGAGGAATAAGCATCGGCTAACTC CGTGCCAGCAGCCGCGTAATACGGAGGATGCAAGCG TTATCCGGAATGATTGGGCGTAAAGGGTCCGCAAGTG GCACTGTAAAGTCTGCTGTCAAARARCAAGGSTCAACC TTGTAAAGGCGAGTGGAACTACAGARCTAGAGTACGT TCGGGGCAGAAGGAATTCCTGGTGTAGCGGTGAAATG SGTAGAGATCAGGAAGAACACCGGTGGCGAAAGCGTT CTGCTAGGCCTGTACTGACACTGAGGGACGAAAGCTA GGGGAGCGAATGGGATTAGATACCCC	
NCBI Accession	MK929011		NCBI Accession	MN866122	
Project info	TAGEM/12/AR-GE/13 - TAGEM/16/AR-GE/44		Project info	TAGEM/12/AR-GE/13 - TAGEM/16/AR-GE/44	
EMBL / Gen Bank No	Name of the strain	Homology	EMBL / Gen Bank No	Name of the strain	Homology
KY807532.1	<i>Trichormus</i> sp. MACC 643	95%	AY274616.1	<i>Anabaena variabilis</i> CIBNOR 23	97%

6.3 Effect of Inoculum

The Cyanobacteria species used in this study were all diazotrophic species with good growth ability in BG11-N medium. Thus, the Cyanobacteria species which were used in this study could be considered as acclimated to nitrogen deprivation for 20 months since the progress and used as the experimental reference for PHB production [111].

6.4 Screening and Selecting the Best PHB Producer Cyanobacteria Species





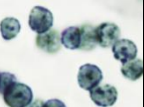
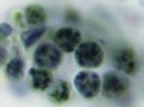
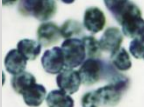
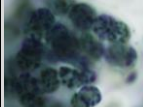

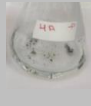
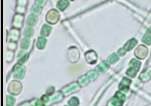

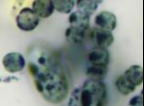
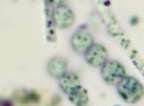

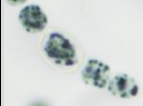
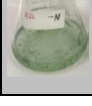



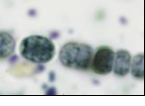

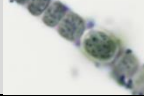
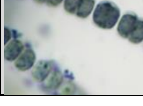
Cyanobacterial species were incubated in BG11-N (control), and BG11-NP medium for investigating the effect of nitrogen and phosphorous, and enhancing PHB production. Light microscope imaging, Sudan black B measurement, FTIR, chlorophyll-a, carotenoid, and phycobiliprotein analysis have been performed.

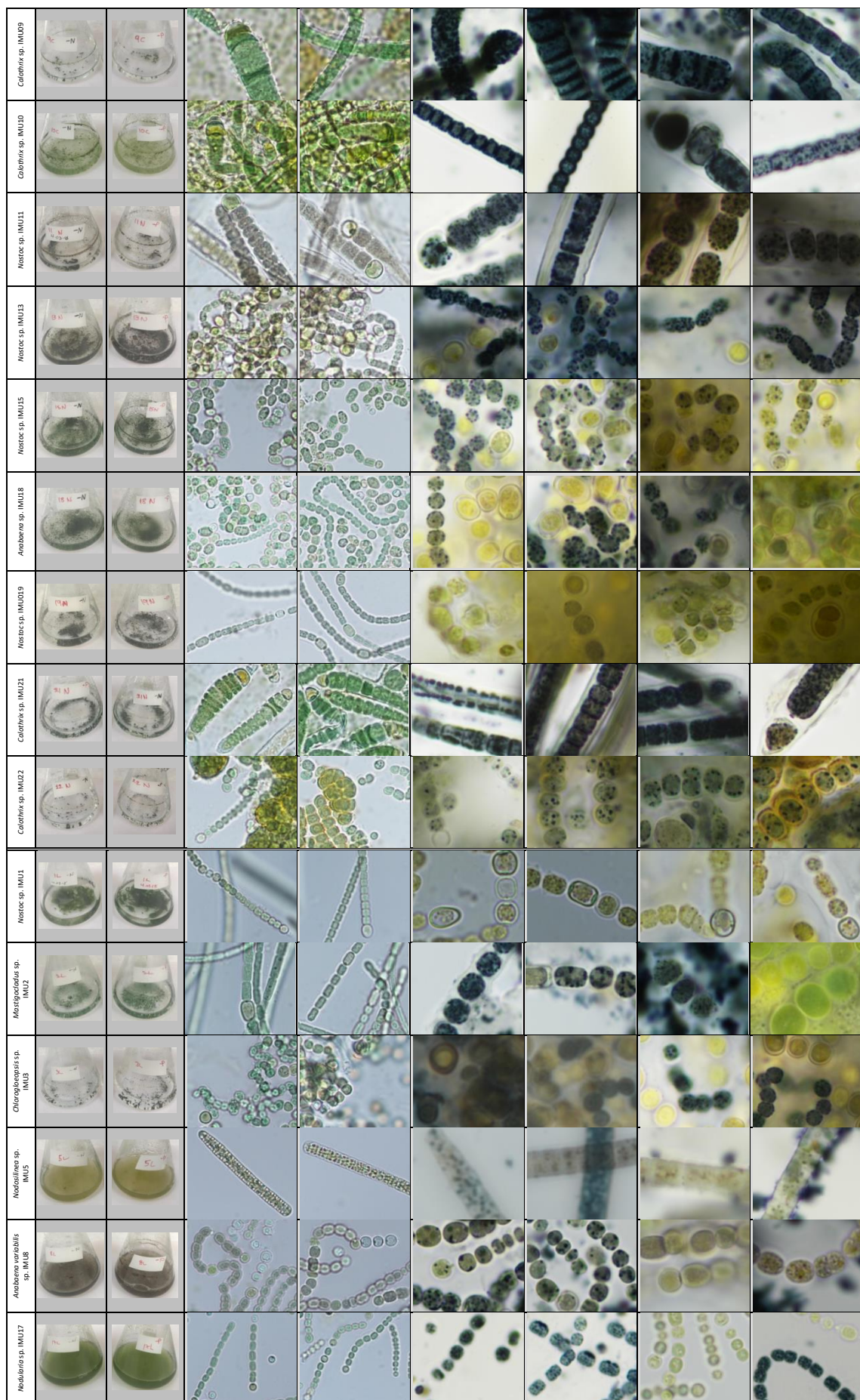
Light microscope imaging showed that there was not a big morphologically difference of cells, which grew in BG11-N and BG11-NP media (Table 6.7). Also, from the images of flasks growth of the species observed qualitatively (Table 6.7).

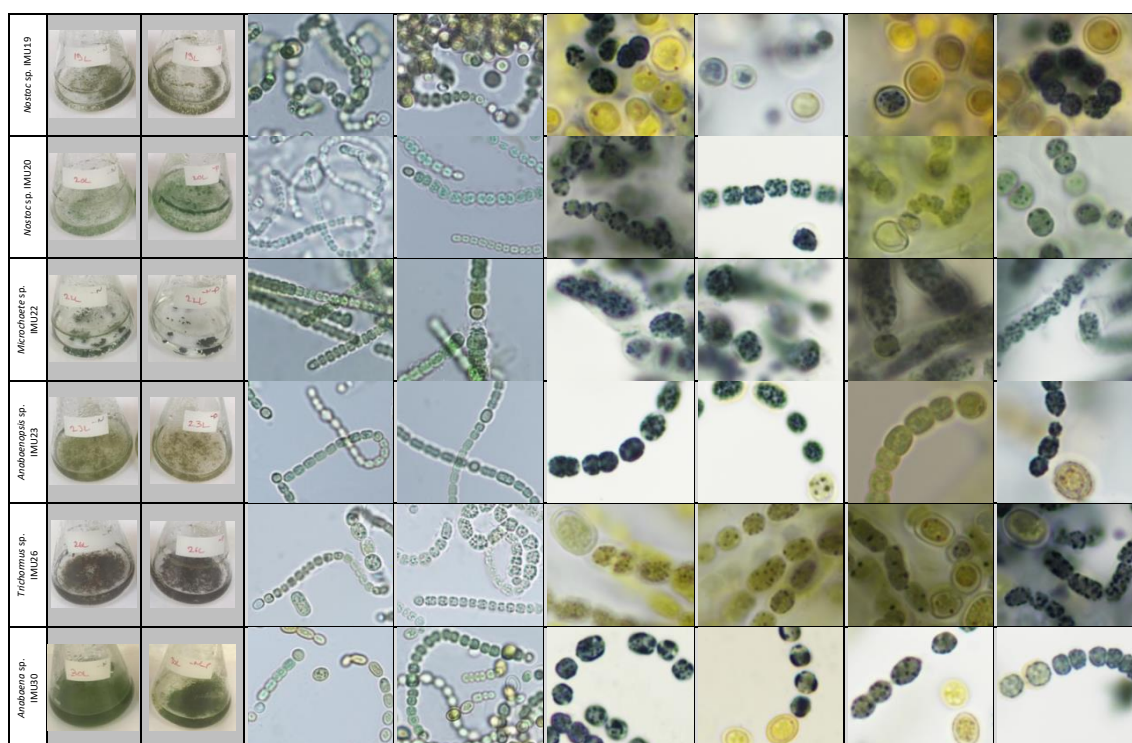
PHB production capacities have been measured by using Sudan black-B dye and FTIR. Qualitative analyses of PHB have been imagined by the Sudan black B dye method with the solubility of the dye in lipids and PHB granules, which observed as black dots in the cells by light microscope imaging (Table 6.8).

Table 6.8 Images of Cyanobacteria in BG11-N and BG11-NP medium

*The width of each picture of cells 50μm, Sudan Black B stained cells 20μm

Name	Culture Images (10th Day)		Light Microscope Images (10th Day)		Sudan Black B stained cells (5th Day)		Sudan Black B stained cells (10th Day)	
	-N	-NP	-N	-NP	-N	-NP	-N	-NP
Nostoc sp. IM02								
Cylindrocapsa sp. IM04								
Cylindrocapsa sp. IM05								





6.4.1 Quantitative Analyzes of PHB

6.4.1.1 Sudan Black B Measurements

PHB analyzes by the Sudan black B method were performed on A₆₇₀ by UV measurements. With this aim, the first calibration curve (Fig. 6.5) was obtained to calculate PHB content (Fig. 6.6). The value of R² showed low reliability with the number of 0.8209, which was expected to be around 0.98 (should be closer to 1) due to curves after A_{0.6}-1000 µg/ml. As a result, the parameters above the UV absorbance A_{0.6} and PHB content above than 1000 µg/ml was accepted not trustable due to Sudan black B calibration curve which means the values of PHB content (Fig. 6.6) between 1000-3700 µg/ml may not show a critical difference. Also, error bars of PHB content (Fig. 6.6) indicate low reliability.

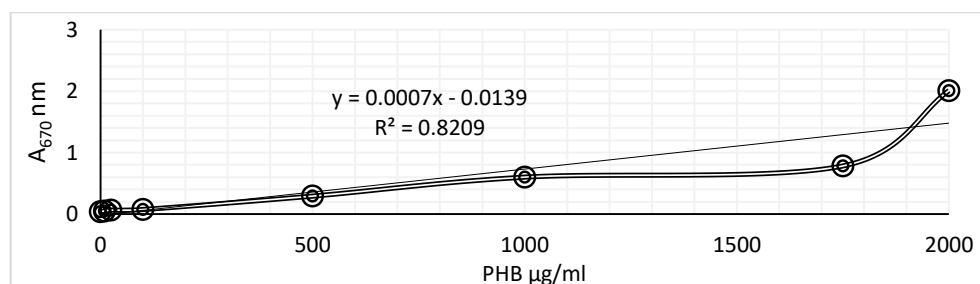


Figure 6.5 Sudan black B method PHB calibration curve

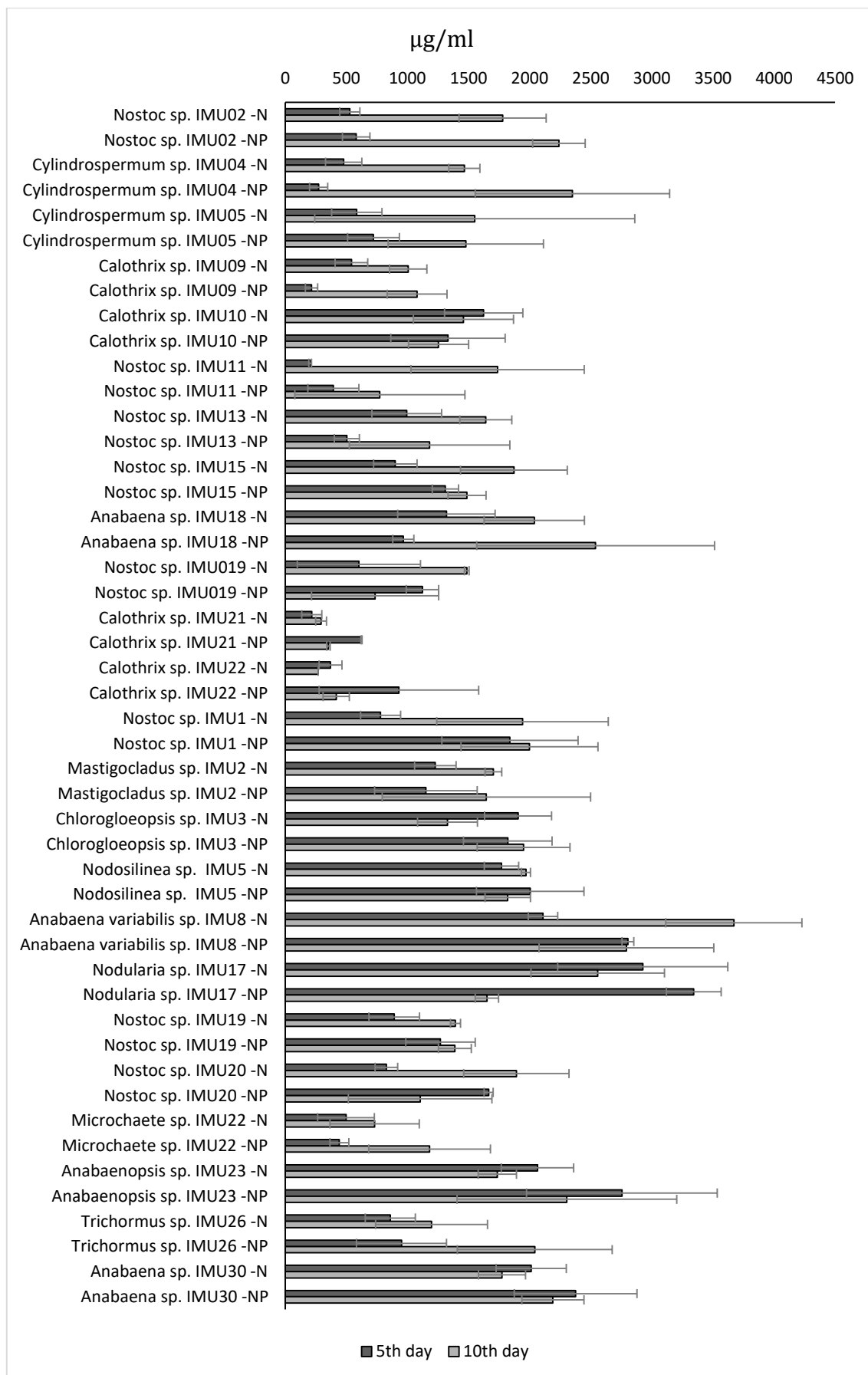


Figure 6.6 PHB content of Cyanobacteria species by Sudan black B method

6.4.1.2 FTIR Measurements

FTIR analysis was performed to select the best PHB producer Cyanobacteria by measuring transmissions at 1720 cm^{-1} (Fig. 6.7), 1735 cm^{-1} (Fig. 6.8), and their ratio to 1652 cm^{-1} (amide I band) (Fig. 6.9,10) separately. The two bands at 1720 cm^{-1} , 1735 cm^{-1} were not showed any significant diversity from each other owing to their close numbered values as expected. Single-band measurements gave the best PHB producer Cyanobacteria, which were *Nostoc* sp. IMU11 and *Calothrix* sp. IMU10. On the other hand, when results of peaks normalization by amide I band ratio were investigated, it has been clarified that *Anabaena* sp. IMU18 had more PHB accumulation than other species. The difference between the two results of *Anabaena* sp. IMU18 may proceed from the species cell ratio in the media. In this respect *Anabaena* sp. IMU18 gave promising PHB enhancement by increasing the growth ratio by modifying growth parameters.

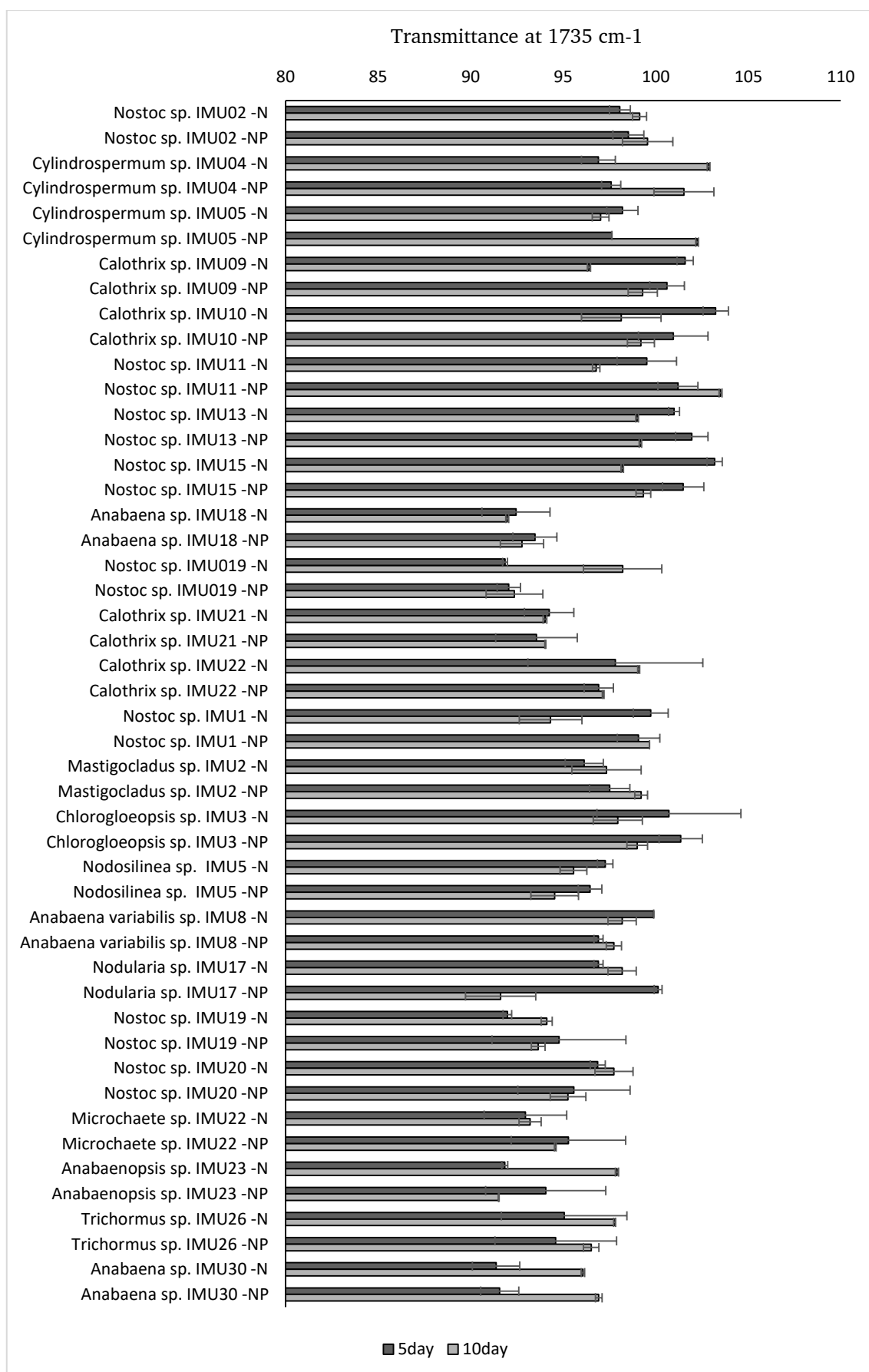


Figure 6.7 PHB responsible FTIR peak at 1720 cm⁻¹

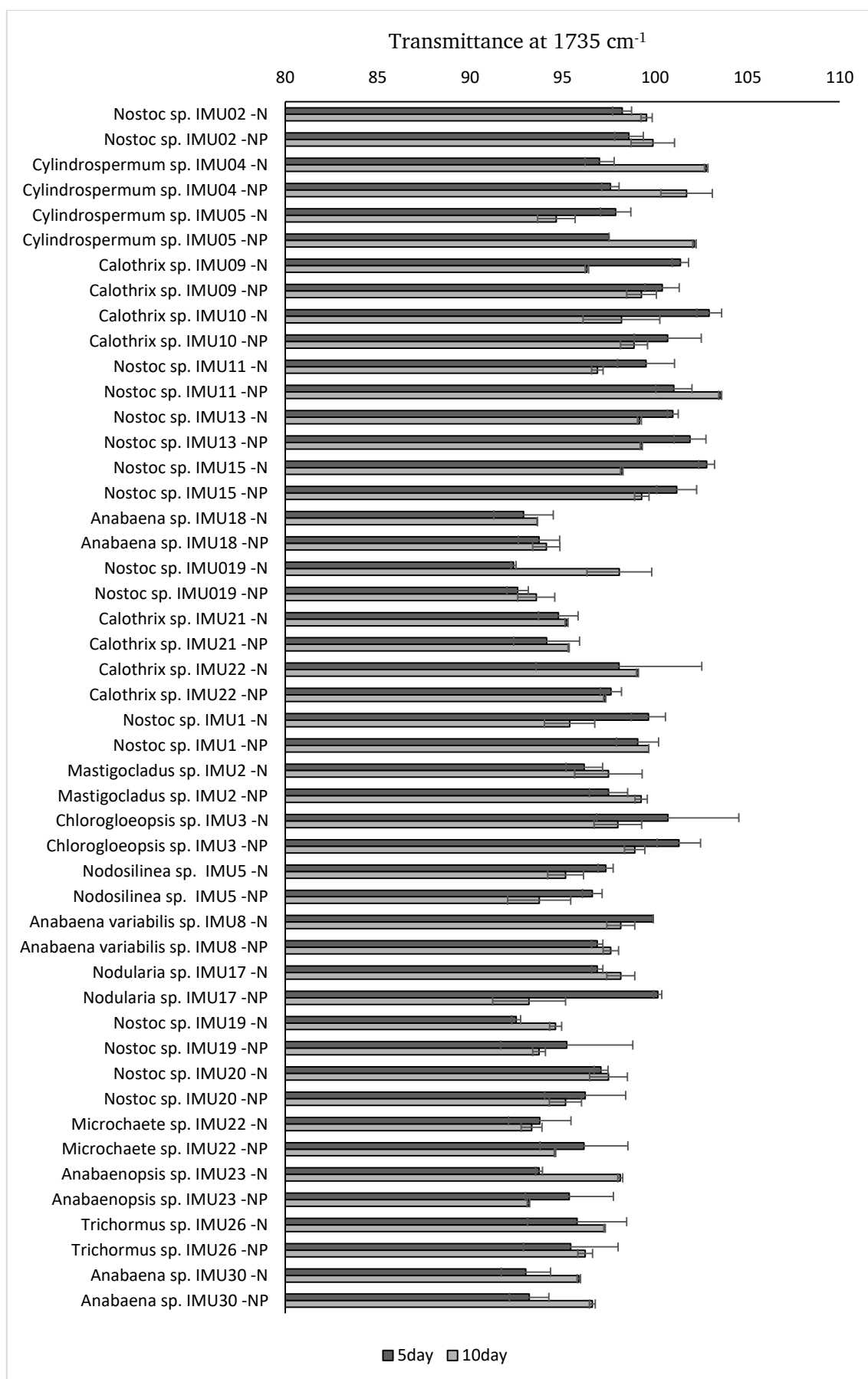


Figure 6.8 PHB responsible FTIR peak at 1735 cm⁻¹

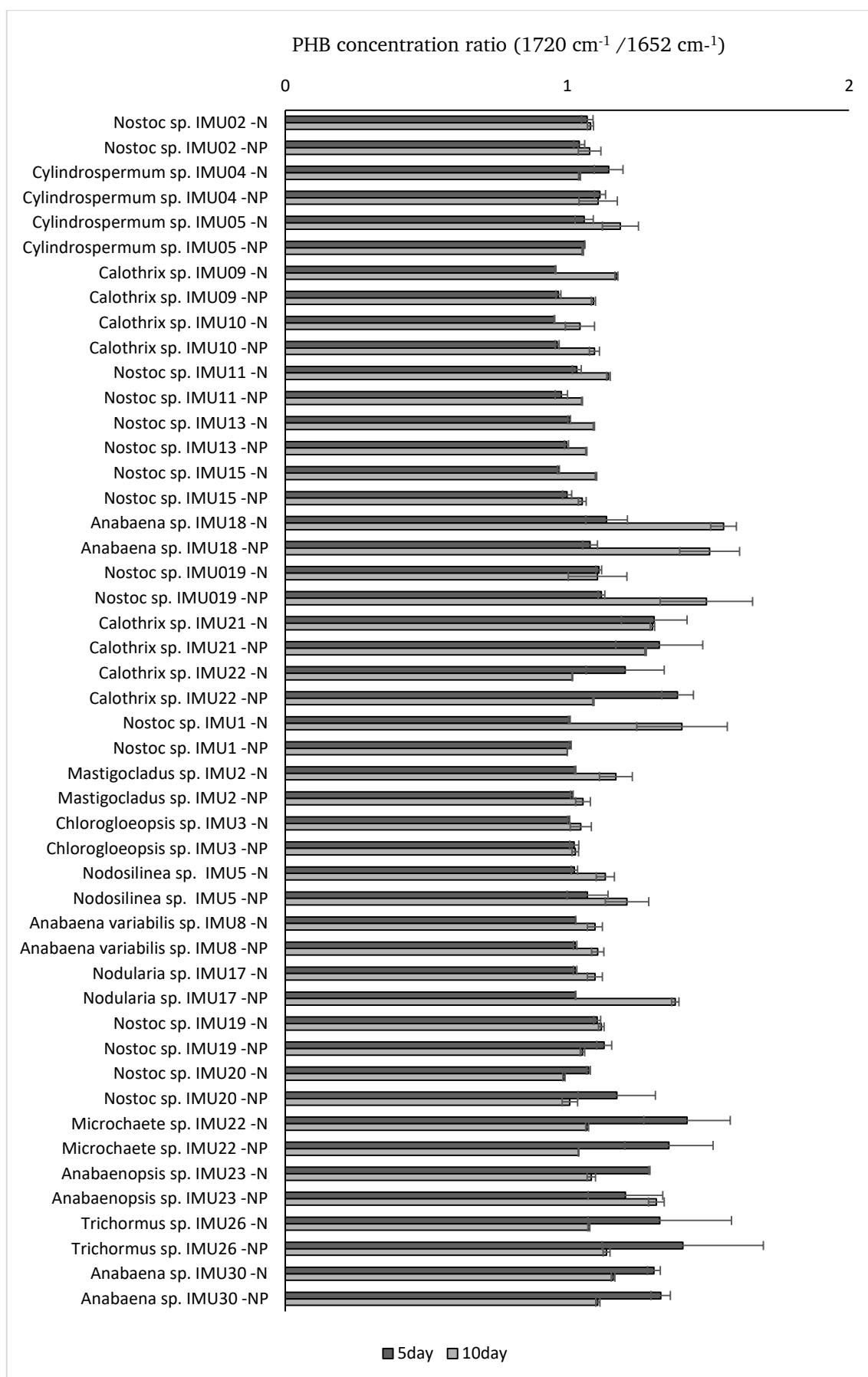


Figure 6.9 PHB concentration ratio of 1720 cm⁻¹/1652 cm⁻¹

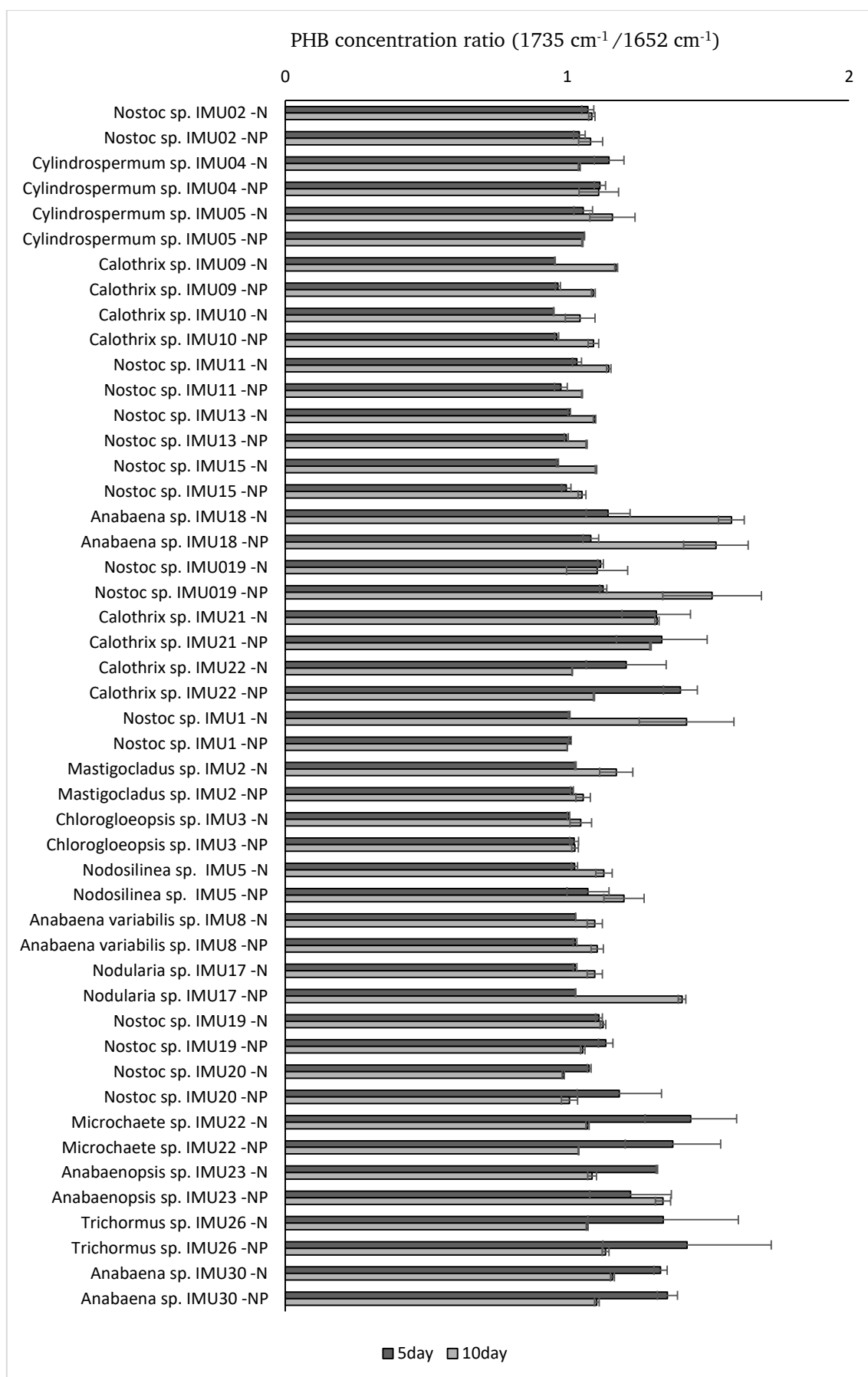


Figure 6.10 PHB concentration ratio of $1735\text{ cm}^{-1}/1652\text{ cm}^{-1}$

In consideration of FTIR data with the sporting qualitative analysis (Table 6.8), *Calothrix* sp. IMU10, *Nostoc* sp. IMU11, and *Anabaena* sp. IMU18 were selected for their PHB production capacities.

6.4.2 Other Measurements

6.4.2.1 TAG, Oligosaccharide, and Polysaccharide Analysis by FTIR

FTIR analysis was performed on the 7th day of incubation to investigate Cyanobacterial TAG and carbohydrate (oligosaccharide and polysaccharide) levels.

TAG concentration ratio ($1744\text{ cm}^{-1}/1652\text{ cm}^{-1}$) was found high in the *Nostoc* sp. IMU20, *Calothrix* sp. IMU09, *Calothrix* sp. IMU10, *Nostoc* sp. IMU11, and *Nostoc* sp. IMU13, respectively (Fig. 6.11).

Oligosaccharide ($1145\text{ cm}^{-1}/1652\text{ cm}^{-1}$) and polysaccharide ($1045\text{ cm}^{-1}/1652\text{ cm}^{-1}$) concentration ratios were observed high in the *Nostoc* sp. IMU20, *Microchaete* sp. IMU22, *Nostoc* sp. IMU19, *Calothrix* sp. IMU09, *Nostoc* sp. IMU11, *Nostoc* sp. IMU13, and *Calothrix* sp. IMU10, respectively, as well as with higher oligosaccharide ratio than polysaccharide ratio (Fig. 6.12).

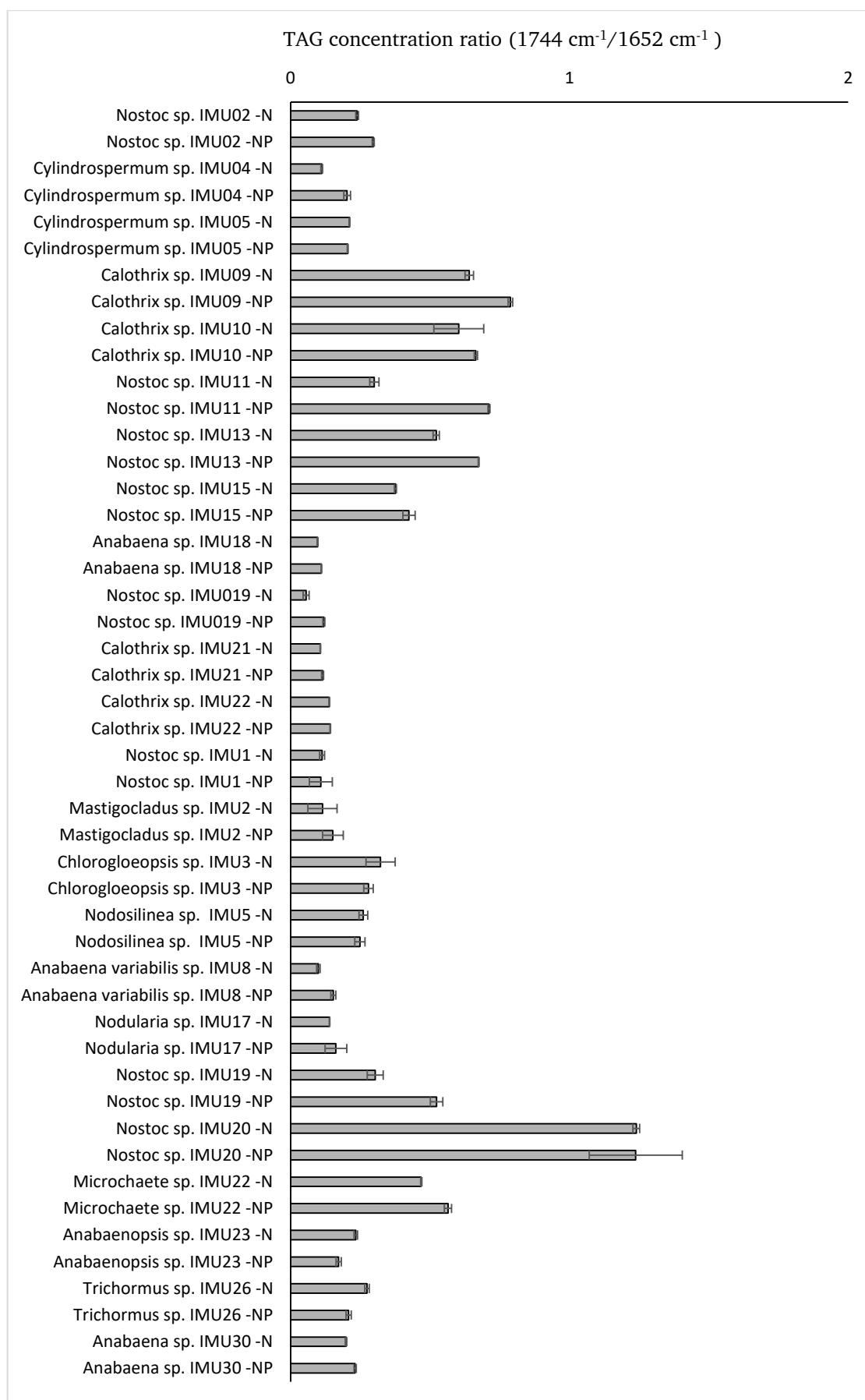


Figure 6.11 TAG concentration ratio of Cyanobacteria species

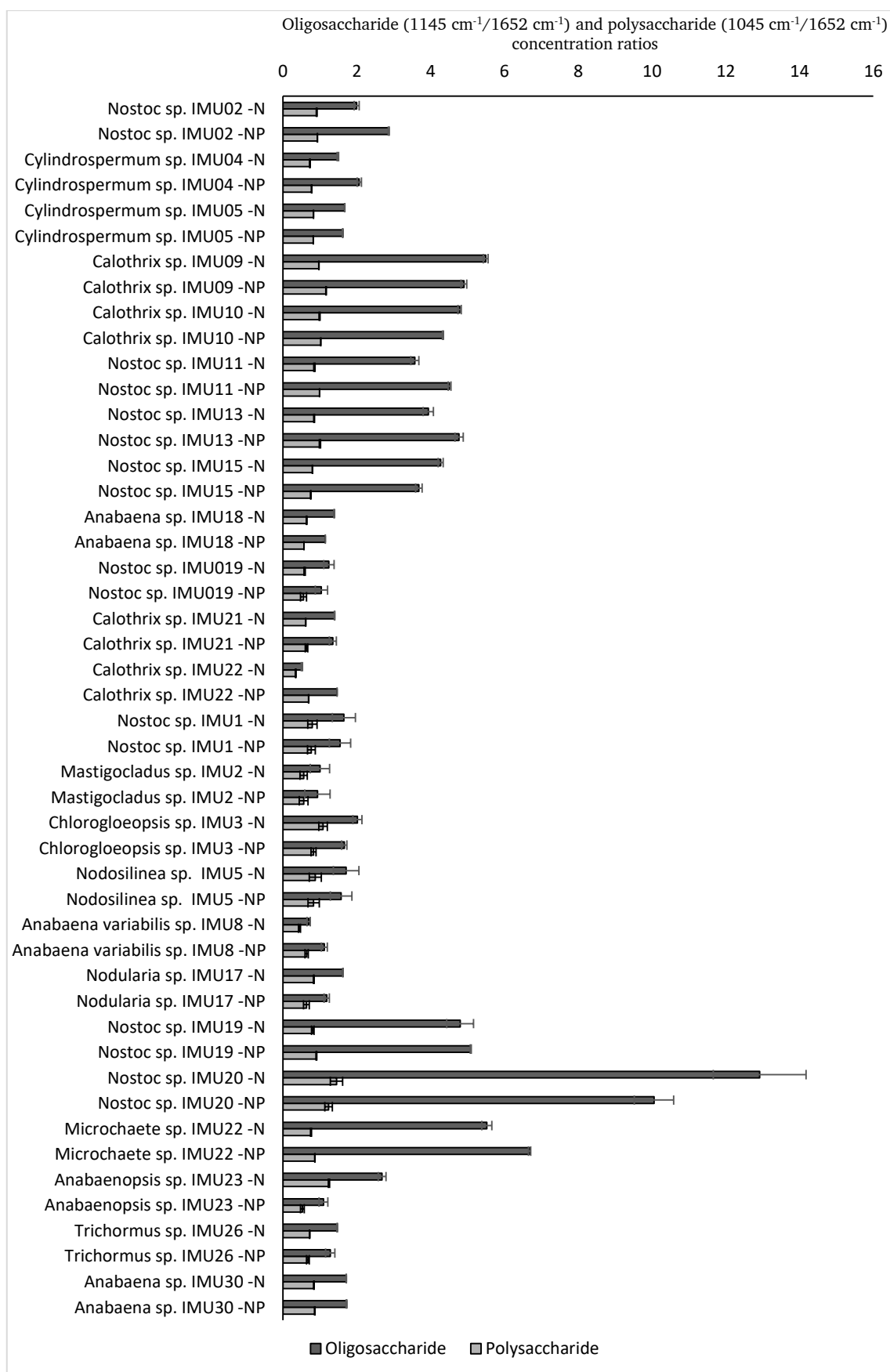


Figure 6.12 Oligosaccharide and polysaccharide concentration ratios of Cyanobacteria species

6.4.2.2 Total Chlorophyll-a & Carotenoid Measurements

Cyanobacterial species had been investigated on the changes of total chlorophyll-a and carotenoid contents on the 5th and 10th day of incubation.

Total chlorophyll-a concentration was found high in the *Nostoc* sp. IMU019, *Anabaena* sp. IMU18, *Nostoc* sp. IMU13, *Anabaena* sp. IMU30, and *Nostoc* sp. IMU11, respectively with the more accumulations on the 10th days except for *Anabaena variabilis* sp. IMU8 in the BG11-NP medium (Fig. 6.13).

Total carotenoid concentration was observed high in the *Calothrix* sp. IMU21, *Nostoc* sp. IMU15, *Anabaena* sp. IMU18, *Nodularia* sp. IMU17, *Nostoc* sp. IMU019, and *Nostoc* sp. IMU11 respectively, together with close accumulations on incubation days but high for the 10th day especially (Fig. 6.14)

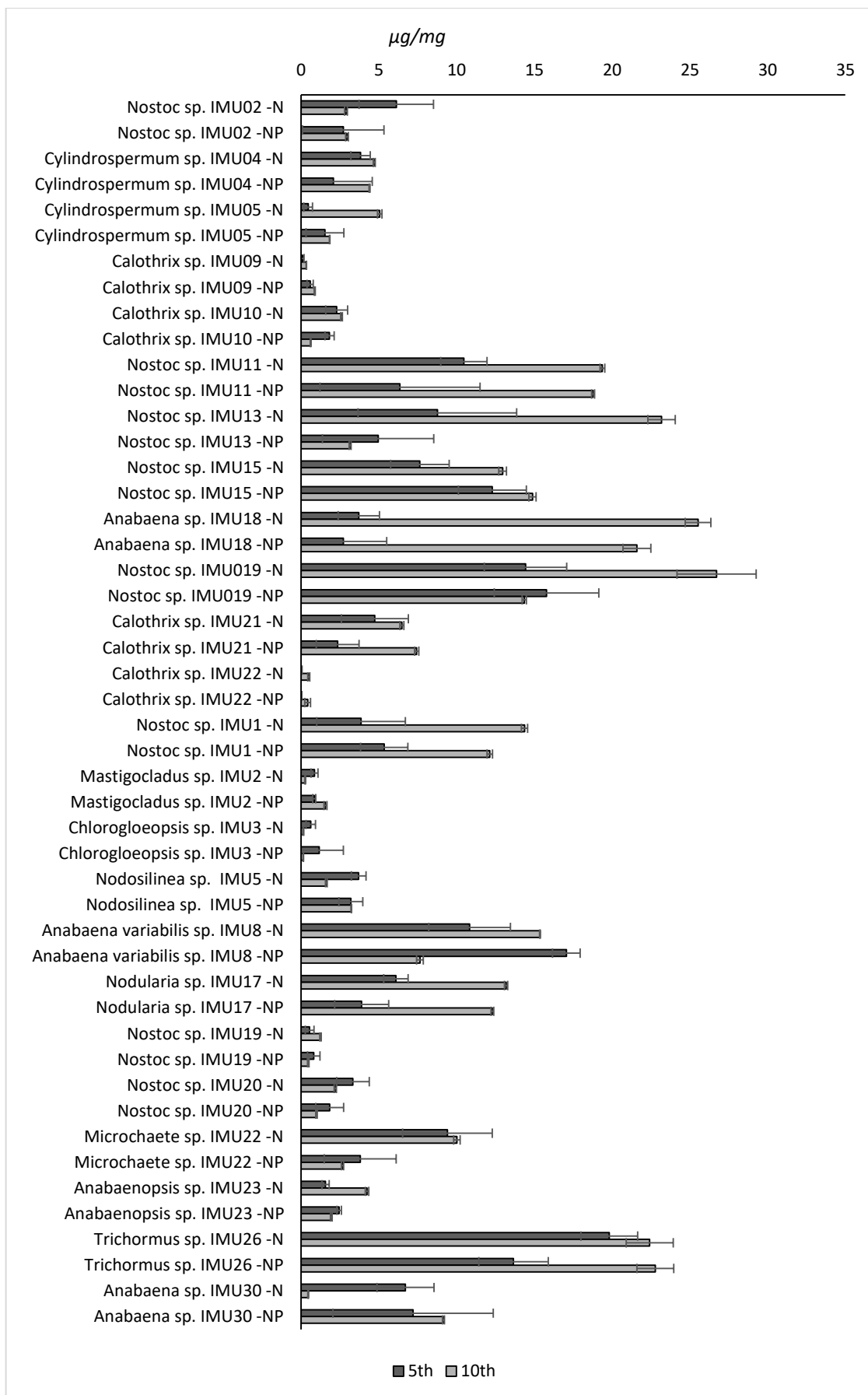


Figure 6.13 Total chlorophyll-a concentration in Cyanobacteria species

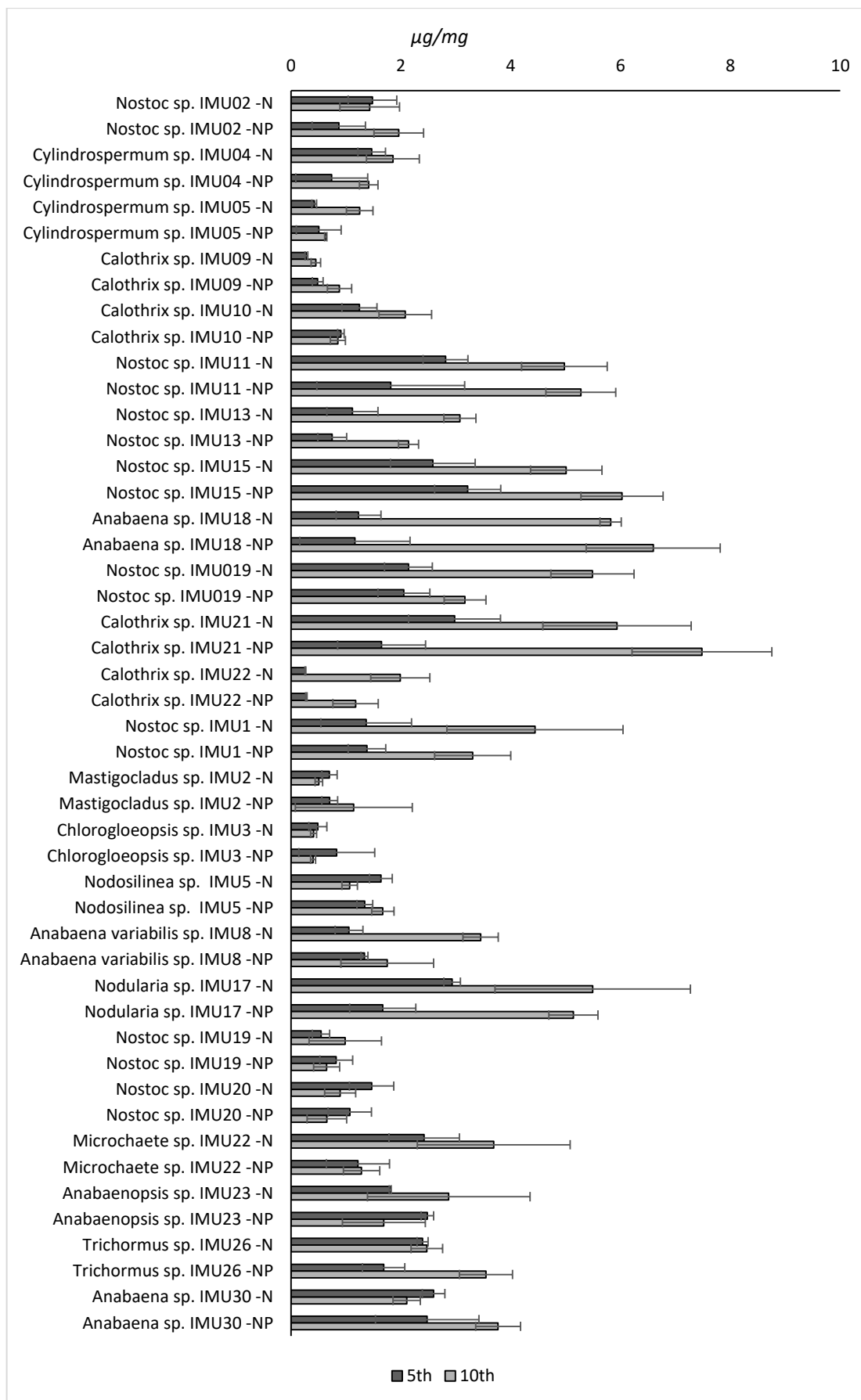


Figure 6.14 Total carotenoid concentration in Cyanobacteria species

6.4.2.3 Phycobiliprotein Measurements

Cyanobacterial species had been investigated on the changes of phycoerythrin, phycocyanine, and allophycocyanine concentrations.

Phycoerythrin concentration was observed high in the *Nostoc* sp. IMU13, *Trichormus* sp. IMU26, *Anabaena variabilis* sp. IMU8, *Nostoc* sp. IMU019, *Calothrix* sp. IMU10, and *Nostoc* sp. IMU1, respectively with the more accumulations on the 10th days except for *Anabaena variabilis* sp. IMU8 in the BG11-NP medium (Fig. 6.15).

Phycoerythrin concentration was investigated high in the *Nostoc* sp. IMU13, *Trichormus* sp. IMU26, *Calothrix* sp. IMU10, *Anabaenopsis* sp. IMU23, *Nostoc* sp. IMU1, and *Anabaena* sp. IMU18, respectively (Fig. 6.16).

Allophycocyanine concentration was observed high, especially in the *Calothrix* sp. IMU10, then it followed by *Microchaete* sp. IMU22, *Trichormus* sp. IMU26, *Nodosilinea* sp. IMU5, *Nostoc* sp. IMU1, *Nostoc* sp. IMU13, and *Anabaena variabilis* sp. IMU8, respectively (Fig. 6.17).

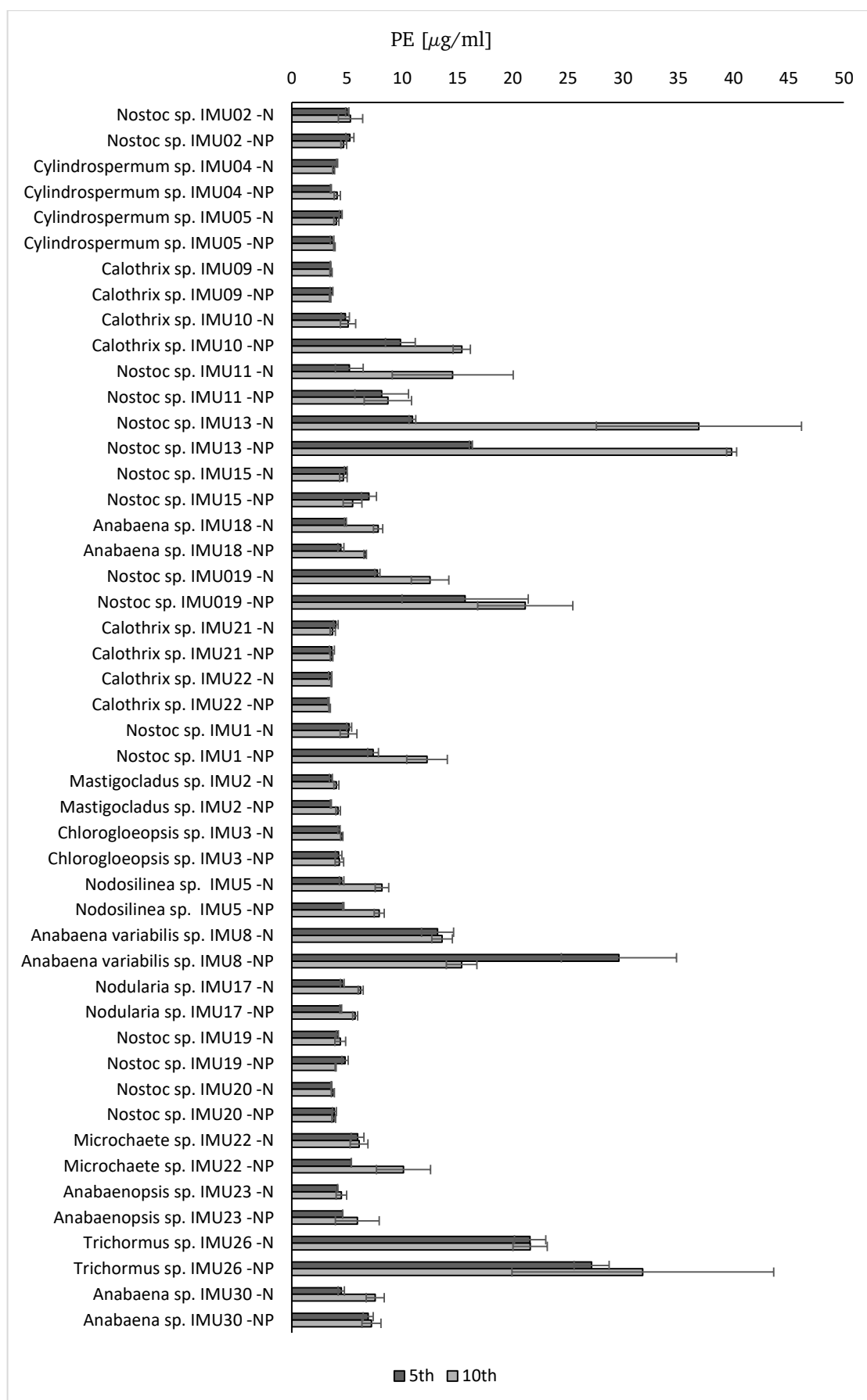


Figure 6.15 Phycoerythrin concentration changes in Cyanobacteria species

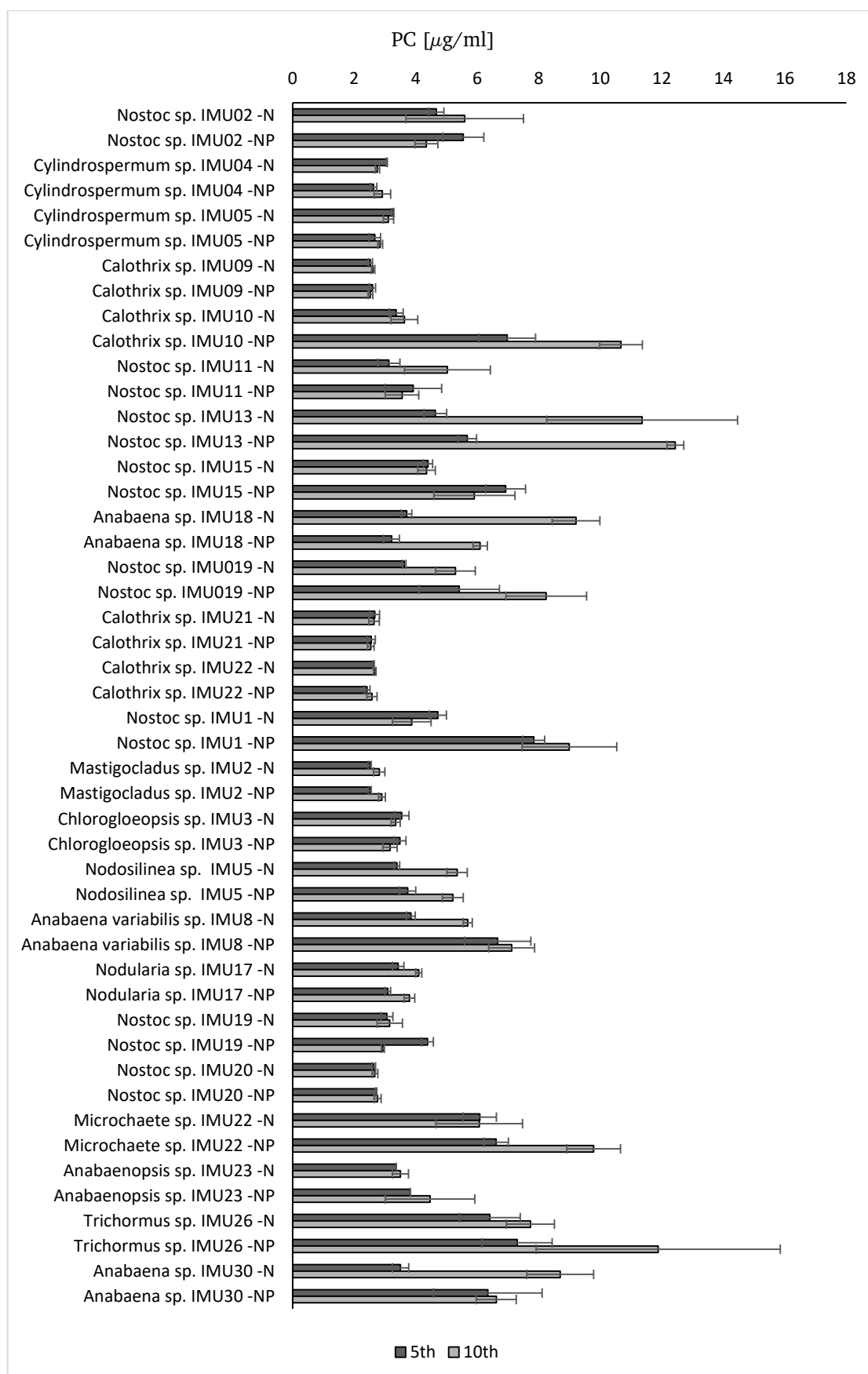


Figure 6.16 Phycocyanine concentration changes in Cyanobacteria species

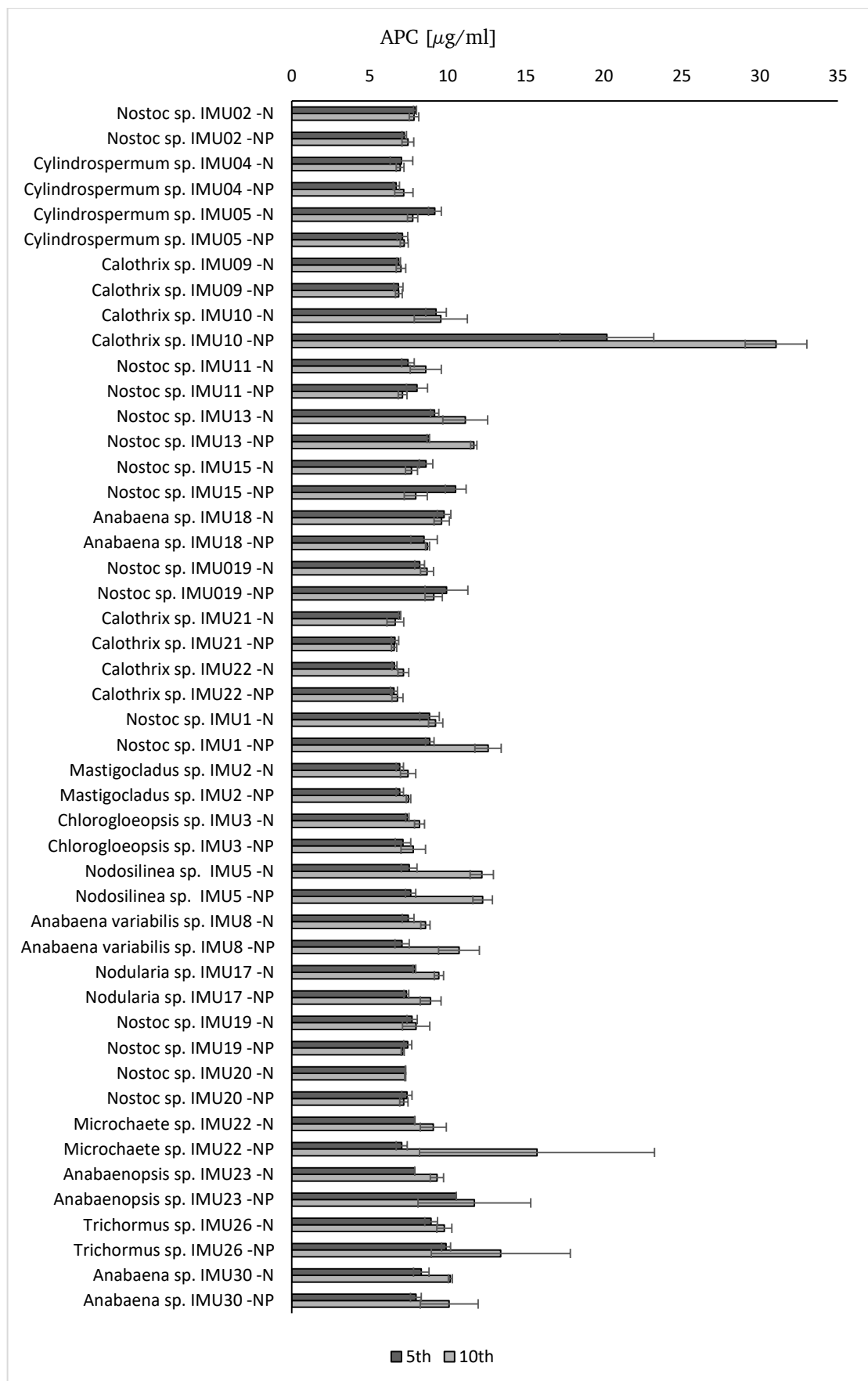







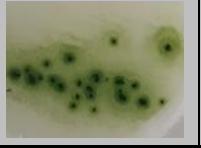




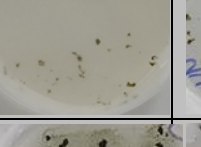


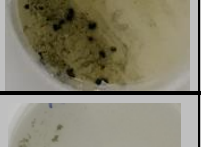
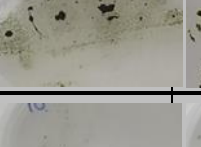

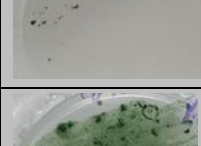

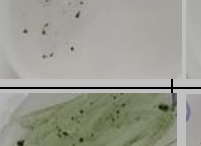
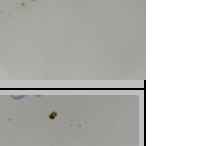
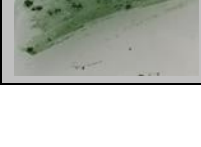

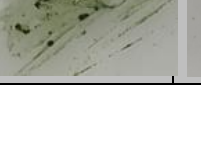

Figure 6.17 Allophycocyanine concentration changes in Cyanobacteria species

6.5 Studies on Selected Species

6.5.1 Medium Trial

Allen, BG11, FW, and Z8 medium plates were tried to find the best Cyanobacterial growth on selected species. BG11 was chosen best medium for growth (Table 6.9).

Table 6.9 Allen, BG11, FW, and Z8 medium trial

<i>Species</i>	<i>Day</i>	<i>Allen</i>	<i>BG11</i>	<i>FW</i>	<i>Z8</i>
<i>Calothrix</i> sp. IMU10	5th				
	10th				
<i>Nostoc</i> sp. IMU11	5th				
	10th				
<i>Anabaena</i> sp. IMU18	5th				
	10th				

6.5.2 HPLC Analysis

Cyanobacterial lutein, zeaxanthin, canthaxanthin, chlorophyll-a, alpha-carotene, beta-carotene, and riboflavin (B₂ vitamin) contents were obtained by HPLC analysis. Error band was high, especially for the lutein data, and some species had no data on zeaxanthin and canthaxanthin content, which may occur from low sample amounts.

Lutein compositions (Fig. 6.18) were observed high, especially in the *Anabaena* sp. IMU18, then it was followed by *Nostoc* sp. IMU11 and *Calothrix* sp. IMU10.

The best lutein production was for both *Calothrix* sp. IMU10 and *Nostoc* sp. IMU11 on the 5th day, instead of *Anabaena* sp. IMU18 on the 10th day incubation, also nitrogen starvation was the best for all species to produce Lutein.

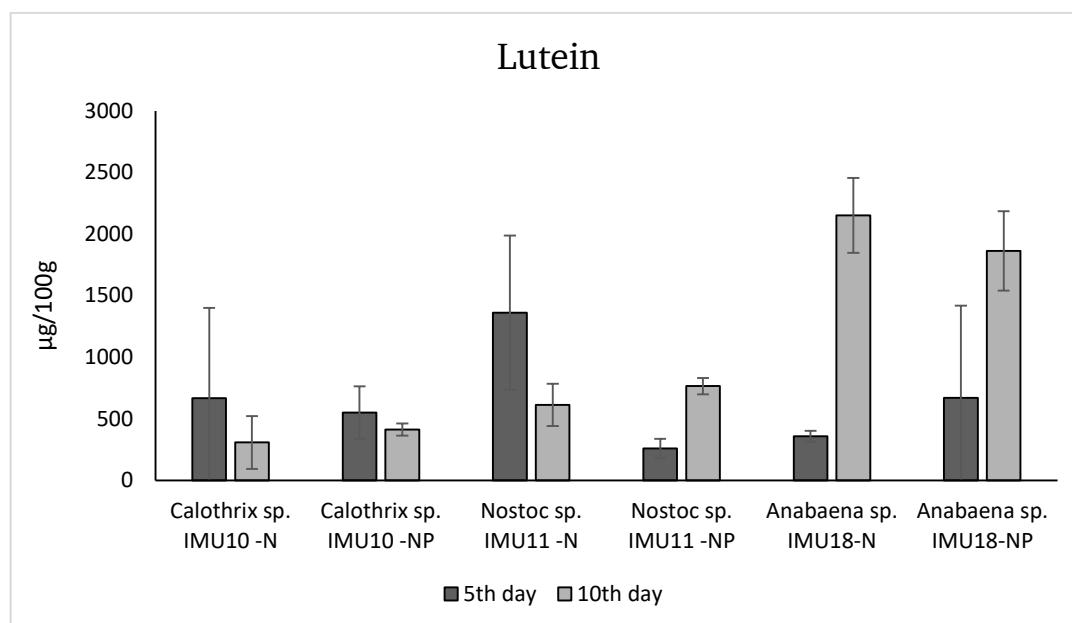


Figure 6.18 Lutein concentrations in selected Cyanobacteria

Zeaxanthin compositions (Fig. 6.19) were so low on the 5th day, and also on the 10th day, except for only *Anabaena* sp. IMU18. *Calothrix* sp. IMU10 produced zeaxanthin only in nitrogen deprived culture conditions. All species' zeaxanthin content was high on the 5th day. *Anabaena* sp. IMU18 has selected the best zeaxanthin producer species, which had so low zeaxanthin content on the 5th day, as well as with no zeaxanthin production in the nitrogen starvation for the five days.

Canthaxanthin compositions (Fig. 6.20) were so low, especially on the 5th day, except for *Nostoc* sp. IMU11 which showed only inspectable data on the 5th day. The best canthaxanthin producer species was *Anabaena* sp. IMU18, then it followed by *Calothrix* sp. IMU10. Nitrogen deprived culture conditions were the most suitable medium for canthaxanthin production for all species.

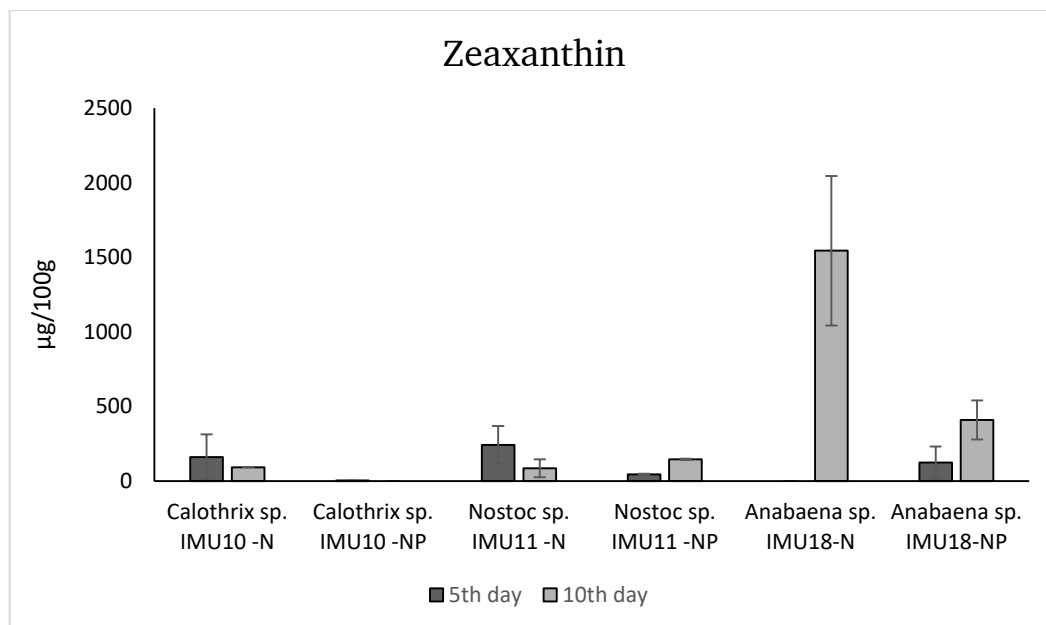


Figure 6.19 Zeaxanthin concentrations in selected Cyanobacteria

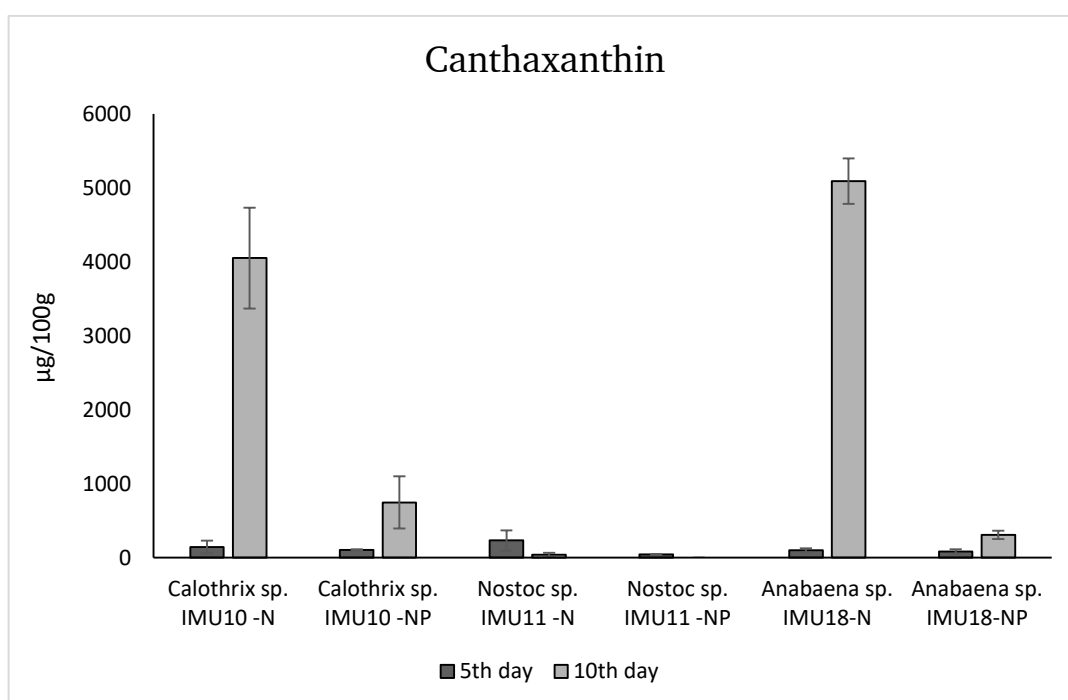


Figure 6.20 Canthaxanthin concentrations in selected Cyanobacteria

Chlorophyll-a compositions (Fig. 6.21) were higher on the 10th day in general, and nitrogen starvation was the best condition for all species instead of *Nostoc* sp. IMU11 with questionable error bands. *Calothrix* sp. IMU10 was the best chlorophyll-a producer species.

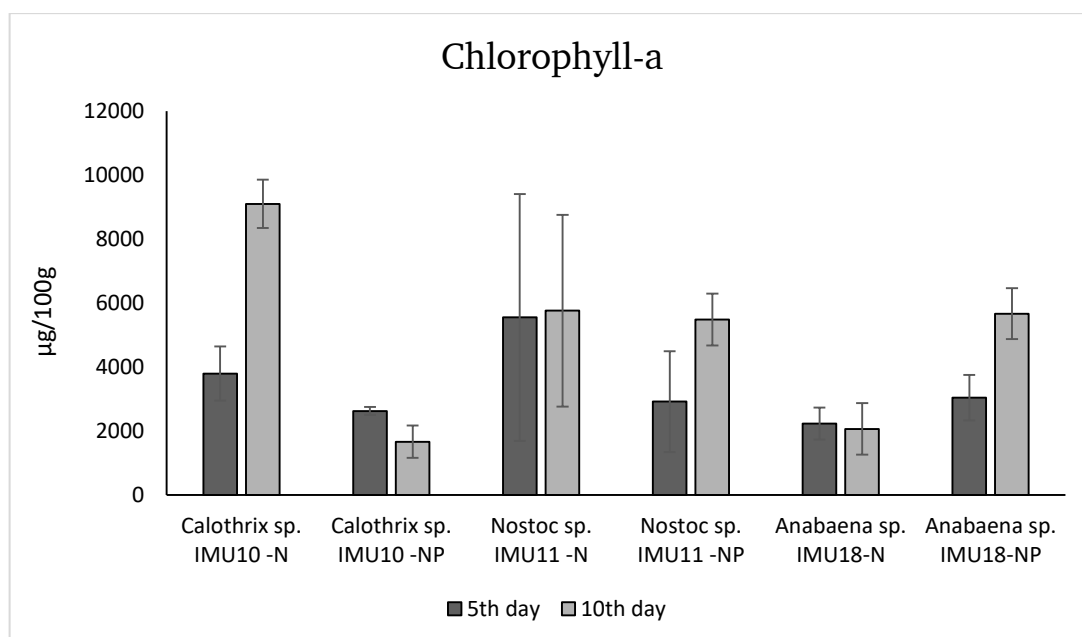


Figure 6.21 Chlorophyll-a concentrations in selected Cyanobacteria

Alpha-carotene compositions (Fig. 6.22) were maximum on the 10th day, except for *Nostoc* sp. IMU11, which was cultivated in the nitrogen deprived medium, as well as *Calothrix* sp. IMU10 in nitrogen and phosphorous medium. The best culture condition for alpha-carotene production was nitrogen starvation for all Cyanobacteria species and the best species was determined as *Anabaena* sp. IMU18, then followed by *Nostoc* sp. IMU11 and *Calothrix* sp. IMU10.

Beta-carotene compositions (Fig. 6.23) were high on the 5th day, except for *Anabaena* sp. IMU18. The best beta-carotene producer species was identified as *Nostoc* sp. IMU11 and followed by nitrogen starved *Calothrix* sp. IMU10 and *Anabaena* sp. IMU18, the again nitrogen and phosphorous starved *Calothrix* sp. IMU10. Nitrogen deprived culture conditions were the most suitable medium for beta-carotene production for all species.

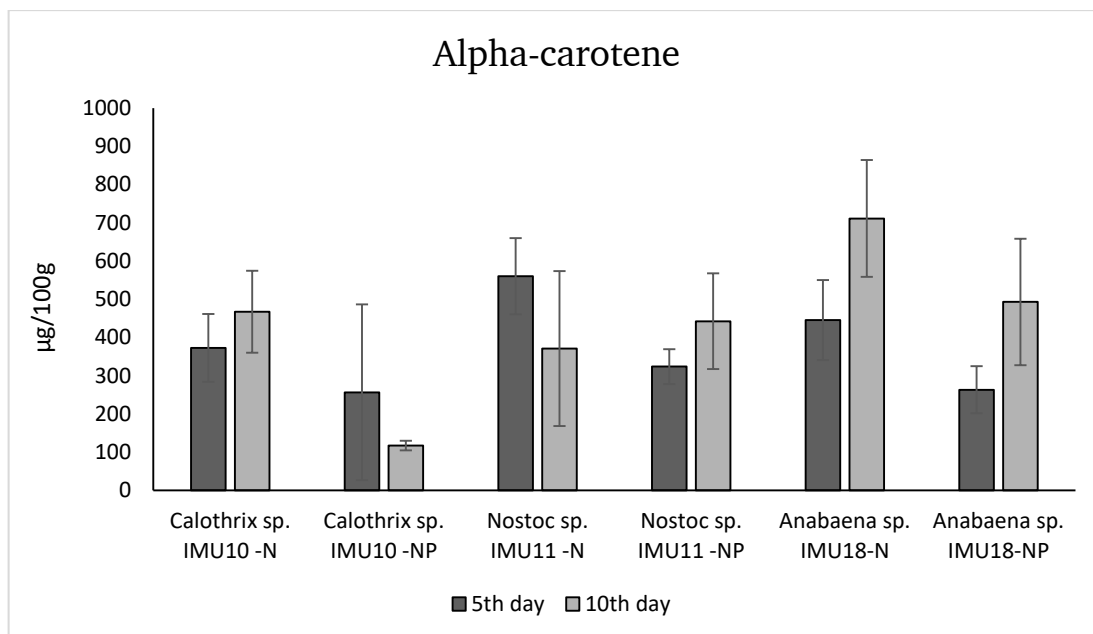


Figure 6.22 Alpha-carotene concentrations in selected Cyanobacteria

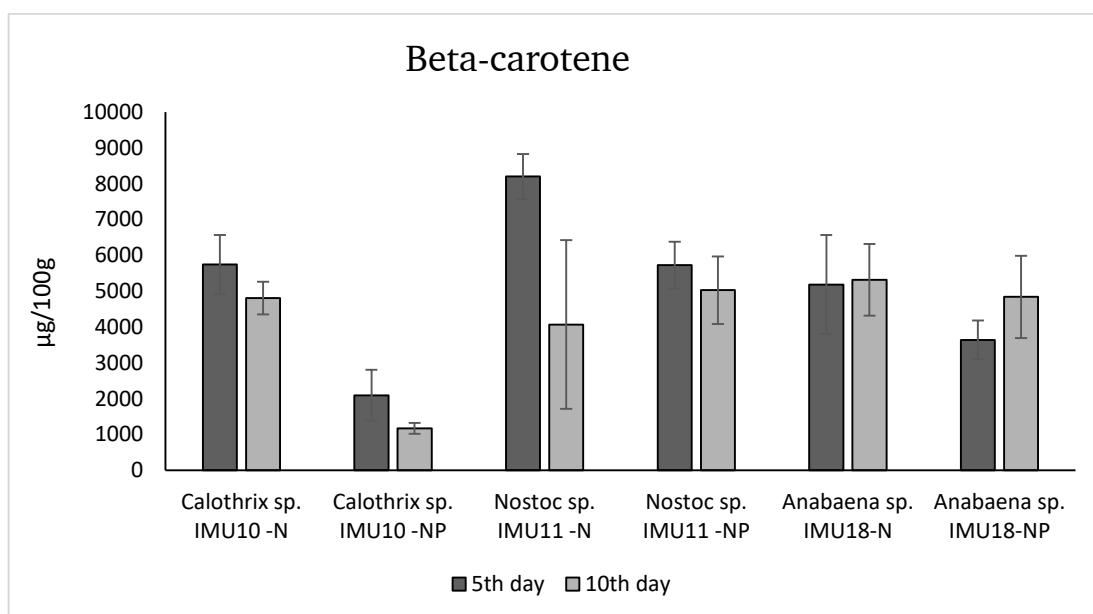


Figure 6.23 Beta-carotene concentrations in selected Cyanobacteria

Riboflavin (B_2 vitamin) production (Fig 6.24) increased by the following days except for *Nostoc* sp. IMU11. The best culture conditions were nitrogen depleted medium, instead of nitrogen and phosphorous, depleted medium for *Anabaena* sp. IMU18 and nitrogen and phosphorus-depleted medium for *Calothrix* sp. IMU10.

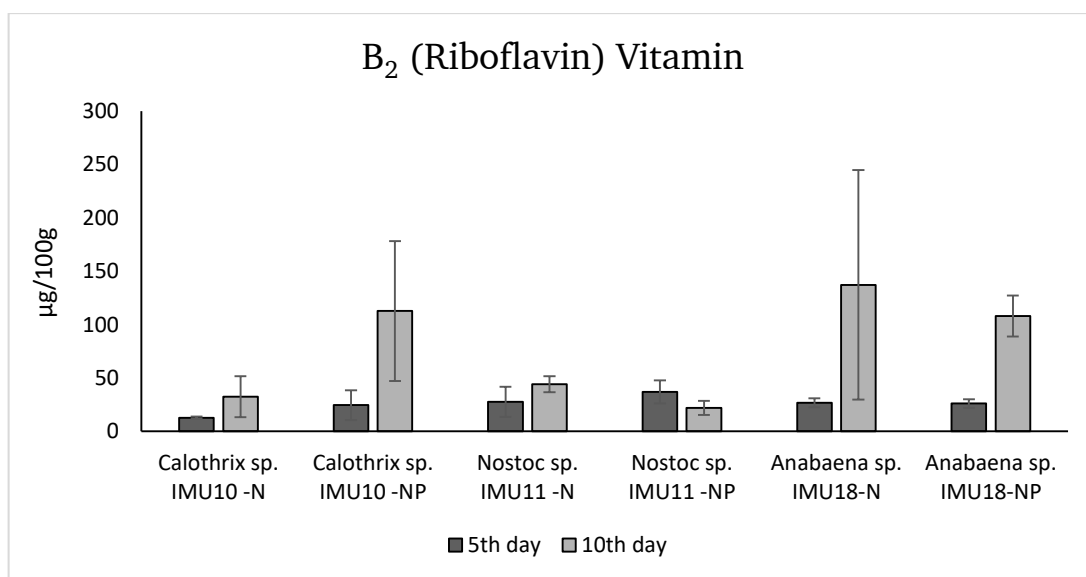


Figure 6.24 B₂ vitamin concentrations in selected Cyanobacteria

6.5.3 Detailed Experiments on Selected Species

BG11 medium (+) was used as the negative control while the BG11-N medium (-N) was used as the control, and the BG11-NP medium (-NP) was used as an experimental group.

6.5.3.1 PHB Measurements

Sulphuric acid digestion method had been compared with the Sudan black B dye method and investigated both for determination PHB production of Cyanobacterial species. With this aim calibration curve calculated for the sulphuric acid digestion method (Fig. 6.25) and the curve was showed very reliable data with the 0.9977 numbered R² value contrary to the Sudan black B dye method. PHB percentage in dry weight (DW) had been calculated by calibration cure (Fig. 6.26). The best day for collecting samples was found on the 5th day and the best cultivation as nitrogen depleted BG11 for all species, and the best PHB producer species as *Calothrix* sp. IMU10, *Nostoc* sp. IMU11, and *Anabaena* sp. IMU18.

The Sudan black B dye method results (Fig. 6.26) corroborate with the sulphuric acid digestion method resulting from the best cultivation condition, which is Nitrogen depleted BG11 media. But unreliable calibration curve, big error bars, and unparallel values were confirmed UV measurements by Sudan black B dye method was not applicable for PHB analysis.

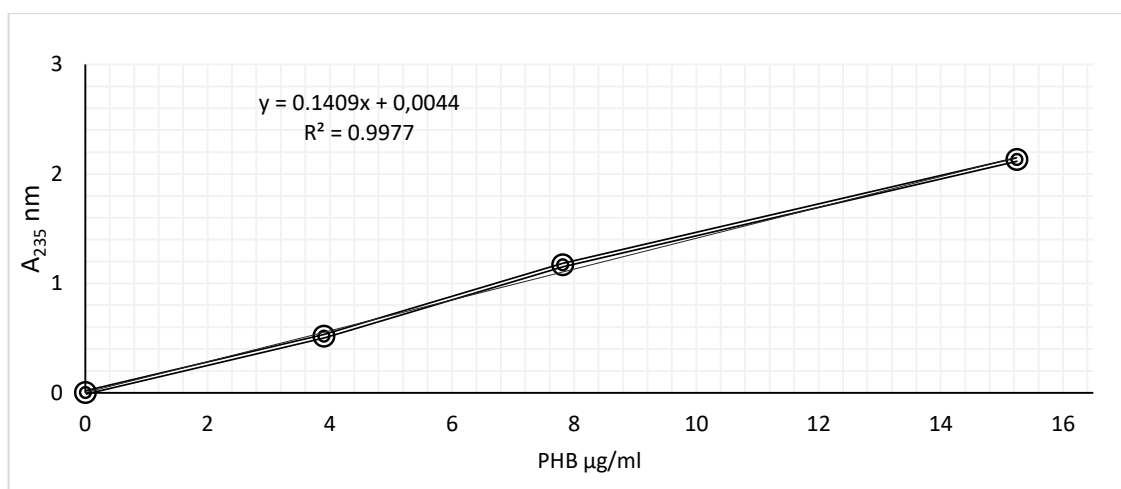


Figure 6.25 PHB calibration curve of sulphuric acid digestion in the quartz tube

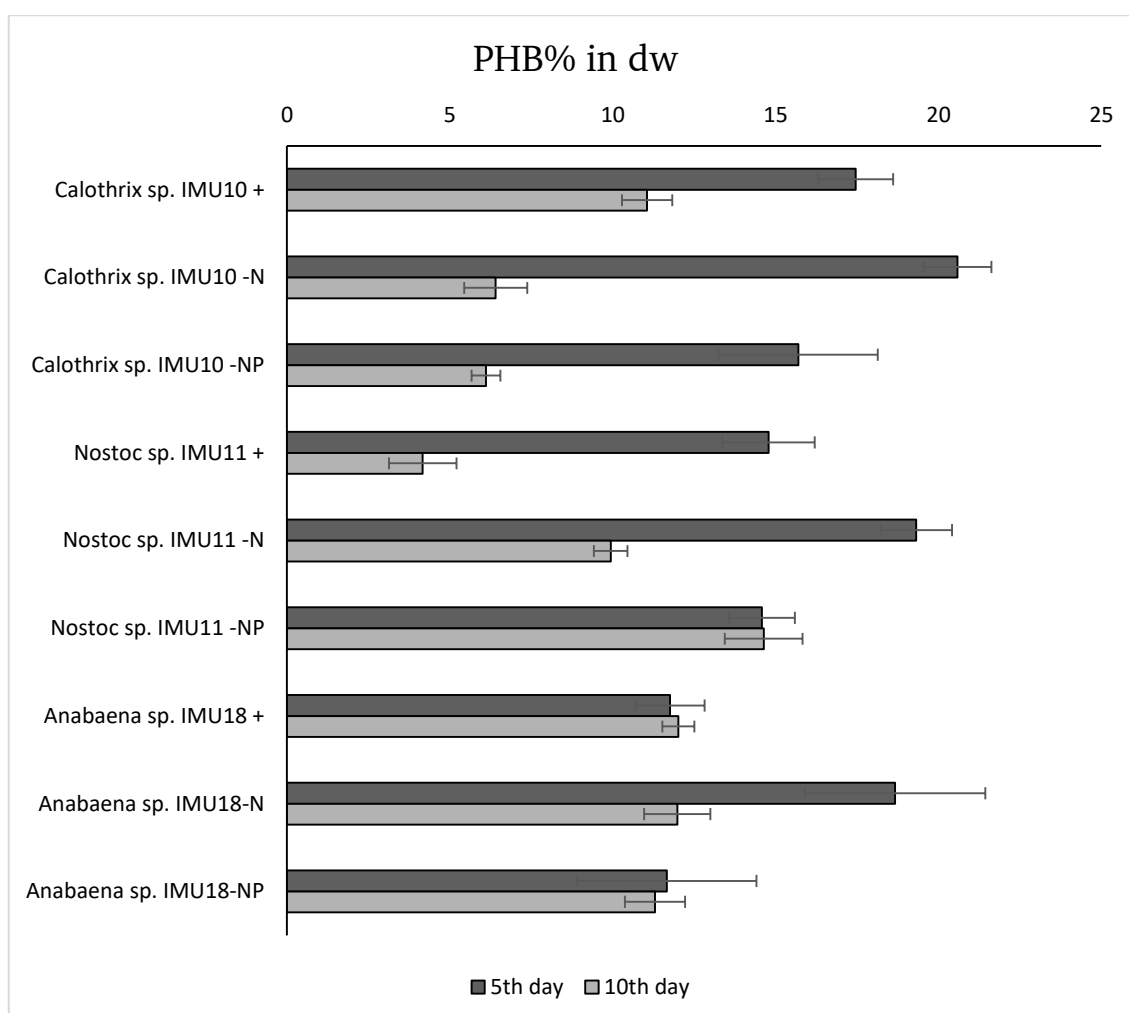


Figure 6.26 PHB percentage in dry weight (dw) by sulphuric acid digestion method

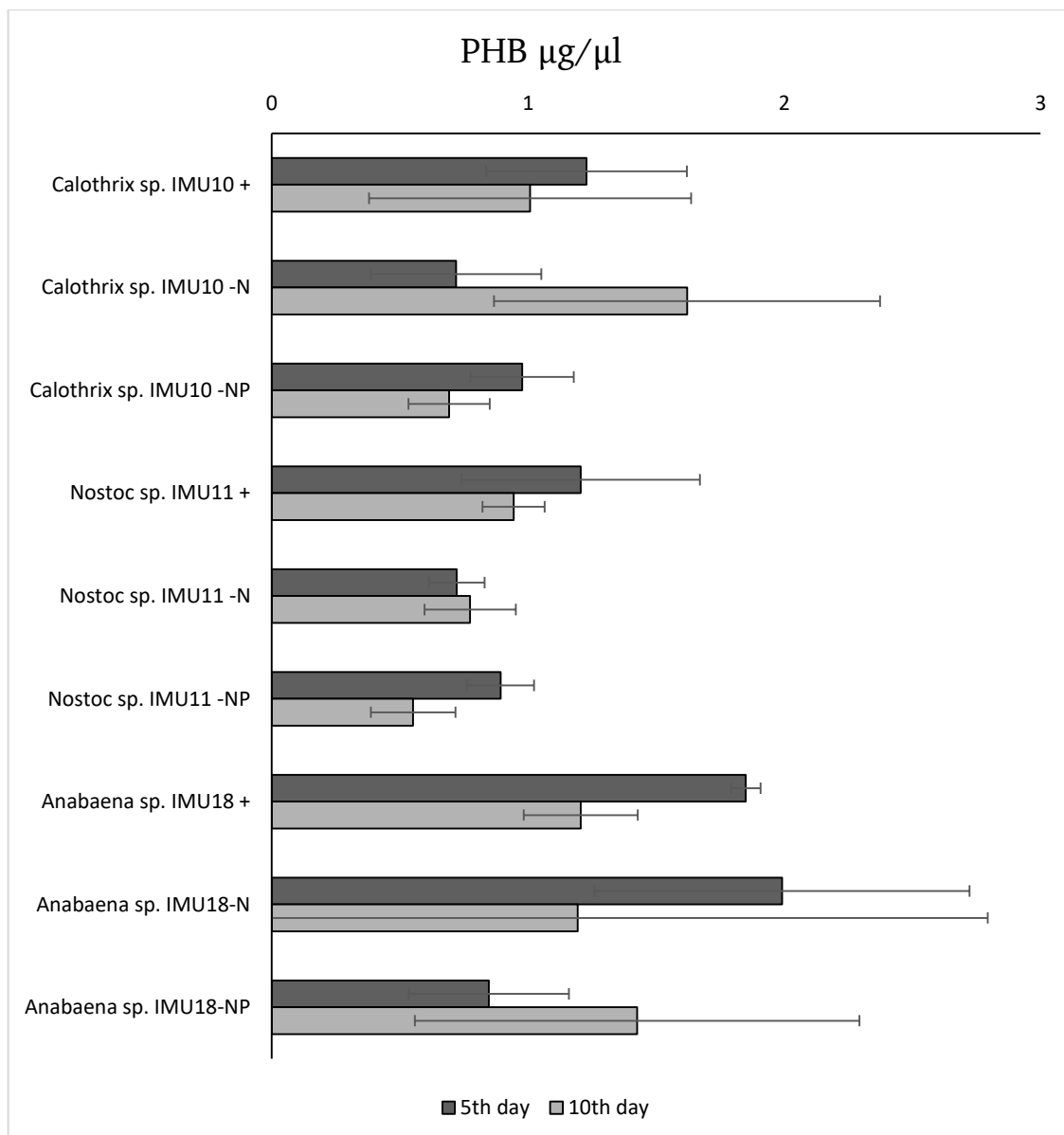
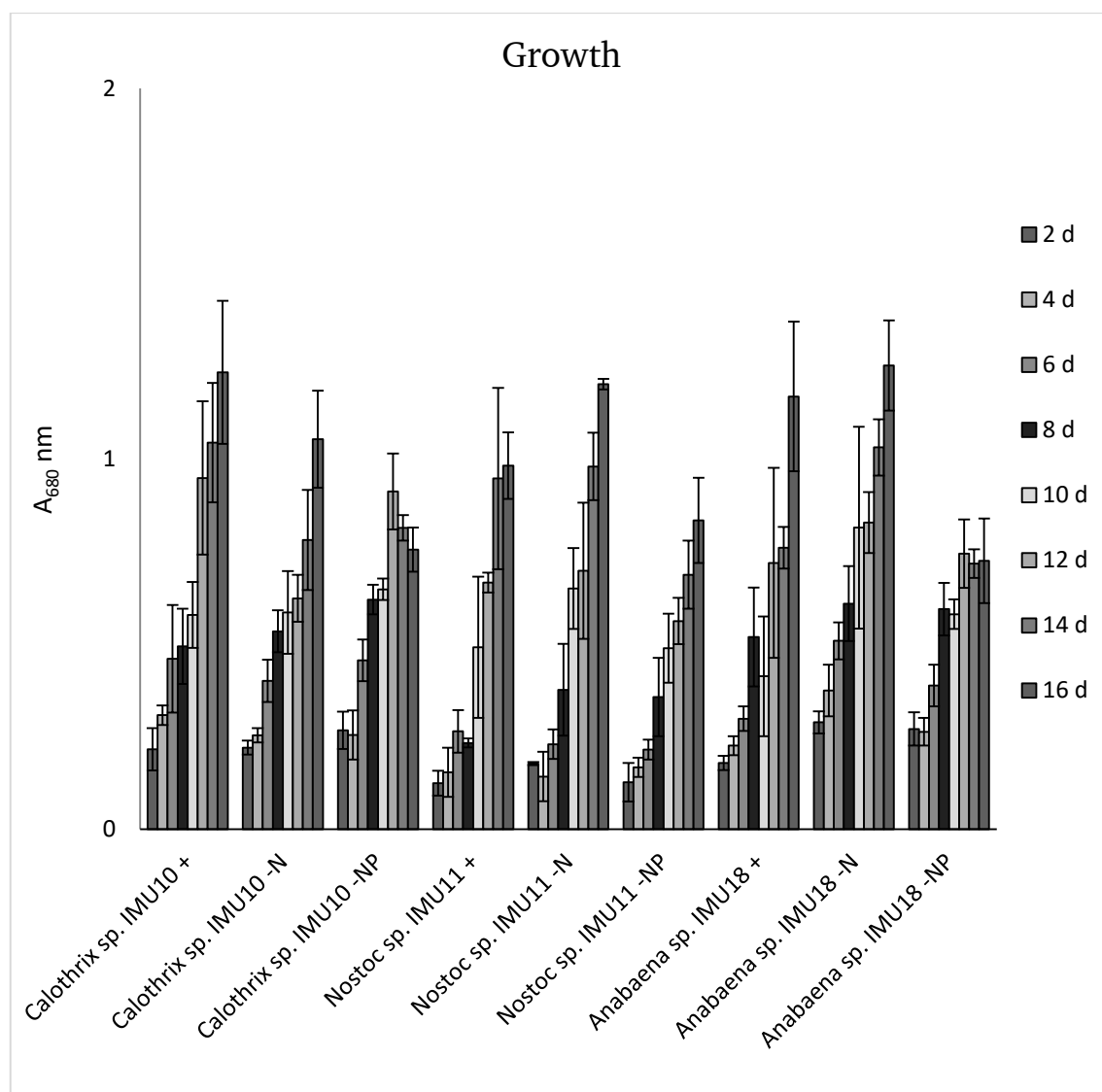


Figure 6.27 PHB concentration by Sudan black B dye method

6.5.3.2 Growth

Cyanobacterial growth was recorded at A_{680} , and it was investigated with increasing growth rate by days (Fig. 6.28). The best growth rate was observed in nitrogen derived BG11, normal BG11, and nitrogen and phosphorous deprived BG11 media for *Anabaena* sp. IMU18 and *Nostoc* sp. IMU11 respectively, except for normal BG11, nitrogen derived BG11, and nitrogen and phosphorous deprived BG11 media for *Calothrix* sp. IMU10 with the lowest rate.



+: BG11/ -N: BG11-N/ -P: BG11-P / 2,4,6,8,10,12,14,16: Sampling day*

Figure 6.28 Cyanobacterial growth rates

6.5.3.3 Chlorophyll-a & Carotenoid Measurements

It had been determined that the best condition for chlorophyll-a production is nitrogen deprived BG11 medium except for *Calothrix* sp. IMU10 and the worse parameter was nitrogen and phosphorous deprived BG11 medium (Fig. 6.29). Growth and chlorophyll-a data were showed the same analogy. Chlorophyll-a and carotenoid amounts (Fig. 6.30) had been raised by the following days in general.

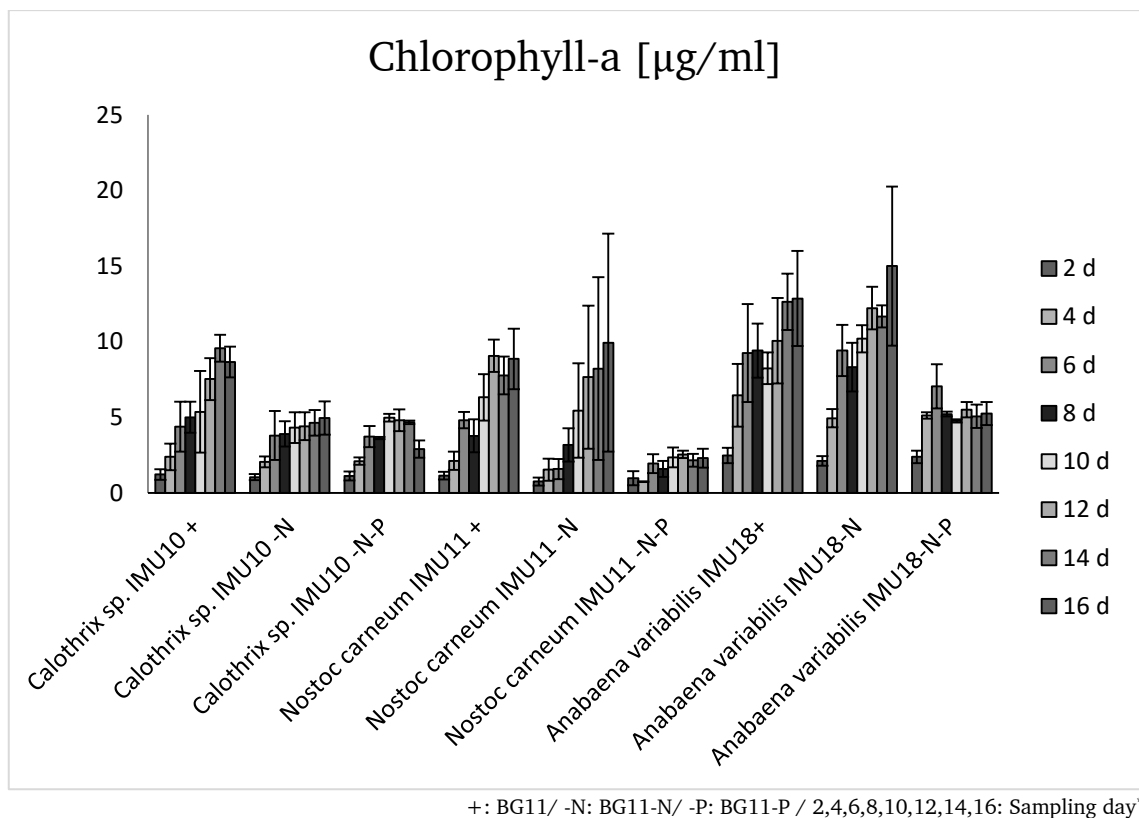


Figure 6.29 Chlorophyll-a amounts in selected species

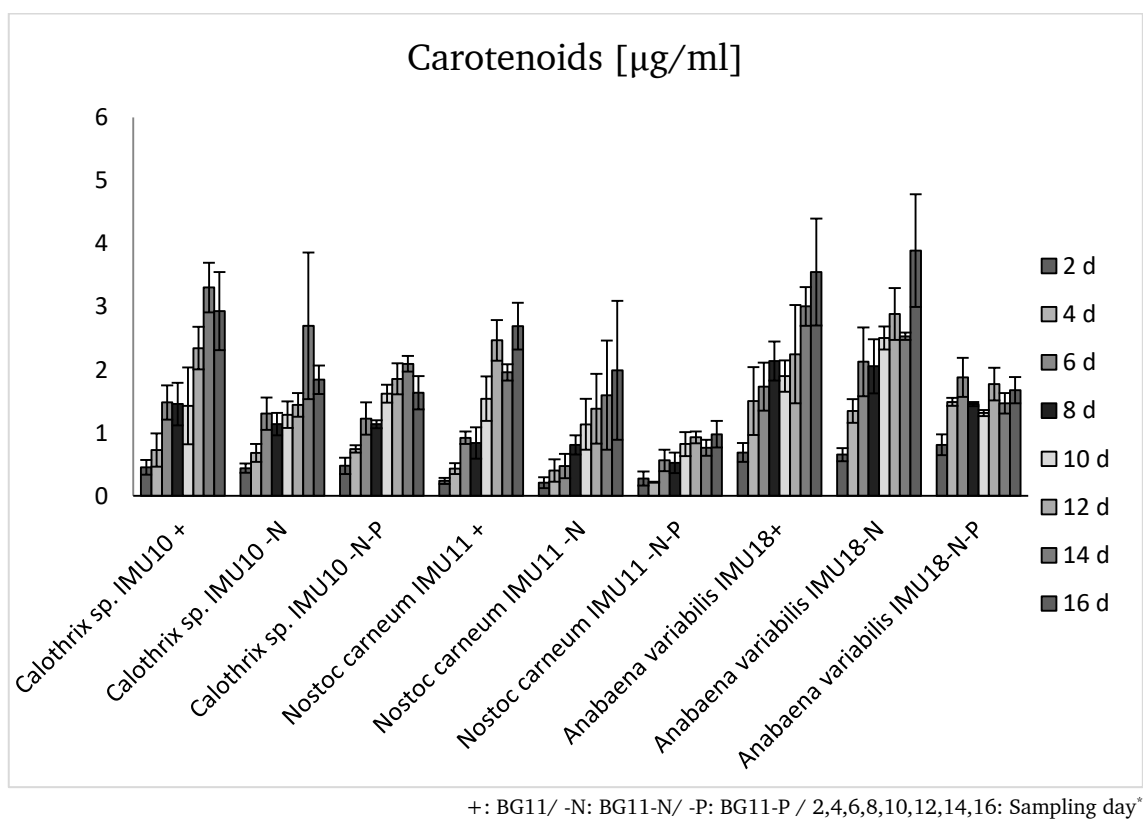


Figure 6.30 Carotenoid amounts in selected species

6.5.3.4 Saccharide Measurements

The saccharide production was calculated by calibration curve (Fig. 6 .31) and the best saccharide production had been identified on the day of 10, and the best culture conditions were nitrogen and phosphorous depleted BG11 medium, nitrogen depleted BG11 medium, and normal BG11 medium, respectively, except for the *Anabaena* sp. IMU18 (Fig. 6 .32).

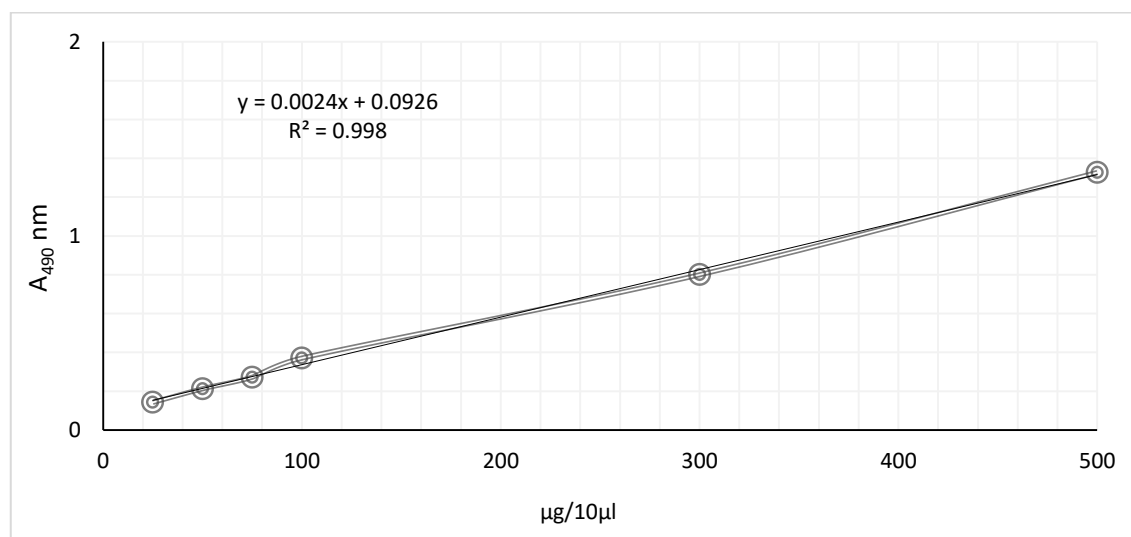


Figure 6.31 Saccharide calibration curve

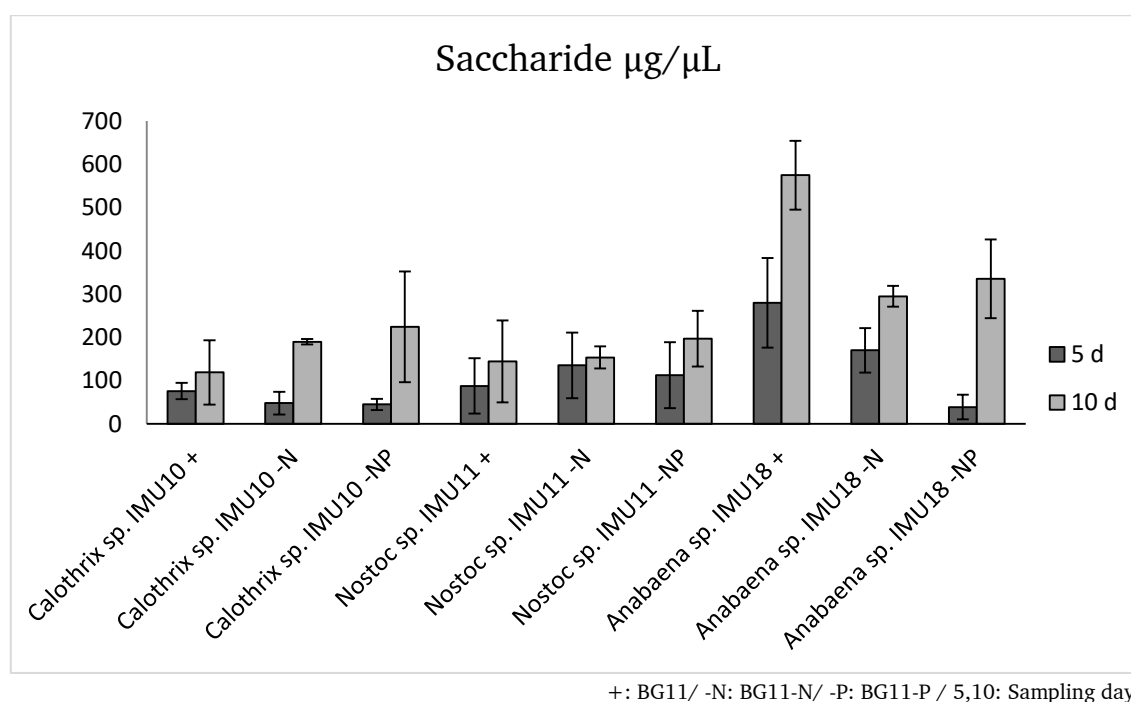


Figure 6.32 Total saccharide amounts in selected species

6.5.3.5 Protein Measurements

Protein productions were calculated by calibration curve (Fig. 6 .33) and were observed in increasing by the following days, and the best culture conditions were BG11, nitrogen depleted BG11 medium, and nitrogen and phosphorous, depleted BG11 medium especially for *Anabaena* sp. IMU18 (Fig. 6 .34).

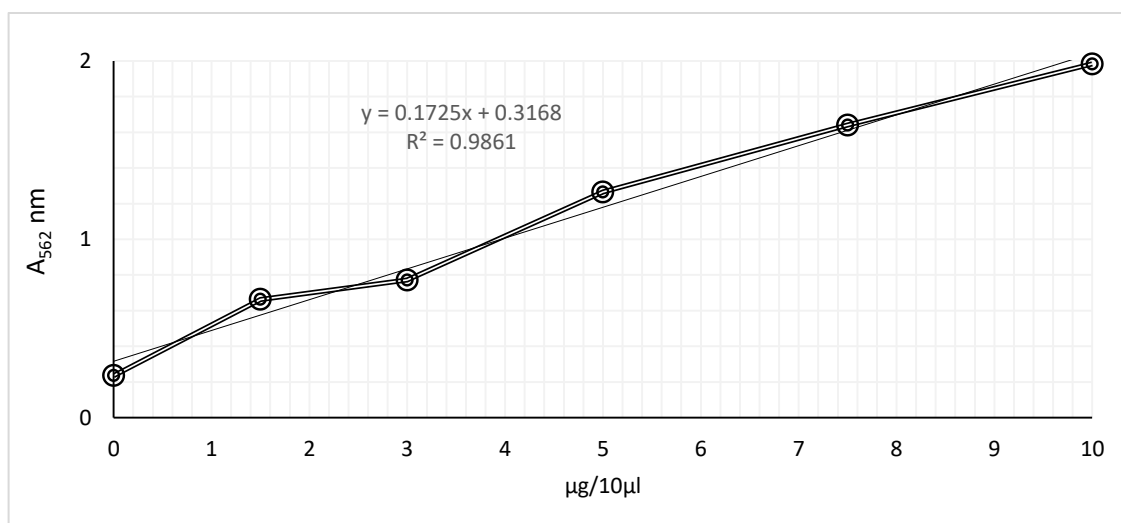


Figure 6.33 Protein calibration curve

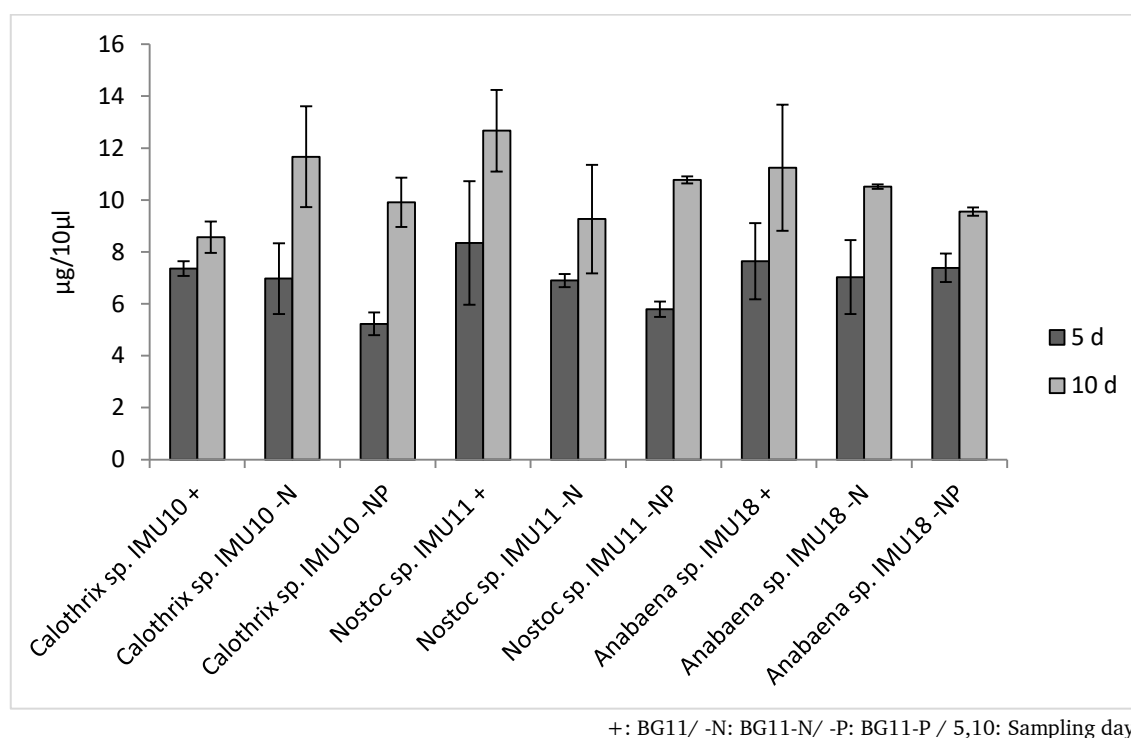


Figure 6.34 Protein amounts in selected species

6.5.3.6 Nile Red Imaging

Cyanobacterial lipids and PHB contents were imaged by fluorescent microscope with high illuminations, which gave promising results (Fig. 6.35).

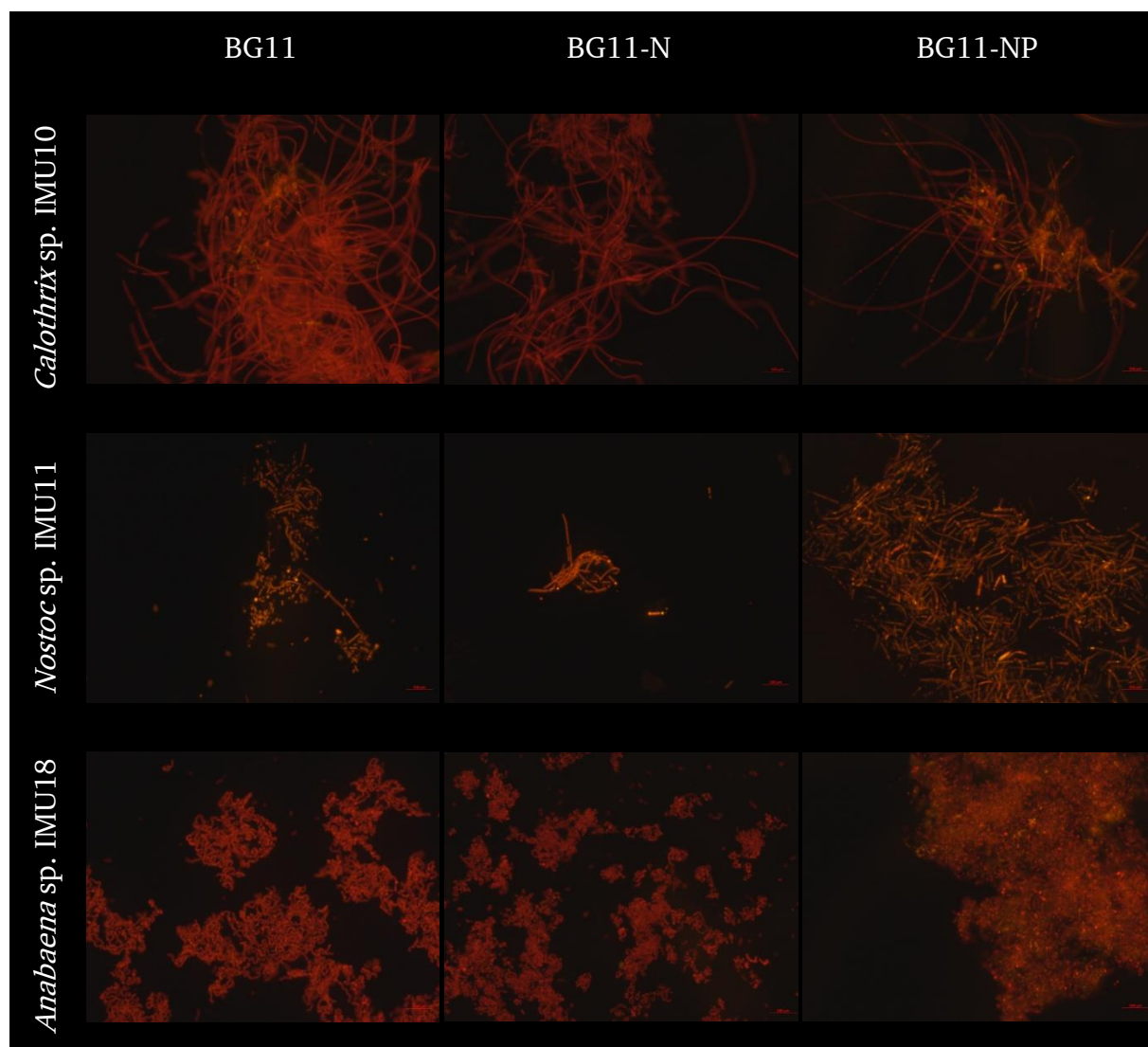


Figure 6.35 Nile red images

6.5.4 Maximization of Extraction Techniques

Sodium hypochlorite extraction could not have resulted due to the weight loss of the Cyanobacterial cells by hardly rinsing from sodium hypochlorite.

Soxhlet extraction maximization results (Fig. 6.36) showed no significant differences in *Calothrix* sp. IMU10 and *Nostoc* sp. IMU11, which means the classic extraction method was better, except for the *Anabaena* sp. IMU18 using

chloroform with dichloromethane (CD) instead of chloroform (C) showed promising results with a 1.59 fold increase.

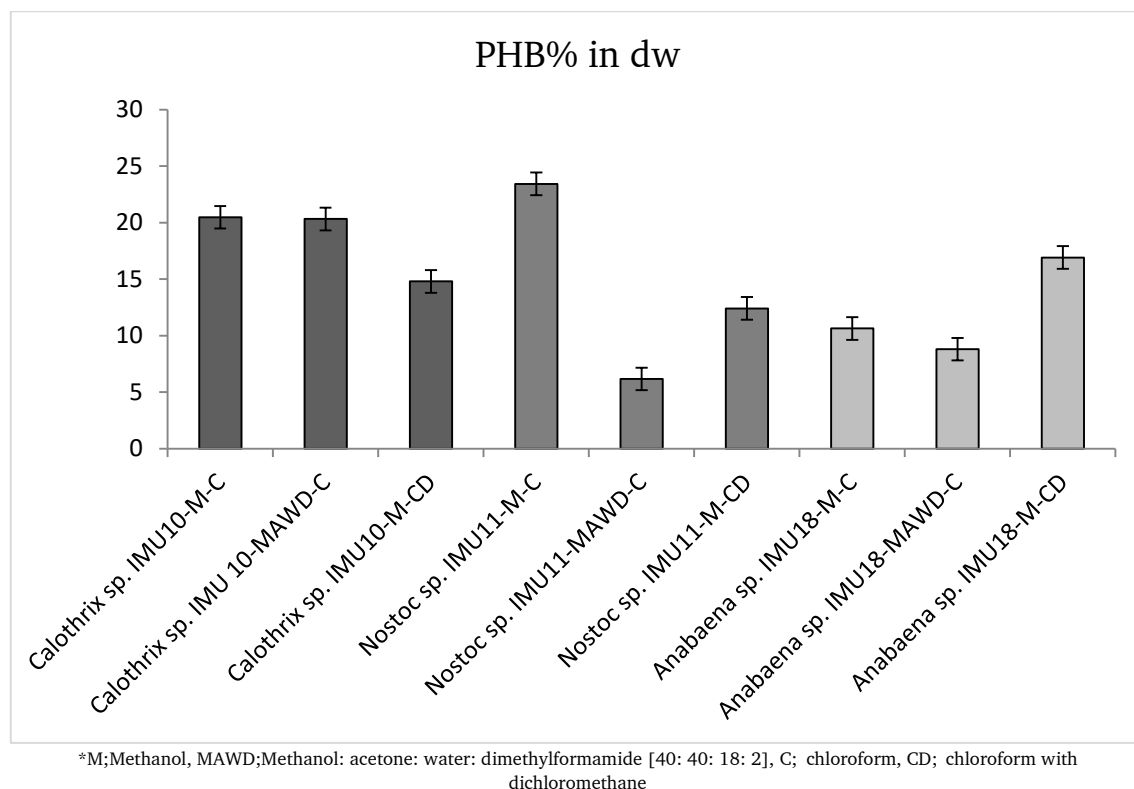


Figure 6.36 PHB percentage in dry weight (dw) of selected species after different extraction manipulations

6.5.5 Environmental Stress Applications

6.5.5.1 PHB Analysis

Stress applications experiment was summarized as following Table 6.10:

Table 6.10 Culture flasks during inoculation by various media

* +: BG11; N: BG11-N; P: BG11-NP; A: BG11-N + %0.4 AcOH/ dark; B: BG11-N + %0.4 AcOH/ dark/ pH:8.5; C: BG11-N + %0.4 AcOH/ dark/ 10°C

	<i>Group +</i>	<i>Group N</i>	<i>Group P</i>	<i>Group A</i>	<i>Group B</i>	<i>Group C</i>
<i>Calothrix</i> sp. IMU10 0th Day						
<i>Calothrix</i> sp. IMU10 5th Day						
<i>Calothrix</i> sp. IMU10 10th Day						
<i>Nostoc</i> sp. IMU11 0th Day						
<i>Nostoc</i> sp. IMU11 5th Day						
<i>Nostoc</i> sp. IMU11 10th Day						
<i>Anabaena</i> sp. IMU18 0th Day						
<i>Anabaena</i> sp. IMU18 5th Day						
<i>Anabaena</i> sp. IMU18 10th Day						

Results had been estimated by the crotonic acid method. Also, GREINER UV STAR F Bottom 96 well microplate was used to the comparison of quartz tubes, which had been used for the sulphuric acid digestion method. The microplate was measured at UV 235nm, and results were calculated by generated formulas from calibration curves (Fig 6.37). GREINER UV STAR F Bottom 96 well microplate results showed inconsistent results comparing to the literally-known quartz tube calibration curve (Fig 6.25) and method with big error bars.

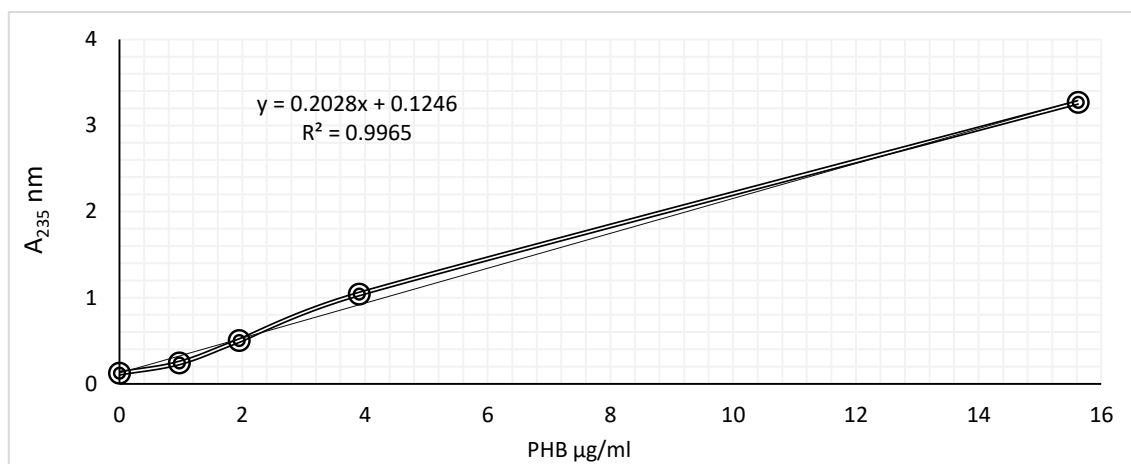


Figure 6.37 Calibration curve of PHB in the microplate

6.5.5.1.1 PHB Production of *Calothrix* sp. IMU10

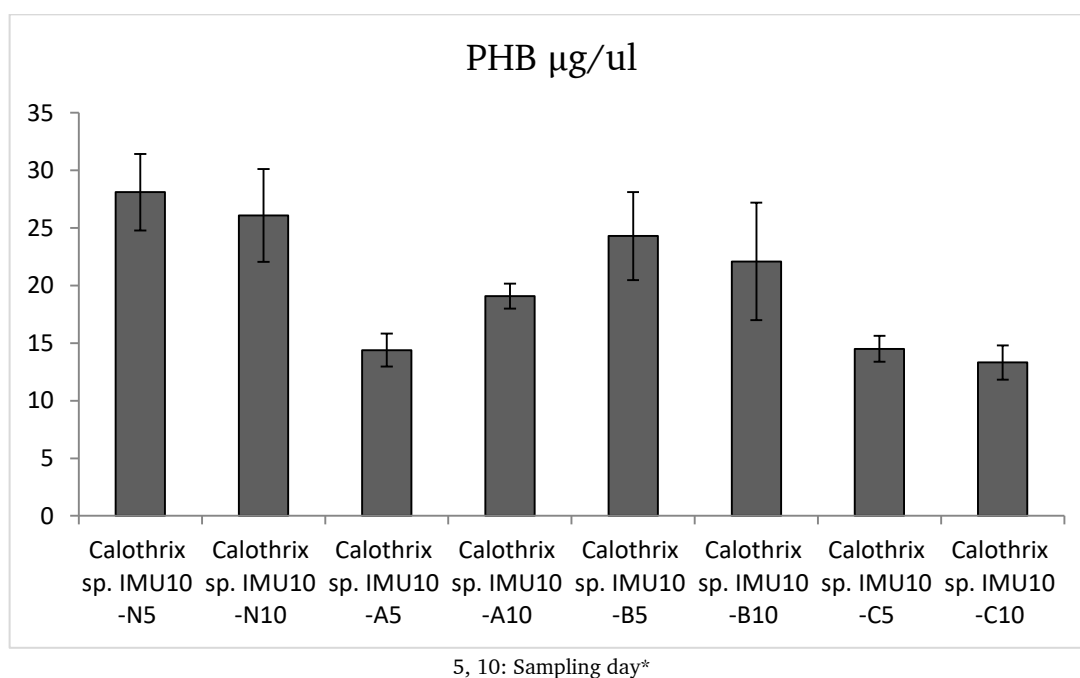


Figure 6.38 PHB amounts of *Calothrix* sp. IMU10 in the quartz tubes

PHB production amounts on *Calothrix* sp. IMU10 was not increased on the experimental groups of environmental effects (Fig. 6.38). The best medium was determined as nitrogen deprived BG11, which was the control group of the experiment, and followed by the group the B, A, and C. Cyanobacterial PHB was decreased by days instead of for the group A.

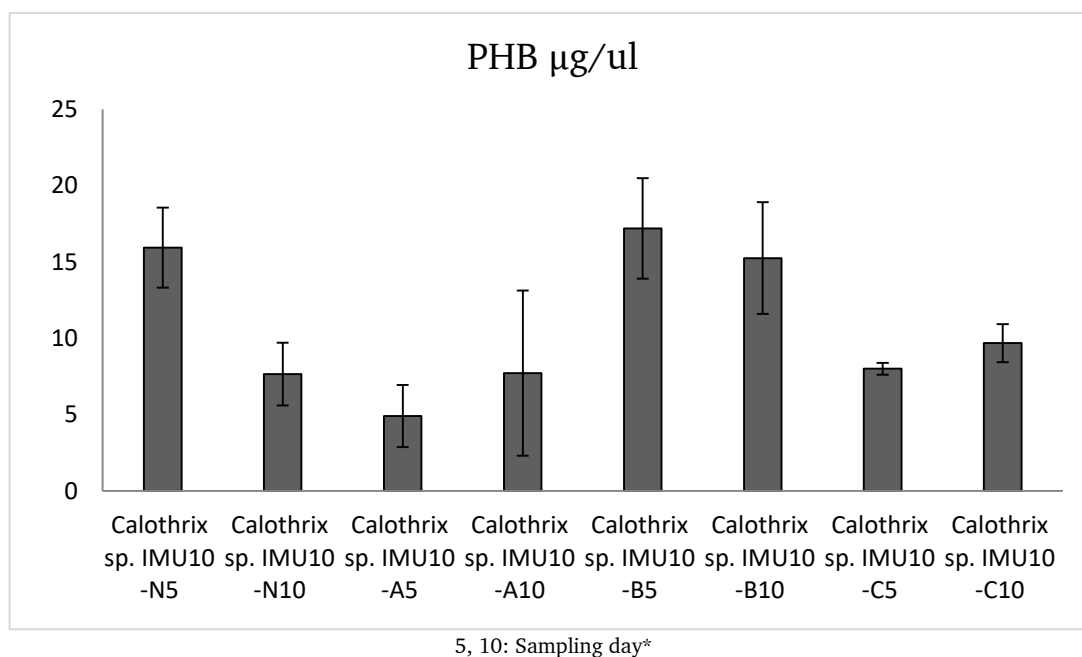


Figure 6.39 PHB amounts of *Calothrix* sp. IMU10 in the microplate

The best medium for PHB production of *Calothrix* sp. IMU10 in microplates were identified as Group B, and followed by the groups the N (Control), C, and A (Fig. 6.39), which were inconsistent with the literally-known quartz tube method. Cyanobacterial PHB was decreased by days except for groups A and C.

6.5.5.1.2 PHB Production of *Nostoc* sp. IMU11

The experimental groups were not shown any significant differences according to the control group (Fig. 6.40). The succeeding media were determined as groups B, C, and A, respectively. Cyanobacterial PHB was decreased by days instead of for group A.

Microplate experimental groups were not shown any significant differences comparing to the control group (Fig. 6.40). The succeeding media were determined as groups B, C, and A, respectively. Cyanobacterial PHB was decreased by days instead of for group A.

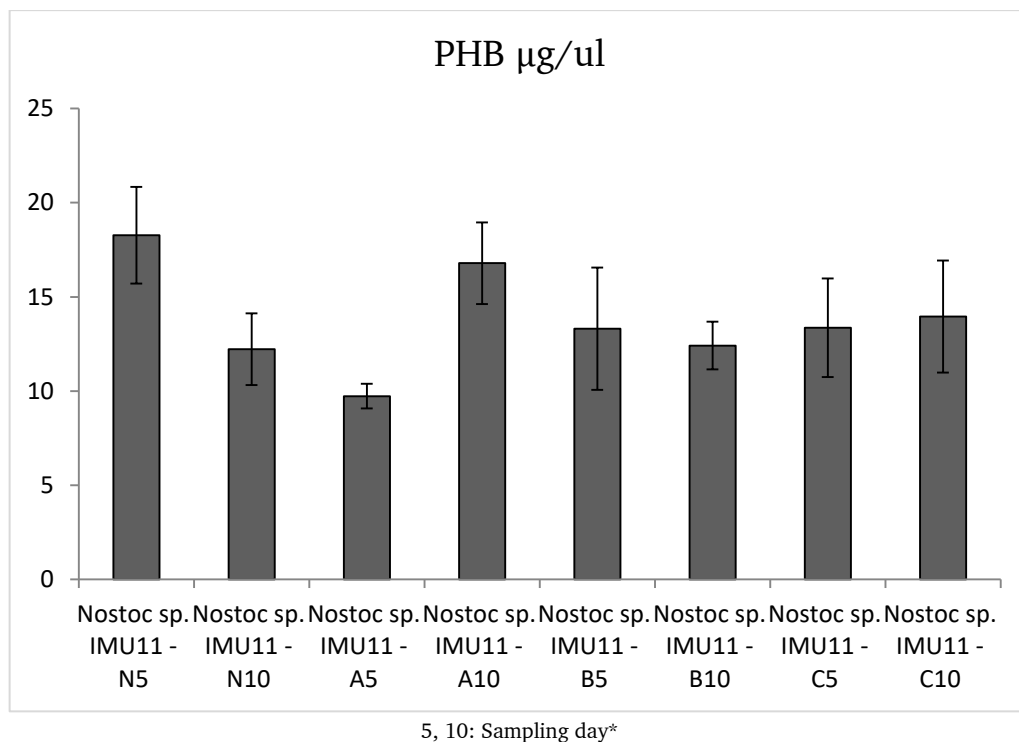


Figure 6.40 PHB amounts of *Nostoc* sp. IMU11 in the quartz tubes

PHB yield was measured in microplates as C, A, B, and N, respectively (Fig. 6.41), which was inconsistent with the quartz tube method's results. PHB was decreased in group C and N by days except for groups A and C.

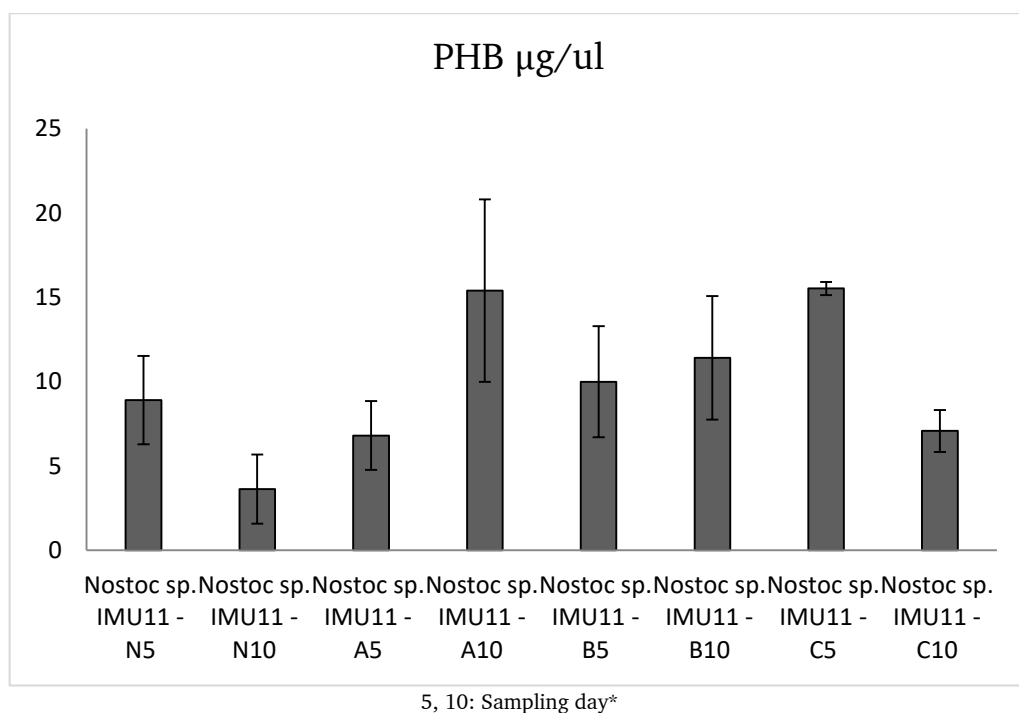


Figure 6.41 PHB amounts of *Nostoc* sp. IMU11 in the microplate

6.5.5.1.3 PHB Production of *Anabaena* sp. IMU18

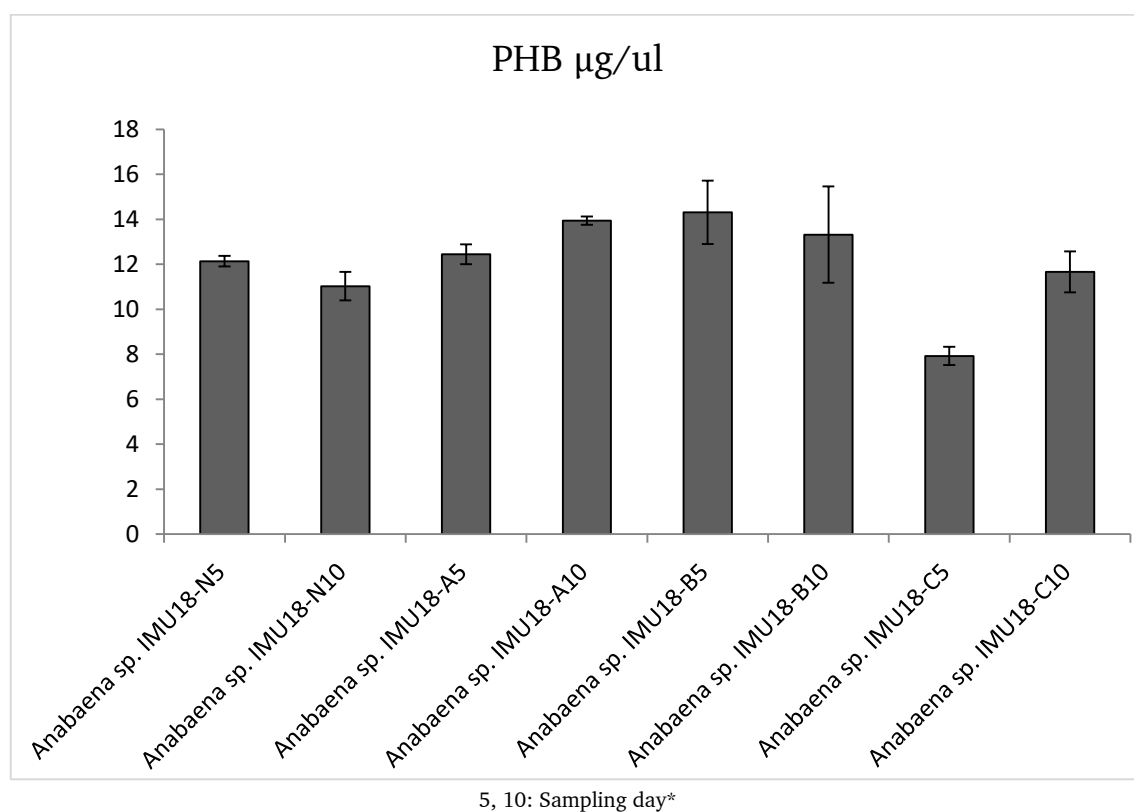


Figure 6.42 PHB amounts of *Anabaena* sp. IMU18 in the quartz tubes

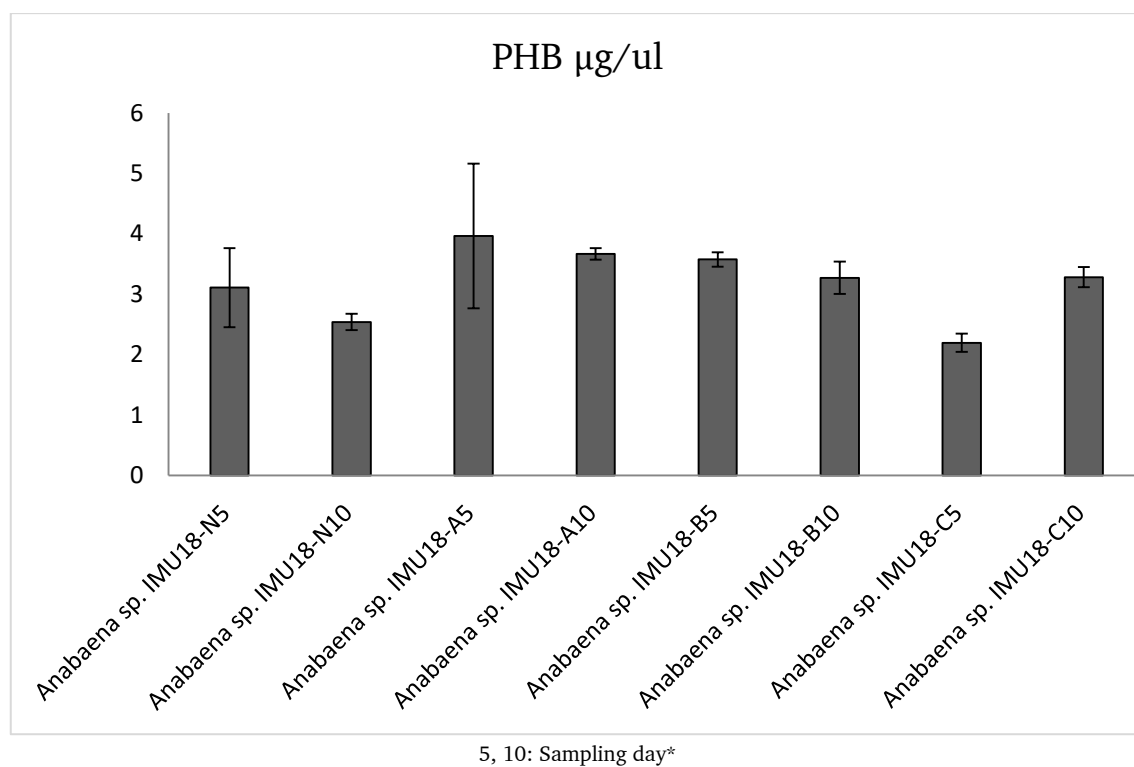


Figure 6.43 PHB amounts of *Anabaena* sp. IMU18 in the microplate

Environmental stress parameters gave promising results for *Anabaena* sp. IMU18 except for Group C. The best PHB producer was estimated as group B, and followed by A, N, and C (Fig. 6.42). Cyanobacterial PHB was decreased by days instead of for group A.

Environmental stress parameters were sporting the results which were gained from the quartz tube, except for the wrong calculations. PHB yield, which measured in microplates, was ordered as following C, A, B, and N (Fig. 6.43). Results had almost parallel consistent with the quartz tube method's results. PHB was decreased in groups by days instead of C.

6.5.5.1.4 Discussion of PHB Analysis Results

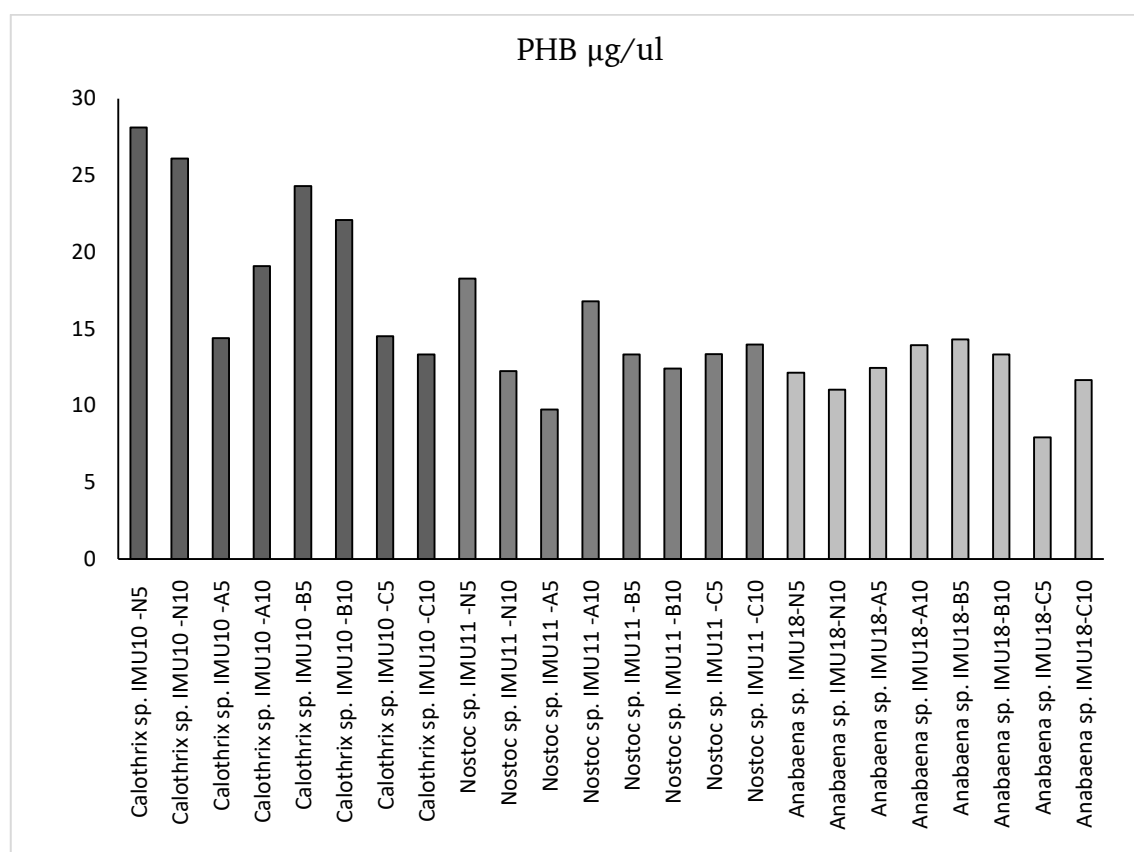


Figure 6.44 PHB amounts of selected Cyanobacteria against environmental manipulation

Environmental stress addition to Cyanobacteria has not indicated promising results apart from *Anabaena* sp. IMU18 (Fig. 6.43). Comparing with the different parameters, the best PHB producer was determined as *Calothrix* sp. IMU10, and followed by *Nostoc* sp. IMU11 and *Anabaena* sp. IMU18 respectively.

6.5.5.2 Chlorophyll-a & Carotenoid Measurements

Investigations of Cyanobacterial growth were also determined by chlorophyll-a concentrations, whereas Cyanobacterial growth parameters were hard to measure for their filamentous forms. Chlorophyll-a amounts were showed that the growth of the species had been raised by the following days of the incubation, which were resulted in best in the control group, then followed by groups A, C, and B in general (Fig. 6.45).

General results of carotenoid values were almost parallel to the chlorophyll-a graph and showed that the growth of the species had been increased by the following days of incubation with no significant change in group B especially. The best carotenoid amount resulted in the control group then followed by groups A, C, and B in general, which means environmental stress application was not promising (Fig. 6.46).

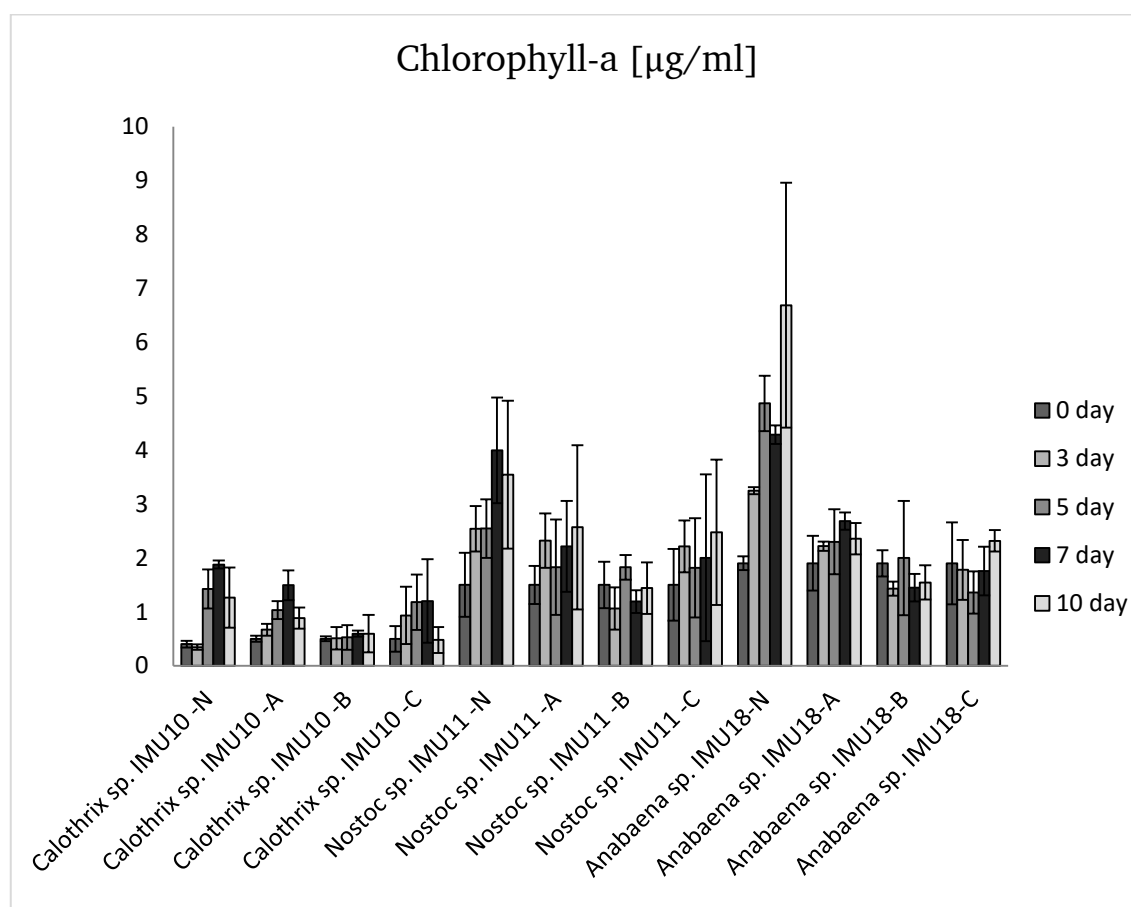


Figure 6.45 Chlorophyll-a amounts of selected species in different stress conditions

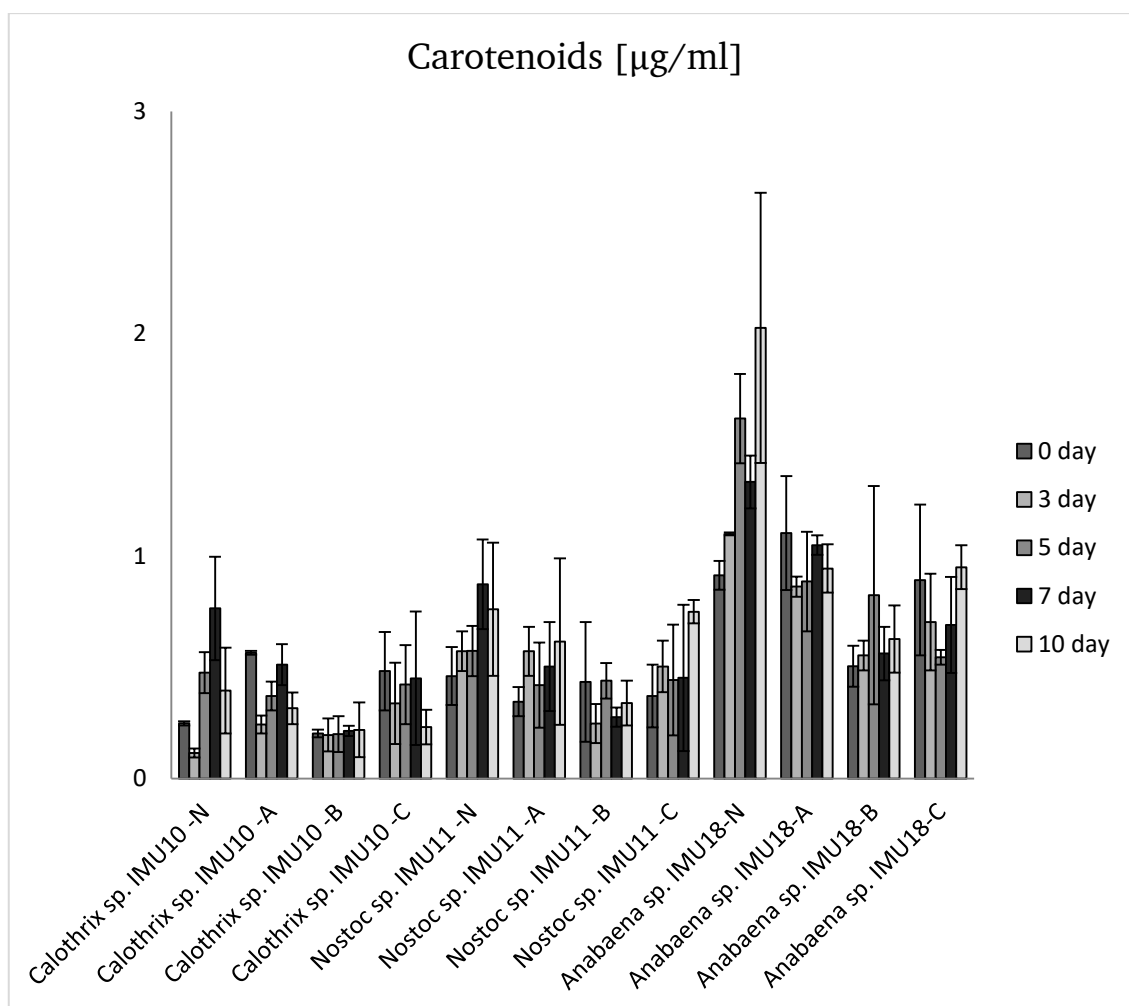


Figure 6.46 Carotenoid amounts of selected species in different stress conditions

6.5.5.3 GC Measurements of FAME Products

Fatty acyl methyl ester (FAME) analysis was identified by Gas chromatography (GC) and FAME standard optimization [112] for the Cyanobacteria species in their selected culture media, which were BG11-N for *Calothrix* sp. IMU10 (Fig. 6.47) and *Nostoc* sp. IMU11 (Fig. 6.48), and BG11-N with %0.4 AcOH addition in the dark culturing for *Anabaena* sp. IMU18 (Fig. 6.49). FAME analysis of selected Cyanobacteria in selected conditions for PHB production gave promising and accessible results for biodiesel production. The best FAME products for three species were determined as cis-10-pentadecenoic acid methyl ester (C15:1), methyl octadecanoate (C18:0), methyl arachidate (C20:0), methyl palmitate (C16:0), and cis-10-heptadecenoic acid methyl ester (C17:1), respectively.

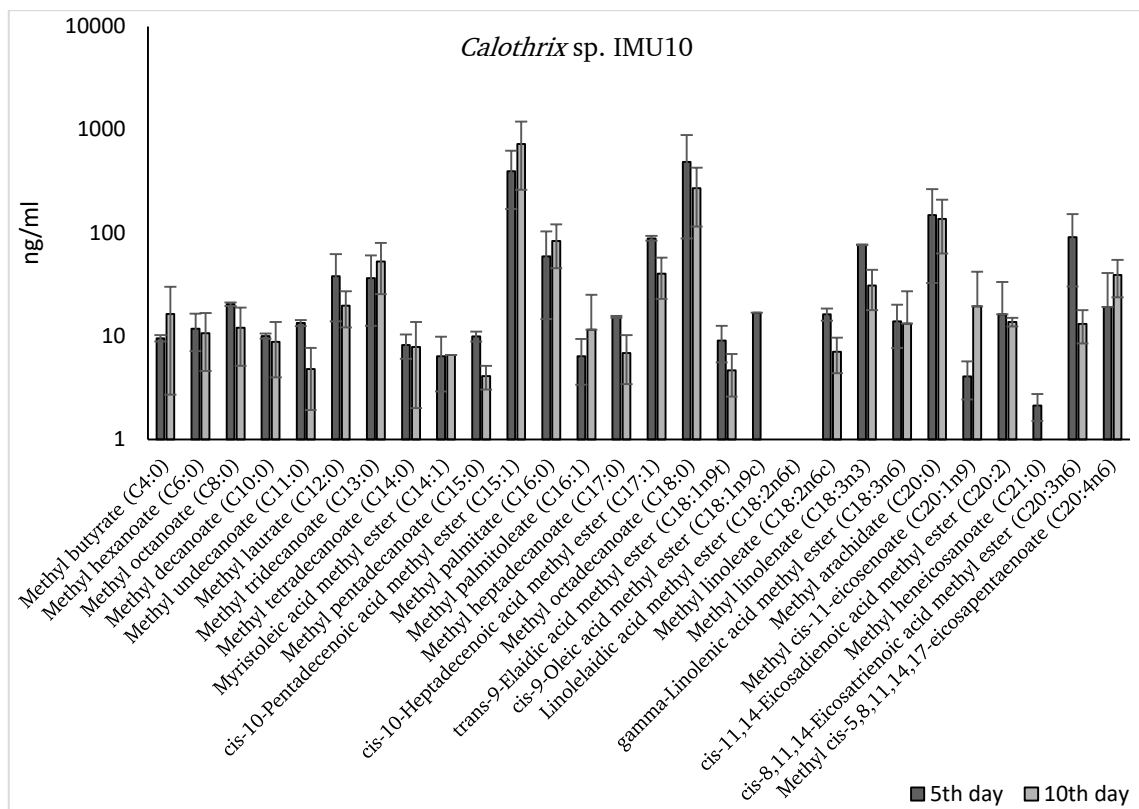


Figure 6.47 FAME analysis of *Calothrix* sp. IMU10 * In a logarithmic scale

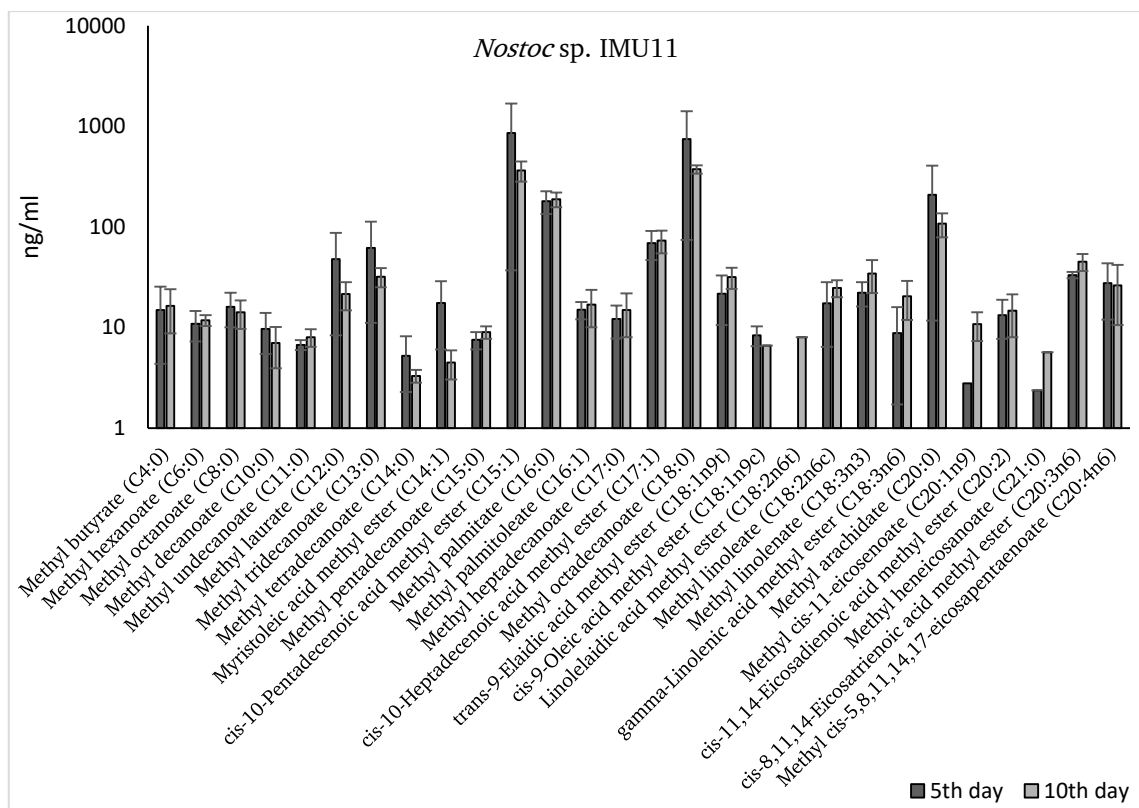


Figure 6.48 FAME analysis of *Nostoc* sp. IMU11 * In a logarithmic scale

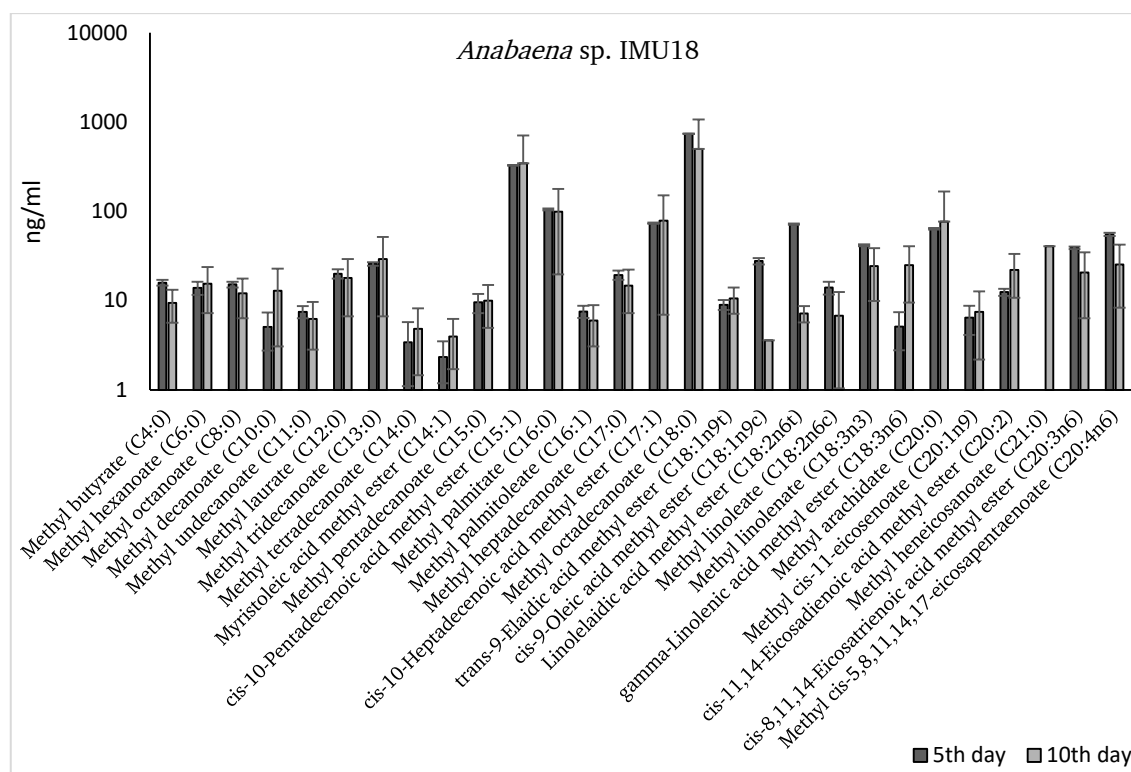


Figure 6.49 FAME analysis of *Anabaena* sp. IMU18 *In a logarithmic scale

6.5.6 Identification of PHB by FTIR Analysis

Extracted PHB by soxhlet extraction was determined by FTIR. PHB extracts from *Calothrix* sp. IMU10 (Fig. 6.50), *Nostoc* sp. IMU11 (Fig. 6.51), and *Anabaena* sp. IMU18 (Fig. 6.52) were identified by FTIR and the leading PHB bands described in Table 6.11 [91]. The FTIR spectrums showed prominent peaks at ~ 1735 to ~ 1710 cm^{-1} and also, adsorption bands obtained at 1363, ~ 1476 , ~ 2920 – ~ 2849 , and ~ 3381 cm^{-1} denote the $-\text{CH}_3$, $-\text{CH}_2$, $-\text{CH}$, and O-H groups respectively.

Table 6.11 Band assignments of FTIR

<i>Wavenumber value (cm⁻¹)</i>	<i>Assignment*</i>	<i>Comments</i>
~3400	$\delta_{(\text{H-O-H})}$ of nitrogen compounds	H bonded OH groups of alcohol, phenol, organic acids and also H bonded N-H groups
~2930	$\nu_{\text{as}} (\text{C-H})$ of saturated CH	Positions of saturated CH associated with lipids, alkanes and may also contain contributions from PHB
~2850	$\nu_{\text{s}} (\text{C-H})$ of saturated CH	Positions of saturated CH associated with lipids, alkanes and may also contain contributions from PHB
~1,735	$\nu_{\text{C=O}}$ of ester functional groups primarily from lipids, fatty acids, and PHB	The exact position of PHB absorbance depends on the degree of crystallinity of the PHB
~1,650	$\nu_{\text{C=O}}$ of amides associated with proteins	Usually called the amide I band; may also contain contributions from C=C stretches of olefinic and aromatic compounds
~1,540	$\delta_{(\text{N-H})}$ of amides associated with proteins	Usually called the amide II band; may also contain contributions from C=N stretches
~1,455	$\delta_{\text{as}} (\text{CH}_3)$ and $\delta_{\text{as}} (\text{CH}_2)$ of proteins	Positions of these assignments can vary; contributions also from PHB
~1,398	$\delta_{\text{s}} (\text{CH}_3)$ and $\delta_{\text{s}} (\text{CH}_2)$ of proteins, $\nu_{\text{s}} (\text{C-O of COO}^-)$ groups	Positions of these assignments can vary; contributions also from PHB
~1,242	$\nu_{\text{as}} (\text{P=O})$ of the phosphodiester backbone of nucleic acids (DNA and RNA)	May also be due to the presence of phosphorylated proteins and polyphosphate storage products
~1,080	$\nu_{\text{s}} (\text{P=O})$ of the phosphodiester backbone of nucleic acids (DNA and RNA)	May also be due to the presence of phosphorylated proteins and polyphosphate storage products
1,200–900	$\nu_{(\text{C-O-C})}$ of polysaccharides	Contributions also from PHB

* ν_{as} , asymmetric stretch; ν_{s} , symmetric stretch; δ_{as} , asymmetric deformation (bend); δ_{s} , symmetric deformation (bend)

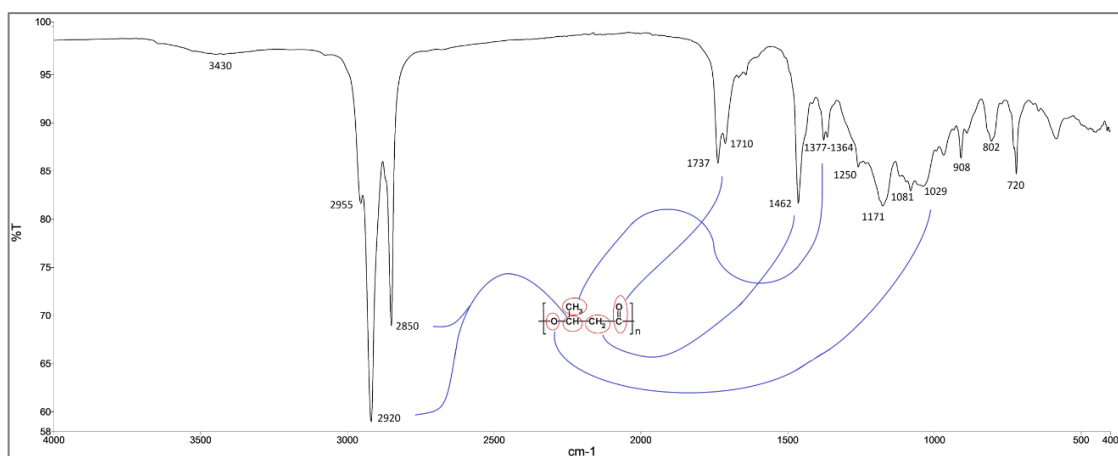


Figure 6.50 FTIR spectra of *Calothrix* sp. IMU10

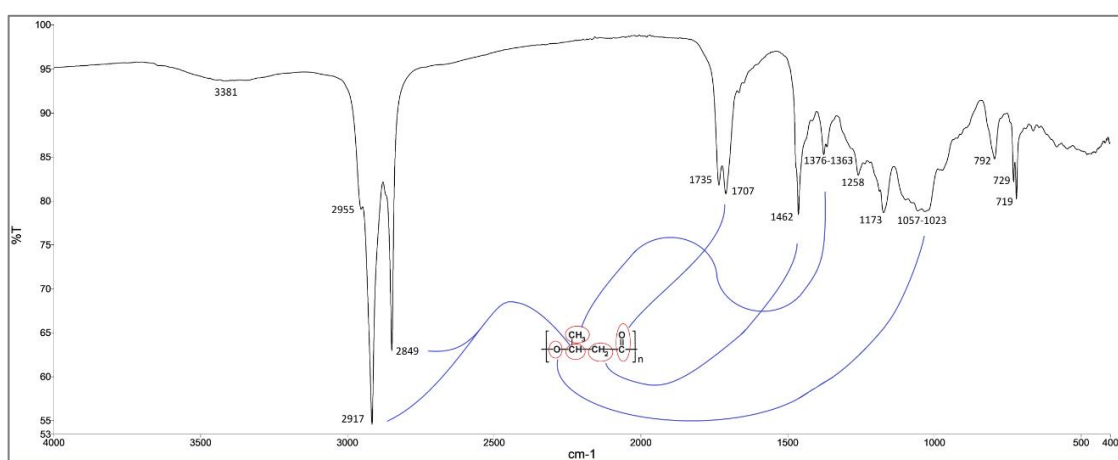


Figure 6.51 FTIR spectra of *Nostoc* sp. IMU11

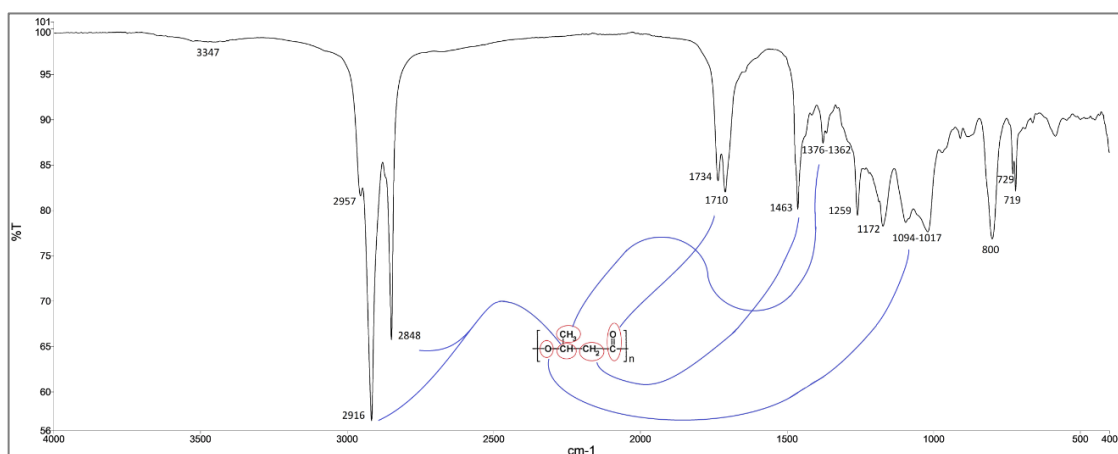


Figure 6.52 FTIR spectra of *Anabaena* sp. IMU18

6.6 Conclusions

Cyanobacteria have been investigated to find the best PHB producer species, the best extraction procedure, culture media, stress conditions, and their by-product contents. The species have been sustained in BG11-N medium since isolation in May 2017, which had been considered as a well-established time for the species to adapt to nitrogen starvation, day by day.

Nostoc sp. IMU02, *Cylindrospermum* sp. IMU04, *Cylindrospermum* sp. IMU05, *Calothrix* sp. IMU09, *Calothrix* sp. IMU10, *Nostoc* sp. IMU11, *Nostoc* sp. IMU13, *Nostoc* sp. IMU15, *Anabaena* sp. IMU18, *Nostoc* sp. IMU019, *Calothrix* sp. IMU21, and *Calothrix* sp. IMU22 species from paddy fields of Edirne and also *Nostoc* sp. IMU1, *Mastigocladus* sp. IMU2, *Chlorogloeopsis* sp. IMU3, *Nodosilinea* sp. IMU5, *Anabaena variabilis* sp. IMU8, *Nodularia* sp. IMU17, *Nostoc* sp. IMU19, *Nostoc* sp. IMU20, *Microchaete* sp. IMU22, *Anabaenopsis* sp. IMU23, *Trichormus* sp. IMU26, and *Anabaena* sp. IMU30 species from IMU culture library have been identified, and their PHB, TAG, chlorophyll-a, carotenoid, oligosaccharide, polysaccharide, and phycobiliprotein (phycoerythrin, phycocyanine, and allophycocyanine) measurements have been completed.

FTIR measurement (relative) and sulphuric acid digestion method (% in dw) have been compared for PHB determination against Sudan black B UV measurement, and it has been found that these measurements have more reliable data to measure PHB content analytically. But also, Sudan black B dyeing has been given a respectable microscope screening of PHB. Moreover, the effect of the quartz tube and the GREINER UV STAR F Bottom 96 well microplate on the sulphuric acid digestion method have been compared, and measurement by the quartz tube has been found to be more accurate.

Sodium hypochlorite and soxhlet extraction have been compared to investigate the best PHB extraction method where sodium hypochlorite extraction was showed week applicability with high weight loss. Additionally, the maximization of soxhlet extraction has been studied for classical pre-extraction by methanol and extraction by chloroform (C). Results have shown no significant difference for *Calothrix* sp. IMU10 and *Nostoc* sp. IMU11, while *Anabaena* sp. IMU18 gave

promising PHB results with a 1.59 fold increase by chloroform and dichloromethane (1:1) extraction (CD).

Calothrix sp. IMU10, *Nostoc* sp. IMU11, and *Anabaena* sp. IMU18 species have been selected as the best PHB producer species. Five days of incubation in the BG11-N medium has been determined as the best stress condition except for *Anabaena* sp. IMU18, while dark incubation and %0.4 AcOH addition in BG11-N, has been defined the best for PHB production.

FAME, protein, saccharide, chlorophyll-a, carotenoid, and also detailed lutein, zeaxanthin, canthaxanthin, chlorophyll-a, alpha-carotene, beta-carotene, and riboflavin contents of the selected species have been determined. Particularly, FAME analysis has been resulted in promising biodiesel usage, which has been also supported by fluorescence imaging of the selected Cyanobacteria by Nile red dyeing as it was expected due to nitrogen deprivation was known to increase the FAME contents as well as the PHB [113].

References

- [1] R. C. Thompson, S. H. Swan, C. J. Moore, and F. S. Vom Saal, "Our plastic age," *Philos. Trans. R. Soc. B Biol. Sci.*, vol. 364, no. 1526, pp. 1973–1976, 2009.
- [2] A. A. Shah, F. Hasan, A. Hameed, and S. Ahmed, "Biological degradation of plastics: A comprehensive review," *Biotechnol. Adv.*, vol. 26, no. 3, pp. 246–265, 2008.
- [3] S. Seena, D. Graça, A. Bartels, and J. Cornut, "Does nanosized plastic affect aquatic fungal litter decomposition?," *Fungal Ecol.*, vol. 39, pp. 388–392, 2019.
- [4] N. J. Beaumont, M. Aanesen, M. C. Austen, T. Börger, J. R. Clark, M. Cole, T. Hooper, P. K. Lindeque, C. Pascoe, K. J. Wyles, "Global ecological, social and economic impacts of marine plastic," *Mar. Pollut. Bull.*, vol. 142, pp. 189–195, 2019.
- [5] M. Bergmann, S. Mützel, S. Primpke, M. B. Tekman, J. Trachsel, and G. Gerdt, "White and wonderful? Microplastics prevail in snow from the Alps to the Arctic," *Sci. Adv.*, vol. 5, no. 8, pp. 1–11, 2019.
- [6] B. Garcia, M. M. Fang, and J. Lin, "All Hands on Deck: Addressing the Global Marine Plastics Pollution Crisis in Asia", vol. 8, no. 19, pp. 1–30, 2019.
- [7] M. Tekman, M.B., Gutow, L., Macario, A., Haas, A., Walter, A., Bergmann, "Litterbase," Alfred Wegener Institute Helmholtz Centre for Polar and Marine Research, 2019. [Online]. Available: <https://litterbase.awi.de/>. [Accessed: 12-Dec-2019].
- [8] A. Shrivastava, "Polymerization," in *Introduction to Plastics Engineering*, Elsevier, pp. 17–48, 2018.
- [9] M. C. Andrade, K. O. Winemiller, P. S. Barbosa, A. Fortunati, D. Chelazzi, A. Cincinelli, and T. Giarrizzo, "First account of plastic pollution impacting freshwater fishes in the Amazon: Ingestion of plastic debris by piranhas and other serrasalmids with diverse feeding habits," *Environ. Pollut.*, vol. 244, pp. 766–773, 2019.
- [10] C. Wilcox, E. Van Seville, B. D. Hardesty, and J. A. Estes, "Threat of plastic pollution to seabirds is global, pervasive, and increasing," *Proc. Natl. Acad. Sci. U. S. A.*, vol. 112, no. 38, pp. 11899–11904, 2015.
- [11] J. H. Kandziora, N. van Toulon, P. Sobral, H.L. Taylor, A.J. Ribbink, J.R. Jambeck, and S. Werner, "The important role of marine debris networks to prevent and reduce ocean plastic pollution," *Mar. Pollut. Bull.*, vol. 141, no. July 2018, pp. 657–662, 2019.
- [12] M. Nazareth, M. R. C. Marques, M. C. A. Leite, and Í. B. Castro, "Commercial plastics claiming biodegradable status: Is this also accurate for marine

- environments?,” J. Hazard. Mater., vol. 366, pp. 714–722, 2019.
- [13] PAGEV, “Türkiye Plastik Sektör İzleme Raporu,” PAGEV, pp. 9–10, 2019. [Online]. Available: <https://www.pagev.org/turkiye-plastik-sektor-izleme-raporu-2019-3>.
 - [14] V. D. Mendhulkar and L. A. Shetye, “Synthesis of Biodegradable Polymer Polyhydroxyalkanoate (PHA) in Cyanobacteria *Synechococcus elongates* Under Mixotrophic Nitrogen- and Phosphate-Mediated Stress Conditions,” Ind. Biotechnol., vol. 13, no. 2, pp. 85–93, 2017.
 - [15] Brigham and Sinskey, “Applications of Polyhydroxyalkanoates in the Medical Industry,” Int. J. Biotechnol. Wellness Ind., pp. 53–60, 2012.
 - [16] W. Sabra, A.-P. Zeng, H. Lunsdorf, and W.-D. Deckwer, “Effect of Oxygen on Formation and Structure of *Azotobacter vinelandii* Alginate and Its Role in Protecting Nitrogenase,” Appl. Environ. Microbiol., vol. 66, no. 9, pp. 4037–4044, 2000.
 - [17] M. Schlebusch and K. Forchhammer, “Requirement of the Nitrogen Starvation-Induced Protein Sll0783 for Polyhydroxybutyrate Accumulation in *Synechocystis* sp. Strain PCC 6803,” Appl. Environ. Microbiol., vol. 76, no. 18, pp. 6101–6107, 2010.
 - [18] T. Osanai, K. Numata, A. Oikawa, A. Kuwahara, H. Iijima, Y. Doi, K. Tanaka, K. Saito, and M. Y. Hirai, “Increased Bioplastic Production with an RNA Polymerase Sigma Factor SigE during Nitrogen Starvation in *Synechocystis* sp. PCC 6803,” DNA Res., vol. 20, no. 6, pp. 525–535, 2013.
 - [19] E. Rezzonico, L. Moire, and Y. Poirier, “Polymers of 3-hydroxyacids in plants,” Phytochem. Rev., vol. 1, no. 1, pp. 87–92, 2002.
 - [20] C. S. . Reddy, R. Ghai, Rashmi, and V. . Kalia, “Polyhydroxyalkanoates: an overview,” Bioresour. Technol., vol. 87, no. 2, pp. 137–146, 2003.
 - [21] M. E. Floccari, N. I. López, B. S. Méndez, U. P. Fürst, and A. Steinbüchel, “Isolation and partial characterization of *Bacillus megaterium* mutants deficient in poly(3-hydroxybutyrate) synthesis,” Can. J. Microbiol., vol. 41, no. 13, pp. 77–79, 1995.
 - [22] H. Zhang, V. Obias, K. Gonyer, and D. Dennis, “Production of polyhydroxyalkanoates in sucrose-utilizing recombinant *Escherichia coli* and *Klebsiella* strains,” Appl. Environ. Microbiol., vol. 60, no. 4, pp. 1198–205, 1994.
 - [23] J.-U. Ackermann and W. Babel, “Growth-associated synthesis of poly(hydroxybutyric acid) in *Methylobacterium rhodesianum* as an expression of an internal bottleneck,” Appl. Microbiol. Biotechnol., vol. 47, no. 2, pp. 144–149, 1997.
 - [24] D. Bourque, Y. Pomerleau, and D. Groleau, “High-cell-density production of poly- β -hydroxybutyrate (PHB) from methanol by *Methylobacterium extorquens*: production of high-molecular-mass PHB,” Appl. Microbiol. Biotechnol., vol. 44, no. 3–4, pp. 367–376, 1995.
 - [25] M. Takeda, H. Matsuoka, H. Hamana, and M. Hikuma, “Biosynthesis of poly-

- 3-hydroxybutyrate by *Sphaerotilus natans*,” *Appl. Microbiol. Biotechnol.*, vol. 43, no. 1, pp. 31–34, 1995.
- [26] L. Lama, B. Nicolaus, V. Calandrelli, M. C. Manca, I. Romano, and A. Gambacorta, “Effect of growth conditions on endo- and exopolymer biosynthesis in *Anabaena cylindrica* 10 C,” *Phytochemistry*, vol. 42, no. 3, pp. 655–659, 1996.
 - [27] N. G. Carr, “The occurrence of poly- β -hydroxybutyrate in the blue-green alga, *Chlorogloea fritschii*,” *Biochim. Biophys. Acta - Biophys. Incl. Photosynth.*, vol. 120, no. 2, pp. 308–310, 1966.
 - [28] L. Sharma and N. Mallick, “Accumulation of poly- β -hydroxybutyrate in *Nostoc muscorum*: regulation by pH, light–dark cycles, N and P status and carbon sources,” *Bioresour. Technol.*, vol. 96, no. 11, pp. 1304–1310, 2005.
 - [29] L. Sharma, A. Kumar Singh, B. Panda, and N. Mallick, “Process optimization for poly- β -hydroxybutyrate production in a nitrogen fixing cyanobacterium, *Nostoc muscorum* using response surface methodology,” *Bioresour. Technol.*, vol. 98, no. 5, pp. 987–993, 2007.
 - [30] N. Mallick, S. Gupta, B. Panda, and R. Sen, “Process optimization for poly(3-hydroxybutyrate-co-3-hydroxyvalerate) co-polymer production by *Nostoc muscorum*,” *Biochem. Eng. J.*, vol. 37, no. 2, pp. 125–130, 2007.
 - [31] S. M. Haase, B. Huchzermeyer, and T. Rath, “PHB accumulation in *Nostoc muscorum* under different carbon stress situations,” *J. Appl. Phycol.*, vol. 24, no. 2, pp. 157–162, 2012.
 - [32] S. Ansari and T. Fatma, “Cyanobacterial Polyhydroxybutyrate (PHB): Screening, Optimization and Characterization,” *PLoS One*, vol. 11, no. 6, pp. 1–20, 2016.
 - [33] L. J. Stal, “Poly(hydroxyalkanoate) in cyanobacteria: an overview,” *FEMS Microbiol. Lett.*, vol. 103, no. 2–4, pp. 169–180, 1992.
 - [34] R. De Philippis, C. Sili, and M. Vincenzini, “Glycogen and poly- β -hydroxybutyrate synthesis in *Spirulina maxima*,” *J. Gen. Microbiol.*, vol. 138, no. 8, pp. 1623–1628, 1992.
 - [35] M. Vincenzini, C. Sili, R. de Philippis, A. Ena, and R. Materassi, “Occurrence of poly-beta-hydroxybutyrate in *Spirulina* species.,” *J. Bacteriol.*, vol. 172, no. 5, pp. 2791–2792, 1990.
 - [36] M. Miyake, M. Erata, and Y. Asada, “A thermophilic cyanobacterium, *Synechococcus* sp. MA19, capable of accumulating poly- β -hydroxybutyrate,” *J. Ferment. Bioeng.*, vol. 82, no. 5, pp. 512–514, 1996.
 - [37] M. Nishioka, K. Nakai, M. Miyake, Y. Asada, and M. Taya, “Production of poly- β -hydroxybutyrate by thermophilic cyanobacterium, *Synechococcus* sp. MA19, under phosphate-limited conditions,” *Biotechnol. Lett.*, vol. 23, no. 14, pp. 1095–1099, 2001.
 - [38] D. Kamravamanesh, S. Pflügl, W. Nischkauer, A. Limbeck, M. Lackner, and C. Herwig, “Photosynthetic poly- β -hydroxybutyrate accumulation in unicellular cyanobacterium *Synechocystis* sp. PCC 6714,” *AMB Express*, vol.

7, no. 1, p. 143, 2017.

- [39] B. Panda, P. Jain, L. Sharma, and N. Mallick, "Optimization of cultural and nutritional conditions for accumulation of poly- β -hydroxybutyrate in *Synechocystis* sp. PCC 6803," *Bioresour. Technol.*, vol. 97, no. 11, pp. 1296–1301, 2006.
- [40] R. Bhati, "Biodegradable Plastics Production by Cyanobacteria," in *Biotechnology Products in Everyday Life*, Springer, Cham, 2019, pp. 131–143.
- [41] D. Hosler, S. L. Burkett, and M. J. Tarkanian, "Prehistoric polymers: Rubber processing in ancient Mesoamerica," *Science*, vol. 284, no. 5422, pp. 1988–1991, 1999.
- [42] A. L. Andrady and M. A. Neal, "Applications and societal benefits of plastics," *Philos. Trans. R. Soc. B Biol. Sci.*, vol. 364, no. 1526, pp. 1977–1984, 2009.
- [43] J. A. Jansen, "Plastics - It's All About Molecular Structure," *Plast. Eng.*, vol. 72, no. 8, pp. 44–49, 2016.
- [44] Ferdinand Rodriguez, "Plastic," *Encyclopædia Britannica*, 2019. [Online]. Available: <https://www.britannica.com/science/plastic>. [Accessed: 02-Nov-2019].
- [45] EFSA, "Bisphenol A," 2018. [Online]. Available: <https://www.efsa.europa.eu/en/topics/topic/bisphenol> [Accessed: 04-Dec-2019].
- [46] J. Yang, W. Song, X. Wang, Y. Li, J. Sun, W. Gong, and C. Sun, "Migration of phthalates from plastic packages to convenience foods and its cumulative health risk assessments," *Food Addit. Contam. Part B Surveill.*, vol. 12, no. 3, pp. 151–158, 2019.
- [47] Z. Cao, Q. Chen, X. Li, Y. Zhang, M. Ren, L. Sun, M. Wang, X. Liu, and G. Yu, "The non-negligible environmental risk of recycling halogenated flame retardants associated with plastic regeneration in China," *Sci. Total Environ.*, vol. 646, pp. 1090–1096, 2019.
- [48] Y. Tokiwa, B. Calabia, C. Ugwu, and S. Aiba, "Biodegradability of Plastics," *Int. J. Mol. Sci.*, vol. 10, no. 9, pp. 3722–3742, 2009.
- [49] M. Shimao, "Biodegradation of plastics," *Curr. Opin. Biotechnol.*, vol. 12, no. 3, pp. 242–247, 2001.
- [50] Å. M. Ronkvist, W. Xie, W. Lu, and R. A. Gross, "Cutinase-Catalyzed hydrolysis of poly(ethylene terephthalate)," *Macromolecules*, vol. 42, no. 14, pp. 5128–5138, 2009.
- [51] P. Bombelli, C. J. Howe, and F. Bertocchini, "Polyethylene bio-degradation by caterpillars of the wax moth *Galleria mellonella*," *Curr. Biol.*, vol. 27, no. 8, pp. 292–293, 2017.
- [52] Y. Yang, J. Yang, and L. Jiang, "Comment on "a bacterium that degrades and assimilates poly(ethylene terephthalate)"", *Science*, vol. 353, no. 6301,

p. 759, 2016.

- [53] S. Su, R. Kopitzky, S. Tolga, and S. Kabasci, "Polylactide (PLA) and Its Blends with Poly(butylene succinate) (PBS): A Brief Review," *Polymers (Basel)*, vol. 11, no. 7, p. 1193, 2019.
- [54] C. Namrata, "Ketosis," *Biochemistry for Medics*, 2013. [Online]. Available: <https://www.namrata.co/ketosis-part-1/>. [Accessed: 12-Nov-2019].
- [55] M. Miyake, K. Kataoka, M. Shirai, and Y. Asada, "Control of poly-beta-hydroxybutyrate synthase mediated by acetyl phosphate in cyanobacteria," *J. Bacteriol.*, vol. 179, no. 16, pp. 5009–5013, 1997.
- [56] P. B. S. Albuquerque and C. B. Malafaia, "Perspectives on the production, structural characteristics and potential applications of bioplastics derived from polyhydroxyalkanoates," *Int. J. Biol. Macromol.*, vol. 107, no. PartA, pp. 615–625, 2018.
- [57] S. Philip, T. Keshavarz, and I. Roy, "Polyhydroxyalkanoates: biodegradable polymers with a range of applications," *J. Chem. Technol. Biotechnol.*, vol. 82, no. 3, pp. 233–247, 2007.
- [58] B. A. Whitton and P. A. Roger, "Use of blue-green algae and *Azolla* in rice culture," *Soc. Gen. Microbiol.*, vol. 25, pp. 89–100, 1989.
- [59] P. A. Holmes, "Applications of PHB - a microbially produced biodegradable thermoplastic," *Phys. Technol.*, vol. 16, no. 1, pp. 32–36, 1985.
- [60] Brown TA., "Genomes 2nd edition," in Oxford: Wiley-Liss, 2nd ed., BIOS Scientific Publishers Ltd, p. 686, 2002.
- [61] W. F. Vincent, "Protists, Bacteria and Fungi: Planktonic and Attached - Cyanobacteria," in *General psychology for college students.*, New York: MacMillan Co, pp. 226–232, 2015.
- [62] S. J. van Vuuren, J. Taylor, C. Van Ginkel, and A. Gerber, "Easy identification of the most common Freshwater Algae: A guide for the identification of microscopic algae in South African freshwaters", no. 32(3). School of Environmental Sciences and Development: Botany North-West University, pp. 15–33, 2006.
- [63] M. P. Starr and J. M. Schmidt, "The Prokaryotes", 1st ed. Berlin, Heidelberg: Springer Berlin Heidelberg, pp. 198–200, 1981.
- [64] R. E. Lee, "Phycology", 4th ed. Cambridge University Press, pp. 33–49, 2008.
- [65] B. Yilmaz Ozturk, B. Asikkutlu, C. Akkoz, and T. Atici, "Molecular and morphological characterization of several cyanobacteria and chlorophyta species isolated from lakes in turkey," *Turkish J. Fish. Aquat. Sci.*, vol. 19, no. 8, pp. 635–643, 2019.
- [66] M. R. Hons, "Screening and selection of a cyanobacteria for production of poly-B-hydroxybutyrate in a closed photobioreactor," *University of Adelaide*, pp. 7–28, 2009.
- [67] G. M. M.D. Guiry in Guiry, M.D. & Guiry, "AlgaeBase," World-wide electronic publication, National University of Ireland, Galway. [Online].

Available:

https://www.algaebase.org/search/genus/detail/?genus_id=42976.

[Accessed: 12-Jan-2020].

- [68] M. A. Schneegurt, "Cyanosite," Purdue University and Wichita State University. [Online]. Available: <http://www-cyanosite.bio.purdue.edu/images/images.html>. [Accessed: 12-Jan-2020].
- [69] R. Radzi, N. Muangmai, P. Broady, W. M. W. Omar, S. Lavoue, P. Convey, and F. Merican, "Nodosilinea signiensis sp. nov. (Leptolyngbyaceae, Synechococcales), a new terrestrial cyanobacterium isolated from mats collected on Signy Island, South Orkney Islands, Antarctica," *PLoS One*, vol. 14, no. 11, pp. 1–13, 2019.
- [70] R. Y. Stanier, R. Kunisawa, M. Mandel, and G. Cohen-Bazire, "Purification and properties of unicellular blue-green algae (order Chroococcales).," *Bacteriol. Rev.*, vol. 35, no. 2, pp. 171–205, 1971.
- [71] UTEX, "BG-11 Medium," UTEX Culture Collection of Algae. [Online]. Available: <https://utex.org/products/bg-11-medium?variant=30991786868826>. [Accessed: 02-Feb-2015].
- [72] UTEX, "BG-11(-N) Medium," UTEX Culture Collection of Algae, 2009. [Online]. Available: <https://utex.org/products/bg-11-n-medium?variant=30991786311770>. [Accessed: 27-Feb-2016].
- [73] M. Costa, M. Garcia, J. Costa-Rodrigues, M. S. Costa, M. J. Ribeiro, M. H. Fernandes, P. Barros, A. Barreiro, V. Vasconcelos, and R. Martins, "Exploring Bioactive Properties of Marine Cyanobacteria Isolated from the Portuguese Coast: High Potential as a Source of Anticancer Compounds," *Mar. Drugs*, vol. 12, no. 1, pp. 98–114, 2013.
- [74] Cyanosite, "Z8 Medium," Cyanosite. [Online]. Available: <http://www-cyanosite.bio.purdue.edu/media/table/media.html>. [Accessed: 20-Jun-2005].
- [75] Cyanosite, "Allen Medium," Cyanosite. [Online]. Available: <http://www-cyanosite.bio.purdue.edu/media/table/allen.html>. [Accessed: 20-Jun-2005].
- [76] CCCryo, "FW medium," CCCryo - Culture Collection of Cryophilic Algae. [Online]. Available: <http://cccryo.fraunhofer.de/sources/files/medien/fwDiatom.pdf>. [Accessed: 20-Jun-2005].
- [77] E. Sahinkaya, A. Yurtsever, Ö. Aktaş, D. Ucar, and Z. Wang, "Sulfur-based autotrophic denitrification of drinking water using a membrane bioreactor," *Chem. Eng. J.*, vol. 268, pp. 180–186, 2015.
- [78] S. Aljanabi, "Universal and rapid salt-extraction of high quality genomic DNA for PCR- based techniques," *Nucleic Acids Res.*, vol. 25, no. 22, pp. 4692–4693, 1997.
- [79] M. W. Fawley and P. Karen, "Note a Simple and Rapid Technique for the Isolation of Dna," *Algae*, vol. 225, no. 40, pp. 223–225, 2004.

- [80] X. Wu, A. Zarka, and S. Boussiba, "A simplified protocol for preparing DNA from filamentous cyanobacteria," *Plant Mol. Biol. Report.*, vol. 18, no. 4, pp. 385–392, 2000.
- [81] T. Nolan, J. Huggett, and E. Sanchez, "Good Practice Guide for the Application of Quantitative PCR (qPCR)," *Natl. Meas. Syst.*, pp. 10–17, 2013.
- [82] P. Rajaniemi, "Phylogenetic and morphological evaluation of the genera *Anabaena*, *Aphanizomenon*, *Trichormus* and *Nostoc* (Nostocales, Cyanobacteria)," *Int. J. Syst. Evol. Microbiol.*, vol. 55, no. 1, pp. 11–26, 2005.
- [83] T. Kurobe, D. Baxa, C. Mioni, R. Kudela, T. Smythe, S. Waller, A. Chapman, and S. Teh, "Identification of harmful cyanobacteria in the Sacramento-San Joaquin Delta and Clear Lake, California by DNA barcoding," *Springerplus*, vol. 2, no. 1, p. 491, 2013.
- [84] U. Nübel, F. Garcia-Pichel, and G. Muyzer, "PCR primers to amplify 16S rRNA genes from cyanobacteria," *Appl. Environ. Microbiol.*, vol. 63, no. 8, pp. 3327–3332, 1997.
- [85] M. Scheer, "Charakterisierung der Diversität von Mikroorganismen im Nationalpark 'Unteres Odertal'," *Technische Universität Dresden*, pp. 33–35, 2010.
- [86] J. Martins, L. Peixe, and V. Vasconcelos, "Cyanobacteria and bacteria co-occurrence in a wastewater treatment plant: absence of allelopathic effects," *Water Sci. Technol.*, vol. 62, no. 8, pp. 1954–1962, 2010.
- [87] M. A. Porras, M. A. Villar, and M. A. Cubitto, "Novel spectrophotometric technique for rapid determination of extractable PHA using Sudan black dye," *J. Biotechnol.*, vol. 255, no. May, pp. 28–32, 2017.
- [88] A. G. de A. Barros, J. Liu, G. A. Lemieux, B. C. Mullaney, and K. Ashrafi, "Analyses of *C. elegans* Fat Metabolic Pathways," in *Methods in Cell Biology*, vol. 107, pp. 383–407, 2012.
- [89] T. Cakmak, P. Angun, Y. E. Demiray, A. D. Ozkan, Z. Elibol, and T. Tekinay, "Differential effects of nitrogen and sulfur deprivation on growth and biodiesel feedstock production of *Chlamydomonas reinhardtii*," *Biotechnol. Bioeng.*, vol. 109, no. 8, pp. 1947–1957, 2012.
- [90] L. F. Rivas, S. A. Casarin, N. C. Nepomuceno, M. I. Alencar, J. Augusto, M. Agnelli, E. S. Medeiros, A. O. W. Neto, M. P. Oliveira, A. M. Medeiros, and A. S. F. Santos, "Reprocessability of PHB in extrusion: ATR-FTIR, tensile tests and thermal studies," *Polímeros*, vol. 27, no. 2, pp. 122–128, 2017.
- [91] M. Kansiz, H. Billman-Jacobe, and D. McNaughton, "Quantitative Determination of the Biodegradable Polymer Poly(β -hydroxybutyrate) in a Recombinant *Escherichia coli* Strain by Use of Mid-Infrared Spectroscopy and Multivariate Statistics," *Appl. Environ. Microbiol.*, vol. 66, no. 8, pp. 3415–3420, 2000.
- [92] A. P. Dean, D. C. Sigee, B. Estrada, and J. K. Pittman, "Using FTIR

- spectroscopy for rapid determination of lipid accumulation in response to nitrogen limitation in freshwater microalgae,” *Bioresour. Technol.*, vol. 101, no. 12, pp. 4499–4507, 2010.
- [93] S. W. Jeffrey and G. F. Humphrey, “New spectrophotometric equations for determining chlorophylls a, b, c1 and c2 in higher plants, algae and natural phytoplankton,” *Biochem. und Physiol. der Pflanz.*, vol. 167, no. 2, pp. 191–194, 1975.
- [94] J. B. Simeunovic, S. B. Markovic, D. J. Kovac, A. C. Misan, A. I. Mandic, and Z. B. Svircev, “Filamentous cyanobacteria from Vojvodina region as source of phycobiliprotein pigments as potencial natural colorants,” *Food Feed Res.*, vol. 39, no. 1, pp. 23–31, 2012.
- [95] J. Schierle, B. Pietsch, A. Ceresa, C. Fizet, and E. H. Waysek, “Method for the determination of beta-carotene in supplements and raw materials by reversed-phase liquid chromatography: single laboratory validation,” *J. AOAC Int.*, vol. 87, no. 5, pp. 1070–82, 2008.
- [96] M. Yaman, “Beslenmede Gıda Kompozisyonu Analiz Yöntemleri”. Istanbul Sabahattin Zaim University, Faculty of Health Sciences, Department of Nutrition and Dietetics, pp. 117–166, 2007.
- [97] E. S. P. Reyes and L. Subryan, “An improved method of simultaneous HPLC and thiamin in selected cereal products,” *J. Food Compos. Anal.*, vol. 2, no. 1, pp. 41–47, 1989.
- [98] N. U. Maheswari and K. Ahilandeswari, “Production of bioplastic using *Spirulina platensis* and comparison with commercial plastic,” *Res. Environ. Life Sci.*, vol. 4, no. 3, pp. 133–136, 2011.
- [99] A. Hoseinabadi, I. Rasooli, and M. Taran, “Isolation and Identification of Poly β -Hydroxybutyrate Over-Producing Bacteria and Optimization of Production Medium,” *Jundishapur J. Microbiol.*, vol. 8, no. 7, 2015, [Online]. Available: <http://jjmicrobiol.com/en/articles/18875.html>. [Accessed: 03-Feb-2017].
- [100] M. Jahn, V. Vialas, J. Karlsen, G. Maddalo, F. Edfors, B. Forsström, M. Uhlén, L. Käll, and E. P. Hudson, “Growth of Cyanobacteria Is Constrained by the Abundance of Light and Carbon Assimilation Proteins,” *Cell Rep.*, vol. 25, no. 2, pp. 478–486, 2018.
- [101] L. Guidi, M. Tattini, and M. Landi, “How Does Chloroplast Protect Chlorophyll Against Excessive Light?,” in *Chlorophyll*, no. June, InTech, pp. 21–33, 2017.
- [102] T. Zavřel, M. Sinetova, and J. Červený, “Measurement of Chlorophyll a and Carotenoids Concentration in Cyanobacteria,” *Bio-Protocol*, vol. 5, no. 9, pp. 1–5, 2015.
- [103] T. Zavřel, P. Očenášová, M. Sinetova, and J. Červený, “Determination of Storage (Starch/Glycogen) and Total Saccharides Content in Algae and Cyanobacteria by a Phenol-Sulfuric Acid Method,” *Bio-Protocol*, vol. 8, no. 15, pp. 1–13, 2018.

- [104] P. Held and K. Raymond, "Determination of Algal Cell Lipids Using Nile Red - Using Microplates to Monitor Neutral Lipids in *Chlorella Vulgaris*," *Biofuel Res. Appl. Notes*, vol. 071211, no. 8, pp. 1–5, 2011.
- [105] M. G. de Moraes, C. Stillings, R. Dersch, M. Rudisile, P. Pranke, J. A. V. Costa, and J. Wendorff, "Extraction of poly(3-hydroxybutyrate) from *Spirulina* LEB 18 for developing nanofibers," *Polímeros*, vol. 25, no. 2, pp. 161–167, 2015.
- [106] Yellore and Desai, "Production of poly- 3- hydroxybutyrate from lactose and whey by *Methylobacterium* sp. ZP24," *Lett. Appl. Microbiol.*, vol. 26, no. 6, pp. 391–394, 1998.
- [107] S. Ansari, D. Yasin, and T. Fatma, "Key Insights of Natural Bioplastic Polyhydroxybutyrate (PHB) Synthesis In Cyanobacteria," *Am. J. PharmTech Res.*, vol. 6, no. 4, pp. 110–127, 2016.
- [108] T. Matthew, W. Zhou, J. Rupprecht, L. Lim, S. R. Thomas-Hall, A. Doebbe, O. Kruse, B. Hankamer, U. C. Marx, S. M. Smith, and P. M. Schenk, "The Metabolome of *Chlamydomonas reinhardtii* following Induction of Anaerobic H₂ Production by Sulfur Depletion," *J. Biol. Chem.*, vol. 284, no. 35, pp. 23415–23425, 2009.
- [109] S. Van Wycken, K. Ramirez, and L. M. L. Laurens, "Determination of Total Lipids as Fatty Acid Methyl Esters (FAME) by in situ Transesterification: Laboratory Analytical Procedure (LAP)," Golden, CO (United States), pp. 1–12, 2016.
- [110] E. G. Bellinger and D. C. Sigee, "Freshwater Algae: Identification and Use as Bioindicators", Wiley-Blackwell Publishing, pp. 137–174, 2010.
- [111] M. F. Haddad, T. Dayioglu, M. Yaman, B. Nalbantoglu, and T. Cakmak, "Long-term diazotrophic cultivation of *Trichormus* sp. IMU26: evaluation of physiological changes related to elevated phycobiliprotein content," *Journal of Applied Phycology*, 2020. [Online]. Available: <http://link.springer.com/10.1007/s10811-019-02012-3>. [Accessed: 03-Feb-2020].
- [112] F. David, P. Sandra, and A. K. Vickers, "Column selection for the analysis of fatty acid methyl esters," *Food Anal. Appl. Palo Alto, CA Agil. Technol.*, pp. 1–12, 2005.
- [113] A. M. P. Anahas and G. Muralitharan, "Characterization of heterocystous cyanobacterial strains for biodiesel production based on fatty acid content analysis and hydrocarbon production," *Energy Convers. Manag.*, vol. 157, no. September 2017, pp. 423–437, 2018.

Publications from the Thesis

Contact Information: t.dayioglu@yahoo.com

Papers

1. M. F. Haddad, T. Dayioglu, M. Yaman, B. Nalbantoglu, and T. Cakmak, "Long-term diazotrophic cultivation of *Trichormus* sp. IMU26: evaluation of physiological changes related to elevated phycobiliprotein content," *J. Appl. Phycol.*, Jan. 2020. [Online]. Available: <http://link.springer.com/10.1007/s10811-019-02012-3>.

Conference Oral Presentations

1. M. Fadhil Haddad*, T. Dayioglu, B. Nalbantoglu, and T. Cakmak, (2019). "Screening Indigenous Cyanobacteria for Phycobiliprotein Production", II. International Green Biotechnology Congress 2019 (09-11 September in Istanbul).
2. T. Dayioglu.*, Z. Elibol Cakmak, M. Haddad, T. Cakmak, "Polyhydroxybutyrate Production Potential of Some Indigenous Cyanobacteria", IPSAT (II. International Plant Science and Technology Congress), 07-10.10.2018, Bodrum, TURKEY.
3. Z. Elibol Cakmak*, T. Dayioglu., M. Haddad, T. Cakmak, "Diazotrophic Cyanobacteria Isolated from Paddy Fields in Edirne Province", IPSAT (II. International Plant Science and Technology Congress), 07-10.10.2018, Bodrum, TURKEY.
4. M. Haddad*, Z. Elibol Cakmak, T. Dayioglu, T. Cakmak, " Phycobiliproteins Producing Cyanobacteria Isolated from Paddy Fields in Edirne Province ", IPSAT (II. International Plant Science and Technology Congress), 07-10.10.2018, Bodrum, TURKEY.

Projects

1. Republic of Turkey Ministry of Agriculture and Forestry General Directorate of Agricultural Research and Policies (TAGEM) Grant No: TAGEM/16/AR-GE/44